Investigating permeation of anti-mycobacterial agents in *Mycobacterium tuberculosis* and *M. tuberculosis*-infected macrophages *in vitro* as a model for early stage tuberculosis drug discovery

Amanda N. Mabhula

Supervisor: Professor Kelly Chibale
Department of Chemistry
& Institute of Infectious Disease and Molecular Medicine, University of Cape Town

Co-Supervisor: Professor Digby F. Warner
Department of Pathology
& Institute of Infectious Disease and Molecular Medicine, University of Cape Town

Co-Supervisor: Associate Professor Lubbe Wiesner
Department of Medicine, University of Cape Town

A thesis presented for the degree of Doctor of Philosophy in the Department of Chemistry, University of Cape Town

June 2020

DECLARATION

I, **Amanda N. Mabhula**, hereby declare that:

i) This thesis is my own unaided work, both in concept, execution and data interpretation, and that apart from the normal guidance of my supervisors, I have received no assistance apart from that acknowledged.

ii) This thesis is being submitted for the degree of Doctor of Philosophy at the University Cape Town, and neither the substance nor any part of the thesis has been submitted, or is to be submitted for a degree or examination in this or any other university.

iii) I grant the University permission to reproduce the thesis, in whole or in part, for the purposes of research.

Signed: Signed by candidate Date: 24 June 2020

ACKNOWLEDGEMENTS

I would like to give my sincerest thank you to everyone who contributed in any way, however minor it may seem, on my journey towards this PhD.

A special thank you to my supervisor Prof. Kelly Chibale, you inspired this young woman as an undergraduate at the University of Fort Hare, years before I would come to UCT. When I joined your group, you became a mentor and a scientific father figure. Thank you for all your patience, guidance and support through the constant challenges during the course of this work and the enormous scientific knowledge you have imparted upon me.

To my co-supervisors, Prof. Digby Warner and Assoc Prof. Lubbe Wiesner thank you welcoming me into your research groups and making me feel at home. I appreciate our discussions that challenged me to continue to grow my scientific capabilities, your guidance and motivation to push through during those 'stuck in the cloud' moments.

Prof. Val Mizrahi, as a leading woman in science, you inspire me every day. Your insightful comments and constructive criticism during MMRU journal club and work-in-progress meetings are appreciated.

Dr. Mathew Njoroge, thank you for the insightful discussions, technical support with LC-MS/MS method development and data interpretation. I would also like to thank Drs. Gabriel Mashabela and Pooja Agarwal who inducted me into the labs; and with whom I worked closely during optimization of some methods. The countless discussions and advice are much appreciated. Drs. Gurminder Kaur, Godwin Dzirwonu and Paul Njaria whose exceptional skills in organic synthesis yielded the compounds that were crucial for this work, I could not have done it without you. A special thank you to all members of the Kelly Chibale research group, MMRU and Lubbe Wiesner research group who gave constructive criticism during our group meetings. Ditshego Ralefeta, thank for you for assistance with microscopy image acquisition and analysis. I am also grateful to H3D support, particularly from Mr. Warren Olifant and Ms. Nesia Barnes (Division of Clinical Pharmacology) who ran the PAMPA and selected solubility assays as part of routine screening; Ms. Zama Nqgumba and Mr. Ronald Olckers for technical support. To Ms. Tando Ntsabo and Ms. Ronnett Seldon (TB screening lab), thank you for assistance in testing for MICs of selected compounds.

Ms. Elaine Rutherfoord-Jones, Ms. Lameeza Jakoet, Ms. Dierdre Brooks and Ms. Saroja Naicker your unmatched administrative prowess made this journey smooth. Berenice Arendse, Fadwah Booley, Rayanna Fredericks and Shaheeda Johnson, thank for your support in the maintenance of equipment and laboratories.

I am also grateful for the support which made this work possible through funding: the Department of Science and Technology, through the South Africa Research Chairs Initiative (SARChI) administered by the National Research Foundation (NRF), Department of Chemistry and the Institute of Infectious Diseases and Molecular Medicine (IDM), University of Cape Town; and The Novartis Research Foundation.

To my friends, thank you for constantly checking up on me and lending your ears to listen to me vent when things were not going great in the lab.

To the most important people in my life, my family: my mom, my dad, Gugu, Nombu, Sandra, Brandy, Theo, Mzo noNkosi, thank you guys! I am really lucky to have your support, constant encouragement and your prayers from day one!

Most importantly, this would not have been possible without God's Will and Grace. *ENkosi Bawo*!

ABSTRACT

Tuberculosis (TB) is the leading cause of death due to a single infectious disease and remains a major threat to global public health. The increasing emergence of multi-drug resistance to current anti-TB drugs, exacerbated by the long treatment duration, highlights the need for new effective treatments or strategies to shorten the treatment duration, improve patient adherence and curb the alarming rates of resistance. A key challenge to current strategies employed in the development of anti-TB drugs is the complexity in TB disease pathology which presents as a wide spectrum of lesions in patients presenting with the disease. These lesions occur at different anatomical loci in the same individual and at different stages as the disease progresses. In addition, the interaction between the causative agent, *Mycobacterium tuberculosis*, and its obligate human host induces physiologic and metabolic changes in the infecting bacillus that are specific to each lesion compartment, and dynamic. This is likely to influence *M. tuberculosis* susceptibility to antibiotic treatment and, consequently, affect treatment duration and possibly the development of drug resistance. A major limitation in current strategies to address this problem is translation of *in vitro* compound potency to *in vivo* efficacy. To reach the target site, a drug must first distribute and accumulate in the lesion microenvironments where bacteria reside: the macrophage host cell and the caseum.

This thesis focused on the development of an *in vitro* infection model that could be used to predict drug penetration into *M. tuberculosis*-infected macrophages. Of particular interest was the extent to which host intracellular drug concentrations translate into effective antimycobacterial activity. To this end, the thesis comprised three key aspects: (i) characterization of physicochemical properties, antimycobacterial activities and *M. tuberculosis*-mediated metabolism of selected anti-TB compounds; (ii) determination of intracellular drug permeation in resting, activated and foamy macrophages; and (iii) determination of the correlation (or not) between intracellular drug concentration and effective *M. tuberculosis* growth inhibition.

The highly lipophilic natural product, fusidic acid (FA), its known human metabolite, 3-ketofusidic (3-ketoFA or GKFA37), and two C-3 alkyl esters (GKFA16 and GKFA17) as FA prodrugs were utilized in the study. In addition, another chemical class, the less lipophilic benzoxazole-based oxime derivatives were also investigated. Moxifloxacin (MXF), levofloxacin (LVF), bedaquiline (BDQ), rifampicin (RIF) and clofazimine (CFZ) were included for reference as known anti-TB drugs with varying lipophilicities. In chapter 2, FA and derivatives showed potent

antimycobacterial activity (~1 µM) with selectivity indices (SI) >20 against the THP-1 macrophage cell line. Predicted artificial membrane permeability assay (PAMPA) results suggested that FA and derivatives would readily permeate the cell membrane. *M. tuberculosis* metabolized the C-3 alkyl-ester prodrug GKFA17 to form both FA and 3-ketoFA, with complete hydrolysis of the prodrug. FA was metabolized to 3-ketoFA, but the low levels of the metabolite suggested that another unidentified metabolite, presumed to be 3-epifusidic acid (3-epiFA), was formed. *In vitro* assays revealed that the potent benzoxazole-based oxime carbamates (PMN1-201, PMN1-136 and PMN2-09) were rapidly hydrolyzed by *M. tuberculosis* and were also susceptible to spontaneous degradation in media, forming the poorly active corresponding free oximes (PMN1-199, PMN1-135 and PMN1-157).

In chapter 3, the *in vitro* macrophage drug uptake assay showed that FA C-3 alkyl prodrugs, GKFA16 and GKFA17, accumulated in significantly higher amounts in resting macrophages in comparison to FA and GKFA37. Accumulation of MXF was comparable to the least accumulated FA derivative, GKFA37, and showed steady state intracellular concentrations over a 6-day period. While GKFA16 and GKFA17 showed continued increasing accumulation, intracellular concentrations of FA and GKFA37 decreased after 48 hours, suggesting a likely susceptibility to macrophage efflux. In infected macrophages, the presence of intracellular bacteria or increasing bacterial burden did not affect the host cell ability to accumulate the drugs.

FA and derivatives exhibited bacteriostatic inhibition of intracellular mycobacterial growth. MXF showed a potent bactericidal effect, reducing intracellular bacterial counts significantly at 10x MIC, with complete sterilization at 50x MIC even though MXF accumulation was significantly less than that of FA alkyl esters. These results suggested that both the inherent activity of a compound and ability to accumulate within host cells drive cellular efficacy. Given that the C-3 alkyl ester prodrugs accumulated at significantly higher concentrations than FA and GKFA37, this demonstrates the limitations of this assay in ascertaining the impact of intracellular concentration on drug efficacy for bacteriostatic drugs while highlighting its ability to correlate drug penetration and intracellular activity for cidal drugs. The prodrug GKFA17 was shown to undergo metabolism in resting host cells and during infection to form FA and then 3-ketoFA. Therefore, the prodrug strategy could be used to increase intracellular exposure of FA as GKFA17 showed superior macrophage accumulation. Benzoxazole-based oxime carbamates and their corresponding free oximes failed to accumulate in host macrophages and this was corroborated by their failure to

control host cell bacterial growth despite the potent *in vitro* activity against *M. tuberculosis* of the carbamates, suggesting that they are poorly permeable.

Chapter 4 investigated drug permeation in different macrophage phenotypes known to exist in the granuloma during TB disease, including foamy and activated macrophages. The activation state of the host cell did not affect the ability to accumulate anti-TB drugs such as RIF and BDQ. However, FA and its prodrug GKFA17 were significantly reduced in M1 activated macrophages. Despite the significantly reduced intracellular concentration, activated macrophages treated with FA and derivatives showed superior intracellular *M. tuberculosis* growth inhibition, suggesting that macrophage activation potentiates the activity of these compounds.

In order to assess the effect of foamy macrophage lipid bodies (LBs) on drug uptake and intracellular localization, oleic acid-induced foamy macrophages were treated with selected anti-TB drugs and experimental compounds. FA and derivatives showed early increased accumulation in foamy cells compared to resting macrophages, while MXF, BDQ and RIF levels were not significantly changed. Intracellular:extracellular (I/E) ratios increased with increase in lipophilicity, with FA C-3 alkyl prodrugs exhibiting the highest I/E ratios of >100. Despite exhibiting increased foamy macrophage concentrations, FA and derivatives exhibited a similar reduction (bacteriostatic) in bacterial counts in both resting and foamy macrophages. The intracellular activity of RIF was also not affected by presence of LBs in foamy macrophages. BDQ, LVF and MXF, however, showed reduced intracellular efficacy against *M. tuberculosis* in foamy macrophages compared to resting macrophages, suggesting a role for LBs to impact intracellular drug distribution.

In conclusion, this thesis demonstrates the potential utility in combining advanced analytical methods and an *in vitro* infection model to determine cellular drug permeation profiles that might be applied to prioritize compounds and combinations optimized for distribution to target bacterial populations. This will facilitate well-informed decision-making processes in progression of lead compounds in pre-clinical development and, therefore, may offer the potential to reduce high rates of attrition of compounds which enter clinical phase of development.

PUBLICATIONS AND CONFERENCES

Poster Presentation: Investigating permeation of anti-mycobacterial agents in macrophages as an *in vitro* model for early stage TB drug discovery. Tuberculosis Drug Discovery and Development: Gordon Research Seminar (GRS) (24th – 25th June 2017) and Gordon Research Conference (GRC) (25th – 30th June 2017). Renaissance Tuscany Il Ciocco, Lucca (Barga), Italy.

Amanda Mabhula and Vinayak Singh. Drug resistance in *M. tuberculosis*: where we stand. *Med Chem Comm*. 2019; 10(8):1342-1360. doi:10.1039/c9md00057g.

TABLE OF CONTENTS

LIST OF FIGURES

LIST OF TABLES

ABBREVIATIONS

ADME absorption, distribution, metabolism, excretion

AMK amikacin

ART antiretroviral therapy

ATP adenosine triphosphate

AUC area under the curve

AZT azithromycin

BCG bacille Calmette-Guerin

BDQ bedaquiline

BPaL bedaquiline-pretomanid-linezolid

BPaMZ bedaquiline-pretomanid-moxifloxacin-pyrazinamide

CFU colony forming unit

CFZ clofazimine

cKD conditional knockdown

CLogP calculated log P

C_{max} maximum concentration

CPX ciprofloxacin

CRISPRi clustered regularly inter-spaced short palindromic repeats interference

D-CS D-cycloserine

Ddn deazaflavin-dependent nitroreductase

DLM delamanid

DNA deoxyribonucleic acid

DOTS directly observed therapy short-course

DR-TB drug-resistant TB

DS-TB drug-susceptible TB

EBA early bactericidal activity

EDTA ethylenediaminetetraacetic acid

EF-G elongation factor-G

EMB ethambutol

ETH ethionamide

FA fusidic acid

FASII fatty acid synthase II

FGD1 F_{420}-dependent glucose-6-phosphate dehydrogenase

GDP guanosine diphosphate

GTP guanosine triphosphate

GTX gatifloxacin

HIV human immunodeficiency virus

HLM human liver microsomes

HTS high throughput screening

I/E intracellular/ extracellular

IFN-γ interferon gamma

ILI intracytoplasmic lipid inclusions

IMPDH inosine monophosphate dehydrogenase

INH isoniazid

IS internal standard

LAM lipoarabinomannan

LB lipid bodies

LC-MS/MS liquid chromatography tandem mass spectrometry

LPS lipopolysaccharide

LTBI latent tuberculosis infection

LVF levofloxacin

LZD linezolid

M. bovis *Mycobacterium bovis*

M. smegmatis *Mycobacterium smegmatis*

M. tuberculosis *Mycobacterium tuberculosis*

MALDI-MSI matrix assisted laser desorption ionization –mass spectrometry imaging

MBC minimum bactericidal concentration

MDR-TB multi-drug resistant TB

MIC minimum inhibitory concentration

MLM mouse liver microsomes

MOI multiplicity of infection

MR mannose receptors

MRP multidrug resistance protein

MRSA methicillin-resistant *Staphylococcus aureus*

MW molecular weight

MXF moxifloxacin

NAD nicotinamide adenine dinucleotide

NADH nicotinamide adenine dinucleotide hydrogen

NO nitric oxide

PAMP pathogen-associated molecular pattern

PAMPA predicted artificial membrane permeability assay

PAR peak area ratio

PAS para aminosalicylic acid

PD pharmacodynamics

PET/CT positron emission tomography-computed tomography

PGL phenolic glycolipids

PI propidium iodide

PI3P phosphatidylinositol-3-phosphate

PK pharmacokinetic

PK/PD pharmacokinetic-pharmacodynamic

POA pyrazinoic acid

PRR pattern recognition patterns

PtpA protein tyrosine phosphatase

PZA pyrazinamide

RFB rifabutin

RFP rifapentine

RIF rifampicin

RLM rat liver microsomes

RNAP ribonucleic acid polymerase

RNI reactive nitrogen intermediates

ROI reactive oxygen intermediates

ROS reactive oxygen species

SAR structure activity relationship

SPM streptomycin

TAG triacylglyceride

TB tuberculosis

TB/HIV tuberculosis-human immunodeficiency virus

TB-IRIS TB immune reconstitution inflammatory syndrome

TDM therapeutic drug monitoring

TMM trehalose monomycolate

TNF-α tumor necrosis factor alpha

UN United Nations

WHO World Health Organization

XDR-TB extensively-drug resistant TB

CHAPTER 1

INTRODUCTION AND LITERATURE REVIEW

1.1 TB disease: A global health burden

Mortality rates due to *Mycobacterium tuberculosis* infections are currently higher than those of any single infectious agent (WHO 2019a). Tuberculosis (TB), the disease caused by *M. tuberculosis*, is estimated to have caused approximately 1.4 million deaths, while 10.0 million people were estimated to have developed the disease in 2018 (WHO 2019a). Factors including underfunding of research, resource and programmatic challenges in the prevention and treatment of TB, and the emergence of the human immunodeficiency virus (HIV) in recent decades, have caused a significant upsurge in mortality and morbidity due to TB. TB was declared a public health emergency by the World Health Organization (WHO) in 1993 (WHO 1994). In 2018, 8.6% of TB cases were of people living with HIV, of which approximately 251 000 died from this co-infection.

The success of antiretroviral therapy (ART) regimens has significantly reduced HIV-associated mortality rates, particularly in the African region where the disease was driving TB incidence at the height of the HIV pandemic. HIV, however, remains a leading risk factor for TB. Diabetes mellitus, which affects about 422 million globally, also increases the risk of TB disease, surpassing HIV in certain geographical areas (WHO 2019a; Al-Rifai et al. 2017). In addition, an estimated 1.7 billion individuals are latently infected with TB, potentially providing a reservoir of future disease (WHO 2019a; Houben and Dodd 2016).

Two-thirds of people who develop TB disease reside in only 8 countries, and 30 countries referred to as high burden countries (HBCs) contribute 87% of the global TB disease. The WHO South-East Asian region accounted for 44%, the African region 24%, and the Western Pacific region 18%, while the Americas, European and Eastern Mediterranean regions accounted for a combined 12.2% of estimated TB cases (Figure 1.1) (WHO 2019a). The majority of this distribution in TB prevalence could be explained by factors which increase the risk of acquiring TB, such as high HIV prevalence (most notably in the African region where 72% of TB patients are also HIV infected), development of drug-resistant forms of TB, presence of non-infectious comorbidities such as diabetes mellitus, poorly resourced and inadequate health systems, high economic burden, and overcrowding amongst other factors.

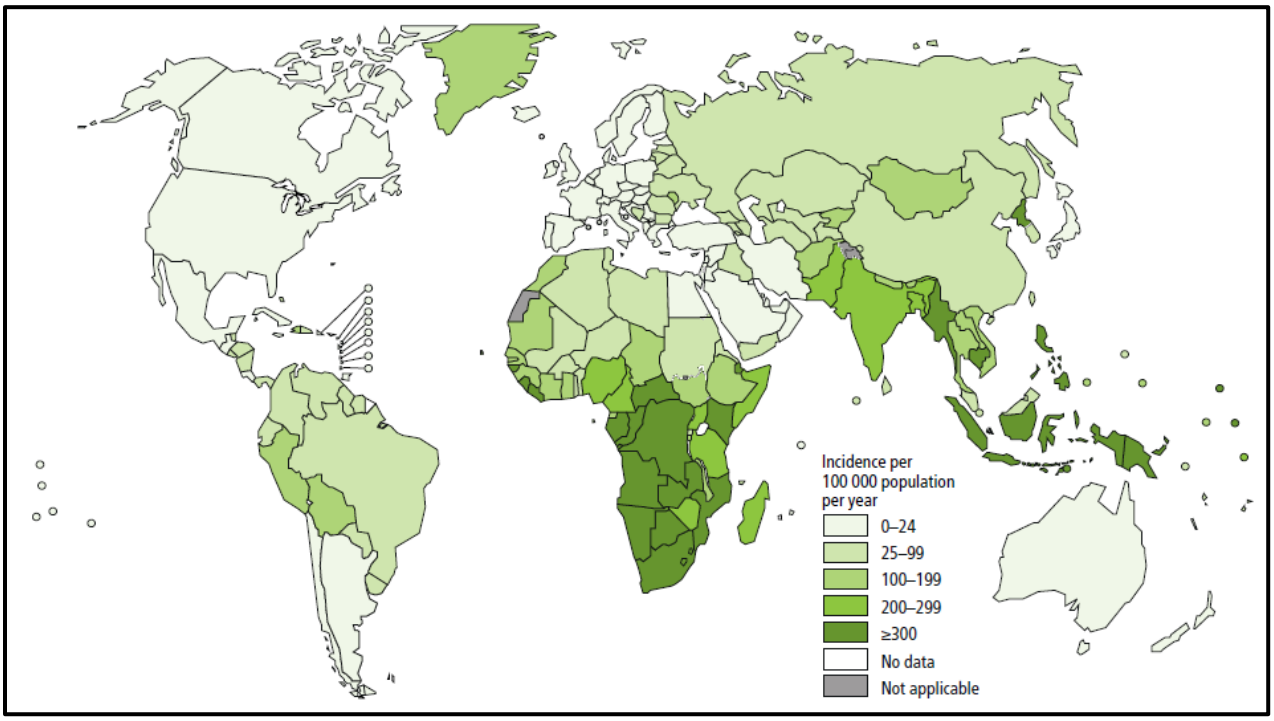

Figure 1.1. Global distribution of estimated new TB cases in 2018 **(WHO 2019a)**.

In the face of the TB epidemic, 2018 saw a high-level United Nations (UN) meeting in which countries and their governments re-committed to the Sustainable Development Goals and the WHO End TB Strategy to achieve defined milestones and targets by 2020 and 2030, respectively. Specific commitments were made to improve access to treatment for people with TB disease, provide preventive treatment for latent TB infection (LTBI), improve access to diagnosis and care, and commit more funding to research (WHO 2019a).

1.2 Limitations of current TB treatment and the search for new antimycobacterial agents

While many governments are complicit in the failure to deliver effective TB treatment as a result of insufficient resources and inadequate health systems, pre-clinical and clinical TB drug development programs are equally liable in not producing successful clinical candidates and, consequently, therapies (Dartois and Barry 2013). The last five decades were characterized by very slow progress in the discovery and development of new TB drugs (Mitchison and Davies 2012), with only three recent drugs, bedaquiline (BDQ), delamanid (DLM) and pretomanid (PA-824) approved since pyrazinamide (PZA) in the early 1980s (Ryan and Lo 2014; Mahajan 2013; Keam 2019) (https://www.tballiance.org/news/fda-approves-new-treatment-highly-drug-resistant-forms-tuberculosis, accessed 17th May, 2020).

1.2.1 Drug-susceptible TB therapy

The first effective anti-TB drugs were introduced in the late 1940s to early 1950s, following the discoveries of streptomycin (SPM), isoniazid (INH) and para-aminosalicylic acid (PAS) which were first tested in clinical trials as monotherapies (Mitchison and Davies 2012; Fox, Ellard, and

Mitchison 1999). The development of resistance to the early monotherapies, particularly SPM, led to extensive discovery efforts and clinical trials which saw the inception of combination regimens (Mitchison and Davies 2012). In the 1960s, the discoveries of rifampicin (RIF) and ethambutol (EMB), which were tested in a number of combinations in clinical trials, significantly improved cure rates when used together with INH (Fox, Ellard, and Mitchison 1999). However, it was over a decade later through the addition of a nicotinamide derivative, PZA, that treatment duration was reduced to six months. Thus, the standard TB drug regimen in use today was determined (Figure 1.2) (Mitchison and Davies 2012; Murray, Schraufnagel, and Hopewell 2015).

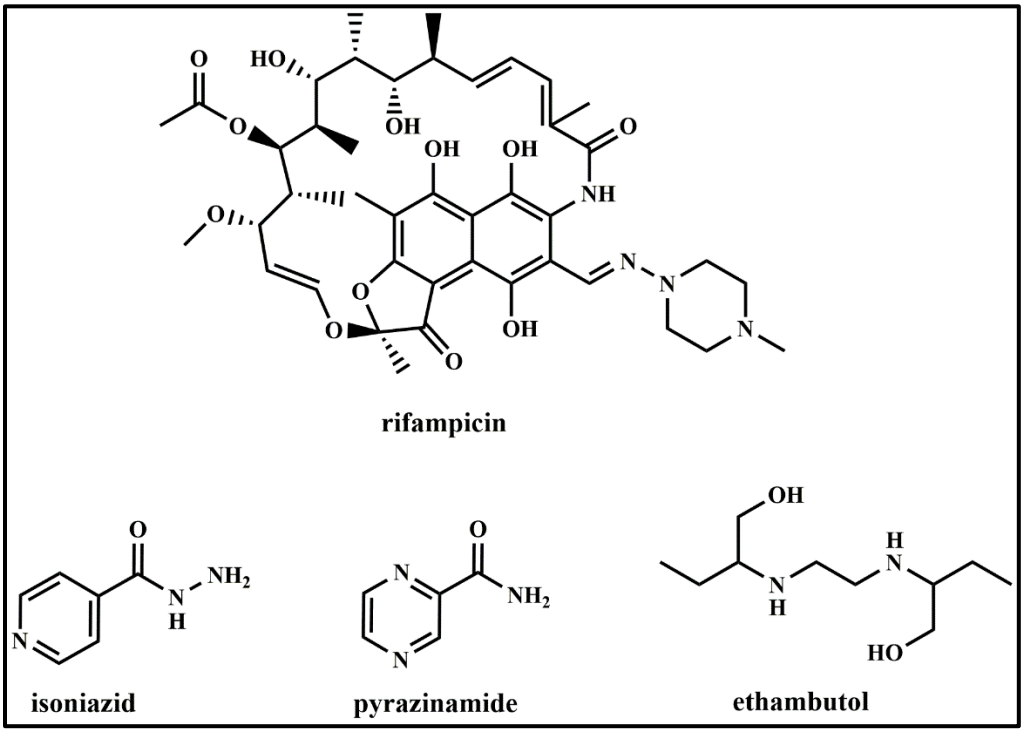

Figure 1.2. Current first-line drugs for drug-susceptible TB (DS-TB).

This regimen, born of necessity to combat the emergence of drug resistance while minimizing therapy duration, consists of these four drugs given in a 6 months course for drug susceptible TB

(DS-TB): INH, EMB, RIF and PZA (Figure 1.2) are taken in an initial 2-month "intensive" phase followed by a 4 months "continuation" phase comprising INH and RIF alone. This therapy is highly effective, with 85% cure rates in patients treated for DS-TB (WHO 2019a). However, despite implementation of this curative Directly Observed Therapy Short-course (DOTS), TB mortality statistics remain astonishingly high. A major limitation of this multidrug regimen is that it is too long: 6 months daily intake (in some cases going up to 9 months) of multiple drugs imposes an enormous pill burden on TB patients. Coupled with reported toxicity and related adverse side effects, the resulting poor patient adherence drives development of resistance to the standard drugs. In TB/HIV co-infected patients, the added pill burden of ART and possible drug-drug interactions drives further toxicity, poor treatment adherence and increases the risk of developing immune reconstitution inflammatory syndrome (TB-IRIS) (Michailidis et al. 2005; Koul et al. 2011). Consequent treatment failure, relapse and emergence of resistance impose further limitations on the first-line TB therapy, leading to even lengthier and more toxic treatments for drug-resistant TB (DR-TB).

1.2.2 Multi-drug and extensively-drug resistant TB treatment

In recent years, there has been renewed vigor in TB drug discovery and development efforts, and significant advances have been made with more drug candidates in the development pipeline now than ever (Figure 1.3) (www.newtbdrugs.org). The newly approved BDQ, DLM and PA-824; and repurposed drugs linezolid (LZD) and clofazimine (CFZ), all form part of multi-drug resistant TB (MDR-TB) and extensively-drug resistant TB (XDR-TB) treatment regimens ((WHO 2019b; Lee et al. 2012; Tang et al. 2015). MDR-TB is defined as the failure to respond to at least INH and RIF, the most important drugs in the first-line regimen for DS-TB; while XDR-TB is defined as

MDR-TB plus resistance to any fluoroquinolone and at least one of the second-line injectable drugs used in MDR-TB treatment (WHO 2019b).

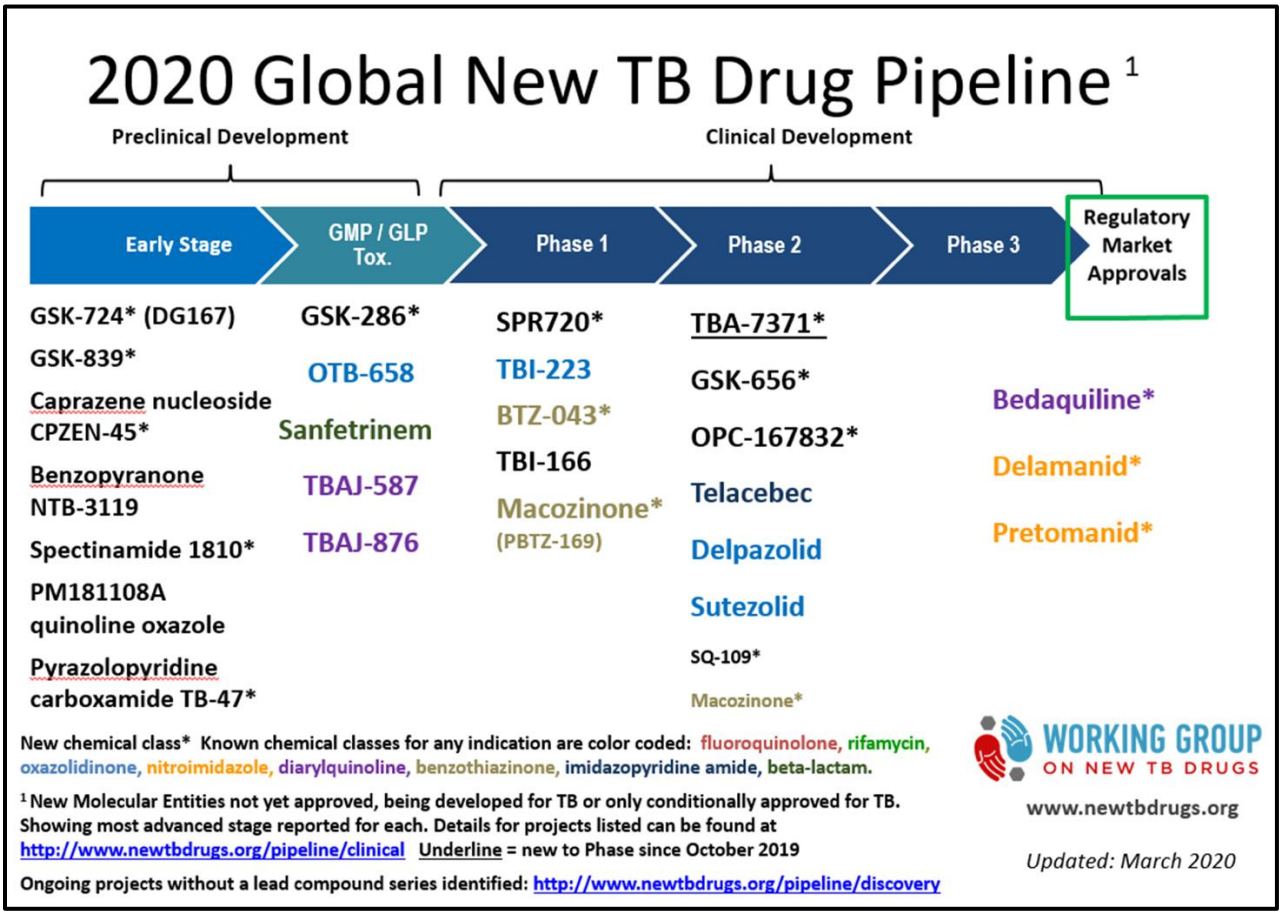

Figure 1.3. The current global TB drug pipeline (www.newtbdrugs.org; accessed on 26th April 2020).

The new WHO guidelines for treatment of DR-TB include 'shorter' and more standardized regimens (9-12 months) recommended for use in the absence of resistance to fluoroquinolones and second-line injectables and less than a month of previous usage of second-line drugs, if any (WHO 2019b). The longer regimens lasting 18 months or more may be standardized or individualized based on patient history, response to treatment and toxicity (WHO 2019b). Success rates for treatment of MDR-TB were as low as 56% with further reduction for XDR-TB to 39%, owing to

treatment failure and loss to follow-up (WHO 2019a). While it is worthy to note the potential contribution of the new and repurposed drugs to curb further development of resistance to existing DR-TB drugs, these regimens are even longer than DS-TB, less effective and some drugs such as LZD have severely toxic side effects (Lee et al. 2012).

1.2.3 Current paradigm in discovery and preclinical TB drug development

The failure of current anti-TB drugs to translate potent *in vitro* activity into *in vivo* clinical efficacy and shortened treatment duration raises questions about the strategies employed to develop and optimize clinical candidates (Dartois and Barry 2013). As more drugs populate the development pipeline (Evans and Mizrahi 2018), it raises a question of whether the *in vitro* screening assays and *in vitro*/*in vivo* models used in the early phases of discovery and development algorithms are sufficient to deliver drugs or combinations that will effectively predict and translate into clinical efficacy (Dartois and Barry 2013). The 'target product profile(s)' for a new TB drug or combination requires that it must: i) shorten treatment duration for both DS-TB and DR-TB; ii) be effective against MDR and/or XDR strains; iii) reduce the current pill burden on TB patients; iv) reduce the dosing frequency and; v) allow for co-administration with anti-HIV treatment and other chronic illness medications such as diabetes, with no drug-drug interactions (Koul et al. 2011).

The first-line anti-TB drugs were discovered and developed based on empirical methods, solely reliant on phenotypic measures of response in *in vitro* assays and/or *in vivo* animal models, and immediately followed by extensive clinical trials (Fox, Ellard, and Mitchison 1999). For example, PZA was discovered through screening in *M. tuberculosis*-infected mice without prior *in vitro* susceptibility testing (Mitchison and Davies 2012; Fox, Ellard, and Mitchison 1999). This strategy

however proved beneficial, as PZA demonstrated inactivity in neutral pH standard culture medium in a study by McDermott and Tompsett (1954), cited by (Chakraborty and Rhee 2015), and would probably not have been pursued further (Lamont, Dillon, and Baughn 2020). INH, another nicotinamide derivative, was discovered through murine testing after the parent compound had shown activity against *M. tuberculosis* in a guinea pig model (Chakraborty and Rhee 2015). Similarly, EMB came from screening of compounds in mice in a study by Thomas et al., (1961), cited by (Chakraborty and Rhee 2015). RIF, a semisynthetic natural product derivative was discovered through screening of culture extracts against *M. tuberculosis*, followed by isolation, derivatization and optimization of the active compound (Chakraborty and Rhee 2015). It was only after these drugs had been in clinical use for over a few decades that their molecular targets and mechanisms of action were identified, mainly through elucidating genetic and then molecular resistance mechanisms (Zhang et al. 1992; Telenti et al. 1993; Taniguchi et al. 1996; Sreevatsan et al. 1997; Scorpio and Zhang 1996). For PZA, however, the mechanism of action remains under investigation, with new evidence suggesting coenzyme A biosynthesis pathway as potential target (Sun et al. 2020; Gopal et al. 2020; Gopal, Nartey, et al. 2017; Lamont, Dillon, and Baughn 2020).

Such lengthy empirical approaches are not feasible to address the need for anti-TB drugs in modern society and to sustain the development pipeline. In addition, the use of murine and other animal models as a primary screening tool has been heavily debated. Consequently, in the last few decades, drug discovery platforms have shifted to develop better screening tools and preclinical models to predict clinical drug efficacy and improve the rates of new drug development (Dartois and Barry 2013). The annotation of *M. tuberculosis* genome sequence (Cole et al. 1998) led to a new era of TB drug discovery, supported by advancement of molecular genetic tools such as whole-genome transcriptomics, proteomics, comparative genomics and structural genomics

(Lechartier et al. 2014). The two main approaches (Figure 1.4) used in modern drug discovery – phenotypic or whole-cell (drug-to-target) screening and target-based (target-to-drug) screening (Cole 2016) – are described briefly below. In addition, although not routinely included, some TB drug discovery programs include intracellular screens utilizing infected host cells to mimic a disease-relevant environment.

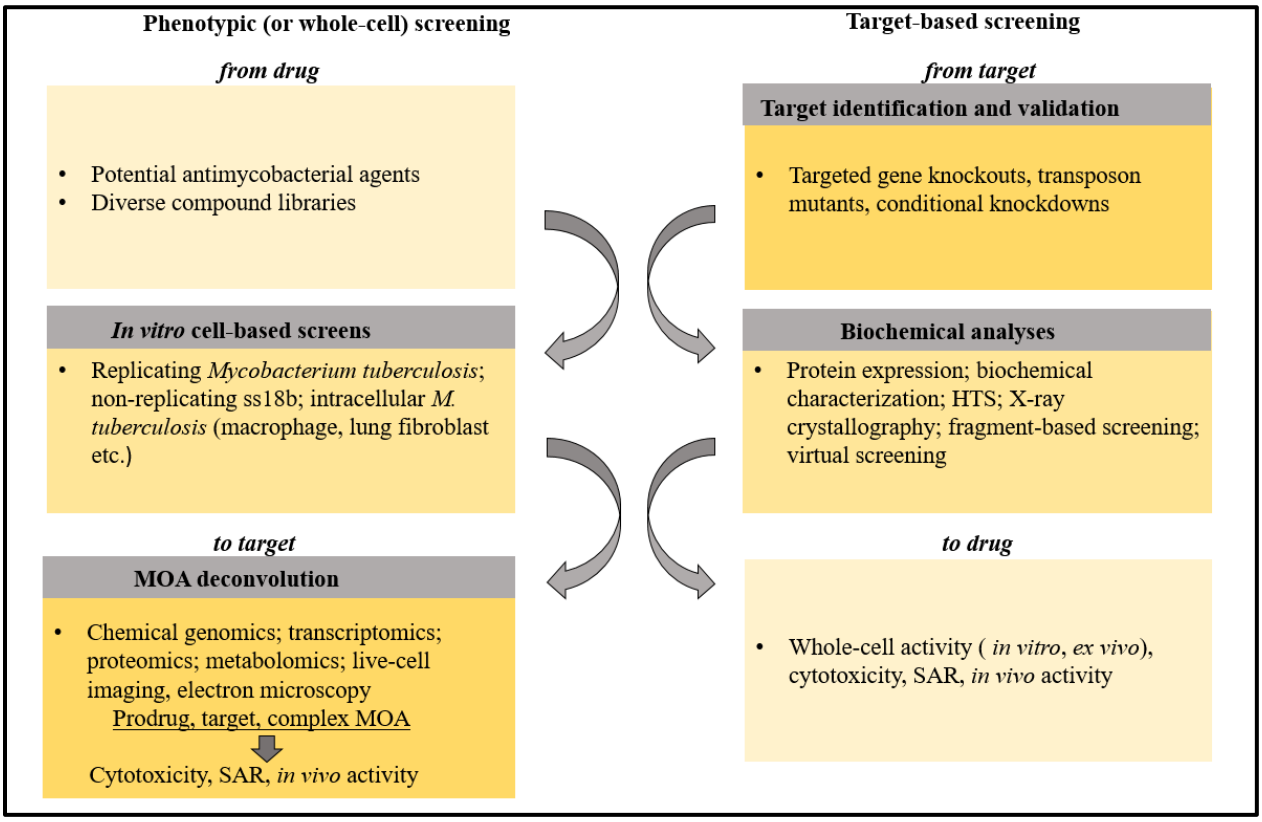

Figure 1.4. Main TB drug discovery strategies: phenotypic (drug-to-target) and target-based (target-to-drug) screening. Adapted from (Singh and Mizrahi 2017). MOA, mechanism of action; SAR, structure-activity-relationship; HTS, high-throughput screening.

i) Phenotypic screening

This approach involves screening of chemically diverse compound libraries or focused libraries derived from a specific pharmacophore for *in vitro* activity against *M. tuberculosis* or, in some cases, against surrogate mycobacteria including *M. smegmatis* and *M. bovis* BCG (Altaf et al. 2010), to determine minimum inhibitory/bactericidal concentrations (MIC/MBC) (Franzblau et al. 2012). The use of *M. smegmatis* or *M. bovis* BCG is particularly attractive for high-throughput screening (HTS) to circumvent the slow-growth of *M. tuberculosis* and its pathogenicity that requires handling in high safety laboratories. For example, BDQ was discovered through phenotypic HTS on *M. smegmatis* (Andries et al. 2005).

Thousands of compounds are evaluated through HTS and compounds with known activity against *M. tuberculosis* ('actives') are identified (Grzelak et al. 2019). This approach relies on phenotypic measures of mycobacterial growth inhibition in cellular assays that are designed to mimic physiological conditions and bacterial phenotypes encountered during host infection such as replicating, non-replicating and intracellular *M. tuberculosis* infection assays (Franzblau et al. 2012; Warrier et al. 2015; Tantry et al. 2015; Pethe et al. 2010; Grant et al. 2013). Subsequent target identification and validation, and *in vivo* efficacy studies, follow and can inform the pharmacological optimization steps taken to deliver compounds for clinical development.

This approach has been reasonably successful in preloading the TB drug pipeline with new and chemically diverse drugs and drug candidates (Figure 1.3) such as BDQ (diarylquinoline) (Koul et al. 2007; Andries et al. 2005), DLM and PA-824 (nitroimidazoles) (Stover et al. 2000; Matsumoto et al. 2006), Q203 (imidazopyridine

amide) (Pethe et al. 2013), SQ109 (diethylamine) (Protopopova et al. 2005) and the benzothiazinones (PBTZ-169 and BTZ-043) (Makarov et al. 2009). An important characteristic of phenotypic screening is that it yields compounds with demonstrated whole-cell activity; that is, the ability to penetrate the mycobacterial cell to reach its molecular target. However, despite the fact that many 'active' compounds belong to chemically diverse classes, whole-genome sequencing data from resistant mutants revealed common targets such as QcrB, MmpL3 and DprE1 (Figure 1.5). Interestingly, these 'promiscuous' targets are membrane-associated, suggesting a bias in whole-cell screening approaches that has been associated with compound hydrophobicity (Goldman 2013; Cole 2016). MmpL3, targeted by SQ109 amongst other compounds, is an essential outer membrane protein responsible for the transport of trehalose monomycolates (TMMs) required for mycolic acid biosynthesis (Tahlan et al. 2012). DprE1, a target of benzothiazinones (PBTZ-169 and BTZ-043), is an essential membrane-associated protein subunit of decaprenylphosphoryl-b-D-ribose epimerase which is involved in arabinogalactan and lipoarabinomannan synthesis (Makarov et al. 2009). Other membrane-associated targets to emerge from whole-cell screening are respiratory targets, AtpE and QcrB. AtpE, target of BDQ, is a component of the ATP synthase complex essential for ATP production (Koul et al. 2007; Haagsma et al. 2011). QcrB is a cytochrome *c* reductase component of the cytochrome *bc*1 complex in the mycobacterial electron transport chain (Pethe et al. 2013).

ii) Target-based screening

Our understanding of *M. tuberculosis* biology has considerably increased owing to the whole genome sequencing of this mycobacterium and the subsequent advancements in

post-genomic tools (Lechartier et al. 2014). This led to identification of essential genes required for *M. tuberculosis* growth and survival both *in vitro* and *in vivo* (Sassetti, Boyd, and Rubin 2003). A core principle informing drug discovery is that targets identified must be essential, selective and demonstrate vulnerability under conditions that recapitulate host environment (Singh and Mizrahi 2017; Cole 2016). Subsequent HTS of compound libraries or structure-guided drug design allows for identification of compounds that inhibit the biochemical function of the target of interest. Target selectivity means human hosts lack a particular target that is essential in *M. tuberculosis*, or the human homolog has significant structural difference to avoid drug toxicity (Singh and Mizrahi 2017). While some targets were validated as being essential *in vitro* by genetic means (Sassetti and Rubin 2003), they were found to be non-essential *in vivo* owing to genetic redundancy or the capacity of *M. tuberculosis* for metabolic scavenging (Singh et al. 2017; Park et al. 2017). This highlighted that target validation is an essential consideration to translate *in vitro* target-drug interactions into successful clinical outcome. In this regard, conditional knockdown (cKD) mutant strains generated through transcriptional silencing or clustered regularly inter-spaced short palindromic repeats interference (CRISPRi) have become critical genetic tools for validation of targets i*n vitro*, *ex vivo*, and *in vivo* (Evans and Mizrahi 2015; Singh and Mizrahi 2017).

While target-based drug discovery has the potential to identify potent inhibitors of novel targets due to its targeted, rational approach utilizing biochemical assays, three-dimensional structural information, and demonstrated biological function, it often fails to translate into whole-cell activity against *M. tuberculosis.* As a result, not much success has been realized with target-based approaches. It is often thought that poor cell penetration

owing to the complex and hydrophobic cell wall of tubercle bacilli, efflux mechanisms or *M. tuberculosis* metabolism renders the compound effectively inactive. Functional redundancy or the ability of the bacillus to scavenge metabolites from the host cell may explain the disconnect between IC_{50} and MIC (Cole 2016).

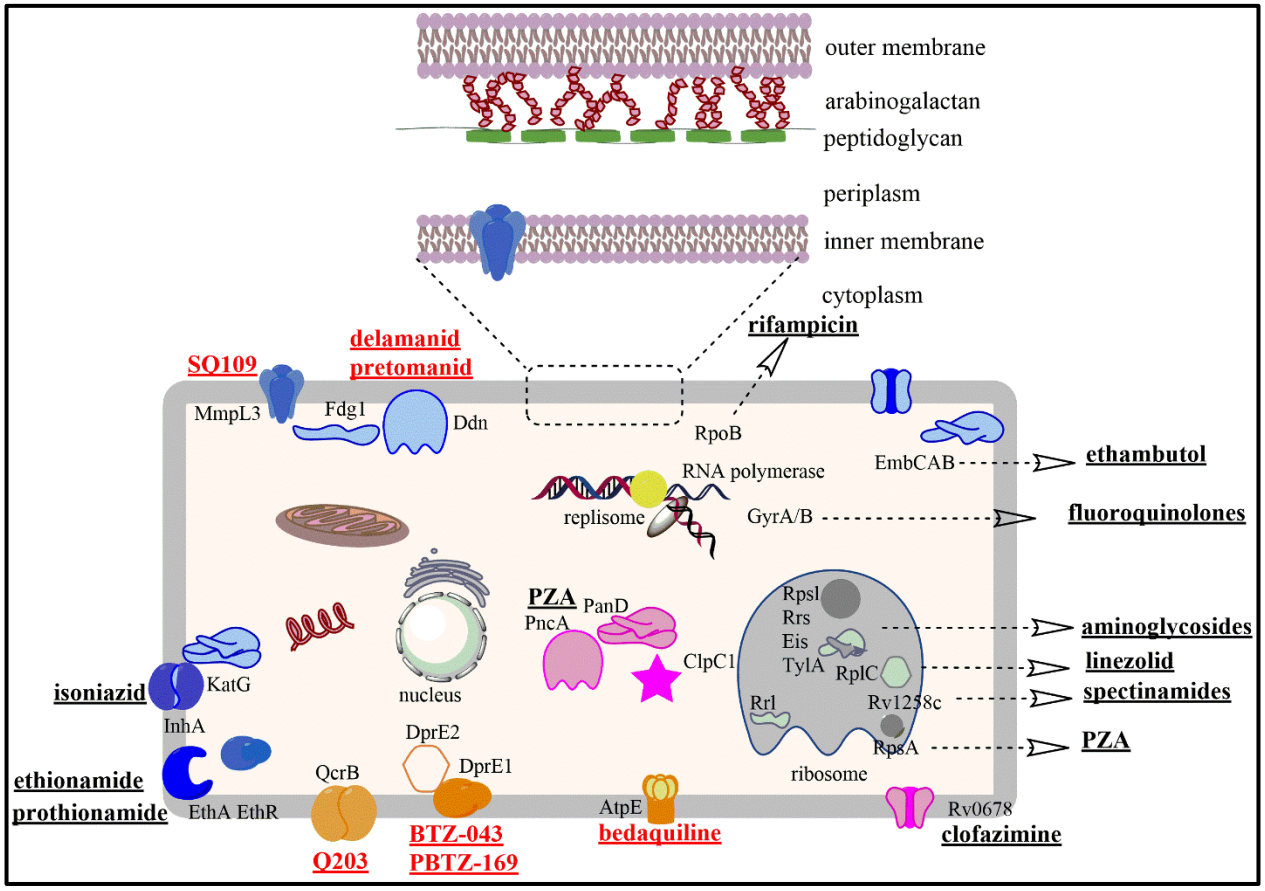

Figure 1.5. Newly approved TB drugs and leading clinical candidates discovered through phenotypic (whole-cell) screening (**red**) and known TB drugs (**black**). Target-based approaches have failed to deliver clinical candidates. Adapted from (Mabhula and Singh 2019)

A new approach combining these two strategies, target-based whole-cell screening (TB-WCS), first described in *M. tuberculosis* by Abrahams et al., (2012), is now the preferred strategy employed in drug discovery and preclinical development programs. TB-WCS utilizes conditional mutant strains with differential expression of a target gene to potentially sensitize the strain to inhibitors that act on or biochemically downstream of that target (Abrahams et al. 2012; Moreira et al. 2015; Soto et al. 2018). It identifies compounds that are biologically active against *M. tuberculosis* and act on a specific known target or pathway. More recently, Johnson et al., (2019) described an advanced TB-WCS approach, screening compound libraries against large pools of *M. tuberculosis* hypomorphs called PROSPECT (primary screening of strains to prioritize expanded chemistry and targets) identifying new scaffolds against known targets, and efflux pump EfpA as a new target (Johnson et al. 2019).

iii) Screening against *M. tuberculosis*-infected cells

Assays utilizing *M. tuberculosis*-infected macrophages for screening of new antimycobacterial compounds are not routinely done. However, some TB drug discovery programs have found advantages with this approach as it may yield compounds with host cell and *M. tuberculosis* penetration properties, while also providing cytotoxicity information early in the discovery phase (Cole 2016). Perhaps the most advantageous aspect of intracellular screening is the utility of high-content imaging using confocal fluorescence microscopy to directly identify compounds with activity against replicating *M. tuberculosis*. Some compounds with potent intracellular antimycobacterial efficacy

have been identified utilizing such screens (Christophe et al. 2009; Christophe et al. 2010), including the QcrB inhibitors that led to the drug candidate Q203 (Pethe et al. 2013).

iv) Limitations in current *in vitro/in vivo* lead optimization strategies

MIC or MBC values are often used as the criterion to progress compounds for optimization of *in vitro* absorption, distribution, metabolism and excretion (ADME) parameters, which subsequently inform *in vivo* pharmacokinetic-pharmacodynamic (PK/PD) proof of concept studies in animal models (Dartois and Barry 2013). *In vitro*/*in vivo* PK parameters indicate how much of the drug becomes available in the host circulation and organ tissues while PD parameters provide a correlation between drug concentration and therapeutic effect observed (Nielsen and Friberg 2013). PK/PD parameters in modern drug discovery have been used as a critical measure for drug-dosing strategies, clinical efficacy and drug combinations (Dartois 2014). However, PK/PD tools post-dated the development of the current standard TB regimen, meaning its design was based on inadequate understanding of exposure–response relationships (Dartois 2014). Furthermore, incorporation of PK/PD modeling in subsequent clinical investigations has mostly relied on plasma-based PK/PD parameters.

Standard PK/PD indices, *f*AUC/MIC, *f*C_{max}/MIC and $T_{>MIC}$, are generated based on a summary measure of drug exposure in relation to MIC of the specific infecting *M. tuberculosis* strain and used as predictors of efficacy (Nielsen and Friberg 2013). AUC is defined as area under the concentration-time curve; C_{max} is the maximum drug concentration reached; $T_{>MIC}$ is the cumulative percentage of a 24-hour period that the

concentration is above MIC, and *f* refers to unbound, free drug fraction (Nielsen and Friberg 2013). Concerning the design of dosing strategies and shortening of TB treatment duration, pharmacological studies have focused on investigating adjustment and optimization of dosages of current TB drugs to determine if increasing plasma PK exposure could have an effect on reducing treatment duration (Davies and Nuermberger 2008).

For example, it has been shown that increasing the dosage of RIF to 600 mg favorably increases AUC and AUC/MIC ratios, and that there is a linear increase in bactericidal activity up to a dose of 1200 mg (Diacon et al. 2007). However, recent phase 2 studies present conflicting results regarding reduction in culture conversion time in smear-positive TB patients given high-dose RIF combination therapies (Peloquin et al. 2017; Boeree et al. 2015; Aarnoutse et al. 2017). On the other hand, utilizing the *ex vivo* hollow fibre model, Gumbo and colleagues established a correlation in efficacy between first-line anti-TB drugs and their PK/PD responses, successfully predicting the failure of moxifloxacin (MXF) to shorten treatment in trials (Pasipanodya, Srivastava, and Gumbo 2012; Pasipanodya et al. 2013; Pasipanodya et al. 2015; Gumbo et al. 2015; Gumbo et al. 2004). These studies, amongst others, raise questions about how predictive plasma-based PK/PD data are of clinical efficacy, and whether the *in vitro/vivo* models used are sufficient to predict clinical outcome.

1.3 A new paradigm for preclinical development

Our understanding of the complex biology of *M. tuberculosis* has improved in the last two decades, accompanied by superior screening methods and technological advances which have contributed

to more drugs and new targets under investigation in the development pipeline. However, given the length of treatment, which is reflective of the inability to sterilize *M. tuberculosis* during host infection, questions arise about the effectiveness of the *in vitro*/*in vivo* models to predict clinical efficacy. Furthermore, none of the therapies tested in recent years has shortened treatment duration. Lead candidates with potent *in vitro* activity often fail to translate into *in vivo* clinical efficacy.

In efforts to address this gap, Dartois and Barry highlighted that "anti-tuberculosis drugs do not exert their effect in the plasma, where their levels are traditionally measured, but in defined target tissues and lesions where they must be distributed" (Dartois and Barry 2010). The authors noted that clinical data pertaining to drug penetration in pulmonary and other TB lesions were limited, citing a few studies over 30 years ago by Kislitsyna (1980, 1985) and by Canetti (1965) that were limited to RIF and INH (Dartois and Barry 2010). The authors proposed that rational medicinal chemistry approaches that utilize *in vitro/in vivo* lead optimization assays and models which consider the complex disease pathology, the physiology of the infecting bacilli and drug chemical properties, were needed in order to translate *in vitro* compound potency to *in vivo* efficacy (Dartois and Barry 2013; Tanner et al. 2018). In the last decade, studies utilizing positron emission tomography and computed tomography (PET/CT) imaging techniques on non-human primates and human lungs revealed the dynamic nature of TB pathology, with lesion heterogeneity reported between and within individuals (Barry et al. 2009; Lenaerts, Barry, and Dartois 2015; Via et al. 2013). This further highlighted that a simple linear strategy that excludes TB disease pathology considerations would be insufficient to predict clinical efficacy and suggested that a shift in our current thinking around strategies and criteria used in lead optimization was required (Dartois and Barry 2013).

In pioneering work utilizing a rabbit model of TB infection that recapitulates human infection, Dartois and colleagues demonstrated that INH, RIF, PZA and MXF had variable lung tissue and lesion penetration properties, and that lesion concentrations were poorly correlated with those observed in plasma (Kjellsson et al. 2012). Although the authors acknowledged that rabbit lesions were much less differentiated than human lesions, this work prompted investigations into lesion-centered PK/PD analyses in efforts to understand clinical outcomes. A seminal review by Dartois (2014), highlighted the need to interrogate host distribution of anti-TB drugs from circulation to their *M. tuberculosis* molecular targets, with rational lead optimization strategies that include PK/PD parameters at the site of disease (Figure 1.6) (Dartois 2014). Owing to complex and highly heterogeneous TB disease pathology (Lenaerts, Barry, and Dartois 2015), antimycobacterial agents must first distribute into the lung tissue, penetrate into lesions and lesion microenvironments, including the multiple cell types, to reach the intracellular bacilli. At cellular level, penetration into the infected cell and through the *M. tuberculosis* cell wall is required to reach the molecular target. Thus strongly suggests that extrapolation of plasma-based PK/PD indices maybe insufficient to inform lesion-specific drug distribution (Dartois 2014).

Importantly, the Dartois review emphasized that understanding physicochemical and pharmacological parameters which drive drug distribution from plasma and accumulation into dynamic TB lung lesions, in both architecture and *M. tuberculosis* subpopulations present, could enable effective dosing strategies and design of complementary regimens.

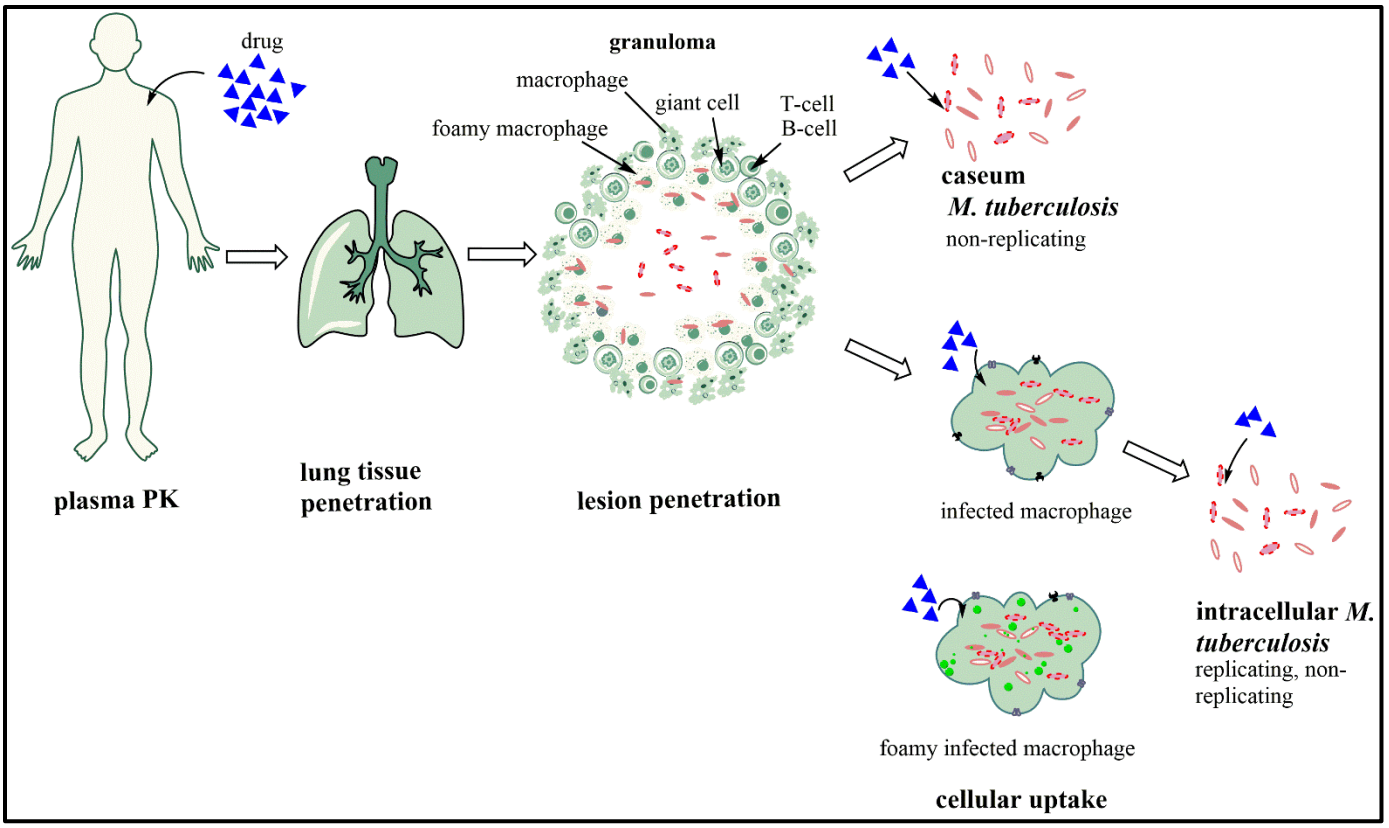

Figure 1.6. The complex path of antimycobacterial drugs to reach the bacilli in TB infected persons. When a TB drug is administered, usually orally, it must be absorbed in the gut and into circulation where it will subsequently have to penetrate the lung tissue. In the lung, the drug must penetrate various lesions and lesion compartments. An avascular environment limits diffusion into the caseum, where persister (non-replicating) extracellular bacilli exist. In the cellular compartment, different macrophage phenotypes and bacilli subpopulations exist, which the drug must penetrate to reach the molecular target at effective concentrations. Adapted from (Dartois 2014).

1.3.1 Diversity in TB pathology: The relationship between the bacillus and the host

1.3.1.1 *M. tuberculosis* pathogenicity

M. tuberculosis is an airborne pathogen that is spread through inhalation of aerosolized bacilli. It is mainly a pulmonary infection although cases of extra-pulmonary disease can occur following dissemination of the bacilli from the lungs into other tissues such as the lymph nodes, bone and meninges (O'Garra et al. 2013). Our current understanding of early events in *M. tuberculosis* infection stems from extensive *in vitro* and *in vivo* animal model studies which support observed human pathology. Following inhalation of *M. tuberculosis* bacilli, alveolar macrophages in the alveolar space phagocytose the bacilli, and are trafficked to the lung interstitium where a cascade of immunological events is triggered (Flynn, Chan, and Lin 2011). During the innate immune phase, *M. tuberculosis* establishes infection in various phagocytic immune cells including macrophages, dendritic cells, monocytes, eosinophils and neutrophils (Wolf et al. 2007; Ernst 2012; Cadena, Flynn, and Fortune 2016). These innate immune responses, while essential in establishing an environment that allows for initiation of an adaptive response, may not be protective as bacterial burden in the initial granuloma is relatively high, with very minimal *M. tuberculosis* killing (Lin et al. 2014)). It is thought that the pathogen selectively recruits and invades permissive macrophages as a means to evade host mechanisms (Cambier et al. 2014), and uses infected macrophages for expansion (Davis and Ramakrishnan 2009).

Considerable evidence indicates that *M. tuberculosis* employs different mechanisms to manipulate the early stages of infection, for example, mycobacterial cell wall lipids (pthiocerol-containing lipids) mask the pathogen-associated molecular patterns (PAMPs) (Cambier et al. 2014). Another surface lipid, phenolic glycolipid (PGL), is thought to induce the macrophage chemokine CCL2 to recruit growth-permissive macrophages

(Cambier et al. 2014). More recently, alveolar macrophages were determined to display a fatty acid metabolic signature and were more permissive for *M. tuberculosis* growth while the ontologically different and glycolytic interstitial macrophages restricted growth (Huang et al. 2018). Furthermore, neutrophils were found to be the predominantly infected cell type in TB patients (Eum et al. 2010), and have been implicated in both disease control and progression (Yang et al. 2012; Lowe et al. 2012; Dallenga and Schaible 2016). A recent study described a less characterized granulocyte subset favourable for *M. tuberculosis* growth (Lovewell et al. 2020). These data suggest heterogeneity in host cells recruited during antimycobacterial infection, which may influence the outcome of early granuloma. When the adaptive immune response is triggered, the recruitment of various adaptive immune cells to control and/or eliminate *M. tuberculosis* infection, subsequently leads to the maturation of the early granuloma (Urdahl, Shafiani, and Ernst 2011; Flynn, Chan, and Lin 2011).

The granuloma is the hallmark pathologic feature of *M. tuberculosis* infection, where it is thought a counter-balance exists between host immunological responses, particularly macrophages which attempt to kill *M. tuberculosis* and prevent dissemination of infection, and the bacilli which attempt to subvert host mechanisms and replicate within infected cells (Orme and Basaraba 2014). Earliest descriptions of *M. tuberculosis* pathology in histopathological autopsy examinations by Canetti (1955) (cited by Cambier et al., (2014)) support our current understanding of granuloma events (Cambier et al. 2014). The early granuloma is a cellular structure which comprises an aggregate of macrophages, dendritic cells (DCs), T cells, B cells, and other immune cells localized at the site of infection.

However, granulomas differentiate and mature independent of each other, in response to their localized immune response (Marakalala et al. 2016).

Within an individual host, some granulomas control infection and limit *M. tuberculosis* growth while, in active disease, lack of infection control leads to formation of the classical caseous granuloma (Figure 1.6) (Flynn, Chan, and Lin 2011; Lin et al. 2014). The general architecture of a caseous granuloma consists of a central acellular necrotic core with a 'cheese-like' appearance called the caseum, surrounded by a peripheral fibrotic ring and an outer cellular layer of various immune cells. Even though a caseous granuloma can resolve through a process of calcification, which represents a successful immune response, caseum necrosis can lead to cavitation and subsequent release of *M. tuberculosis* into the airways and therefore disease transmission (Flynn, Chan, and Lin 2011).

1.3.1.2 Host cell-*M. tuberculosis* interactions

Macrophages, the primary host cells infected by *M. tuberculosis*, are designed to effect a vast antimicrobial mechanism against the invading pathogen to resolve the infection. How *M. tuberculosis* bacilli escape these mechanisms and manage to grow in such a hostile intracellular environment remains an area of focus. Numerous key macrophage-mycobacterium interactions drive *M. tuberculosis* escape from host immune responses, and explain the physiological and metabolic changes that enable its resistance to anti-TB drugs. A few key measures and counter-measures between host and *M. tuberculosis* and their effect on infection outcome are briefly described below:

i) M. tuberculosis manipulates macrophage entry and phagosome maturation

Phagocytosis delivers *M. tuberculosis* bacilli to the intracellular vesicle, the phagosome, that must undergo a maturation process through lysosome fusion to form the antimicrobial phagolysosome (Armstrong and Hart 1971). Phagolysosomes are characterized by an acidic pH, restricted nutrients required by *M. tuberculosis* for growth such as iron, increased toxic metals such as Zn, and lysosomal hydrolase enzymes that can degrade *M. tuberculosis*. Initial interactions between *M. tuberculosis* and host phagocytic cells occurs through mycobacterial pathogen-associated molecular patterns (PAMPs) and host pattern recognition receptors (PRRs) which initiate bacterial phagocytosis (Philips and Ernst 2012).

A study by Cambier et al., (2014) showed that *M. tuberculosis* manipulates macrophage uptake through PRRs by recruiting and infecting only permissive cells at the site of infection in order to increase its chance of survival (Cambier et al. 2014). *M. tuberculosis* mannose-caped lipoarabinomannan (LAM) was reported to bind mannose receptors (MR) on the macrophage surface and MR was implicated in blocking phagosome maturation through a phosphatidylinositol-3-phosphatase (PI3P)-mediated mechanism (Rajaram et al. 2017; Fratti et al. 2003). *M. tuberculosis* was also reported to disrupt RAB protein function (Rab5 – early endocytic events and Rab7 – for late endocytic events) to dysregulate phagosome-lysosome membrane fusion events and therefore prevent phagosome maturation.

Additionally, the H+ V-ATPase vesicular proton pump responsible for acidification of the phagosome was reported to be inhibited by *M. tuberculosis* through the secreted protein tyrosine phosphatase (PtpA) (Wong et al. 2011; Sun-Wada et al. 2009), while a second *M. tuberculosis*-induced mechanism was reported to selectively target the

subunit A of H+ V-ATPase for ubiquitination and degradation (Queval et al. 2017). Another study using *M. marinum*, a close genetic relative of *M. tuberculosis*, showed that some bacteria replicate in the phagolysosome compartment indicating acid tolerance (Levitte et al. 2016). NADPH oxidase, responsible for generation of reactive oxygen species (ROS) is another host protein complex targeted by *M. tuberculosis*, which expresses ROS detoxifying enzymes.

ii) M. tuberculosis invades the host cytosol

The seminal work by Armstrong and Hart (1971) allowed for visualization of phagosome-resident *M. tuberculosis* and BCG (the attenuated *M. bovis* vaccine strain) in phagosomes with blocked lysosome fusion. Later studies demonstrated the ability of *M. tuberculosis* (but not BCG) to access the host cytosol, implicating a role for ESX-1 (a type VII secretion system deleted in BCG) in *M. tuberculosis* escape from the phagosome (van der Wel et al. 2007; Simeone et al. 2012). Furthermore, recent work reported that the mycobacterial lipid, pthiocerol dimycocerosate (PDIM), along with EsxA induced phagosomal damage (Augenstreich et al. 2017). The ultimate outcome of phagosome perforation is bacterial access to the cytosol and determines bacterial and host cell fate.

The presence of *M. tuberculosis* in the cytosol triggers the inflammasome and autophagy, a homeostatic process that removes defective organelles, protein aggregates and invading bacteria through autophagosomes (Wong and Jacobs 2011). *M. tuberculosis* impairs and evades autophagic responses; moreover, while the

inflammasome provides protection against *M. tuberculosis*, it may not be sufficient to halt *M. tuberculosis* replication, and may even cause damage (Wong and Jacobs 2011; Romagnoli et al. 2012; Ouimet et al. 2016).

iii) M. tuberculosis 'hijacks' host cell death mechanisms for its proliferation

Infected cell death occurs via two mechanisms, apoptosis, also referred to as programmed cell death, and necrosis. It has been reported that apoptotic death favours host protection mechanisms minimizing inflammation and eliminating dead, intact infected cells through internalization by uninfected macrophages in a process called efferocytosis (Martin et al. 2012; Behar, Divangahi, and Remold 2010). It has also been argued that *M. tuberculosis* induces apoptotic death and uses phagocytosis of apoptotic-mediated dead infected macrophages for expansion (Davis and Ramakrishnan 2009). Necrosis, however, is thought to favour *M. tuberculosis* proliferation. *M. tuberculosis* has been reported to induce necrosis by breaking down inner mitochondrial membranes (Duan et al. 2002; Chen, Gan, and Remold 2006) and utilizing ESX-1 mediated depletion of NAD (Sun et al. 2015). Necrotic macrophages lyse and release *M. tuberculosis* into the extracellular milieu, where the bacillus subsequently infects additional host macrophages in a repeated cycle of infections. Mahamed et al., (2017) recently suggested that *M. tuberculosis* replicates to form huge bacillary aggregates in necrosis-induced dead cells and that ingestion of these dead cells by macrophages leads to a higher probability of cell death, initiating a chain of positive feedback events (Mahamed et al. 2017). Necrotic death is coupled with tissue destruction and

subsequent collapse of local capillaries leading to formation of the granuloma caseum, and eventually cavitation within granuloma foci and transmission.

1.3.2 TB disease heterogeneity: implications for TB treatment

During infection, different microenvironments exist within the lung owing to the unique architecture of TB lesions in which *M. tuberculosis* must survive. As discussed above, the infected macrophage represents a key cellular microenvironment where bacteria replicate and drives processes for its dissemination, although non-replicating bacteria have also been reported (Levitte et al. 2016). The necrotic caseum, on the other hand, lacks vasculature and subjects extracellular bacilli to oxygen and nutrient deficient conditions. To ensure survival in such a hostile environment, caseum *M. tuberculosis* assumes a non-replicating state in which bacilli become phenotypically resistant to both host and antibiotic stress (Connolly, Edelstein, and Ramakrishnan 2007). *M. tuberculosis* effects metabolic and physiological adaptations selectively in these specific niches and, critically, these adaptations are thought to subvert drug efficacy and result in a prolonged treatment duration (Lenaerts, Barry, and Dartois 2015; Connolly, Edelstein, and Ramakrishnan 2007).

To achieve efficacy at the site of infection, physicochemical and pharmacological properties of TB drugs should be considered to ensure a rational design and development of TB drugs with properties to drive their distribution to the specific microenvironment where they must accumulate at effective concentrations, and for sufficient duration, to target the diverse *M. tuberculosis* subpopulations (Dartois 2014). In addition, investigating these lesion-specific PK/PD properties

could provide insight into why drugs fail to shorten treatment duration in clinical investigation and help guide dosing strategies and drug combinations to avoid further fueling drug resistance (Dartois 2014).

Recent work by Dartois and others has focused on investigating distribution of current TB drugs into lesion microenvironments to test this hypothesis. Utilizing advanced matrix-assisted laser desorption ionization-mass spectrometry imaging (MALDI-MSI) techniques, one of the earlier studies provided evidence correlating anti-TB drug lesion distribution in lesions with sterilizing activity (Prideaux et al. 2015). Subsequently, there has been growing evidence that correlates drug lesion penetration with efficacies observed from current clinical drug use. The relationship between physicochemical properties of known TB drugs, their lesion penetrating properties and potential implications in clinical outcome are discussed below.

1.3.2.1 Molecular mechanisms, physicochemical and lesion penetration properties of first-line TB drugs

Rifampicin:

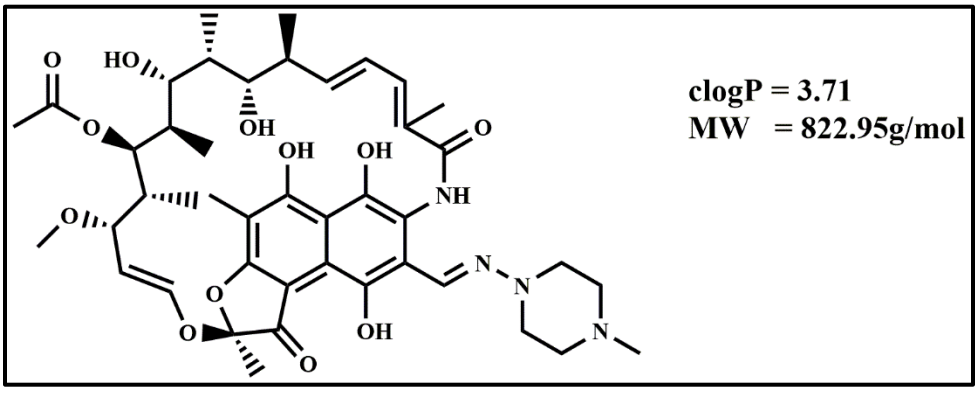

Figure 1.7. Rifampicin.

RIF (Figure 1.7), a semisynthetic rifamycin, is a key sterilizing drug in the first-line regimen. It is bactericidal against *M. tuberculosis* and targets RNA transcription through inhibition of the *rpoB*-encoded β subunit of DNA-dependent RNA polymerase (RNAP), resulting in cell death (Telenti et al. 1993; Taniguchi et al. 1996).

Following oral administration, maximum RIF plasma concentrations are reached within approximately 4 hours (h) (T_{max}), and an elimination half-life, ($t_{1/2}$), of between 1.8-6.1 h has been reported (Peloquin et al. 2017; Boeree et al. 2015; Aarnoutse et al. 2017). RIF undergoes extensive metabolism to from 25-desacetyl-RIF, which retains much of its activity (Nakajima et al. 2011). Due to lack of PK/PD considerations in the 1960s, distribution of TB drugs including RIF from plasma to lungs and lung lesions was poorly understood (Dartois, 2014). A few earlier RIF lesion penetration studies by Kislitsyna., (1980, 1985) and by Canetti., (1965); cited by (Dartois and Barry 2010) seemed to indicate variability in RIF distribution between plasma, lung tissue and lesions, likely indicating limitations in the methods used to collect the data. However, some of the studies are in agreement with recently reported RIF plasma concentrations being greater than in lung tissue and lesions in a rabbit PK model (Kjellsson et al. 2012). Furthermore, this study also reported higher RIF levels in uninvolved lung tissue than in lesions, results which seem to suggest RIF may distribute poorly into lesion microenvironments. This would contradict the well-established role of RIF as a sterilizing drug in the regimen, reducing treatment duration in clinical studies over 50 years ago (Fox, Ellard, and Mitchison 1999; Mitchison and Davies 2012).

However, recent spatial distribution data using MALDI-MSI showed a steady-state accumulation of RIF in lesion caseum compartment, providing a strong correlating with its ability to sterilize infection (Prideaux et al. 2015). The slow but sustained accumulation in the necrotic core of the caseum where anaerobic, extracellular persister *M. tuberculosis* populations reside suggested that

sufficient RIF concentrations are reached in caseum to sterilize infection (Prideaux et al. 2015). Previously, the sterilizing effect of RIF had been attributed to its mechanism of action as a RNAP inhibitor and the metabolic phenotype of *M. tuberculosis* subpopulations present in lesion compartments (Mitchison and Coates 2004; Mitchison 1985). The authors suggested that RIF's known *in vitro* activity against both replicating aerobic and slowly- or non-replicating anaerobic bacilli translates to susceptibility of these subpopulations *in vivo* (Mitchison and Coates 2004; Mitchison 1985).

While caseum bacilli exhibit reduced susceptibility to treatment, RIF and other rifamycins achieved lower caseum MBC_{90} (i.e., the minimum concentration required to kill 90% of the bacterial population in the caseum), and sterilized the bacilli in an *ex vivo* caseum model (Sarathy et al. 2018) and in the *in vitro* 'Wayne and Loebel' assay (Lakshminarayana et al. 2015). These data suggest that RIF reaches the persister population at the necrotic core at sufficient concentrations to achieve its sterilizing activity. In addition, RIF's moderate lipophilicity (clogP 3.71) is thought to promote sufficient caseum binding to sustain adequate concentrations. The distribution of RIF into both the cellular and caseum environments therefore suggests it is well positioned to exert its bactericidal effect on both replicating and slowly- or non-replicating persister populations in the caseum.

Isoniazid:

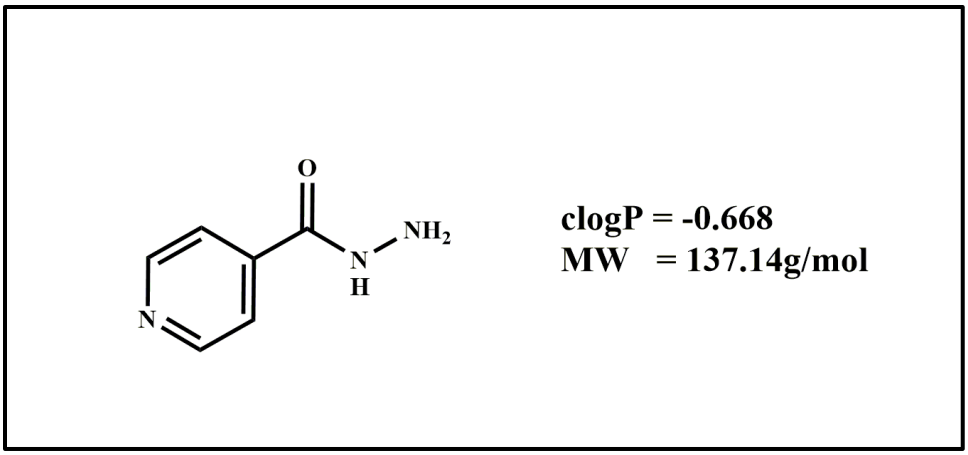

Figure 1.8. Isoniazid.

INH (isonicotinyl hydrazine) (Figure 1.8) is a prodrug that targets the synthesis of mycolic acids, a key structural component of *M. tuberculosis* cell wall. It requires bioactivation by the KatG catalase-peroxidase enzyme to form INH-nicotinamide adenosine dinucleotide (INH-NAD) adducts which inhibit a NADH dependent enoyl-ACP-reductase (a FASII – fatty acid synthase - enzyme), an enzyme directly involved in mycolic acid biosynthesis (Zhang et al. 1992; Rozwarski et al. 1999; Lei, Wei, and Tu 2000; Vilcheze et al. 2000).

Metabolically quiescent, slowly- or non-replicating bacteria show tolerance to INH in both *in vitro* 'Wayne and Loebel' assays (Lakshminarayana et al. 2015) and in the *ex vivo* caseum assay (Sarathy et al. 2018). Thus, INH's contribution in the TB first-line regimen has always been regarded as its bactericidal activity against replicating bacilli (Mitchison and Coates 2004; Mitchison 1985), as they are actively utilizing mycolic acid biosynthesis machinery. Following a 300mg oral administration, INH reaches C_{max} in approximately 2.5-3.0 h (Aarnoutse et al. 2017). It has a median half-life of about 1.0 to 4.0 h depending on whether patients are rapid or slow acetylators (Verbeeck et al. 2016; Aarnoutse et al. 2017). While INH undergoes metabolism in the liver to form several metabolites, N-acetylation is the major metabolic process. Similarly to RIF,

INH plasma and lung tissue distribution data have been inconsistent (Dartois and Barry 2010). Spatial imaging data using the INH metabolite, acetyl-INH, as a surrogate showed homogenous accumulation in both the cellular and caseum compartments; however, while most lesions achieved above MIC concentrations, the minimum anaerobic cidal concentration (MAC) of INH was never reached (Prideaux et al. 2015). INH is a small molecule (MW, 137.1 g/mol) with low lipophilicity (clogP, -0.67) suggesting its homogeneous distribution in cellular and caseum microenvironments is likely explained by passive diffusion. Despite favorable caseum distribution, the inherent inactivity of INH against non-replicating bacilli suggests it will not exert activity against caseum resident bacilli.

Pyrazinamide:

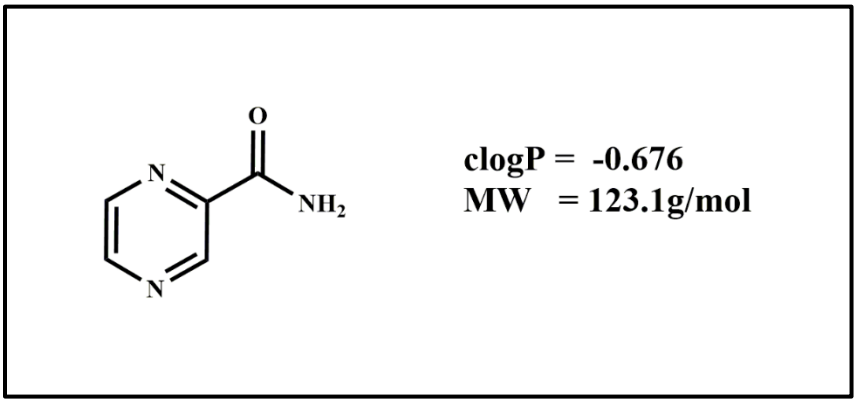

Figure 1.9. Pyrazinamide.

PZA is also a low molecular weight prodrug (123.1g/mol) with low lipophilicity (clogP, -0.676), structurally similar to INH (Figure 1.9). PZA requires bioactivation, mediated by the *pncA*-encoded pyrazinamidase enzyme, to release pyrazinoic acid (POA) (Zhang and Mitchison 2003; Scorpio and Zhang 1996; Lemaitre et al. 2001). Its exact mechanism of action however remains unclear (Lamont, Dillon, and Baughn 2020). Membrane energetics (Zhang et al. 2003), trans-

translation (Shi et al. 2011) and, the pantothenate and coenzyme A biosynthesis pathway (Shi et al. 2014; Gopal, Nartey, et al. 2017) have been implicated as targerts of PZA activity. The latter has been supported through the identification of PanD (aspartate α-decarboxylase) as the primary target of PZA, by showing that POA competitively inhibits the active site of PanD (Sun et al. 2020). Further evidence indicates that POA binding induces degradation of PanD, mediated by the caseinolytic protease ClpC1-ClpP (Gopal et al. 2020; Gopal et al. 2019). Mutations in the *clpC1*, encoding the unfoldase component of the ClpC1–ClpP, are known to indirectly cause PZA resistance (Gopal, Tasneen, et al. 2017; Yee, Gopal, and Dick 2017).

The unique sterilizing activity of PZA, which reduced treatment duration by 3 months, was attributed to its acidic pH-dependent activity *in vitro* (Mitchison 1985), leading to belief that TB lesions were acidic. However, subsequent mice studies suggested that the caseum pH was neutral, as PZA failed to sterilize infection in the Kramnik (C3HeB/FeJ) mouse model while efficacious in BALB/c (Lanoix et al. 2016). PZA inhibited *in vitro* non-replicating *M. tuberculosis* under neutral conditions (Lakshminarayana et al. 2015), and in an *ex vivo* caseum assay, against the highly drug tolerant persister phenotype (Sarathy et al. 2018) albeit at a very high MIC range. Recent lesion-centric pharmacological evidence utilizing MALDI-MSI provides insight into PZA sterilizing effect. Firstly, PZA plasma PK/PD studies indicate that it reaches C_{max} within 2-4h following oral administration, with concentrations increasing linearly with dose over the clinically applicable range. It undergoes metabolism to form 2-pyrazinoic acid, 5-hydroxy-PZA, 5-hydroxy-POA and pyrazinuric acid etc. metabolites, and has $t_{1/2}$ of approximately 5.8 h to 10 h (Aarnoutse et al. 2017; Verbeeck et al. 2016). In terms of tissue distribution, PZA exhibits relatively similar plasma and lung tissue or lesion concentrations, indicating favorable exposure even at the difficult-to-reach caseum (Prideaux et al. 2015; Blanc, Sarathy, et al. 2018). Its low molecular weight likely

drives PZA caseum distribution through passive diffusion, and low lipophilicity causes low caseum-binding (Sarathy et al. 2016) in contrast to more hydrophobic drugs like CFZ. This data indicates that both PZA and/or its active metabolite POA accumulate to reach caseum non-replicating persisters and bacilli in cellular lesion compartments, where the phagolysosome of activated macrophages is acidic.

Conflicting evidence exists regarding PZA-mediated sterilizing effect in the caseum (Ahmad, Fraig, et al. 2011; Lanoix et al. 2016; Lanoix, Betoudji, and Nuermberger 2016; Blanc, Sarathy, et al. 2018). The differences in treatment outcome seem to be a function of lesion heterogeneity, which varies in murine, guinea pig and rabbit models used in these studies. In the rabbit model, which recapitulates lesions observed during TB disease in humans, PZA is distributed into the different lesions types and microenvironments including the caseum, which was found to have a pH range of 6.1-8.0 (Blanc, Sarathy, et al. 2018), corroborating penetration and pH in human lung lesions and caseum (Prideaux et al. 2015; Kempker et al. 2017). Furthermore, this was associated with a slow onset of bactericidal activity in necrotic lesions, likely because the PZA concentrations required to exert a sterilizing effect against caseum bacilli are extremely high, as observed in *ex vivo* caseum assays (Blanc, Sarathy, et al. 2018; Sarathy et al. 2018). Finally, PK/PD modeling of TB drugs in human lesions suggested that PZA achieves suboptimal concentrations showing the longest below-MIC periods in the caseum of ‘at-risk’ patients, at the currently used dosages (Strydom et al. 2019). These findings provide a pharmacological explanation of PZA sterilizing activity, why treatment fails to sterilize infection in certain patients and may guide dose optimization strategies to improve PZA caseum exposure.

Ethambutol:

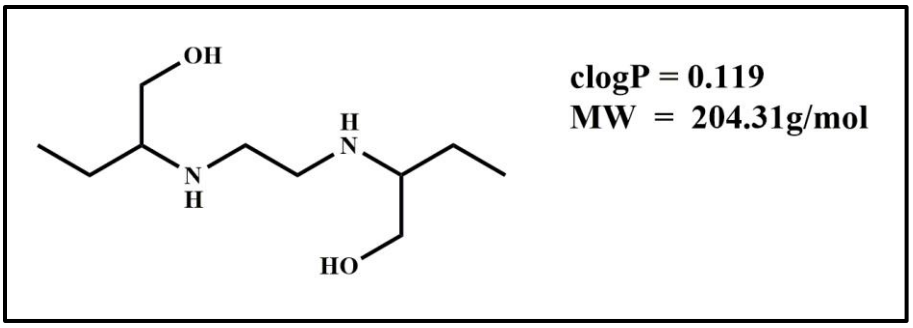

Figure 1.10. Ethambutol.

EMB (Figure 1.10) is a cell wall synthesis inhibitor, targeting replicating bacteria by interfering with arabinogalactan synthesis – a key structural feature of the mycobacterial cell wall (Takayama and Kilburn 1989; Forbes, Kuck, and Peets 1962). EMB targets mycobacterial membrane-associated arabinosyl transferases encoded by three genes, *embA*, *embB* and *embC*, which are organized as 10-kb operon (Telenti et al. 1997; Takayama and Kilburn 1989; Goude et al. 2009; Belanger et al. 1996).

In the starvation and anaerobic non-replicating *in vitro* assays to mimic caseum resident bacilli, EMB is poorly active, with MIC values 30-fold greater compared to replicating bacteria against which it exerts bactericidal activity (Lakshminarayana et al. 2015). Under clinical conditions, EMB reaches peak plasma concentrations in 2-3 h and has $t_{1/2}$ of 2-4 h (Verbeeck et al. 2016). In addition to its moderate *in vitro* activity, a rabbit PK model showed that EMB plasma concentrations were likely inadequate to achieve PK/PD parameters associated with clinical efficacy (Zimmerman et al. 2017). A key observation however, which likely explains why EMB remains part of the cornerstone TB regimen, was its significant accumulation in the lung tissue and cellular lesion microenvironment, while slowly diffusing into the caseum (Zimmerman et al. 2017). With a clogP of 0.41, EMB was predicted to have less caseum binding hence the observed slow caseum diffusion. Its lack of sterilizing activity against non-replicating bacilli means it is

ineffective in the caseum (Lakshminarayana et al. 2015) however EMB accumulation into the cellular environment and its activity against replicating bacteria suggest that it is responsible for its role in the standard combination regimen (Zimmerman et al. 2017).

1.3.2.2 Molecular mechanisms and lesion PK/PD for MDR-TB and XDR-TB drugs

As a guiding principle, DR-TB patient therapies are generally individualized based on a patient's treatment and resistance profile. The WHO recently introduced a new grading system to guide building regimens for DR-TB patients, prioritizing second and third-line anti-TB drugs based on individual contribution to treatment outcomes versus toxicity (WHO 2019b). Classified in the A category are the fluoroquinolones, MXF and levofloxacin (LVF), along with BDQ and LZD; drugs considered the most effective for DR-TB and recommended for inclusion in all DR-TB regimens unless pre-determined resistance exists (WHO 2019b). In group B are clofazimine (CFZ) and cycloserine or terizidone, while all the remaining second-line drugs form the Group C (Figure 1.4) recommended for use in completing a regimen and when drugs in the A and B groups cannot be used. Group C drugs include DLM, PZA, EMB, PAS, aminoglycosides (SPM and amikacin (AMK)), thioamides (ethionamide (ETH) and prothionamide), and β-lactams (meropenem or imipenem-cilastin; only used in combination with clavulanate) (WHO 2019b).

Plasma-based PK profiles exist for these drugs, and are used in conjunction with their MICs to inform PK/PD parameters that drive clinical efficacy (Dartois and Barry 2010). Since DR-TB drugs are generally less effective, more toxic and require even lengthier treatment duration, therapeutic drug monitoring (TDM) based on plasma PK/PD is utilized to inform dosing strategies. While this may facilitate favorable treatment outcomes, it is now recognized that plasma concentrations may not translate into lesion drug exposure. Drug penetration and exposure at the

site of action remains less explored, as this is a new developing strategy. However, as shown with lesion-penetration data of first-line drugs, penetration and exposure in lesion microenvironments is drug-specific and critical to clinical outcome. Therefore, in addition to patient resistance profile, DR-TB therapies should consider lesion-centric PK/PD optimizations to ensure drug combinations that are complementary in targeting bacilli, their mechanism of action and lesion-penetration properties to prevent further resistance. Since lesion-penetration considerations are a new strategy in TB drug discovery and development, only a few of the DR-TB drugs have been included in lesion-centric PK studies and, are discussed below:

Fluoroquinolones:

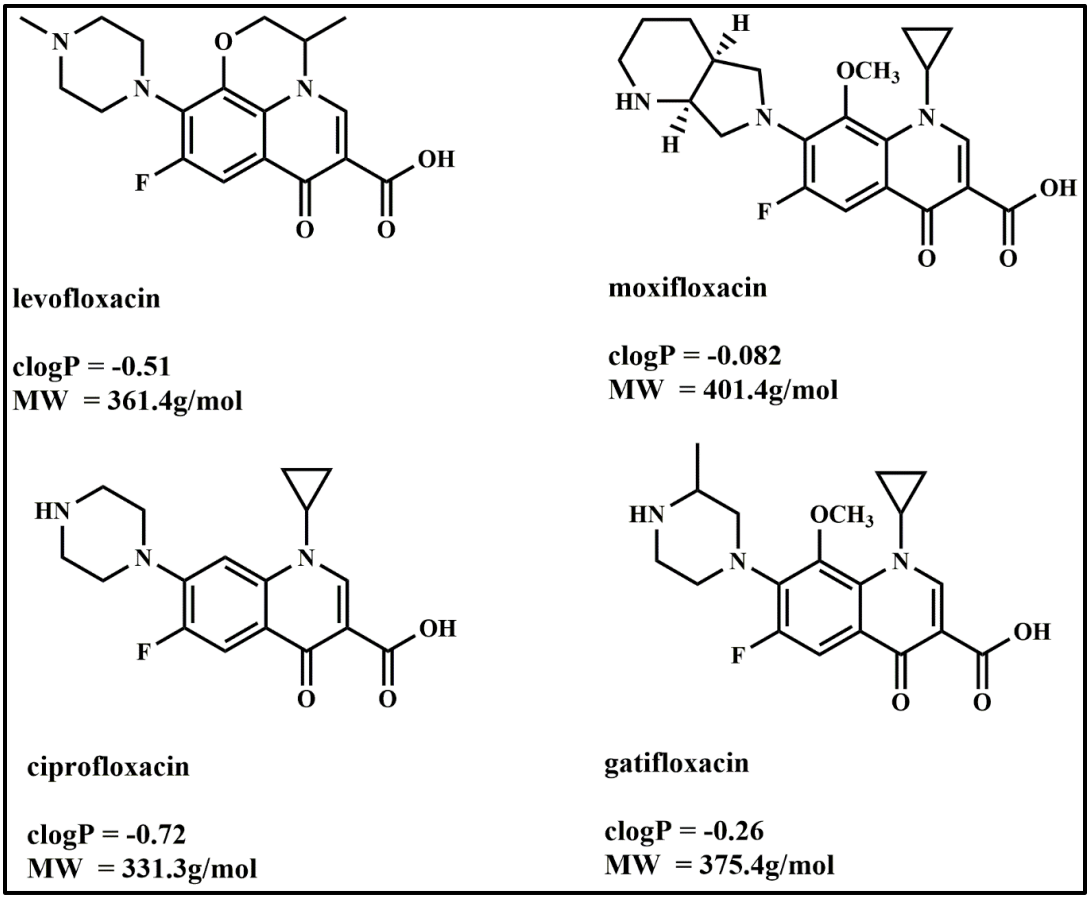

Figure 1.11. Examples of fluoroquinolones, including moxifloxacin, levofloxacin and gatifloxacin currently approved for inclusion in DR-TB therapies.

Fluoroquinolones (Figure 1.11) are broad-spectrum antibacterials that target bacterial type II and type IV topoisomerases. *M. tuberculosis* lacks topoisomerase IV genes and only encodes gyrase (Cole et al. 1998; Aubry et al. 2004). DNA gyrase is an ATP-dependent enzyme required for DNA replication and recombination and RNA transcription through introduction of negative supercoils into the double-stranded DNA helix (Drlica and Zhao 1997). Fluoroquinolones are bactericidal against *M. tuberculosis*, and exert their activity by intercalating into DNA, therefore trapping the gyrase-DNA complexes. The GyrB subunit is involved in ATP hydrolysis to supply energy to the GyrA subunit which binds DNA to form double-stranded breaks (Drlica et al. 2008). Currently, only MXF and LVF are recommended for inclusion in DR-TB regimens (WHO 2019b)

MXF plays a key role in current DR-TB regimens and is also under investigation for potential use in DS-TB therapies (www.newtbdrugs.org). Earlier studies showed that MXF exerts bactericidal activity against both replicating and non-replicating bacilli *in vitro* and in animal efficacy models (Nuermberger, Yoshimatsu, Tyagi, O'Brien, et al. 2004; Kjellsson et al. 2012; Nuermberger, Yoshimatsu, Tyagi, Williams, et al. 2004), which informed its inclusion in clinical investigations towards efforts to shorten TB treatment duration for DS-TB. Following administration, MXF reaches t_{max} in about 1-4 h, with a median $t_{1/2}$ of approximately 6.6 h (Peloquin et al. 2008). With favorable plasma PK/PD and lung tissue accumulation these data suggested that MXF would exert sterilizing activity in human lesions; however, it failed to shorten the treatment duration in phase III clinical trials (Gillespie et al. 2014).

Subsequently, studies have provided insights into the observed clinical paradox of MXF efficacy. Imaging data on lesion-specific partitioning of MXF revealed its heterogeneous accumulation, with preferred distribution into peripheral cellular layers while it failed to penetrate and reach effective concentrations in the acellular caseum (Prideaux et al. 2015; Blanc, Daudelin, et al. 2018; Prideaux et al. 2011). Failure to reach critical concentrations in the caseum could explain why MXF would not sterilize persisters in the caseum, hence the observed clinical phenotype (Pienaar et al. 2017; Blanc, Daudelin, et al. 2018). This spatial distribution of MXF highlighted the drawbacks in mouse models utilized for predicting clinical efficacy, as some do not recapitulate human disease (Warner and Mizrahi 2014). Earlier *in vivo* model data was generated using BALB/c mice, known to exclusively develop cellular lesions where MXF is now known to concentrate, explaining the observed sterilizing effect. In addition, MXF lesion-centric PK/PD and efficacy were superior to that of other fluoroquinolones currently in clinical investigations, LVF and gatifloxacin (GTX) (Sarathy et al. 2019).

Repurposed drugs:

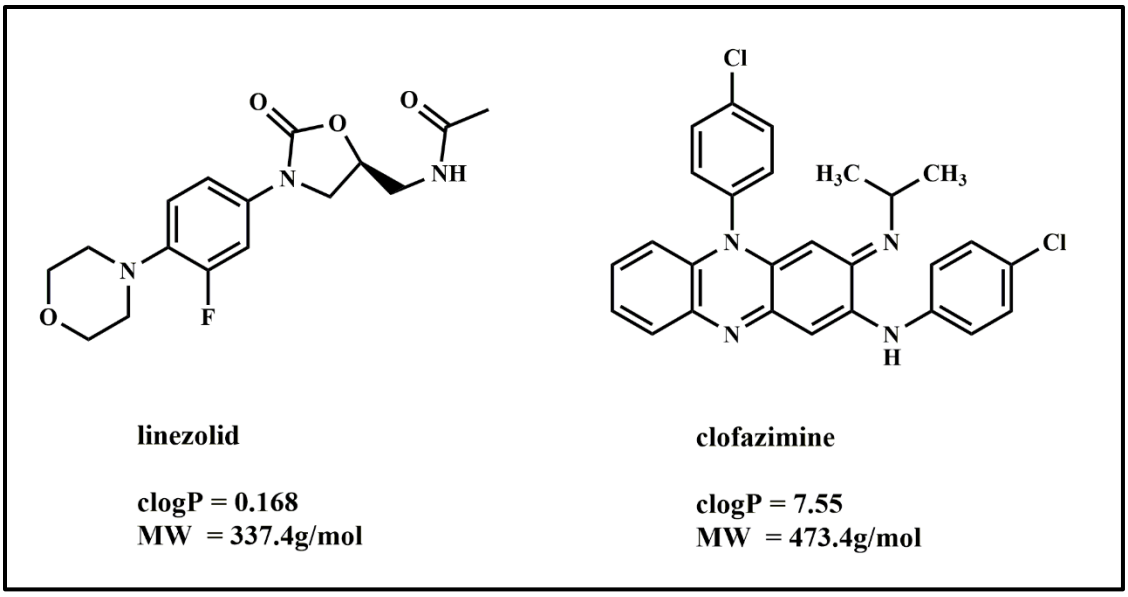

Figure 1.12. Repurposed drugs, clofazimine and linezolid.

LZD (Figure 1.12) belongs to the oxazolidinone class of antibiotics and has been in clinical use for treatment of drug-resistant bacterial infections such as the Gram-positive streptococci and methicillin-resistant *Staphylococcus aureus* (MRSA). Oxazolidinones target bacterial protein synthesis by binding to the 23S rRNA of the 50S ribosomal subunit, inhibiting protein translation (Zhou et al. 2002). LZD is bactericidal in both BALB/c mice, with cellular lesions, and C3HeB/FeJ mice with human-like pathology (Driver et al. 2012). It is effective in treatment of DR-TB in non-human primates and humans (Yew, Chau, and Wen 2008; von der Lippe, Sandven, and Brubakk 2006; Lee et al. 2012; Coleman et al. 2014), and currently recommended for inclusion in DR-TB clinical regimens. However, a major drawbacks is its toxicity, with drug-induced neurologic, hematologic and ophthalmologic adverse effects often reported (Schecter et al. 2010). Newer generation oxazolidinones including sutezolid and delpazolid are currently in the development pipeline and LZD combination regimens and dose-ranging optimization are investigated.

Following administration, LZD reaches maximum plasma concentrations in approximately 1-4 h, with $t_{1/2}$ of 1.5-7 h (Dietze et al. 2008). With regards to distribution into lung tissue, a recent study using ion-imaging data showed that LZD spatial distribution was homogenous across the cellular and caseum lesion compartments, suggesting a potential to reach multiple bacilli subpopulations (Strydom et al. 2019). In addition, PK/PD modeling data suggested that LZD exhibited favorable patient target attainment across multiple lesion microenvironments (Strydom et al. 2019). Given that the caseum environment is likely to suffer sub-therapeutic drug exposure, and hence constitutes a more likely environment for resistant *M. tuberculosis*, LZD accumulation in the caseum may explain its observed efficacy in DR-TB patients (Lee et al. 2012) and its contribution to bactericidal and sterilizing activity (Tasneen et al. 2016; Driver et al. 2012).

CFZ (Figure 1.12) is a riminophenazine previously used for treatment of leprosy until recent studies showed its potential utility for MDR-TB (Cholo et al. 2017). CFZ was initially discovered as an anti-TB drug in 1957 (Barry et al. 1957), but it failed to show efficacy in monotherapies at the time, and was repurposed for leprosy treatment. The exact mechanism of action of CFZ is still not well understood. A redox-mediated mechanism that involves the enzymatic reduction of CFZ by NADH dehydrogenase (NDH-2), followed by a spontaneous, non-enzymatic O_2 oxidation to form reactive oxygen species (ROS) has been reported in *M. smegmatis* (Yano et al. 2011). There is no specific target for ROS, and no known NDH-2 mutations associated with CFZ resistance.

However, CFZ resistance has been reported to be conferred by non-target mutations in *Rv0678*, encoding a transcriptional regulator of neighboring *mmpS5* and *mmpL5* genes associated with upregulation of the MmpS5-MmpL5 efflux system (Xu et al. 2017; Hartkoorn, Uplekar, and Cole 2014). These non-target mutations were shown to cause cross-resistance with BDQ suggesting that

both drugs could be substrates of MmpL5 and can select for non-target based, efflux resistance (Hartkoorn, Uplekar, and Cole 2014; Andries et al. 2014). MmpL (mycobacterial membrane large proteins) proteins are multisubstrate efflux pumps which form part of the resistance nodulation and cell division (RND) superfamily in *M. tuberculosis* (Domenech, Reed, and Barry 2005). Efflux pump inhibitor, verapamil, improved the activity of CFZ and BDQ by 8-fold or more suggesting the potential of verapamil for inhibiting efflux pumps relevant to these drugs, at least *in vitro* (Gupta et al. 2014). Recently, however, the potentiating effect of verapamil has been attributed to its effect on membrane energetics, which is targeted by both BDQ (AtpE) and CFZ (NDH-2), rather than increased drug accumulation as a result of efflux inhibition (Chen et al. 2018).

CFZ is a highly lipophilic (clogP, 755), low aqueous solubility drug, with a peculiar PK profile. CFZ shows favorable distribution into tissues compared to plasma and has a previously reported long terminal half-life of 70 days in tissue sites (Levy 1974; Gopal et al. 2013) A recent PK model study estimated a median terminal half-life of 34.2 days, which was significantly longer for women (49.5 days) compared to men (21.8 days), owing to differences in body composition (Abdelwahab et al. 2020). CFZ has been reported to accumulate readily in human mononuclear phagocytes to achieve very high levels, (Baik and Rosania 2012; Harbeck et al. 1999), which can lead to organ damage caused by crystal deposition. *In vivo* TB infection mouse models revealed superior efficacy of CFZ in BALB/c mice in comparison to the C3HeB/FeJ model, which develops necrotic lesions (Irwin et al. 2014). In addition, TB lesion penetration data showed a contrasting distribution between the caseum and cellular lesion compartments, with higher accumulation observed in the cellular layer surrounding the caseum (Prideaux et al. 2015; Strydom et al. 2019). PK/PD modeling data, assuming $T_{> MIC}$ of 90% as the PK/PD index required for CFZ efficacy, suggested that this target was reached across lesions except for caseum cavity (Strydom et al. 2019). These data may

explain the observed inefficacy of CFZ in C3HeB/FeJ mice (Irwin et al. 2014). In addition to poor caseum penetration, CFZ is poorly active against non-replicating bacilli (Sarathy et al. 2018).

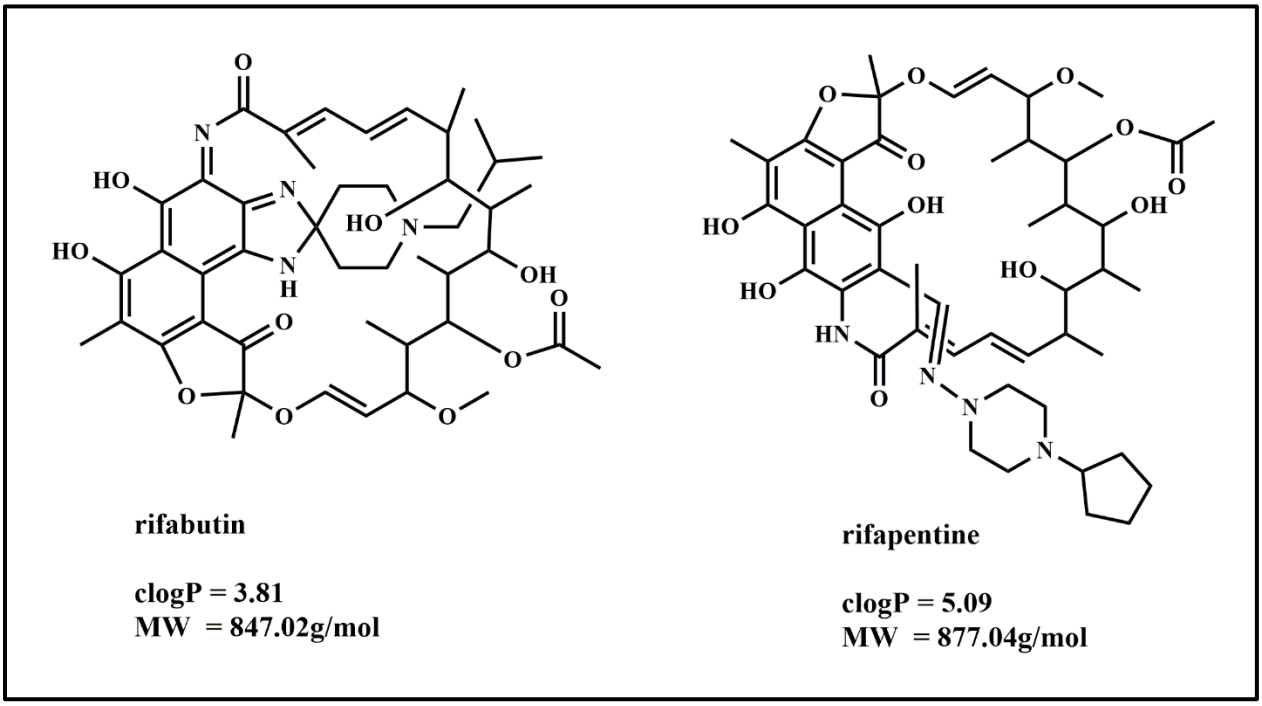

Figure 1.13. New generation rifamycins, rifabutin and rifapentine.

Rifamycins including rifapentine (RFP) and rifabutin (RFB) (Figure 1.13) inhibit *M. tuberculosis* growth by the same mechanism as RIF. They are effective against both active and latent TB but cross-resistance with RIF due to mutations in the *rpoB* gene has been observed (Jamieson et al. 2014; Sirgel et al. 2005). These rifamycins exhibit comparable or better activity than RIF against replicating and non-replicating bacilli *in vitro* (Lakshminarayana et al. 2015) and in the *ex vivo* rabbit caseum model suggesting their potential to sterilize persisters in TB lesions (Sarathy et al. 2018). RFP has been pursued as a potential substitute for RIF (Dorman et al. 2012; Dooley et al. 2012), with promising treatment shortening ability (Rosenthal et al. 2007). However, clinical

investigation of RFP in phase 2 studies failed to deliver more efficacious outcomes in comparison to RIF (Dorman et al. 2015), despite promising shortening treatment in murine models.

RFB and RFP reach peak plasma concentrations in 3-4 h and ~5 h respectively, but both have significantly longer half-life values in comparison to RIF, 32-67 h and 14-18 h respectively (Burman, Gallicano, and Peloquin 2001). Both rifamycins are metabolized similarly to RIF, via a desacetylation at position 25. RFP was reported to reach higher Cmax than RIF when both administered at 600mg (Burman, Gallicano, and Peloquin 2001). Recent PK/PD studies showed that RFP, similarly to RIF, penetrated into all lesions microenvironments, but its caseum levels were lower than RIF (Rifat et al. 2018). This may, in part, explain the clinical observations. RFP and RFB are more lipophilic than RIF, with clogP values of 5.09 and 4.73 respectively, compared to RIF's 3.71. The lower caseum penetration may be explained by their lipophilicities and resulting differences in caseum diffusion and macromolecular binding (Sarathy et al. 2016). Unbound RIF levels were 10 times higher than RFP in rabbit caseum *ex vivo*.(Sarathy et al. 2016). Increasing RFP dosing would likely achieve adequate caseum concentration; however, dose-optimization studies indicate that high dosage may not be tolerable, and patients with larger cavitary lesions had similar outcome to those receiving RIF (Dooley et al. 2015). RFP and RFB may offer an alternative option for treatment of patients with known RIF-resistance (Sirgel et al. 2013). While RFP is not recommended for HIV co-infected patients owing to high risk of developing RIF resistance, RFB has fewer drug-drug interactions than RIF in patients receiving ART (Lee, Meintjes, et al. 2013).

New TB drugs:

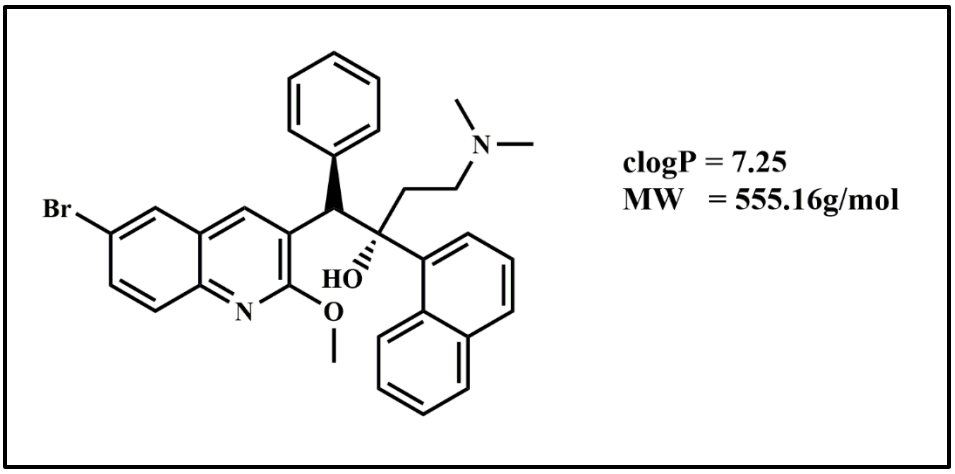

Figure 1.14. Structure of newly approved bedaquiline.

BDQ (Figure 1.14) acts through the inhibition of the C-subunit of membrane-bound adenosine triphosphate (ATP) synthase, inhibiting *M. tuberculosis* energy metabolism (Koul et al. 2007; Haagsma et al. 2011). It is active against both replicating and non-replicating bacillary sub-populations (Koul et al. 2007; Lakshminarayana et al. 2015). Utilizing *M. tuberculosis*-infected *in vivo* animal models, BDQ was shown to be more efficacious in BALB/c mice, while C3HeB/FeJ mice were much more refractory to BDQ treatment (Irwin et al. 2016).

BDQ is well absorbed and reaches Cmax in 4-6 h following oral administration (Rustomjee et al. 2008). It undergoes hepatic metabolism to form a major N-monodesmethyl metabolite (M2), which is less active (van Heeswijk, Dannemann, and Hoetelmans 2014). Both BDQ and M2 have long terminal $t_{1/2}$ in plasma, approximately 164 days (range 62-408 days) for BDQ, and 159 days (range 69-407 days) for M2 metabolite (Diacon et al. 2012). BDQ generally showed preferential accumulation into tissues relative to plasma (van Heeswijk, Dannemann, and Hoetelmans 2014). Further analysis detailing spatial drug partitioning revealed that the highly lipophilic BDQ (clogP, 7.25), similar to CFZ, had higher distribution into the lung tissues, particularly the cellular lesion environment than the caseum, explaining its reduced efficacy in C3HeB/FeJ mice (Irwin et al.

2016). The *ex vivo* rabbit caseum model showed modest activity of BDQ against non-replicating bacilli (Sarathy et al. 2018). These data suggesting that significantly higher caseum drug concentrations would be required for BDQ to sterilize caseum bacilli. However, its poor caseum penetration owing to poor diffusion and lipid binding (Sarathy et al. 2016) seem to suggest that target concentrations are less likely to be attained.

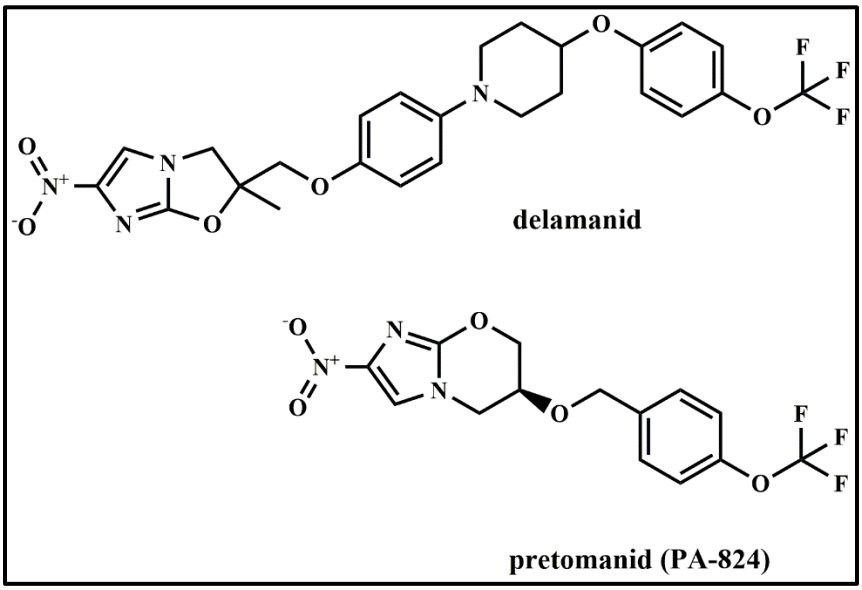

Figure 1.15. Newly approved nitroimidazoles, delamanid and pretomanid.

Nitroimidazoles DLM and PA-824 (Figure 1.15) were discovered through phenotypic screening and have been shown to effect killing of *M. tuberculosis* through two distinct mechanisms (Stover et al. 2000; Matsumoto et al. 2006). Both are prodrugs that require activation through a deazaflavin-dependent nitroreductase (Ddn) and F_{420}-dependent glucose-6-phosphate dehydrogenase (FGD1) two-enzyme system. DLM acts by inhibiting mycolic acid biosynthesis; while PA-824 effects nitric oxide-mediated killing of *M. tuberculosis* (Matsumoto et al. 2006; Manjunatha, Boshoff, and Barry 2009; Cellitti et al. 2012). They both show potent *in vitro* and *in*

vivo activity against replicating, non-replicating hypoxic *M. tuberculosis* and MDR-TB strains (Matsumoto et al. 2006; Gler et al. 2012).

While lesion-centric PK data for these drugs in human TB lesions are not yet available, early bactericidal activity (EBA) studies of DLM monotherapy showed a decline of bacterial load, measured by CFU (Diacon et al. 2011). However, plasma exposure of DLM was not dosage-proportional, and plateaued at 300 mg (Diacon et al. 2011). At different dosages, the median Tmax was 4-5 h (Diacon et al. 2011), and a $t_{1/2}$ of 38 h has been reported (Gler et al. 2012). DLM exhibited bactericidal activity against replicating and non-replicating BCG *in vitro* and in a guinea pig model of TB infection (Chen et al. 2017). Histological examination suggested DLM and DLM-containing combinations killed bacilli located in the hypoxic necrotic caseum of guinea pigs (Chen et al. 2017), an indication that DLM diffuses into the caseum core. Furthermore, DLM exhibited a bactericidal effect in a nitric oxide synthase 2 knockout ($Nos2^{-/-}$) mouse model with hypoxic necrotizing human-like granuloma pathology (Gengenbacher et al. 2017).

PK data of PA-824 in EBA studies showed that it was moderately absorbed, reaching peak plasma concentrations in approximately 4.5 h, with an estimated mean $t_{1/2}$ of 17.4 h (Diacon et al. 2010). PA-824 also showed a bactericidal effect, with dosing range of 200-1200 mg daily effecting the same response, suggesting lower dosages could be effective and minimize potential safety issues (Diacon et al. 2010). PA-824 EBA was also linear over 14 days, suggesting that extending beyond that time-period would have a sterilizing effect. Later studies in murine models showed that even at the lowest dosage (200mg), PA-824 is expected to reach the target PK/PD indices (Ahmad, Peloquin, et al. 2011).

1.3.2.3 Building new regimens: complimentary lesion-penetrating properties

To prevent the emergence of drug resistance and to maximize the efficacy of current anti-TB drugs and avoid failure of lead compounds in clinical development, careful consideration should be given to combination regimen design and implementation. Knowledge of physicochemical properties, lesion distribution, site-specific exposure and activity should be considered early in preclinical lead optimizations utilizing relevant *in vitro* and *in vivo* models to inform design of complimentary combinations (Dartois and Barry 2013; Dartois 2014). For example, utilizing lesion-penetration PK/PD modeling data, Strydom et al., (2019) showed that a combination of CFZ, MXF and LZD would be optimal for patients with caseous lesions based on their distribution and activities at the site of infection (Strydom et al. 2019).

For the new combinations under clinical investigation, BDQ, PA-824, MXF and PZA (BPaMZ) or BDQ, PA-824 and LZD (BPaL), the utility of lesion-centric PK/PD may explain the promising clinical outcomes culminating to the recent FDA approval of BPaL for XDR-TB (Conradie et al. 2020; Keam 2019). Additionally, BPaMZ and BPaZ have also demonstrated superior bactericidal activity in DS-TB and rifampicin-resistant TB (RR-TB) patients compared to those receiving the first-line regimen (Tweed et al. 2019). BPaMZ and BPaL demonstrated superior bactericidal activity and sterilizing effect, shortening treatment duration in a mouse model compared to the first line regimen (Li et al. 2017; Tasneen et al. 2016). Variations, through the removal of BDQ, PZA, MXF from the BPaMZ regimen (Li et al. 2017) or PA-824 from both the BPaMZ and BPaL, highlighted the individual contributions of the drugs to the sterilizing effect of these regimens (Xu et al. 2019) in mouse models of varying pathologies, ranging from exclusively cellular lesions to caseous and cavitary lesions. Removal of BDQ had the greatest reduction in efficacy, and while all variations were superior to the first line regimen, increased treatment duration and relapse rates

were observed (Li et al. 2017). The recent study recent study by Xu et al., (2019) utilizing mice with different disease pathologies may provide evidence correlating drug-specific lesion penetration properties with the observed clinical efficacy (Xu et al. 2019).

1.4 *M. tuberculosis* and the macrophage: the "unit of infection"

While most studies have prioritized understanding the dynamics of caseum drug penetration and sterilizing effects on non-replicating bacteria with a view for treatment shortening, the cellular lesion compartment represents a significant component of TB pathogenesis as bacilli are located predominantly within macrophages. A defining feature in *M. tuberculosis* pathogenesis is the ability to infect and replicate within macrophages (VanderVen et al. 2016; Ehrt, Schnappinger, and Rhee 2018), cells otherwise designed with effective microbicidal mechanisms against most invading pathogens, hence the *M. tuberculosis*-infected macrophage represents the "minimal unit of infection".

1.4.1. Heterogeneity in the *M. tuberculosis* infected macrophage

The dynamics of the host-pathogen interactions within the infected macrophage are crucial to therapeutic outcomes. The infecting bacillus responds to macrophage intracellular environment by effecting phenotypic and metabolic changes to ensure its survival; however, the host cell metabolic status may also be altered in response to infection (Rohde et al. 2007; Fortune and Rubin 2007). In addition, the infected cell responds to host immune responses in efforts to kill the invading bacillus and this response maybe heterogeneous (Russell, Huang, and VanderVen 2019). The changes in intracellular metabolic pathways in immune cells that alters their function is referred

to as immunometabolism (Russell, Huang, and VanderVen 2019; O'Neill, Kishton, and Rathmell 2016) while “the ability of an intracellular bacterial pathogen to adapt its own metabolism to the intracellular milieu of the host cell, to modulate the host cell metabolism in favor of its own needs with the help of common and pathogen-specific (virulence) factors, and to adjust the expression of the necessary virulence genes to the intracellular metabolism” is referred to as pathometabolism (Eisenreich et al. 2015).

Changes in *M. tuberculosis* metabolism have wider implications for therapeutic outcomes (Mashabela, de Wet, and Warner 2019). There is a possibility that the non-replicating phenotype observed in the caseum is selected for in the macrophage before cell death and release into the extracellular milieu, therefore the interaction between the macrophage and the infecting bacillus could contribute to the efficacy of an applied drug. *M. tuberculosis* adaptation of its metabolic processes, such as carbohydrate and fatty acid metabolism, are crucial for cellular function and pathogenicity and are required for long-term survival *in vivo* (Marrero et al. 2013; Ehrt, Schnappinger, and Rhee 2018). Most recently, utilization by *M. tuberculosis* of amino acids as nitrogen sources has also been reported (Agapova et al. 2019). However, the interaction between *M. tuberculosis* and host cell lipid metabolism has unique implications on cellular drug distribution, and progression of TB disease; and is discussed more in detail below.

Early studies by Bloch & Segal reported the preferential metabolism of fatty acids by *M. tuberculosis* isolated *in vivo* from mouse lungs and grown *ex vivo* (Bloch and Segal 1956). Later studies revealed the essentiality of both isocitrate lyases 1 and 2 (ICL1 and ICL2) for *in vivo* survival of *M. tuberculosis* in a chronic mouse model (Munoz-Elias and McKinney 2005; McKinney et al. 2000). ICL1 and ICL2 are key enzymes of the glyoxylate cycle that uses fatty

acids for energy generation, suggesting that during chronic infection *M. tuberculosis* bacilli depends on fatty acid metabolism for survival *in vivo*. Transcriptional analyses revealed that intraphagosomal *M. tuberculosis* upregulated *icl* and other genes involved in degradation and β-oxidation of fatty acids (Schnappinger et al. 2003; Rohde et al. 2012). Further studies confirmed that *M. tuberculosis* is able to assimilate and metabolize fatty acids, cholesterol and triacylglycerides (TAG) (Lee, VanderVen, et al. 2013; Daniel et al. 2011), and that the lipid uptake process is facilitated by a controlled network of genes including *lucA, mce1* and *mce4* (Nazarova et al. 2017; Nazarova et al. 2019).

Accumulating evidence suggests that *M. tuberculosis* induces dysregulation of host lipid metabolism, causing macrophages to accumulate TAG, cholesterol and cholesterol esters as lipid bodies (LB) in a foamy phenotype (Peyron et al. 2008; Singh et al. 2012; Ouimet et al. 2016; Kim et al. 2010). The key study by Peyron et al showed that virulent mycobacteria induce LB formation and association of the phagosome with LB, suggesting that mycobacteria might assimilate lipids from LBs to form intracytoplasmic lipid inclusions (ILI) (Peyron et al. 2008; Caire-Brandli et al. 2014). It is believed that these LBs provide a nutrient source for *M. tuberculosis*. However, these findings have been contradicted by others. For example, a recent study has provided evidence suggesting that LB formation is a host immunity driven response and that while *M. tuberculosis* possesses the ability to assimilate lipids, it is unable to do so from LBs present in IFN-γ-activated macrophages *in vitro* and *in vivo* (Knight et al. 2018).

One school of thought proposes that *M. tuberculosis* in foamy macrophages enter a non-replicating state. The association of foamy macrophages with the hypoxic necrotic centre in caseating lesions suggests that these cells play a role in disease progression and mycobacterial persistence in the

granuloma (Russell et al. 2009; Peyron et al. 2008; Daniel et al. 2011). A recent study suggests that *M. tuberculosis* replicates in foamy cells *in vitro*, however at a lower rate compared to non foamy macrophages; and this control of bacterial growth is associated with a pro-inflammatory response (Agarwal et al. 2020). *In vivo*, a chronic animal infection model confirmed increasing lipid accumulation in foamy macrophages and *M. tuberculosis* ILIs associated with disease progression (Caceres et al. 2009). The ultimate goal of *M. tuberculosis* infection is thought to be driving mechanisms for its transmission between hosts, therefore it would seem that the association of foamy macrophages with the caseating necrotic core suggests a role for foamy macrophages in this process (Daniel et al. 2011; Caceres et al. 2009). Furthermore, the necrotic core of caseous granuloma are enriched in these same lipids found in foamy cells and extracellular bacilli in this microenvironment are commonly found embedded in this nutrient-rich material (Kim et al. 2010).

1.4.2. Factors affecting intracellular drug exposure and efficacy in *M. tuberculosis*-infected macrophages

The final target of a drug is to achieve the required concentration at its biological target within the different physiological and metabolic *M. tuberculosis* states (Dartois 2014). A number of factors however, may determine the exposure of a drug (Figure 1.16) in the intracellular environment and are critical to clinical outcome (Mashabela, de Wet, and Warner 2019; Tanner et al. 2018).

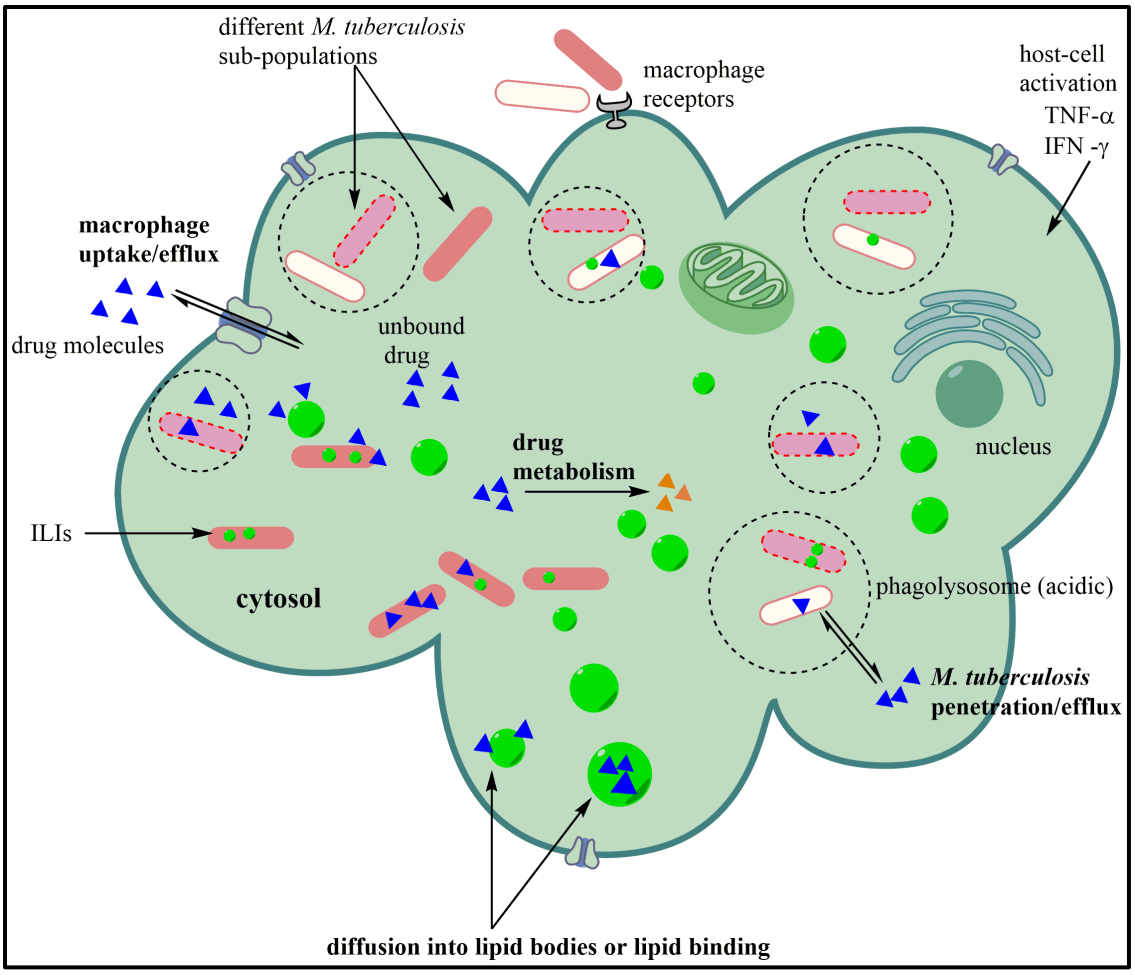

Figure 1.16. Fate of drugs in *M. tuberculosis*-infected macrophages. The interaction between *M. tuberculosis* and the host macrophage influences cellular drug efficacy as a result of processes like efflux, drug metabolism, lipid binding, host cell activation etc. ILIs, intrabacilli lipid inclusions; TNF-α, tumor necrosis alpha; IFN-γ, interferon gamma. Adapted from (Tanner et al. 2018).

i) Efflux

M. tuberculosis is an obligate pathogen, believed to have co-existed with the human host for centuries (Gagneux 2018). For any drug to achieve the desired effect on its *M. tuberculosis* target, it will need the right properties to penetrate and bypass *M. tuberculosis* intrinsic and adapted

mechanisms for tolerance against antimycobacterial agents. Effective concentrations at the molecular target depend on drug influx by either diffusion or active uptake, efflux, ease of reach and affinity to its molecular target, the metabolic state of the bacillus, which may directly affect drug metabolism (Sarathy, Dartois, and Lee 2012). The *M. tuberculosis* cell wall is believed to pose as an impermeable barrier to antimycobacterial agents, owing to its uniquely organized cell envelope architecture and composition (Figure 1.5) (Kalscheuer et al. 2019) which may be modified as bacilli switch from replicating to a non-replicating state. Transport of antimycobacterial agents across the mycobacterial cell wall depends on their size and physicochemical properties. More lipophilic agents are thought to move across via passive diffusion due to the lipid-rich environment of the cell wall, while water-filled porin channels transport small polar molecules (Sarathy, Dartois, and Lee 2012; Danilchanka, Pavlenok, and Niederweis 2008).

Active transport-mediated mechanisms rely on influx and efflux transporters spanning the cell wall, and their function is directly linked to the metabolic state of *M. tuberculosis*, as they may be over-expressed under environmental stress or undergo mutations. (Sarathy, Dartois, and Lee 2012). Infection of macrophages upregulates efflux mechanisms in replicating *M. tuberculosis in vitro* (Adams et al. 2011), causing tolerance to anti-TB drugs, which may be restored with treatment of verapamil (Adams, Szumowski, and Ramakrishnan 2014). Initially thought to inhibit efflux, verapamil instead acts by inhibition of membrane energetics, likely explaining why it restored drug susceptibility, since efflux pumps require energy for function (Chen et al. 2018). The indication of differential induction of bacterial efflux pumps, and thus tolerance, will affect drug efficacy in cellular lesion microenvironments.

Macrophage membranes also express influx and efflux transporters which may influence the capacity for drug penetration and accumulation into the intracellular host environment (Te Brake et al. 2018), and are likely to be immune modulated. Primary human macrophages differentially express membrane transporters such as the organic anion transporting polypeptide transporter, P-glycoprotein, multidrug resistance proteins (MRP) etc., and may respond differently to activation signals (Moreau et al. 2011). For example, as a protection mechanism against cytotoxic levels of NO, activated macrophage cell lines upregulated efflux protein MRP1, which has been implicated in ciprofloxacin efflux (Marquez et al. 2009; Lok et al. 2016).

ii) *M. tuberculosis*-mediated drug metabolism

M. tuberculosis and infected host cells contain enzymes that can mediate biotransformation of drug molecules. These metabolic transformations may be beneficial in the case of prodrugs, or detrimental if the drug molecules are deactivated. Host-focused drug metabolism is typically studied in relation to plasma PK/PD through assessment of pharmacological parameters such as bioavailability, clearance rate and via measurements of potential drug toxicities. Generally, liver metabolism through use of human liver microsomes *in vitro* is used to inform *in vivo* metabolism. For an intracellular pathogen like *M. tuberculosis*, drug interaction with both the host macrophage and the bacilli could lead to biotransformations that may affect drug efficacy due to reduced accumulation of active drug molecules in the host cell. *M. tuberculosis* is known to effect chemical transformations on specific chemical groups. These transformations include ester hydrolysis, addition of alkyl groups and reduction-oxidation reactions to name a few (Awasthi and Freundlich 2017). It may also be important to know which drug-metabolizing enzymes are upregulated in replicating and non-replicating bacteria as this may inform the fate of a drug molecule in specific

lesion niches. Therefore, studying metabolism in the context of the infected host macrophages may provide important information on available drug in the cellular lesion compartment.

1.4.3 Disease-relevant infected macrophage *in vitro* assays

Knowledge of the lesion microenvironments in which *M. tuberculosis* bacilli reside, and the complex interaction between the bacilli and host cell, indicate the importance of developing the so-called "disease-relevant" *in vitro* and *in vivo* assays that mimic host environment conditions, for lead optimization (Franzblau et al. 2012). In addition to traditional antimycobacterial replicating assays utilizing different growth media for determination of MICs or MBCs in axenic culture utilizing laboratory or clinical *M. tuberculosis* strains, non-replicating assays (Wayne and Hayes 1996; Gengenbacher et al. 2010) to mimic the phenotypic variability of *M. tuberculosis* in the cellular and caseum lesion compartments are utilized.

In addition, studies have employed *in vitro* macrophage infection assays to determine host infection outcomes. *In vitro* macrophage manipulations with host-derived stimuli such as IFN-γ ensure that significant pH changes occur in intracellular environment to evaluate the efficacy of drugs such as PZA whose functionality is optimal at low pH conditions (Tanner et al. 2018). Furthermore, recent studies have documented methods to induce foamy macrophages utilizing macrophage-like cell lines *in vitro*, such as treatment of macrophage cell-lines with oleic acid (Sarathy et al. 2016; Sarathy et al. 2017; Agarwal et al. 2020). While surrogate human or mouse-derived macrophage-like cell lines (for example, human-derived THP-1 monocytes or murine-derived J774) have been used particularly for their ease of laboratory handling, primary macrophages may provide host relevant insights. The importance of host cell infection outcomes is perhaps highlighted by the utility of mouse models such as BALB/c and C3HeB/FeJ, which develop distinct pathologies inferring disease-relevant mycobacterial physiological and metabolic

adaptations, as well as innate host defense mechanisms to determine and predict clinical outcomes. In addition, despite not exactly recapitulating the host-tissue microenvironment, the mouse model is a cost-effective tool to assess the bactericidal and sterilizing potencies of individual drugs and drug combinations (Koul et al. 2011).

1.5 Statement of research

1.5.1 Hypothesis

Sterilization of *M. tuberculosis* bacilli in lung lesions is dependent on the ability of the applied drug(s) to penetrate and distribute into heterogeneous environments including the caseum and other infected microenvironments and cellular compartments. This ability is a function of the physicochemical and pharmacological properties of the drug. The infected macrophage is a defining feature of mycobacterial pathogenicity, and is therefore considered essential to understanding disease-relevant physicochemical drug properties in the TB drug discovery cascade

1.5.2 Aim of the study

To develop a proof-of-concept model to study drug permeation of potential anti-TB agents in host macrophage cells during infection with M. tuberculosis in an in vitro system.

This approach (Fig. 1.17) will inform how drug molecules traverse through the cellular lesion compartment, what physicochemical properties drive cellular distribution and how, through predictive means we can prioritize compounds to progress through the drug discovery cascade.

This will inform rational design of compounds that permeate into lesion compartments at physiologically relevant concentrations and have complementary activity in the context of target *M. tuberculosis* populations and therefore will be critical to the outcome of treatment.

The following questions were investigated:

(i) Do the selected compounds have the ability to permeate through the membrane into the infected host cells and accumulate within the intracellular environment?

(ii) In what form are the active compounds found in *M. tuberculosis*-infected macrophages?

(iii) Do compounds permeate infected macrophages to reach target bacterial populations at effective concentrations to effect inhibitory or cidal activity?

(iv) Is there a correlation between lipophilicity driven intracellular accumulation and efficacy of compounds in different macrophage phenotypes?

1.5.3 Specific objectives

1. Determine physicochemical properties and antimycobacterial activities of selected potential anti-TB drug leads.
2. Determine *M. tuberculosis*-mediated drug metabolism and/ or drug uptake.
3. Develop a foamy and non-foamy macrophage infection model using reporter *M. tuberculosis* strains and human macrophage-like cell lines.
4. Determine drug cellular uptake during *in vitro M. tuberculosis* infection and in uninfected (resting, foamy and activated) macrophages.

5. Determine the correlation (or not) between intracellular drug concentration and effective *M. tuberculosis* growth inhibition.

The research objectives of this thesis are summarized in Figure 1.17 below:

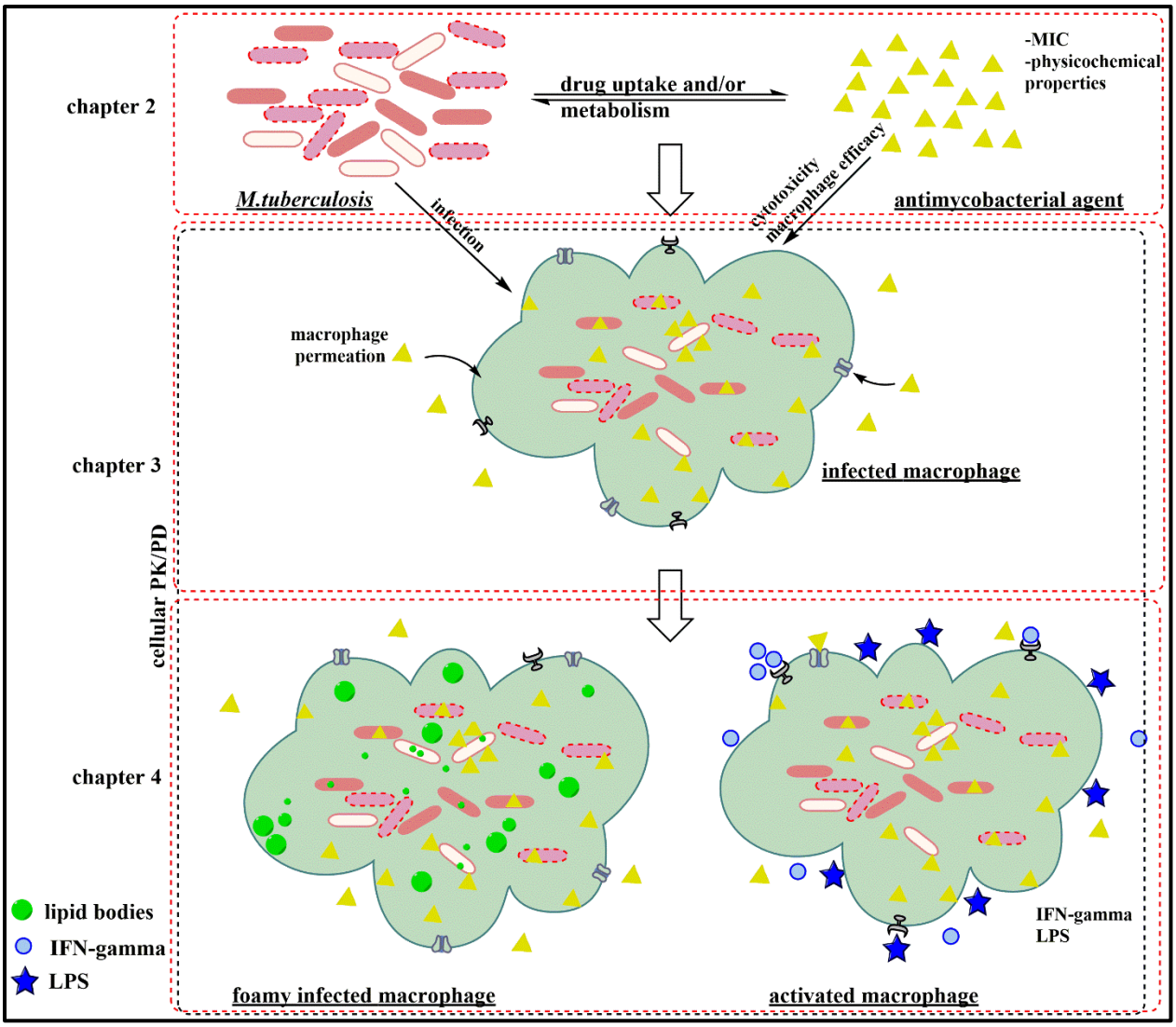

Figure 1.17. Schematic of project research objectives.

1.6 References

Aarnoutse, R. E., G. S. Kibiki, K. Reither, H. H. Semvua, F. Haraka, C. M. Mtabho, S. G. Mpagama, J. van den Boogaard, I. M. Sumari-de Boer, C. Magis-Escurra, M. Wattenberg, J. G. M. Logger, L. H. M. Te Brake, M. Hoelscher, S. H. Gillespie, A. Colbers, P. P. J. Phillips, G. Plemper van Balen, M. J. Boeree, and Acea Consortium Pan. 2017. 'Pharmacokinetics, Tolerability, and Bacteriological Response of Rifampin Administered at 600, 900, and 1,200 Milligrams Daily in Patients with Pulmonary Tuberculosis', *Antimicrobial Agents and Chemotherapy*, 61.

Abdelwahab, M. T., S. Wasserman, J. C. M. Brust, N. R. Gandhi, G. Meintjes, D. Everitt, A. Diacon, R. Dawson, L. Wiesner, E. M. Svensson, G. Maartens, and P. Denti. 2020. 'Clofazimine pharmacokinetics in patients with TB: dosing implications', *Journal of Antimicrobial Chemotherapy*, 75: 3269-77.

Abrahams, G. L., A. Kumar, S. Savvi, A. W. Hung, S. Wen, C. Abell, C. E. Barry, 3rd, D. R. Sherman, H. I. Boshoff, and V. Mizrahi. 2012. 'Pathway-selective sensitization of Mycobacterium tuberculosis for target-based whole-cell screening', *Chemistry and Biology*, 19: 844-54.

Adams, K. N., J. D. Szumowski, and L. Ramakrishnan. 2014. 'Verapamil, and its metabolite norverapamil, inhibit macrophage-induced, bacterial efflux pump-mediated tolerance to multiple anti-tubercular drugs', *Journal of Infectious Diseases*, 210: 456-66.

Adams, K. N., K. Takaki, L. E. Connolly, H. Wiedenhoft, K. Winglee, O. Humbert, P. H. Edelstein, C. L. Cosma, and L. Ramakrishnan. 2011. 'Drug tolerance in replicating mycobacteria mediated by a macrophage-induced efflux mechanism', *Cell*, 145: 39-53.

Agapova, A., A. Serafini, M. Petridis, D. M. Hunt, A. Garza-Garcia, C. D. Sohaskey, and L. P. S. de Carvalho. 2019. 'Flexible nitrogen utilisation by the metabolic generalist pathogen Mycobacterium tuberculosis', *Elife*, 8.

Agarwal, P., T.W. Combes, F. Shojaee-Moradi, B.A. Fielding, S.N. Gordon, V. Mizrahi, and F.O. Martinez. 2020. 'Foam Cells Control Mycobacterium tuberculosis Infection', *Frontiers in Microbiology*.

Ahmad, Z., M. M. Fraig, G. P. Bisson, E. L. Nuermberger, J. H. Grosset, and P. C. Karakousis. 2011. 'Dose-dependent activity of pyrazinamide in animal models of intracellular and

extracellular tuberculosis infections', *Antimicrobial Agents and Chemotherapy*, 55: 1527-32.

Ahmad, Z., C. A. Peloquin, R. P. Singh, H. Derendorf, S. Tyagi, A. Ginsberg, J. H. Grosset, and E. L. Nuermberger. 2011. 'PA-824 exhibits time-dependent activity in a murine model of tuberculosis', *Antimicrobial Agents and Chemotherapy*, 55: 239-45.

Al-Rifai, R. H., F. Pearson, J. A. Critchley, and L. J. Abu-Raddad. 2017. 'Association between diabetes mellitus and active tuberculosis: A systematic review and meta-analysis', *PloS One*, 12: e0187967.

Altaf, M., C. H. Miller, D. S. Bellows, and R. O'Toole. 2010. 'Evaluation of the Mycobacterium smegmatis and BCG models for the discovery of Mycobacterium tuberculosis inhibitors', *Tuberculosis (Edinb)*, 90: 333-7.

Andries, K., P. Verhasselt, J. Guillemont, H. W. Gohlmann, J. M. Neefs, H. Winkler, J. Van Gestel, P. Timmerman, M. Zhu, E. Lee, P. Williams, D. de Chaffoy, E. Huitric, S. Hoffner, E. Cambau, C. Truffot-Pernot, N. Lounis, and V. Jarlier. 2005. 'A diarylquinoline drug active on the ATP synthase of Mycobacterium tuberculosis', *Science*, 307: 223-7.

Andries, K., C. Villellas, N. Coeck, K. Thys, T. Gevers, L. Vranckx, N. Lounis, B. C. de Jong, and A. Koul. 2014. 'Acquired resistance of Mycobacterium tuberculosis to bedaquiline', *PloS One*, 9: e102135.

Armstrong, J. A., and P. D. Hart. 1971. 'Response of cultured macrophages to Mycobacterium tuberculosis, with observations on fusion of lysosomes with phagosomes', *Journal of Experimental Medicine*, 134: 713-40.

Aubry, A., X. S. Pan, L. M. Fisher, V. Jarlier, and E. Cambau. 2004. 'Mycobacterium tuberculosis DNA gyrase: interaction with quinolones and correlation with antimycobacterial drug activity', *Antimicrobial Agents and Chemotherapy*, 48: 1281-8.

Augenstreich, J., A. Arbues, R. Simeone, E. Haanappel, A. Wegener, F. Sayes, F. Le Chevalier, C. Chalut, W. Malaga, C. Guilhot, R. Brosch, and C. Astarie-Dequeker. 2017. 'ESX-1 and phthiocerol dimycocerosates of Mycobacterium tuberculosis act in concert to cause phagosomal rupture and host cell apoptosis', *Cellular Microbiology*, 19.

Awasthi, D., and J. S. Freundlich. 2017. 'Antimycobacterial Metabolism: Illuminating Mycobacterium tuberculosis Biology and Drug Discovery', *Trends in Microbiology*, 25: 756-67.

Baik, J., and G. R. Rosania. 2012. 'Macrophages sequester clofazimine in an intracellular liquid crystal-like supramolecular organization', *PloS One*, 7: e47494.

Barry, C. E., 3rd, H. I. Boshoff, V. Dartois, T. Dick, S. Ehrt, J. Flynn, D. Schnappinger, R. J. Wilkinson, and D. Young. 2009. 'The spectrum of latent tuberculosis: rethinking the biology and intervention strategies', *Nature Reviews: Microbiology*, 7: 845-55.

Barry, V. C., J. G. Belton, M. L. Conalty, J. M. Denneny, D. W. Edward, J. F. O'Sullivan, D. Twomey, and F. Winder. 1957. 'A new series of phenazines (rimino-compounds) with high antituberculosis activity', *Nature*, 179: 1013-5.

Behar, S. M., M. Divangahi, and H. G. Remold. 2010. 'Evasion of innate immunity by Mycobacterium tuberculosis: is death an exit strategy?', *Nature Reviews: Microbiology*, 8: 668-74.

Belanger, A. E., G. S. Besra, M. E. Ford, K. Mikusova, J. T. Belisle, P. J. Brennan, and J. M. Inamine. 1996. 'The embAB genes of Mycobacterium avium encode an arabinosyl transferase involved in cell wall arabinan biosynthesis that is the target for the antimycobacterial drug ethambutol', *Proceedings of the National Academy of Sciences of the United States of America*, 93: 11919-24.

Blanc, L., I. B. Daudelin, B. K. Podell, P. Y. Chen, M. Zimmerman, A. J. Martinot, R. M. Savic, B. Prideaux, and V. Dartois. 2018. 'High-resolution mapping of fluoroquinolones in TB rabbit lesions reveals specific distribution in immune cell types', *Elife*, 7.

Blanc, L., J. P. Sarathy, N. Alvarez Cabrera, P. O'Brien, I. Dias-Freedman, M. Mina, J. Sacchettini, R. M. Savic, M. Gengenbacher, B. K. Podell, B. Prideaux, T. Ioerger, T. Dick, and V. Dartois. 2018. 'Impact of immunopathology on the antituberculous activity of pyrazinamide', *Journal of Experimental Medicine*, 215: 1975-86.

Bloch, H., and W. Segal. 1956. 'Biochemical differentiation of Mycobacterium tuberculosis grown in vivo and in vitro', *Journal of Bacteriology*, 72: 132-41.

Boeree, M. J., A. H. Diacon, R. Dawson, K. Narunsky, J. Bois, and A. Venter. 2015. 'A dose-ranging trial to optimize the dose of rifampin in the treatment of tuberculosis', *American Journal of Respiratory and Critical Care Medicine*, 191.

Burman, W. J., K. Gallicano, and C. Peloquin. 2001. 'Comparative pharmacokinetics and pharmacodynamics of the rifamycin antibacterials', *Clinical Pharmacokinetics*, 40: 327-41.

Caceres, N., G. Tapia, I. Ojanguren, F. Altare, O. Gil, S. Pinto, C. Vilaplana, and P. J. Cardona. 2009. 'Evolution of foamy macrophages in the pulmonary granulomas of experimental tuberculosis models', *Tuberculosis (Edinb)*, 89: 175-82.

Cadena, A. M., J. L. Flynn, and S. M. Fortune. 2016. 'The Importance of First Impressions: Early Events in Mycobacterium tuberculosis Infection Influence Outcome', *mBio*, 7: e00342-16.

Caire-Brandli, I., A. Papadopoulos, W. Malaga, D. Marais, S. Canaan, L. Thilo, and C. de Chastellier. 2014. 'Reversible lipid accumulation and associated division arrest of Mycobacterium avium in lipoprotein-induced foamy macrophages may resemble key events during latency and reactivation of tuberculosis', *Infection and Immunity*, 82: 476-90.

Cambier, C. J., K. K. Takaki, R. P. Larson, R. E. Hernandez, D. M. Tobin, K. B. Urdahl, C. L. Cosma, and L. Ramakrishnan. 2014. 'Mycobacteria manipulate macrophage recruitment through coordinated use of membrane lipids', *Nature*, 505: 218-22.

Cellitti, S. E., J. Shaffer, D. H. Jones, T. Mukherjee, M. Gurumurthy, B. Bursulaya, H. I. Boshoff, I. Choi, A. Nayyar, Y. S. Lee, J. Cherian, P. Niyomrattanakit, T. Dick, U. H. Manjunatha, C. E. Barry, 3rd, G. Spraggon, and B. H. Geierstanger. 2012. 'Structure of Ddn, the deazaflavin-dependent nitroreductase from Mycobacterium tuberculosis involved in bioreductive activation of PA-824', *Structure*, 20: 101-12.

Chakraborty, S., and K. Y. Rhee. 2015. 'Tuberculosis Drug Development: History and Evolution of the Mechanism-Based Paradigm', *Cold Spring Harbor Perspectives in Medicine*, 5: a021147.

Chen, C., S. Gardete, R. S. Jansen, A. Shetty, T. Dick, K. Y. Rhee, and V. Dartois. 2018. 'Verapamil Targets Membrane Energetics in Mycobacterium tuberculosis', *Antimicrobial Agents and Chemotherapy*, 62.

Chen, M., H. Gan, and H. G. Remold. 2006. 'A mechanism of virulence: virulent Mycobacterium tuberculosis strain H37Rv, but not attenuated H37Ra, causes significant mitochondrial inner membrane disruption in macrophages leading to necrosis', *Journal of Immunology*, 176: 3707-16.

Chen, X., H. Hashizume, T. Tomishige, I. Nakamura, M. Matsuba, M. Fujiwara, R. Kitamoto, E. Hanaki, Y. Ohba, and M. Matsumoto. 2017. 'Delamanid Kills Dormant Mycobacteria In

Vitro and in a Guinea Pig Model of Tuberculosis', *Antimicrobial Agents and Chemotherapy*, 61.

Cholo, M. C., M. T. Mothiba, B. Fourie, and R. Anderson. 2017. 'Mechanisms of action and therapeutic efficacies of the lipophilic antimycobacterial agents clofazimine and bedaquiline', *Journal of Antimicrobial Chemotherapy*, 72: 338-53.

Christophe, T., F. Ewann, H. K. Jeon, J. Cechetto, and P. Brodin. 2010. 'High-content imaging of Mycobacterium tuberculosis-infected macrophages: an in vitro model for tuberculosis drug discovery', *Future Medicinal Chemistry*, 2: 1283-93.

Christophe, T., M. Jackson, H. K. Jeon, D. Fenistein, M. Contreras-Dominguez, J. Kim, A. Genovesio, J. P. Carralot, F. Ewann, E. H. Kim, S. Y. Lee, S. Kang, M. J. Seo, E. J. Park, H. Skovierova, H. Pham, G. Riccardi, J. Y. Nam, L. Marsollier, M. Kempf, M. L. Joly-Guillou, T. Oh, W. K. Shin, Z. No, U. Nehrbass, R. Brosch, S. T. Cole, and P. Brodin. 2009. 'High content screening identifies decaprenyl-phosphoribose 2' epimerase as a target for intracellular antimycobacterial inhibitors', *PLoS Pathogens*, 5: e1000645.

Cole, S. T. 2016. 'Inhibiting Mycobacterium tuberculosis within and without', *Philosophical Transactions of the Royal Society of London. Series B: Biological Sciences*, 371.

Cole, S. T., R. Brosch, J. Parkhill, T. Garnier, C. Churcher, D. Harris, S. V. Gordon, K. Eiglmeier, S. Gas, C. E. Barry, 3rd, F. Tekaia, K. Badcock, D. Basham, D. Brown, T. Chillingworth, R. Connor, R. Davies, K. Devlin, T. Feltwell, S. Gentles, N. Hamlin, S. Holroyd, T. Hornsby, K. Jagels, A. Krogh, J. McLean, S. Moule, L. Murphy, K. Oliver, J. Osborne, M. A. Quail, M. A. Rajandream, J. Rogers, S. Rutter, K. Seeger, J. Skelton, R. Squares, S. Squares, J. E. Sulston, K. Taylor, S. Whitehead, and B. G. Barrell. 1998. 'Deciphering the biology of Mycobacterium tuberculosis from the complete genome sequence', *Nature*, 393: 537-44.

Coleman, M. T., R. Y. Chen, M. Lee, P. L. Lin, L. E. Dodd, P. Maiello, L. E. Via, Y. Kim, G. Marriner, V. Dartois, C. Scanga, C. Janssen, J. Wang, E. Klein, S. N. Cho, C. E. Barry, 3rd, and J. L. Flynn. 2014. 'PET/CT imaging reveals a therapeutic response to oxazolidinones in macaques and humans with tuberculosis', *Science Translational Medicine*, 6: 265ra167.

Connolly, L. E., P. H. Edelstein, and L. Ramakrishnan. 2007. 'Why is long-term therapy required to cure tuberculosis?', *PLoS Medicine*, 4: e120.

Conradie, F., A. H. Diacon, N. Ngubane, P. Howell, D. Everitt, A. M. Crook, C. M. Mendel, E. Egizi, J. Moreira, J. Timm, T. D. McHugh, G. H. Wills, A. Bateson, R. Hunt, C. Van Niekerk, M. Li, M. Olugbosi, M. Spigelman, and T. B. Trial Team Nix. 2020. 'Treatment of Highly Drug-Resistant Pulmonary Tuberculosis', *New England Journal of Medicine*, 382: 893-902.

Dallenga, T., and U. E. Schaible. 2016. 'Neutrophils in tuberculosis--first line of defence or booster of disease and targets for host-directed therapy?', *Pathog Dis*, 74.

Daniel, J., H. Maamar, C. Deb, T. D. Sirakova, and P. E. Kolattukudy. 2011. 'Mycobacterium tuberculosis uses host triacylglycerol to accumulate lipid droplets and acquires a dormancy-like phenotype in lipid-loaded macrophages', *PLoS Pathogens*, 7: e1002093.

Danilchanka, O., M. Pavlenok, and M. Niederweis. 2008. 'Role of porins for uptake of antibiotics by Mycobacterium smegmatis', *Antimicrobial Agents and Chemotherapy*, 52: 3127-34.

Dartois, V. 2014. 'The path of anti-tuberculosis drugs: from blood to lesions to mycobacterial cells', *Nature Reviews: Microbiology*, 12: 159-67.

Dartois, V., and C. E. Barry. 2010. 'Clinical pharmacology and lesion penetrating properties of second- and third-line antituberculous agents used in the management of multidrug-resistant (MDR) and extensively-drug resistant (XDR) tuberculosis', *Current Clinical Pharmacology*, 5: 96-114.

Dartois, V., and C. E. Barry, 3rd. 2013. 'A medicinal chemists' guide to the unique difficulties of lead optimization for tuberculosis', *Bioorganic and Medicinal Chemistry Letters*, 23: 4741-50.

Davies, G. R., and E. L. Nuermberger. 2008. 'Pharmacokinetics and pharmacodynamics in the development of anti-tuberculosis drugs', *Tuberculosis (Edinb)*, 88 Suppl 1: S65-74.

Davis, J. M., and L. Ramakrishnan. 2009. 'The role of the granuloma in expansion and dissemination of early tuberculous infection', *Cell*, 136: 37-49.

Diacon, A. H., R. Dawson, M. Hanekom, K. Narunsky, S. J. Maritz, A. Venter, P. R. Donald, C. van Niekerk, K. Whitney, D. J. Rouse, M. W. Laurenzi, A. M. Ginsberg, and M. K. Spigelman. 2010. 'Early bactericidal activity and pharmacokinetics of PA-824 in smear-positive tuberculosis patients', *Antimicrobial Agents and Chemotherapy*, 54: 3402-7.

Diacon, A. H., R. Dawson, M. Hanekom, K. Narunsky, A. Venter, N. Hittel, L. J. Geiter, C. D. Wells, A. J. Paccaly, and P. R. Donald. 2011. 'Early bactericidal activity of delamanid

(OPC-67683) in smear-positive pulmonary tuberculosis patients', *International Journal of Tuberculosis and Lung Disease*, 15: 949-54.

Diacon, A. H., P. R. Donald, A. Pym, M. Grobusch, R. F. Patientia, R. Mahanyele, N. Bantubani, R. Narasimooloo, T. De Marez, R. van Heeswijk, N. Lounis, P. Meyvisch, K. Andries, and D. F. McNeeley. 2012. 'Randomized pilot trial of eight weeks of bedaquiline (TMC207) treatment for multidrug-resistant tuberculosis: long-term outcome, tolerability, and effect on emergence of drug resistance', *Antimicrobial Agents and Chemotherapy*, 56: 3271-6.

Diacon, A. H., R. F. Patientia, A. Venter, P. D. van Helden, P. J. Smith, H. McIlleron, J. S. Maritz, and P. R. Donald. 2007. 'Early bactericidal activity of high-dose rifampin in patients with pulmonary tuberculosis evidenced by positive sputum smears', *Antimicrobial Agents and Chemotherapy*, 51: 2994-6.

Dietze, R., D. J. Hadad, B. McGee, L. P. Molino, E. L. Maciel, C. A. Peloquin, D. F. Johnson, S. M. Debanne, K. Eisenach, W. H. Boom, M. Palaci, and J. L. Johnson. 2008. 'Early and extended early bactericidal activity of linezolid in pulmonary tuberculosis', *American Journal of Respiratory and Critical Care Medicine*, 178: 1180-5.

Domenech, P., M. B. Reed, and C. E. Barry, 3rd. 2005. 'Contribution of the Mycobacterium tuberculosis MmpL protein family to virulence and drug resistance', *Infection and Immunity*, 73: 3492-501.

Dooley, K. E., E. E. Bliven-Sizemore, M. Weiner, Y. Lu, E. L. Nuermberger, W. C. Hubbard, E. J. Fuchs, M. T. Melia, W. J. Burman, and S. E. Dorman. 2012. 'Safety and pharmacokinetics of escalating daily doses of the antituberculosis drug rifapentine in healthy volunteers', *Clinical Pharmacology and Therapeutics*, 91: 881-8.

Dooley, K. E., R. M. Savic, J. G. Park, Y. Cramer, R. Hafner, E. Hogg, J. Janik, M. A. Marzinke, K. Patterson, C. A. Benson, L. Hovind, S. E. Dorman, D. W. Haas, and Actg A. Study Team. 2015. 'Novel dosing strategies increase exposures of the potent antituberculosis drug rifapentine but are poorly tolerated in healthy volunteers', *Antimicrobial Agents and Chemotherapy*, 59: 3399-405.

Dorman, S. E., S. Goldberg, J. E. Stout, G. Muzanyi, J. L. Johnson, and M. Weiner. 2012. 'Substitution of rifapentine for rifampin during intensive phase treatment of pulmonary tuberculosis: study 29 of the tuberculosis trials consortium', *Journal of Infectious Diseases*, 206.

Dorman, S. E., R. M. Savic, S. Goldberg, J. E. Stout, N. Schluger, G. Muzanyi, J. L. Johnson, P. Nahid, E. J. Hecker, C. M. Heilig, L. Bozeman, P. J. Feng, R. N. Moro, W. MacKenzie, K. E. Dooley, E. L. Nuermberger, A. Vernon, M. Weiner, and Consortium Tuberculosis Trials. 2015. 'Daily rifapentine for treatment of pulmonary tuberculosis. A randomized, dose-ranging trial', *American Journal of Respiratory and Critical Care Medicine*, 191: 333-43.

Driver, E. R., G. J. Ryan, D. R. Hoff, S. M. Irwin, R. J. Basaraba, I. Kramnik, and A. J. Lenaerts. 2012. 'Evaluation of a mouse model of necrotic granuloma formation using C3HeB/FeJ mice for testing of drugs against Mycobacterium tuberculosis', *Antimicrobial Agents and Chemotherapy*, 56: 3181-95.

Drlica, K., M. Malik, R. J. Kerns, and X. Zhao. 2008. 'Quinolone-mediated bacterial death', *Antimicrobial Agents and Chemotherapy*, 52: 385-92.

Drlica, K., and X. Zhao. 1997. 'DNA gyrase, topoisomerase IV, and the 4-quinolones', *Microbiology and Molecular Biology Reviews*, 61: 377-92.

Duan, L., H. Gan, D. E. Golan, and H. G. Remold. 2002. 'Critical role of mitochondrial damage in determining outcome of macrophage infection with Mycobacterium tuberculosis', *Journal of Immunology*, 169: 5181-7.

Ehrt, S., D. Schnappinger, and K. Y. Rhee. 2018. 'Metabolic principles of persistence and pathogenicity in Mycobacterium tuberculosis', *Nature Reviews: Microbiology*, 16: 496-507.

Eisenreich, W., J. Heesemann, T. Rudel, and W. Goebel. 2015. 'Metabolic Adaptations of Intracellullar Bacterial Pathogens and their Mammalian Host Cells during Infection ("Pathometabolism")', *Microbiol Spectr*, 3.

Ernst, J. D. 2012. 'The immunological life cycle of tuberculosis', *Nature Reviews: Immunology*, 12: 581-91.

Eum, S. Y., J. H. Kong, M. S. Hong, Y. J. Lee, J. H. Kim, S. H. Hwang, S. N. Cho, L. E. Via, and C. E. Barry, 3rd. 2010. 'Neutrophils are the predominant infected phagocytic cells in the airways of patients with active pulmonary TB', *Chest*, 137: 122-8.

Evans, J. C., and V. Mizrahi. 2015. 'The application of tetracyclineregulated gene expression systems in the validation of novel drug targets in Mycobacterium tuberculosis', *Frontiers in Microbiology*, 6: 812.

———. 2018. 'Priming the tuberculosis drug pipeline: new antimycobacterial targets and agents', *Current Opinion in Microbiology*, 45: 39-46.

Flynn, J. L., J. Chan, and P. L. Lin. 2011. 'Macrophages and control of granulomatous inflammation in tuberculosis', *Mucosal Immunology*, 4: 271-8.

Forbes, M., N. A. Kuck, and E. A. Peets. 1962. 'Mode of action of ethambutol', *Journal of Bacteriology*, 84: 1099-103.

Fortune, S. M., and E. J. Rubin. 2007. 'The complex relationship between mycobacteria and macrophages: it's not all bliss', *Cell Host Microbe*, 2: 5-6.

Fox, W., G. A. Ellard, and D. A. Mitchison. 1999. 'Studies on the treatment of tuberculosis undertaken by the British Medical Research Council tuberculosis units, 1946-1986, with relevant subsequent publications', *International Journal of Tuberculosis and Lung Disease*, 3: S231-79.

Franzblau, S. G., M. A. DeGroote, S. H. Cho, K. Andries, E. Nuermberger, I. M. Orme, K. Mdluli, I. Angulo-Barturen, T. Dick, V. Dartois, and A. J. Lenaerts. 2012. 'Comprehensive analysis of methods used for the evaluation of compounds against Mycobacterium tuberculosis', *Tuberculosis (Edinb)*, 92: 453-88.

Fratti, R. A., J. Chua, I. Vergne, and V. Deretic. 2003. 'Mycobacterium tuberculosis glycosylated phosphatidylinositol causes phagosome maturation arrest', *Proceedings of the National Academy of Sciences of the United States of America*, 100: 5437-42.

Gagneux, S. 2018. 'Ecology and evolution of Mycobacterium tuberculosis', *Nature Reviews: Microbiology*, 16: 202-13.

Gengenbacher, M., M. A. Duque-Correa, P. Kaiser, S. Schuerer, D. Lazar, U. Zedler, S. T. Reece, A. Nayyar, S. T. Cole, V. Makarov, C. E. Barry Iii, V. Dartois, and S. H. E. Kaufmann. 2017. 'NOS2-deficient mice with hypoxic necrotizing lung lesions predict outcomes of tuberculosis chemotherapy in humans', *Scientific Reports*, 7: 8853.

Gengenbacher, M., S. P. Rao, K. Pethe, and T. Dick. 2010. 'Nutrient-starved, non-replicating Mycobacterium tuberculosis requires respiration, ATP synthase and isocitrate lyase for maintenance of ATP homeostasis and viability', *Microbiology*, 156: 81-7.

Gillespie, S. H., A. M. Crook, T. D. McHugh, C. M. Mendel, S. K. Meredith, S. R. Murray, F. Pappas, P. P. Phillips, A. J. Nunn, and R. EMoxTB Consortium. 2014. 'Four-month

moxifloxacin-based regimens for drug-sensitive tuberculosis', *New England Journal of Medicine*, 371: 1577-87.

Gler, M. T., V. Skripconoka, E. Sanchez-Garavito, H. Xiao, J. L. Cabrera-Rivero, D. E. Vargas-Vasquez, M. Gao, M. Awad, S. K. Park, T. S. Shim, G. Y. Suh, M. Danilovits, H. Ogata, A. Kurve, J. Chang, K. Suzuki, T. Tupasi, W. J. Koh, B. Seaworth, L. J. Geiter, and C. D. Wells. 2012. 'Delamanid for multidrug-resistant pulmonary tuberculosis', *New England Journal of Medicine*, 366: 2151-60.

Goldman, R. C. 2013. 'Why are membrane targets discovered by phenotypic screens and genome sequencing in Mycobacterium tuberculosis?', *Tuberculosis (Edinb)*, 93: 569-88.

Gopal, M., N. Padayatchi, J. Z. Metcalfe, and M. R. O'Donnell. 2013. 'Systematic review of clofazimine for the treatment of drug-resistant tuberculosis', *International Journal of Tuberculosis and Lung Disease*, 17: 1001-7.

Gopal, P., G. Gruber, V. Dartois, and T. Dick. 2019. 'Pharmacological and Molecular Mechanisms Behind the Sterilizing Activity of Pyrazinamide', *Trends in Pharmacological Sciences*, 40: 930-40.

Gopal, P., W. Nartey, P. Ragunathan, J. Sarathy, F. Kaya, M. Yee, C. Setzer, M. S. S. Manimekalai, V. Dartois, G. Gruber, and T. Dick. 2017. 'Pyrazinoic Acid Inhibits Mycobacterial Coenzyme A Biosynthesis by Binding to Aspartate Decarboxylase PanD', *ACS Infect Dis*, 3: 807-19.

Gopal, P., J. P. Sarathy, M. Yee, P. Ragunathan, J. Shin, S. Bhushan, J. Zhu, T. Akopian, O. Kandror, T. K. Lim, M. Gengenbacher, Q. Lin, E. J. Rubin, G. Gruber, and T. Dick. 2020. 'Pyrazinamide triggers degradation of its target aspartate decarboxylase', *Nat Commun*, 11: 1661.

Gopal, P., R. Tasneen, M. Yee, J. P. Lanoix, J. Sarathy, G. Rasic, L. Li, V. Dartois, E. Nuermberger, and T. Dick. 2017. 'In Vivo-Selected Pyrazinoic Acid-Resistant Mycobacterium tuberculosis Strains Harbor Missense Mutations in the Aspartate Decarboxylase PanD and the Unfoldase ClpC1', *ACS Infect Dis*, 3: 492-501.

Goude, R., A. G. Amin, D. Chatterjee, and T. Parish. 2009. 'The arabinosyltransferase EmbC is inhibited by ethambutol in Mycobacterium tuberculosis', *Antimicrobial Agents and Chemotherapy*, 53: 4138-46.

Grant, S. S., T. Kawate, P. P. Nag, M. R. Silvis, K. Gordon, S. A. Stanley, E. Kazyanskaya, R. Nietupski, A. Golas, M. Fitzgerald, S. Cho, S. G. Franzblau, and D. T. Hung. 2013. 'Identification of novel inhibitors of nonreplicating Mycobacterium tuberculosis using a carbon starvation model', *ACS Chemical Biology*, 8: 2224-34.

Grzelak, E. M., M. P. Choules, W. Gao, G. Cai, B. Wan, Y. Wang, J. B. McAlpine, J. Cheng, Y. Jin, H. Lee, J. W. Suh, G. F. Pauli, S. G. Franzblau, B. U. Jaki, and S. Cho. 2019. 'Strategies in anti-Mycobacterium tuberculosis drug discovery based on phenotypic screening', *Journal of Antibiotics*, 72: 719-28.

Gumbo, T., A. Louie, M. R. Deziel, L. M. Parsons, M. Salfinger, and G. L. Drusano. 2004. 'Selection of a moxifloxacin dose that suppresses drug resistance in Mycobacterium tuberculosis, by use of an in vitro pharmacodynamic infection model and mathematical modeling', *Journal of Infectious Diseases*, 190: 1642-51.

Gumbo, T., J. G. Pasipanodya, K. Romero, D. Hanna, and E. Nuermberger. 2015. 'Forecasting Accuracy of the Hollow Fiber Model of Tuberculosis for Clinical Therapeutic Outcomes', *Clinical Infectious Diseases*, 61 Suppl 1: S25-31.

Gupta, S., K. A. Cohen, K. Winglee, M. Maiga, B. Diarra, and W. R. Bishai. 2014. 'Efflux inhibition with verapamil potentiates bedaquiline in Mycobacterium tuberculosis', *Antimicrobial Agents and Chemotherapy*, 58: 574-6.

Haagsma, A. C., I. Podasca, A. Koul, K. Andries, J. Guillemont, H. Lill, and D. Bald. 2011. 'Probing the interaction of the diarylquinoline TMC207 with its target mycobacterial ATP synthase', *PloS One*, 6: e23575.

Harbeck, R. J., G. S. Worthen, T. D. Lebo, and C. A. Peloquin. 1999. 'Clofazimine crystals in the cytoplasm of pulmonary macrophages', *Annals of Pharmacotherapy*, 33: 250.

Hartkoorn, R. C., S. Uplekar, and S. T. Cole. 2014. 'Cross-resistance between clofazimine and bedaquiline through upregulation of MmpL5 in Mycobacterium tuberculosis', *Antimicrobial Agents and Chemotherapy*, 58: 2979-81.

Houben, R. M., and P. J. Dodd. 2016. 'The Global Burden of Latent Tuberculosis Infection: A Re-estimation Using Mathematical Modelling', *PLoS Medicine*, 13: e1002152.

Huang, L., E. V. Nazarova, S. Tan, Y. Liu, and D. G. Russell. 2018. 'Growth of Mycobacterium tuberculosis in vivo segregates with host macrophage metabolism and ontogeny', *Journal of Experimental Medicine*, 215: 1135-52.

Irwin, S. M., V. Gruppo, E. Brooks, J. Gilliland, M. Scherman, M. J. Reichlen, R. Leistikow, I. Kramnik, E. L. Nuermberger, M. I. Voskuil, and A. J. Lenaerts. 2014. 'Limited activity of clofazimine as a single drug in a mouse model of tuberculosis exhibiting caseous necrotic granulomas', *Antimicrobial Agents and Chemotherapy*, 58: 4026-34.

Irwin, S. M., B. Prideaux, E. R. Lyon, M. D. Zimmerman, E. J. Brooks, C. A. Schrupp, C. Chen, M. J. Reichlen, B. C. Asay, M. I. Voskuil, E. L. Nuermberger, K. Andries, M. A. Lyons, V. Dartois, and A. J. Lenaerts. 2016. 'Bedaquiline and Pyrazinamide Treatment Responses Are Affected by Pulmonary Lesion Heterogeneity in Mycobacterium tuberculosis Infected C3HeB/FeJ Mice', *ACS Infect Dis*, 2: 251-67.

Jamieson, F. B., J. L. Guthrie, A. Neemuchwala, O. Lastovetska, R. G. Melano, and C. Mehaffy. 2014. 'Profiling of rpoB mutations and MICs for rifampin and rifabutin in Mycobacterium tuberculosis', *Journal of Clinical Microbiology*, 52: 2157-62.

Johnson, E. O., E. LaVerriere, E. Office, M. Stanley, E. Meyer, T. Kawate, J. E. Gomez, R. E. Audette, N. Bandyopadhyay, N. Betancourt, K. Delano, I. Da Silva, J. Davis, C. Gallo, M. Gardner, A. J. Golas, K. M. Guinn, S. Kennedy, R. Korn, J. A. McConnell, C. E. Moss, K. C. Murphy, R. M. Nietupski, K. G. Papavinasasundaram, J. T. Pinkham, P. A. Pino, M. K. Proulx, N. Ruecker, N. Song, M. Thompson, C. Trujillo, S. Wakabayashi, J. B. Wallach, C. Watson, T. R. Ioerger, E. S. Lander, B. K. Hubbard, M. H. Serrano-Wu, S. Ehrt, M. Fitzgerald, E. J. Rubin, C. M. Sassetti, D. Schnappinger, and D. T. Hung. 2019. 'Large-scale chemical-genetics yields new M. tuberculosis inhibitor classes', *Nature*, 571: 72-78.

Kalscheuer, R., A. Palacios, I. Anso, J. Cifuente, J. Anguita, W. R. Jacobs, Jr., M. E. Guerin, and R. Prados-Rosales. 2019. 'The Mycobacterium tuberculosis capsule: a cell structure with key implications in pathogenesis', *Biochemical Journal*, 476: 1995-2016.

Keam, S. J. 2019. 'Pretomanid: First Approval', *Drugs*, 79: 1797-803.

Kempker, R. R., M. T. Heinrichs, K. Nikolaishvili, I. Sabulua, N. Bablishvili, S. Gogishvili, Z. Avaliani, N. Tukvadze, B. Little, A. Bernheim, T. D. Read, J. Guarner, H. Derendorf, C. A. Peloquin, H. M. Blumberg, and S. Vashakidze. 2017. 'Lung Tissue Concentrations of Pyrazinamide among Patients with Drug-Resistant Pulmonary Tuberculosis', *Antimicrobial Agents and Chemotherapy*, 61.

Kim, M. J., H. C. Wainwright, M. Locketz, L. G. Bekker, G. B. Walther, C. Dittrich, A. Visser, W. Wang, F. F. Hsu, U. Wiehart, L. Tsenova, G. Kaplan, and D. G. Russell. 2010.

'Caseation of human tuberculosis granulomas correlates with elevated host lipid metabolism', *EMBO Molecular Medicine*, 2: 258-74.

Kjellsson, M. C., L. E. Via, A. Goh, D. Weiner, K. M. Low, S. Kern, G. Pillai, C. E. Barry, 3rd, and V. Dartois. 2012. 'Pharmacokinetic evaluation of the penetration of antituberculosis agents in rabbit pulmonary lesions', *Antimicrobial Agents and Chemotherapy*, 56: 446-57.

Knight, M., J. Braverman, K. Asfaha, K. Gronert, and S. Stanley. 2018. 'Lipid droplet formation in Mycobacterium tuberculosis infected macrophages requires IFN-gamma/HIF-1alpha signaling and supports host defense', *PLoS Pathogens*, 14: e1006874.

Koul, A., E. Arnoult, N. Lounis, J. Guillemont, and K. Andries. 2011. 'The challenge of new drug discovery for tuberculosis', *Nature*, 469: 483-90.

Koul, A., N. Dendouga, K. Vergauwen, B. Molenberghs, L. Vranckx, R. Willebrords, Z. Ristic, H. Lill, I. Dorange, J. Guillemont, D. Bald, and K. Andries. 2007. 'Diarylquinolines target subunit c of mycobacterial ATP synthase', *Nature Chemical Biology*, 3: 323-4.

Lakshminarayana, S. B., T. B. Huat, P. C. Ho, U. H. Manjunatha, V. Dartois, T. Dick, and S. P. Rao. 2015. 'Comprehensive physicochemical, pharmacokinetic and activity profiling of anti-TB agents', *Journal of Antimicrobial Chemotherapy*, 70: 857-67.

Lamont, E. A., N. A. Dillon, and A. D. Baughn. 2020. 'The Bewildering Antitubercular Action of Pyrazinamide', *Microbiology and Molecular Biology Reviews*, 84.

Lanoix, J. P., F. Betoudji, and E. Nuermberger. 2016. 'Sterilizing Activity of Pyrazinamide in Combination with First-Line Drugs in a C3HeB/FeJ Mouse Model of Tuberculosis', *Antimicrobial Agents and Chemotherapy*, 60: 1091-6.

Lanoix, J. P., T. Ioerger, A. Ormond, F. Kaya, J. Sacchettini, V. Dartois, and E. Nuermberger. 2016. 'Selective Inactivity of Pyrazinamide against Tuberculosis in C3HeB/FeJ Mice Is Best Explained by Neutral pH of Caseum', *Antimicrobial Agents and Chemotherapy*, 60: 735-43.

Lechartier, B., J. Rybniker, A. Zumla, and S. T. Cole. 2014. 'Tuberculosis drug discovery in the post-post-genomic era', *EMBO Molecular Medicine*, 6: 158-68.

Lee, M., J. Lee, M. W. Carroll, H. Choi, S. Min, T. Song, L. E. Via, L. C. Goldfeder, E. Kang, B. Jin, H. Park, H. Kwak, H. Kim, H. S. Jeon, I. Jeong, J. S. Joh, R. Y. Chen, K. N. Olivier, P. A. Shaw, D. Follmann, S. D. Song, J. K. Lee, D. Lee, C. T. Kim, V. Dartois, S. K. Park,

S. N. Cho, and C. E. Barry, 3rd. 2012. 'Linezolid for treatment of chronic extensively drug-resistant tuberculosis', *New England Journal of Medicine*, 367: 1508-18.

Lee, S. S., G. Meintjes, A. Kamarulzaman, and C. C. Leung. 2013. 'Management of tuberculosis and latent tuberculosis infection in human immunodeficiency virus-infected persons', *Respirology*, 18: 912-22.

Lee, W., B. C. VanderVen, R. J. Fahey, and D. G. Russell. 2013. 'Intracellular Mycobacterium tuberculosis exploits host-derived fatty acids to limit metabolic stress', *Journal of Biological Chemistry*, 288: 6788-800.

Lei, B., C. J. Wei, and S. C. Tu. 2000. 'Action mechanism of antitubercular isoniazid. Activation by Mycobacterium tuberculosis KatG, isolation, and characterization of inha inhibitor', *Journal of Biological Chemistry*, 275: 2520-6.

Lemaitre, N., I. Callebaut, F. Frenois, V. Jarlier, and W. Sougakoff. 2001. 'Study of the structure-activity relationships for the pyrazinamidase (PncA) from Mycobacterium tuberculosis', *Biochemical Journal*, 353: 453-8.

Lenaerts, A., C. E. Barry, 3rd, and V. Dartois. 2015. 'Heterogeneity in tuberculosis pathology, microenvironments and therapeutic responses', *Immunological Reviews*, 264: 288-307.

Levitte, S., K. N. Adams, R. D. Berg, C. L. Cosma, K. B. Urdahl, and L. Ramakrishnan. 2016. 'Mycobacterial Acid Tolerance Enables Phagolysosomal Survival and Establishment of Tuberculous Infection In Vivo', *Cell Host Microbe*, 20: 250-8.

Levy, L. 1974. 'Pharmacologic studies of clofazimine', *American Journal of Tropical Medicine and Hygiene*, 23: 1097-109.

Li, S. Y., R. Tasneen, S. Tyagi, H. Soni, P. J. Converse, K. Mdluli, and E. L. Nuermberger. 2017. 'Bactericidal and Sterilizing Activity of a Novel Regimen with Bedaquiline, Pretomanid, Moxifloxacin, and Pyrazinamide in a Murine Model of Tuberculosis', *Antimicrobial Agents and Chemotherapy*, 61.

Lin, P. L., C. B. Ford, M. T. Coleman, A. J. Myers, R. Gawande, T. Ioerger, J. Sacchettini, S. M. Fortune, and J. L. Flynn. 2014. 'Sterilization of granulomas is common in active and latent tuberculosis despite within-host variability in bacterial killing', *Nature Medicine*, 20: 75-9.

Lok, H. C., S. Sahni, P. J. Jansson, Z. Kovacevic, C. L. Hawkins, and D. R. Richardson. 2016. 'A Nitric Oxide Storage and Transport System That Protects Activated Macrophages from Endogenous Nitric Oxide Cytotoxicity', *Journal of Biological Chemistry*, 291: 27042-61.

Lovewell, R. R., C. E. Baer, B. B. Mishra, C. M. Smith, and C. M. Sassetti. 2020. 'Granulocytes act as a niche for Mycobacterium tuberculosis growth', *Mucosal Immunology*.

Lowe, D. M., P. S. Redford, R. J. Wilkinson, A. O'Garra, and A. R. Martineau. 2012. 'Neutrophils in tuberculosis: friend or foe?', *Trends in Immunology*, 33: 14-25.

Mabhula, A., and V. Singh. 2019. 'Drug-resistance in Mycobacterium tuberculosis: where we stand', *Medchemcomm*, 10: 1342-60.

Mahajan, R. 2013. 'Bedaquiline: First FDA-approved tuberculosis drug in 40 years', *Int J Appl Basic Med Res*, 3: 1-2.

Mahamed, D., M. Boulle, Y. Ganga, C. Mc Arthur, S. Skroch, L. Oom, O. Catinas, K. Pillay, M. Naicker, S. Rampersad, C. Mathonsi, J. Hunter, E. B. Wong, M. Suleman, G. Sreejit, A. S. Pym, G. Lustig, and A. Sigal. 2017. 'Intracellular growth of Mycobacterium tuberculosis after macrophage cell death leads to serial killing of host cells', *Elife*, 6.

Makarov, V., G. Manina, K. Mikusova, U. Mollmann, O. Ryabova, B. Saint-Joanis, N. Dhar, M. R. Pasca, S. Buroni, A. P. Lucarelli, A. Milano, E. De Rossi, M. Belanova, A. Bobovska, P. Dianiskova, J. Kordulakova, C. Sala, E. Fullam, P. Schneider, J. D. McKinney, P. Brodin, T. Christophe, S. Waddell, P. Butcher, J. Albrethsen, I. Rosenkrands, R. Brosch, V. Nandi, S. Bharath, S. Gaonkar, R. K. Shandil, V. Balasubramanian, T. Balganesh, S. Tyagi, J. Grosset, G. Riccardi, and S. T. Cole. 2009. 'Benzothiazinones kill Mycobacterium tuberculosis by blocking arabinan synthesis', *Science*, 324: 801-4.

Manjunatha, U., H. I. Boshoff, and C. E. Barry. 2009. 'The mechanism of action of PA-824: Novel insights from transcriptional profiling', *Communicative & Integrative Biology*, 2: 215-8.

Marakalala, M. J., R. M. Raju, K. Sharma, Y. J. Zhang, E. A. Eugenin, B. Prideaux, I. B. Daudelin, P. Y. Chen, M. G. Booty, J. H. Kim, S. Y. Eum, L. E. Via, S. M. Behar, C. E. Barry, 3rd, M. Mann, V. Dartois, and E. J. Rubin. 2016. 'Inflammatory signaling in human tuberculosis granulomas is spatially organized', *Nature Medicine*, 22: 531-8.

Marquez, B., N. E. Caceres, M. P. Mingeot-Leclercq, P. M. Tulkens, and F. Van Bambeke. 2009. 'Identification of the efflux transporter of the fluoroquinolone antibiotic ciprofloxacin in murine macrophages: studies with ciprofloxacin-resistant cells', *Antimicrobial Agents and Chemotherapy*, 53: 2410-6.

Marrero, J., C. Trujillo, K. Y. Rhee, and S. Ehrt. 2013. 'Glucose phosphorylation is required for Mycobacterium tuberculosis persistence in mice', *PLoS Pathogens*, 9: e1003116.

Martin, C. J., M. G. Booty, T. R. Rosebrock, C. Nunes-Alves, D. M. Desjardins, I. Keren, S. M. Fortune, H. G. Remold, and S. M. Behar. 2012. 'Efferocytosis is an innate antibacterial mechanism', *Cell Host Microbe*, 12: 289-300.

Mashabela, G. T., T. J. de Wet, and D. F. Warner. 2019. 'Mycobacterium tuberculosis Metabolism', *Microbiol Spectr*, 7.

Matsumoto, M., H. Hashizume, T. Tomishige, M. Kawasaki, H. Tsubouchi, H. Sasaki, Y. Shimokawa, and M. Komatsu. 2006. 'OPC-67683, a nitro-dihydro-imidazooxazole derivative with promising action against tuberculosis in vitro and in mice', *PLoS Medicine*, 3: e466.

McKinney, J. D., K. Honer zu Bentrup, E. J. Munoz-Elias, A. Miczak, B. Chen, W. T. Chan, D. Swenson, J. C. Sacchettini, W. R. Jacobs, Jr., and D. G. Russell. 2000. 'Persistence of Mycobacterium tuberculosis in macrophages and mice requires the glyoxylate shunt enzyme isocitrate lyase', *Nature*, 406: 735-8.

Michailidis, C., A. L. Pozniak, S. Mandalia, S. Basnayake, M. R. Nelson, and B. G. Gazzard. 2005. 'Clinical characteristics of IRIS syndrome in patients with HIV and tuberculosis', *Antiviral Therapy*, 10: 417-22.

Mitchison, D. A. 1985. 'The action of antituberculosis drugs in short-course chemotherapy', *Tubercle*, 66: 219-25.

Mitchison, D. A., and A. R. Coates. 2004. 'Predictive in vitro models of the sterilizing activity of anti-tuberculosis drugs', *Current Pharmaceutical Design*, 10: 3285-95.

Mitchison, D., and G. Davies. 2012. 'The chemotherapy of tuberculosis: past, present and future', *International Journal of Tuberculosis and Lung Disease*, 16: 724-32.

Moreau, A., M. Le Vee, E. Jouan, Y. Parmentier, and O. Fardel. 2011. 'Drug transporter expression in human macrophages', *Fundamental and Clinical Pharmacology*, 25: 743-52.

Moreira, W., G. J. Ngan, J. L. Low, A. Poulsen, B. C. Chia, M. J. Ang, A. Yap, J. Fulwood, U. Lakshmanan, J. Lim, A. Y. Khoo, H. Flotow, J. Hill, R. M. Raju, E. J. Rubin, and T. Dick. 2015. 'Target mechanism-based whole-cell screening identifies bortezomib as an inhibitor of caseinolytic protease in mycobacteria', *mBio*, 6: e00253-15.

Munoz-Elias, E. J., and J. D. McKinney. 2005. 'Mycobacterium tuberculosis isocitrate lyases 1 and 2 are jointly required for in vivo growth and virulence', *Nature Medicine*, 11: 638-44.

Murray, J. F., D. E. Schraufnagel, and P. C. Hopewell. 2015. 'Treatment of Tuberculosis. A Historical Perspective', *Ann Am Thorac Soc*, 12: 1749-59.

Nakajima, A., T. Fukami, Y. Kobayashi, A. Watanabe, M. Nakajima, and T. Yokoi. 2011. 'Human arylacetamide deacetylase is responsible for deacetylation of rifamycins: rifampicin, rifabutin, and rifapentine', *Biochemical Pharmacology*, 82: 1747-56.

Nazarova, E. V., C. R. Montague, L. Huang, T. La, D. Russell, and B. C. VanderVen. 2019. 'The genetic requirements of fatty acid import by Mycobacterium tuberculosis within macrophages', *Elife*, 8.

Nazarova, E. V., C. R. Montague, T. La, K. M. Wilburn, N. Sukumar, W. Lee, S. Caldwell, D. G. Russell, and B. C. VanderVen. 2017. 'Rv3723/LucA coordinates fatty acid and cholesterol uptake in Mycobacterium tuberculosis', *Elife*, 6.

Nielsen, E. I., and L. E. Friberg. 2013. 'Pharmacokinetic-pharmacodynamic modeling of antibacterial drugs', *Pharmacological Reviews*, 65: 1053-90.

Nuermberger, E. L., T. Yoshimatsu, S. Tyagi, R. J. O'Brien, A. N. Vernon, R. E. Chaisson, W. R. Bishai, and J. H. Grosset. 2004. 'Moxifloxacin-containing regimen greatly reduces time to culture conversion in murine tuberculosis', *American Journal of Respiratory and Critical Care Medicine*, 169: 421-6.

Nuermberger, E. L., T. Yoshimatsu, S. Tyagi, K. Williams, I. Rosenthal, R. J. O'Brien, A. A. Vernon, R. E. Chaisson, W. R. Bishai, and J. H. Grosset. 2004. 'Moxifloxacin-containing regimens of reduced duration produce a stable cure in murine tuberculosis', *American Journal of Respiratory and Critical Care Medicine*, 170: 1131-4.

O'Garra, A., P. S. Redford, F. W. McNab, C. I. Bloom, R. J. Wilkinson, and M. P. Berry. 2013. 'The immune response in tuberculosis', *Annual Review of Immunology*, 31: 475-527.

O'Neill, L. A., R. J. Kishton, and J. Rathmell. 2016. 'A guide to immunometabolism for immunologists', *Nature Reviews: Immunology*, 16: 553-65.

Orme, I. M., and R. J. Basaraba. 2014. 'The formation of the granuloma in tuberculosis infection', *Seminars in Immunology*, 26: 601-9.

Ouimet, M., S. Koster, E. Sakowski, B. Ramkhelawon, C. van Solingen, S. Oldebeken, D. Karunakaran, C. Portal-Celhay, F. J. Sheedy, T. D. Ray, K. Cecchini, P. D. Zamore, K. J. Rayner, Y. L. Marcel, J. A. Philips, and K. J. Moore. 2016. 'Mycobacterium tuberculosis

induces the miR-33 locus to reprogram autophagy and host lipid metabolism', *Nature Immunology*, 17: 677-86.

Park, Y., A. Pacitto, T. Bayliss, L. A. Cleghorn, Z. Wang, T. Hartman, K. Arora, T. R. Ioerger, J. Sacchettini, M. Rizzi, S. Donini, T. L. Blundell, D. B. Ascher, K. Rhee, A. Breda, N. Zhou, V. Dartois, S. R. Jonnala, L. E. Via, V. Mizrahi, O. Epemolu, L. Stojanovski, F. Simeons, M. Osuna-Cabello, L. Ellis, C. J. MacKenzie, A. R. Smith, S. H. Davis, D. Murugesan, K. I. Buchanan, P. A. Turner, M. Huggett, F. Zuccotto, M. J. Rebollo-Lopez, M. J. Lafuente-Monasterio, O. Sanz, G. S. Diaz, J. Lelievre, L. Ballell, C. Selenski, M. Axtman, S. Ghidelli-Disse, H. Pflaumer, M. Bosche, G. Drewes, G. M. Freiberg, M. D. Kurnick, M. Srikumaran, D. J. Kempf, S. R. Green, P. C. Ray, K. Read, P. Wyatt, C. E. Barry, 3rd, and H. I. Boshoff. 2017. 'Essential but Not Vulnerable: Indazole Sulfonamides Targeting Inosine Monophosphate Dehydrogenase as Potential Leads against Mycobacterium tuberculosis', *ACS Infect Dis*, 3: 18-33.

Pasipanodya, J. G., H. McIlleron, A. Burger, P. A. Wash, P. Smith, and T. Gumbo. 2013. 'Serum drug concentrations predictive of pulmonary tuberculosis outcomes', *Journal of Infectious Diseases*, 208: 1464-73.

Pasipanodya, J. G., E. Nuermberger, K. Romero, D. Hanna, and T. Gumbo. 2015. 'Systematic Analysis of Hollow Fiber Model of Tuberculosis Experiments', *Clinical Infectious Diseases*, 61 Suppl 1: S10-7.

Pasipanodya, J. G., S. Srivastava, and T. Gumbo. 2012. 'Meta-analysis of clinical studies supports the pharmacokinetic variability hypothesis for acquired drug resistance and failure of antituberculosis therapy', *Clinical Infectious Diseases*, 55: 169-77.

Peloquin, C. A., D. J. Hadad, L. P. Molino, M. Palaci, W. H. Boom, R. Dietze, and J. L. Johnson. 2008. 'Population pharmacokinetics of levofloxacin, gatifloxacin, and moxifloxacin in adults with pulmonary tuberculosis', *Antimicrobial Agents and Chemotherapy*, 52: 852-7.

Peloquin, C. A., G. E. Velasquez, L. Lecca, R. I. Calderon, J. Coit, M. Milstein, E. Osso, J. Jimenez, K. Tintaya, E. Sanchez Garavito, D. Vargas Vasquez, C. D. Mitnick, and G. Davies. 2017. 'Pharmacokinetic Evidence from the HIRIF Trial To Support Increased Doses of Rifampin for Tuberculosis', *Antimicrobial Agents and Chemotherapy*, 61.

Pethe, K., P. Bifani, J. Jang, S. Kang, S. Park, S. Ahn, J. Jiricek, J. Jung, H. K. Jeon, J. Cechetto, T. Christophe, H. Lee, M. Kempf, M. Jackson, A. J. Lenaerts, H. Pham, V. Jones, M. J.

Seo, Y. M. Kim, M. Seo, J. J. Seo, D. Park, Y. Ko, I. Choi, R. Kim, S. Y. Kim, S. Lim, S. A. Yim, J. Nam, H. Kang, H. Kwon, C. T. Oh, Y. Cho, Y. Jang, J. Kim, A. Chua, B. H. Tan, M. B. Nanjundappa, S. P. Rao, W. S. Barnes, R. Wintjens, J. R. Walker, S. Alonso, S. Lee, J. Kim, S. Oh, T. Oh, U. Nehrbass, S. J. Han, Z. No, J. Lee, P. Brodin, S. N. Cho, K. Nam, and J. Kim. 2013. 'Discovery of Q203, a potent clinical candidate for the treatment of tuberculosis', *Nature Medicine*, 19: 1157-60.

Pethe, K., P. C. Sequeira, S. Agarwalla, K. Rhee, K. Kuhen, W. Y. Phong, V. Patel, D. Beer, J. R. Walker, J. Duraiswamy, J. Jiricek, T. H. Keller, A. Chatterjee, M. P. Tan, M. Ujjini, S. P. Rao, L. Camacho, P. Bifani, P. A. Mak, I. Ma, S. W. Barnes, Z. Chen, D. Plouffe, P. Thayalan, S. H. Ng, M. Au, B. H. Lee, B. H. Tan, S. Ravindran, M. Nanjundappa, X. Lin, A. Goh, S. B. Lakshminarayana, C. Shoen, M. Cynamon, B. Kreiswirth, V. Dartois, E. C. Peters, R. Glynne, S. Brenner, and T. Dick. 2010. 'A chemical genetic screen in Mycobacterium tuberculosis identifies carbon-source-dependent growth inhibitors devoid of in vivo efficacy', *Nat Commun*, 1: 57.

Peyron, P., J. Vaubourgeix, Y. Poquet, F. Levillain, C. Botanch, F. Bardou, M. Daffe, J. F. Emile, B. Marchou, P. J. Cardona, C. de Chastellier, and F. Altare. 2008. 'Foamy macrophages from tuberculous patients' granulomas constitute a nutrient-rich reservoir for M. tuberculosis persistence', *PLoS Pathogens*, 4: e1000204.

Philips, J. A., and J. D. Ernst. 2012. 'Tuberculosis pathogenesis and immunity', *Annual Review of Pathology*, 7: 353-84.

Pienaar, E., J. Sarathy, B. Prideaux, J. Dietzold, V. Dartois, D. E. Kirschner, and J. J. Linderman. 2017. 'Comparing efficacies of moxifloxacin, levofloxacin and gatifloxacin in tuberculosis granulomas using a multi-scale systems pharmacology approach', *PLoS Computational Biology*, 13: e1005650.

Prideaux, B., V. Dartois, D. Staab, D. M. Weiner, A. Goh, L. E. Via, C. E. Barry, 3rd, and M. Stoeckli. 2011. 'High-sensitivity MALDI-MRM-MS imaging of moxifloxacin distribution in tuberculosis-infected rabbit lungs and granulomatous lesions', *Analytical Chemistry*, 83: 2112-8.

Prideaux, B., L. E. Via, M. D. Zimmerman, S. Eum, J. Sarathy, P. O'Brien, C. Chen, F. Kaya, D. M. Weiner, P. Y. Chen, T. Song, M. Lee, T. S. Shim, J. S. Cho, W. Kim, S. N. Cho, K. N.

Olivier, C. E. Barry, 3rd, and V. Dartois. 2015. 'The association between sterilizing activity and drug distribution into tuberculosis lesions', *Nature Medicine*, 21: 1223-7.

Protopopova, M., C. Hanrahan, B. Nikonenko, R. Samala, P. Chen, J. Gearhart, L. Einck, and C. A. Nacy. 2005. 'Identification of a new antitubercular drug candidate, SQ109, from a combinatorial library of 1,2-ethylenediamines', *Journal of Antimicrobial Chemotherapy*, 56: 968-74.

Queval, C. J., O. R. Song, J. P. Carralot, J. M. Saliou, A. Bongiovanni, G. Deloison, N. Deboosere, S. Jouny, R. Iantomasi, V. Delorme, A. S. Debrie, S. J. Park, J. C. Gouveia, S. Tomavo, R. Brosch, A. Yoshimura, E. Yeramian, and P. Brodin. 2017. 'Mycobacterium tuberculosis Controls Phagosomal Acidification by Targeting CISH-Mediated Signaling', *Cell Rep*, 20: 3188-98.

Rajaram, M. V. S., E. Arnett, A. K. Azad, E. Guirado, B. Ni, A. D. Gerberick, L. Z. He, T. Keler, L. J. Thomas, W. P. Lafuse, and L. S. Schlesinger. 2017. 'M. tuberculosis-Initiated Human Mannose Receptor Signaling Regulates Macrophage Recognition and Vesicle Trafficking by FcRgamma-Chain, Grb2, and SHP-1', *Cell Rep*, 21: 126-40.

Rifat, D., B. Prideaux, R. M. Savic, M. E. Urbanowski, T. L. Parsons, B. Luna, M. A. Marzinke, A. A. Ordonez, V. P. DeMarco, S. K. Jain, V. Dartois, W. R. Bishai, and K. E. Dooley. 2018. 'Pharmacokinetics of rifapentine and rifampin in a rabbit model of tuberculosis and correlation with clinical trial data', *Science Translational Medicine*, 10.

Rohde, K. H., D. F. Veiga, S. Caldwell, G. Balazsi, and D. G. Russell. 2012. 'Linking the transcriptional profiles and the physiological states of Mycobacterium tuberculosis during an extended intracellular infection', *PLoS Pathogens*, 8: e1002769.

Rohde, K., R. M. Yates, G. E. Purdy, and D. G. Russell. 2007. 'Mycobacterium tuberculosis and the environment within the phagosome', *Immunological Reviews*, 219: 37-54.

Romagnoli, A., M. P. Etna, E. Giacomini, M. Pardini, M. E. Remoli, M. Corazzari, L. Falasca, D. Goletti, V. Gafa, R. Simeone, G. Delogu, M. Piacentini, R. Brosch, G. M. Fimia, and E. M. Coccia. 2012. 'ESX-1 dependent impairment of autophagic flux by Mycobacterium tuberculosis in human dendritic cells', *Autophagy*, 8: 1357-70.

Rosenthal, I. M., M. Zhang, K. N. Williams, C. A. Peloquin, S. Tyagi, A. A. Vernon, W. R. Bishai, R. E. Chaisson, J. H. Grosset, and E. L. Nuermberger. 2007. 'Daily dosing of rifapentine cures tuberculosis in three months or less in the murine model', *PLoS Medicine*, 4: e344.

Rozwarski, D. A., C. Vilcheze, M. Sugantino, R. Bittman, and J. C. Sacchettini. 1999. 'Crystal structure of the Mycobacterium tuberculosis enoyl-ACP reductase, InhA, in complex with NAD+ and a C16 fatty acyl substrate', *Journal of Biological Chemistry*, 274: 15582-9.

Russell, D. G., P. J. Cardona, M. J. Kim, S. Allain, and F. Altare. 2009. 'Foamy macrophages and the progression of the human tuberculosis granuloma', *Nature Immunology*, 10: 943-8.

Russell, D. G., L. Huang, and B. C. VanderVen. 2019. 'Immunometabolism at the interface between macrophages and pathogens', *Nature Reviews: Immunology*, 19: 291-304.

Rustomjee, R., A. H. Diacon, J. Allen, A. Venter, C. Reddy, R. F. Patientia, T. C. Mthiyane, T. De Marez, R. van Heeswijk, R. Kerstens, A. Koul, K. De Beule, P. R. Donald, and D. F. McNeeley. 2008. 'Early bactericidal activity and pharmacokinetics of the diarylquinoline TMC207 in treatment of pulmonary tuberculosis', *Antimicrobial Agents and Chemotherapy*, 52: 2831-5.

Ryan, N. J., and J. H. Lo. 2014. 'Delamanid: first global approval', *Drugs*, 74: 1041-5.

Sarathy, J., L. Blanc, N. Alvarez-Cabrera, P. O'Brien, I. Dias-Freedman, M. Mina, M. Zimmerman, F. Kaya, H. P. Ho Liang, B. Prideaux, J. Dietzold, P. Salgame, R. M. Savic, J. Linderman, D. Kirschner, E. Pienaar, and V. Dartois. 2019. 'Fluoroquinolone Efficacy against Tuberculosis Is Driven by Penetration into Lesions and Activity against Resident Bacterial Populations', *Antimicrobial Agents and Chemotherapy*, 63.

Sarathy, J. P., V. Dartois, and E. J. Lee. 2012. 'The role of transport mechanisms in mycobacterium tuberculosis drug resistance and tolerance', *Pharmaceuticals (Basel, Switzerland)*, 5: 1210-35.

Sarathy, J. P., H. H. Liang, D. Weiner, J. Gonzales, L. E. Via, and V. Dartois. 2017. 'An In Vitro Caseum Binding Assay that Predicts Drug Penetration in Tuberculosis Lesions', *J Vis Exp*.

Sarathy, J. P., L. E. Via, D. Weiner, L. Blanc, H. Boshoff, E. A. Eugenin, C. E. Barry, 3rd, and V. A. Dartois. 2018. 'Extreme Drug Tolerance of Mycobacterium tuberculosis in Caseum', *Antimicrobial Agents and Chemotherapy*, 62.

Sarathy, J. P., F. Zuccotto, H. Hsinpin, L. Sandberg, L. E. Via, G. A. Marriner, T. Masquelin, P. Wyatt, P. Ray, and V. Dartois. 2016. 'Prediction of Drug Penetration in Tuberculosis Lesions', *ACS Infect Dis*, 2: 552-63.

Sassetti, C. M., D. H. Boyd, and E. J. Rubin. 2003. 'Genes required for mycobacterial growth defined by high density mutagenesis', *Molecular Microbiology*, 48: 77-84.

Sassetti, C. M., and E. J. Rubin. 2003. 'Genetic requirements for mycobacterial survival during infection', *Proceedings of the National Academy of Sciences of the United States of America*, 100: 12989-94.

Schecter, G. F., C. Scott, L. True, A. Raftery, J. Flood, and S. Mase. 2010. 'Linezolid in the treatment of multidrug-resistant tuberculosis', *Clinical Infectious Diseases*, 50: 49-55.

Schnappinger, D., S. Ehrt, M. I. Voskuil, Y. Liu, J. A. Mangan, I. M. Monahan, G. Dolganov, B. Efron, P. D. Butcher, C. Nathan, and G. K. Schoolnik. 2003. 'Transcriptional Adaptation of Mycobacterium tuberculosis within Macrophages: Insights into the Phagosomal Environment', *Journal of Experimental Medicine*, 198: 693-704.

Scorpio, A., and Y. Zhang. 1996. 'Mutations in pncA, a gene encoding pyrazinamidase/nicotinamidase, cause resistance to the antituberculous drug pyrazinamide in tubercle bacillus', *Nature Medicine*, 2: 662-7.

Shi, W., J. Chen, J. Feng, P. Cui, S. Zhang, X. Weng, W. Zhang, and Y. Zhang. 2014. 'Aspartate decarboxylase (PanD) as a new target of pyrazinamide in Mycobacterium tuberculosis', *Emerg Microbes Infect*, 3: e58.

Shi, W., X. Zhang, X. Jiang, H. Yuan, J. S. Lee, C. E. Barry, 3rd, H. Wang, W. Zhang, and Y. Zhang. 2011. 'Pyrazinamide inhibits trans-translation in Mycobacterium tuberculosis', *Science*, 333: 1630-2.

Simeone, R., A. Bobard, J. Lippmann, W. Bitter, L. Majlessi, R. Brosch, and J. Enninga. 2012. 'Phagosomal rupture by Mycobacterium tuberculosis results in toxicity and host cell death', *PLoS Pathogens*, 8: e1002507.

Singh, V., S. Donini, A. Pacitto, C. Sala, R. C. Hartkoorn, N. Dhar, G. Keri, D. B. Ascher, G. Mondesert, A. Vocat, A. Lupien, R. Sommer, H. Vermet, S. Lagrange, J. Buechler, D. F. Warner, J. D. McKinney, J. Pato, S. T. Cole, T. L. Blundell, M. Rizzi, and V. Mizrahi. 2017. 'The Inosine Monophosphate Dehydrogenase, GuaB2, Is a Vulnerable New Bactericidal Drug Target for Tuberculosis', *ACS Infect Dis*, 3: 5-17.

Singh, V., S. Jamwal, R. Jain, P. Verma, R. Gokhale, and K. V. Rao. 2012. 'Mycobacterium tuberculosis-driven targeted recalibration of macrophage lipid homeostasis promotes the foamy phenotype', *Cell Host Microbe*, 12: 669-81.

Singh, V., and V. Mizrahi. 2017. 'Identification and validation of novel drug targets in Mycobacterium tuberculosis', *Drug Discov Today*, 22: 503-09.

Sirgel, F. A., P. B. Fourie, P. R. Donald, N. Padayatchi, R. Rustomjee, J. Levin, G. Roscigno, J. Norman, H. McIlleron, and D. A. Mitchison. 2005. 'The early bactericidal activities of rifampin and rifapentine in pulmonary tuberculosis', *American Journal of Respiratory and Critical Care Medicine*, 172: 128-35.

Sirgel, F. A., R. M. Warren, E. C. Bottger, M. Klopper, T. C. Victor, and P. D. van Helden. 2013. 'The rationale for using rifabutin in the treatment of MDR and XDR tuberculosis outbreaks', *PloS One*, 8: e59414.

Soto, R., E. Perez-Herran, B. Rodriguez, B. M. Duma, M. Cacho-Izquierdo, A. Mendoza-Losana, J. Lelievre, D. B. Aguirre, L. Ballell, L. R. Cox, L. J. Alderwick, and G. S. Besra. 2018. 'Identification and characterization of aspartyl-tRNA synthetase inhibitors against Mycobacterium tuberculosis by an integrated whole-cell target-based approach', *Scientific Reports*, 8: 12664.

Sreevatsan, S., K. E. Stockbauer, X. Pan, B. N. Kreiswirth, S. L. Moghazeh, W. R. Jacobs, Jr., A. Telenti, and J. M. Musser. 1997. 'Ethambutol resistance in Mycobacterium tuberculosis: critical role of embB mutations', *Antimicrobial Agents and Chemotherapy*, 41: 1677-81.

Stover, C. K., P. Warrener, D. R. VanDevanter, D. R. Sherman, T. M. Arain, M. H. Langhorne, S. W. Anderson, J. A. Towell, Y. Yuan, D. N. McMurray, B. N. Kreiswirth, C. E. Barry, and W. R. Baker. 2000. 'A small-molecule nitroimidazopyran drug candidate for the treatment of tuberculosis', *Nature*, 405: 962-6.

Strydom, N., S. V. Gupta, W. S. Fox, L. E. Via, H. Bang, M. Lee, S. Eum, T. Shim, C. E. Barry, 3rd, M. Zimmerman, V. Dartois, and R. M. Savic. 2019. 'Tuberculosis drugs' distribution and emergence of resistance in patient's lung lesions: A mechanistic model and tool for regimen and dose optimization', *PLoS Medicine*, 16: e1002773.

Sun-Wada, G. H., H. Tabata, N. Kawamura, M. Aoyama, and Y. Wada. 2009. 'Direct recruitment of H+-ATPase from lysosomes for phagosomal acidification', *Journal of Cell Science*, 122: 2504-13.

Sun, J., A. Siroy, R. K. Lokareddy, A. Speer, K. S. Doornbos, G. Cingolani, and M. Niederweis. 2015. 'The tuberculosis necrotizing toxin kills macrophages by hydrolyzing NAD', *Nature Structural & Molecular Biology*, 22: 672-8.

Sun, Q., X. Li, L. M. Perez, W. Shi, Y. Zhang, and J. C. Sacchettini. 2020. 'The molecular basis of pyrazinamide activity on Mycobacterium tuberculosis PanD', *Nat Commun*, 11: 339.

Tahlan, K., R. Wilson, D. B. Kastrinsky, K. Arora, V. Nair, E. Fischer, S. W. Barnes, J. R. Walker, D. Alland, C. E. Barry, 3rd, and H. I. Boshoff. 2012. 'SQ109 targets MmpL3, a membrane transporter of trehalose monomycolate involved in mycolic acid donation to the cell wall core of Mycobacterium tuberculosis', *Antimicrobial Agents and Chemotherapy*, 56: 1797-809.

Takayama, K., and J. O. Kilburn. 1989. 'Inhibition of synthesis of arabinogalactan by ethambutol in Mycobacterium smegmatis', *Antimicrobial Agents and Chemotherapy*, 33: 1493-9.

Tang, S., L. Yao, X. Hao, Y. Liu, L. Zeng, G. Liu, M. Li, F. Li, M. Wu, Y. Zhu, H. Sun, J. Gu, X. Wang, and Z. Zhang. 2015. 'Clofazimine for the treatment of multidrug-resistant tuberculosis: prospective, multicenter, randomized controlled study in China', *Clinical Infectious Diseases*, 60: 1361-7.

Taniguchi, H., H. Aramaki, Y. Nikaido, Y. Mizuguchi, M. Nakamura, T. Koga, and S. Yoshida. 1996. 'Rifampicin resistance and mutation of the rpoB gene in Mycobacterium tuberculosis', *FEMS Microbiology Letters*, 144: 103-8.

Tanner, L., P. Denti, L. Wiesner, and D. F. Warner. 2018. 'Drug permeation and metabolism in Mycobacterium tuberculosis: Prioritising local exposure as essential criterion in new TB drug development', *IUBMB Life*, 70: 926-37.

Tantry, S. J., G. Degiacomi, S. Sharma, L. K. Jena, A. Narayan, S. Guptha, G. Shanbhag, S. Menasinakai, M. Mallya, D. Awasthy, G. Balakrishnan, P. Kaur, D. Bhattacharjee, C. Narayan, J. Reddy, C. N. Naveen Kumar, R. Shandil, F. Boldrin, M. Ventura, R. Manganelli, R. C. Hartkoorn, S. T. Cole, M. Panda, S. D. Markad, V. Ramachandran, S. R. Ghorpade, and N. Dinesh. 2015. 'Whole cell screen based identification of spiropiperidines with potent antitubercular properties', *Bioorganic and Medicinal Chemistry Letters*, 25: 3234-45.

Tasneen, R., F. Betoudji, S. Tyagi, S. Y. Li, K. Williams, P. J. Converse, V. Dartois, T. Yang, C. M. Mendel, K. E. Mdluli, and E. L. Nuermberger. 2016. 'Contribution of Oxazolidinones to the Efficacy of Novel Regimens Containing Bedaquiline and Pretomanid in a Mouse Model of Tuberculosis', *Antimicrobial Agents and Chemotherapy*, 60: 270-7.

Te Brake, L. H. M., G. J. de Knegt, J. E. de Steenwinkel, T. J. P. van Dam, D. M. Burger, F. G. M. Russel, R. van Crevel, J. B. Koenderink, and R. E. Aarnoutse. 2018. 'The Role of Efflux

Pumps in Tuberculosis Treatment and Their Promise as a Target in Drug Development: Unraveling the Black Box', *Annual Review of Pharmacology and Toxicology*, 58: 271-91.

Telenti, A., P. Imboden, F. Marchesi, D. Lowrie, S. Cole, M. J. Colston, L. Matter, K. Schopfer, and T. Bodmer. 1993. 'Detection of rifampicin-resistance mutations in Mycobacterium tuberculosis', *Lancet*, 341: 647-50.

Telenti, A., W. J. Philipp, S. Sreevatsan, C. Bernasconi, K. E. Stockbauer, B. Wieles, J. M. Musser, and W. R. Jacobs, Jr. 1997. 'The emb operon, a gene cluster of Mycobacterium tuberculosis involved in resistance to ethambutol', *Nature Medicine*, 3: 567-70.

Tweed, C. D., R. Dawson, D. A. Burger, A. Conradie, A. M. Crook, C. M. Mendel, F. Conradie, A. H. Diacon, N. E. Ntinginya, D. E. Everitt, F. Haraka, M. Li, C. H. van Niekerk, A. Okwera, M. S. Rassool, K. Reither, M. A. Sebe, S. Staples, E. Variava, and M. Spigelman. 2019. 'Bedaquiline, moxifloxacin, pretomanid, and pyrazinamide during the first 8 weeks of treatment of patients with drug-susceptible or drug-resistant pulmonary tuberculosis: a multicentre, open-label, partially randomised, phase 2b trial', *Lancet Respir Med*, 7: 1048-58.

Urdahl, K. B., S. Shafiani, and J. D. Ernst. 2011. 'Initiation and regulation of T-cell responses in tuberculosis', *Mucosal Immunology*, 4: 288-93.

van der Wel, N., D. Hava, D. Houben, D. Fluitsma, M. van Zon, J. Pierson, M. Brenner, and P. J. Peters. 2007. 'M. tuberculosis and M. leprae translocate from the phagolysosome to the cytosol in myeloid cells', *Cell*, 129: 1287-98.

van Heeswijk, R. P., B. Dannemann, and R. M. Hoetelmans. 2014. 'Bedaquiline: a review of human pharmacokinetics and drug-drug interactions', *Journal of Antimicrobial Chemotherapy*, 69: 2310-8.

VanderVen, B. C., L. Huang, K. H. Rohde, and D. G. Russell. 2016. 'The Minimal Unit of Infection: Mycobacterium tuberculosis in the Macrophage', *Microbiol Spectr*, 4.

Verbeeck, R. K., G. Gunther, D. Kibuule, C. Hunter, and T. W. Rennie. 2016. 'Optimizing treatment outcome of first-line anti-tuberculosis drugs: the role of therapeutic drug monitoring', *European Journal of Clinical Pharmacology*, 72: 905-16.

Via, L. E., D. M. Weiner, D. Schimel, P. L. Lin, E. Dayao, S. L. Tankersley, Y. Cai, M. T. Coleman, J. Tomko, P. Paripati, M. Orandle, R. J. Kastenmayer, M. Tartakovsky, A. Rosenthal, D. Portevin, S. Y. Eum, S. Lahouar, S. Gagneux, D. B. Young, J. L. Flynn, and

C. E. Barry, 3rd. 2013. 'Differential virulence and disease progression following Mycobacterium tuberculosis complex infection of the common marmoset (Callithrix jacchus)', *Infection and Immunity*, 81: 2909-19.

Vilcheze, C., H. R. Morbidoni, T. R. Weisbrod, H. Iwamoto, M. Kuo, J. C. Sacchettini, and W. R. Jacobs, Jr. 2000. 'Inactivation of the inhA-encoded fatty acid synthase II (FASII) enoyl-acyl carrier protein reductase induces accumulation of the FASI end products and cell lysis of Mycobacterium smegmatis', *Journal of Bacteriology*, 182: 4059-67.

von der Lippe, B., P. Sandven, and O. Brubakk. 2006. 'Efficacy and safety of linezolid in multidrug resistant tuberculosis (MDR-TB)--a report of ten cases', *Journal of Infection*, 52: 92-6.

Warner, D. F., and V. Mizrahi. 2014. 'Shortening treatment for tuberculosis--to basics', *New England Journal of Medicine*, 371: 1642-3.

Warrier, T., M. Martinez-Hoyos, M. Marin-Amieva, G. Colmenarejo, E. Porras-De Francisco, A. I. Alvarez-Pedraglio, M. T. Fraile-Gabaldon, P. A. Torres-Gomez, L. Lopez-Quezada, B. Gold, J. Roberts, Y. Ling, S. Somersan-Karakaya, D. Little, N. Cammack, C. Nathan, and A. Mendoza-Losana. 2015. 'Identification of Novel Anti-mycobacterial Compounds by Screening a Pharmaceutical Small-Molecule Library against Nonreplicating Mycobacterium tuberculosis', *ACS Infect Dis*, 1: 580-5.

Wayne, L. G., and L. G. Hayes. 1996. 'An in vitro model for sequential study of shiftdown of Mycobacterium tuberculosis through two stages of nonreplicating persistence', *Infection and Immunity*, 64: 2062-9.

WHO. 1994. "A global emergence: WHO Report on TB epidemic." In. Geneva, Switzerland.

———. 2019a. "Global Tuberculosis Report 2019." In. Geneva, Switzerland.

———. 2019b. "WHO consolidated guidelines on drug-resistant tuberculosis treatment." In. Geneva, Switzerland.

Wolf, A. J., B. Linas, G. J. Trevejo-Nunez, E. Kincaid, T. Tamura, K. Takatsu, and J. D. Ernst. 2007. 'Mycobacterium tuberculosis infects dendritic cells with high frequency and impairs their function in vivo', *Journal of Immunology*, 179: 2509-19.

Wong, D., H. Bach, J. Sun, Z. Hmama, and Y. Av-Gay. 2011. 'Mycobacterium tuberculosis protein tyrosine phosphatase (PtpA) excludes host vacuolar-H+-ATPase to inhibit phagosome acidification', *Proceedings of the National Academy of Sciences of the United States of America*, 108: 19371-6.

Wong, K. W., and W. R. Jacobs, Jr. 2011. 'Critical role for NLRP3 in necrotic death triggered by Mycobacterium tuberculosis', *Cellular Microbiology*, 13: 1371-84.

Xu, J., S. Y. Li, D. V. Almeida, R. Tasneen, K. Barnes-Boyle, P. J. Converse, A. M. Upton, K. Mdluli, N. Fotouhi, and E. L. Nuermberger. 2019. 'Contribution of Pretomanid to Novel Regimens Containing Bedaquiline with either Linezolid or Moxifloxacin and Pyrazinamide in Murine Models of Tuberculosis', *Antimicrobial Agents and Chemotherapy*, 63.

Xu, J., B. Wang, M. Hu, F. Huo, S. Guo, W. Jing, E. Nuermberger, and Y. Lu. 2017. 'Primary Clofazimine and Bedaquiline Resistance among Isolates from Patients with Multidrug-Resistant Tuberculosis', *Antimicrobial Agents and Chemotherapy*, 61.

Yang, C. T., C. J. Cambier, J. M. Davis, C. J. Hall, P. S. Crosier, and L. Ramakrishnan. 2012. 'Neutrophils exert protection in the early tuberculous granuloma by oxidative killing of mycobacteria phagocytosed from infected macrophages', *Cell Host Microbe*, 12: 301-12.

Yano, T., S. Kassovska-Bratinova, J. S. Teh, J. Winkler, K. Sullivan, A. Isaacs, N. M. Schechter, and H. Rubin. 2011. 'Reduction of clofazimine by mycobacterial type 2 NADH:quinone oxidoreductase: a pathway for the generation of bactericidal levels of reactive oxygen species', *Journal of Biological Chemistry*, 286: 10276-87.

Yee, M., P. Gopal, and T. Dick. 2017. 'Missense Mutations in the Unfoldase ClpC1 of the Caseinolytic Protease Complex Are Associated with Pyrazinamide Resistance in Mycobacterium tuberculosis', *Antimicrobial Agents and Chemotherapy*, 61.

Yew, W. W., C. H. Chau, and K. H. Wen. 2008. 'Linezolid in the treatment of 'difficult' multidrug-resistant tuberculosis', *International Journal of Tuberculosis and Lung Disease*, 12: 345-6.

Zhang, Y., B. Heym, B. Allen, D. Young, and S. Cole. 1992. 'The catalase-peroxidase gene and isoniazid resistance of Mycobacterium tuberculosis', *Nature*, 358: 591-3.

Zhang, Y., and D. Mitchison. 2003. 'The curious characteristics of pyrazinamide: a review', *International Journal of Tuberculosis and Lung Disease*, 7: 6-21.

Zhang, Y., M. M. Wade, A. Scorpio, H. Zhang, and Z. Sun. 2003. 'Mode of action of pyrazinamide: disruption of Mycobacterium tuberculosis membrane transport and energetics by pyrazinoic acid', *Journal of Antimicrobial Chemotherapy*, 52: 790-5.

Zhou, C. C., S. M. Swaney, D. L. Shinabarger, and B. J. Stockman. 2002. '1H nuclear magnetic resonance study of oxazolidinone binding to bacterial ribosomes', *Antimicrobial Agents and Chemotherapy*, 46: 625-9.

Zimmerman, M., J. Lestner, B. Prideaux, P. O'Brien, I. Dias-Freedman, C. Chen, J. Dietzold, I. Daudelin, F. Kaya, L. Blanc, P. Y. Chen, S. Park, P. Salgame, J. Sarathy, and V. Dartois. 2017. 'Ethambutol Partitioning in Tuberculous Pulmonary Lesions Explains Its Clinical Efficacy', *Antimicrobial Agents and Chemotherapy*, 61.

CHAPTER 2

EVALUATION OF PHYSICOCHEMICAL PROPERTIES, CYTOTOXICITIES, *IN VITRO* ACTIVITIES AND *M. TUBERCULOSIS*-MEDIATED METABOLISM OF FUSIDIC ACID AND BENZOXAZOLE-BASED OXIME DERIVATIVES

2.1 Introduction

The optimization of antimycobacterial compounds in preclinical studies requires comprehensive screening in assays that recapitulate host conditions during infection. *In vitro* screening assays to determine either the MBC or MIC required to kill *M. tuberculosis* or at least halt its growth are a critical first step in drug discovery programs to select potent anti-mycobacterial compounds (Dartois and Barry 2013; Franzblau et al. 2012). Additional screening assays including cytotoxicity determination are equally important to determine potential toxicity effects against the human host (Franzblau et al. 2012). In this chapter, the activities against *M. tuberculosis* of fusidic acid (FA) and its selected derivatives, and of benzoxazole derivatives, were determined under *in vitro* culture conditions. In addition, cytotoxicity screening was performed against a monocyte-derived macrophage-like THP-1 cell line which is used in subsequent infection experiments discussed in chapter 3 and 4.

Intrinsic physicochemical properties of compounds are predicted to be an important factor that drives drug penetration in lung lesions (Sarathy et al. 2016). Physicochemical parameters have long been studied in drug discovery programs and used by chemists to guide the synthesis and optimization of compounds with drug-like properties (O'Shea and Moser 2008; Koul et al. 2011). Lipinski et al. (2001) first reported a correlation between the physicochemical properties of drugs and factors affecting the bioavailability of oral compounds: solubility and

permeability. The authors proposed that a set of physical properties, the so-called 'rule of 5', for molecular weight, lipophilicity, number of hydrogen bond donors and acceptors, were important in determining those compounds that would possess good permeability across the gut membrane (Lipinski et al. 2001).

Most drugs follow Lipinski's 'conventional oral drug space' with cLogP values of 1-4.5 and molecular weight of 300-500 Da (Koul et al. 2011). However, antibacterials and, in particular, antimycobacterial drugs, often deviate from this guideline. TB drugs are represented by a widespread physicochemical space which cannot be defined (Koul et al. 2011; Lakshminarayana et al. 2015). While classical TB drugs, including INH, EMB, PZA, PAS, ETH, occupy a unique chemical space with MW < 250 and cLogP < 2.5, these are in contrast to rifamycins, aminoglycosides, fluoroquinolones, and the newer drugs BDQ and DLM, which have variable clogP and MW values (Figure 2.1). This divergence from conventional drug space is thought to be reflective of the diverse environments encountered by TB drugs in the different host lesions where unique physicochemical properties are required to access either the cellular or caseum microenvironments and the different physiological states of *M. tuberculosis* targeted by each drug (Dartois and Barry 2013). The ability to penetrate lesion microenvironments is drug-specific, suggesting the physicochemical and molecular properties of drugs drive the distinct partitioning observed (Prideaux et al. 2015). For example, hydrophobicity and poor solubility may affect drug caseum penetration and binding to macromolecules, limiting access to persister populations at the necrotic core for drugs such as CFZ and BDQ (Sarathy et al. 2016).

Ultimately, once a drug has penetrated a lesion and reached its site of action, another important factor determines its site-specific efficacy: the metabolic status of *M. tuberculosis.* Different *M. tuberculosis* metabolic states in lesion microenvironments may effect changes in efflux, permeability, drug target expression or drug-metabolizing enzymes (Awasthi and Freundlich

2017; Mashabela, de Wet, and Warner 2019), in response to their local host immunity (Marakalala et al. 2016). Drug uptake by the bacillus may result in efficacious outcomes or *M. tuberculosis*-mediated biotransformation which may lead to inactivation of drug molecules (Awasthi and Freundlich 2017). Alternatively, drug molecules may be eliminated through efflux mechanisms (Adams et al. 2011; Te Brake et al. 2018). For example, non-replicating bacteria have been shown to upregulate efflux mechanisms in response to stress (Pu et al. 2016). Non-replicating bacilli generated through nutrient starvation have a reduced ability to accumulate drugs, though this might not be efflux-mediated, at least for fluoroquinolones and rifamycins (Sarathy et al. 2013).

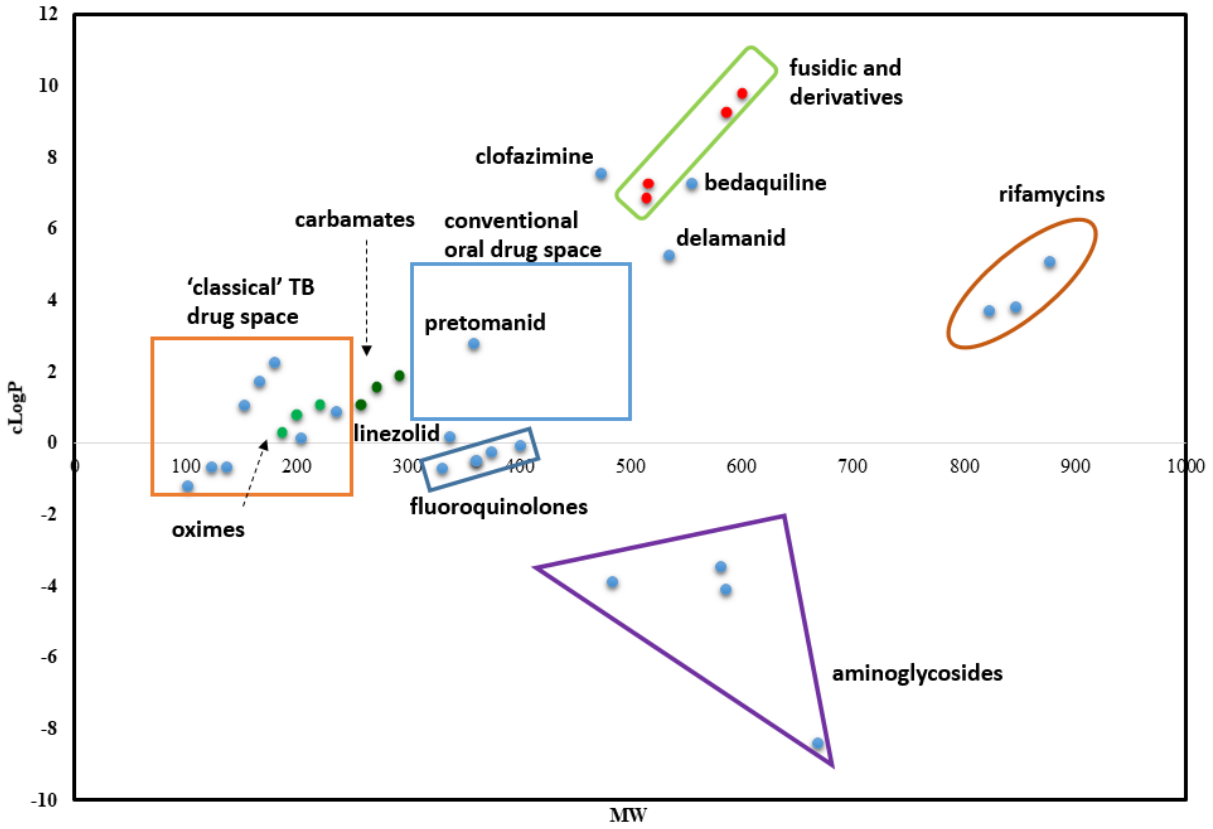

Figure 2.1. A plot of clogP versus molecular weight for known TB drugs. 'Classical' TB drugs include INH, PZA, ETH, EMB, PAS, D-CS, thioacetazone and ETH analogue, prothionamide. Experimental compounds used in this thesis, FA and derivatives (GKFA37, GKFA16 and GKFA17); and benzoxazole-based carbamates (PMN1-201, PMN1-136, PMN2-09) and their corresponding oxime derivatives (PMN1-199, PMN1-135 and PMN1-157) are also included (adapted from (van der Westhuyzen et al. 2015)).

2.2 Fusidic acid and benzoxazole-based oximes as probes for studying drug permeation

2.2.1 Fusidic acid and/or derivatives: potential repurposing and repositioning for TB

Fusidic acid (FA) belongs to the steroidal fusidane-type of antibiotics, which also include helvolic acid and cephalosporin P1, all of which are fungi-derived with narrow spectrum antibiotic activity against Gram-positive bacteria (Shanson 1990; Godtfredsen et al. 1966). They are characterized by a tetracycline ring structure, a Z configuration at the C17-C20 double-bond, a carboxylic acid group at C-21 and an acetoxy group at C-16. The tetracyline ring structure of FA assumes a chair-boat-chair (or trans-syn-trans) confirmation (Figure 2.2), unlike its related fusidane antibiotics, and this conformation is crucial for its function. In addition, the Z configuration at the C17-20 double bond and 16-β acetyl group of FA were determined to be essential for antibacterial activity (Figure 2.3) (Duvold et al. 2001).

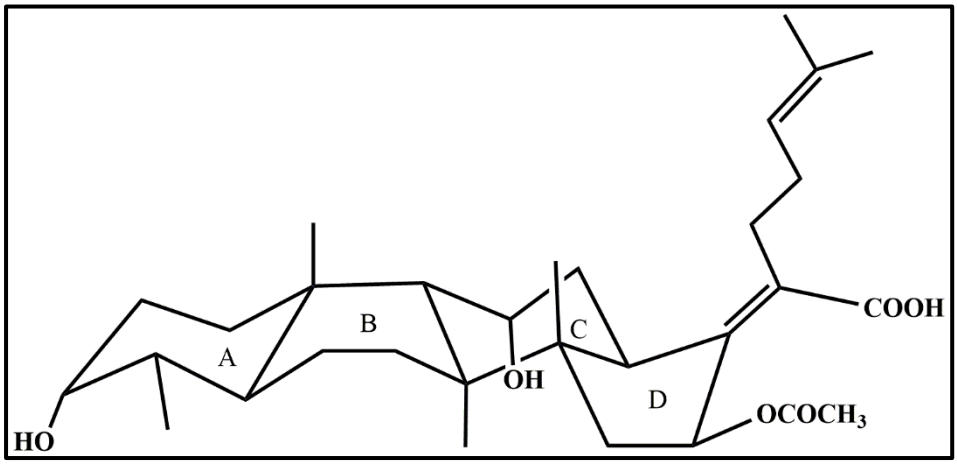

Figure 2.2. *Trans-syn-trans* arrangement of fusidane tetracycline ring system.

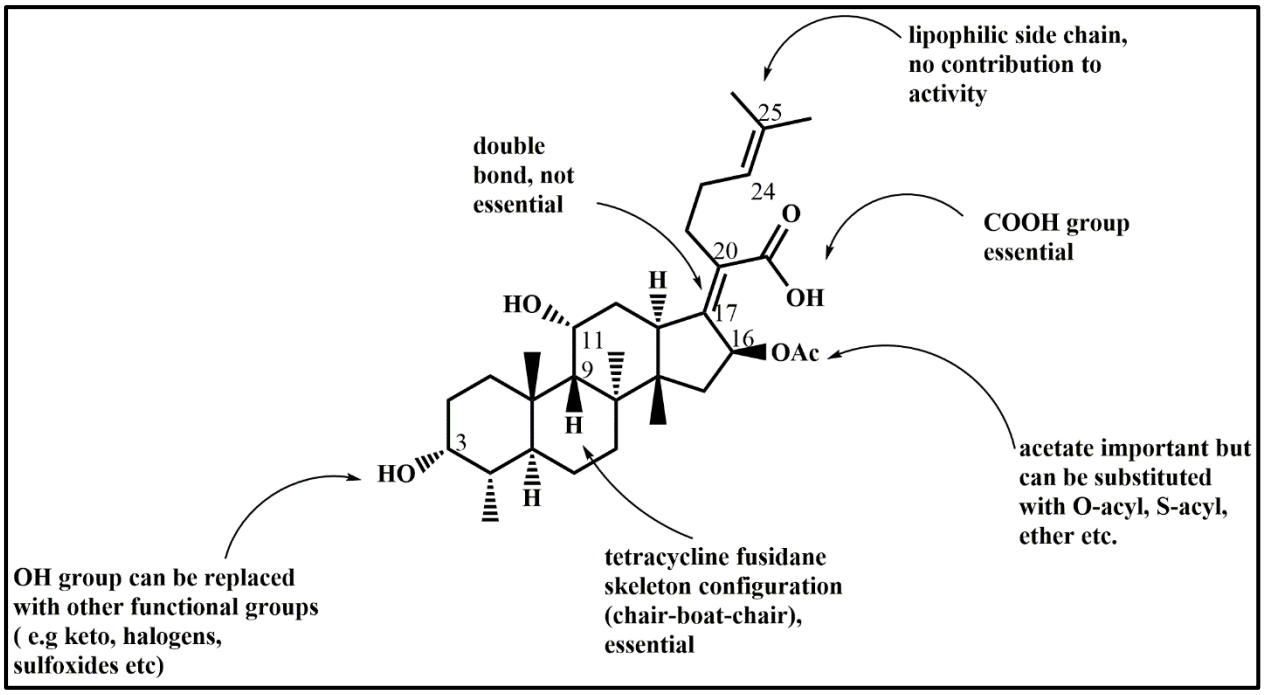

Figure 2.3. Antibacterial structure-activity relationship of FA, showing essential structural features (adapted from (Duvold et al. 2001).

Fusidic acid was first isolated from the fungus *Fusidium coccineum* by Godtfredsen and later developed as a sodium salt due to its hydrophobicity (Godtfredsen et al. 1966). It has been in clinical use for nearly 60 years for the treatment of skin infections caused by *Staphylococcus aureus*. Despite being widely used in Europe, Australia, Canada and Africa, resistance rates remain relatively low. FA has potent activity against methicillin-resistant *S. aureus* (MRSA) and shows very little cross-resistance with other commonly used antibiotics. FA is known to be bacteriostatic, which refers to inhibition of bacterial growth, without killing or exerting cidal activity. FA acts as a protein synthesis inhibitor by targeting the protein translocation process of elongation. FA exerts its activity by binding to a pocket between domain I, II, and III of a five-domain protein complex, elongation factor G (EF-G) (Collignon and Turnidge 1999). EF-G is essential for shifting the nascent polypeptide chain from the A site on the 30S subunit to the P site, during peptide translocation, and also interacts with the ribosome release factor (RRF) to release the ribosome complex on reaching the stop codon during protein synthesis.

FA binding results in a conformational intermediate structure between GDP and GTP-bound forms (Collignon and Turnidge 1999), and as a result prevents both the translocation and ribosome disassembly processes. Resistance to FA has been mapped to the *fusA* gene which encodes for EF-G in *S. aureus* (Turnidge and Collignon 1999; Besier et al. 2003). Chromosomal point mutations that cause amino acid substitutions and therefore altering domain III of the EF-G FA binding site have been reported as one of the mechanisms of resistance (Laurberg et al. 2000).

A number of studies have reported on the activity of FA against mycobacterial species and demonstrated susceptibility of *M. tuberculosis* to FA (Van Caekenberghe 1990; Fuursted, Askgaard, and Faber 1992; Collignon and Turnidge 1999). A review by Collignon & Turnidge (1999) reported MIC values ranging from 4-32 and 16-64 mg/L. Another later study tested 170 *M. tuberculosis* clinical isolates using an agar proportion dilution method to test for activity of FA and a few standard first-line TB drugs. The MIC values of FA were below 16 mg/L and only 1.8% of the strains tested were resistant to FA. A total number of 19 isolates were found to be resistant to at least one of the first-line drugs, with 4 of these showing resistance to at least two drugs (Cicek-Saydam et al. 2001). In addition, none of the resistant strains showed cross-resistance with FA.

Recent work in our research group has focused on the medicinal chemistry of FA towards improving its biological activity and pharmacological parameters. Njoroge et al. (2019), reported on the species-specific differences in the metabolism of FA between human and mouse/rat metabolism (Figure 2.4) (Njoroge et al. 2019). Results showed humans metabolized FA in a reversibly manner to form 3-ketofusidic, an active major metabolite; while rodent surrogates exhibited a highly stereo-selective metabolism resulting in the less active 3-epifusidic acid. These findings highlight how using *in vitro* assays can inform which animal model would be suitable to test for *in vivo* efficacy. In addition, exploration of FA as a

combination drug to potentiate activity of current TB drugs is underway, with data indicating a role for synergy with spectinomycin and chlorpromazine (Omollo et al. 2019).

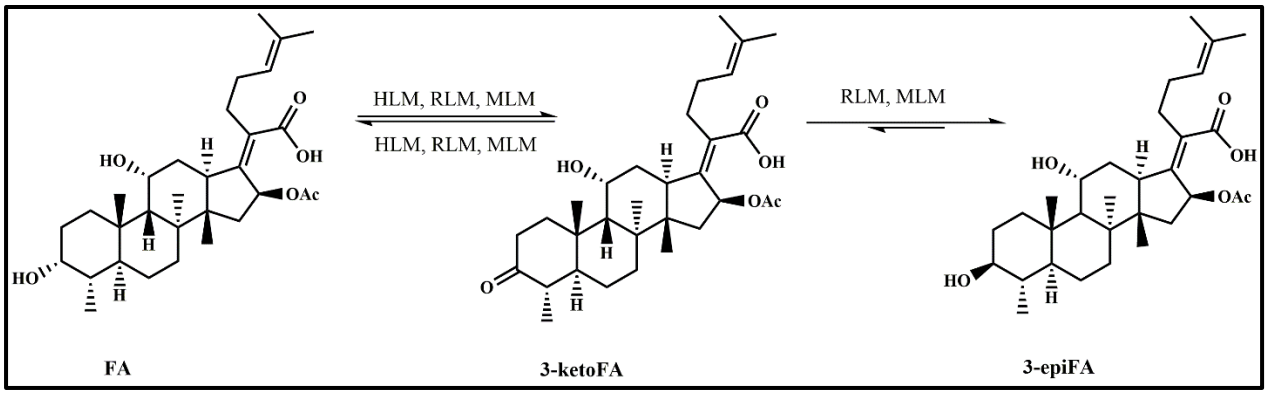

Figure 2.4. Proposed FA metabolism in humans and rodent models of TB (Njoroge et al. 2019). HLM, RLM, MLM are abbreviations for human, mice and rat liver microsomes respectively.

2.2.2 Benzoxazole-based oxime derivatives

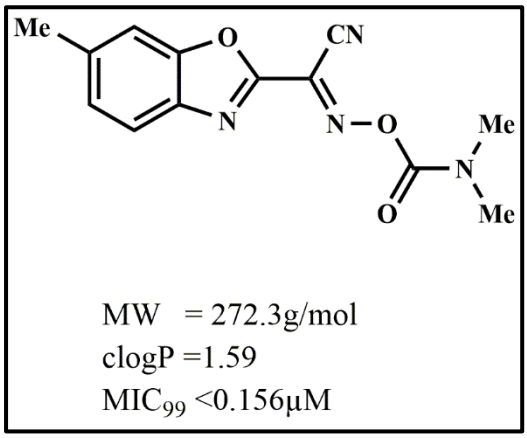

Figure 2.5. Hit compound from NITD HTS of a focused library.

Screening of a library of 'leadlike' compounds at the Novartis Institute for Tropical Diseases (NITD), with defined physicochemical properties of molecular weight (MW) <350 Da, total polar surface area (TPSA) <140Å^2 and clogP values of <3 led to a hit compound with a benzoxazole-based heterocyclic skeleton structure (Figure 2.5). Further exploration of the SAR

was undertaken and led to a number of derivatives with potent *in vitro* activity against *M. tuberculosis*. Limited previous literature exists on benzoxazole-based oximes; however, benzoxazoles or oximes have separately been shown to exhibit antibacterial properties.

The benzoxazole heterocyclic core, derived from the fusion of a benzene ring and the nitrogen- and oxygen-fused ring of the oxazole core, is considered a privileged structure in medicinal chemistry with a wide spectrum of pharmacological properties (Zhang, Zhao, and Zhou 2018). Naturally occurring antibiotics, calcimycin (an ionophore derived from *Streptomyces chartreusensis*), and chlorzoxazone (a *Streptomyces*-derived centrally acting muscle relaxant) are examples of marketed drugs bearing a benzoxazole active core. In addition, a number of synthetic benzoxazole derivatives have been investigated for antiviral, anticancer, antifungal, and antibacterial activities (Byrd et al. 2013; Zhang, Zhao, and Zhou 2018; Rida et al. 2005). While none of the current anti-TB drugs or compounds in clinical development possess the benzoxazole heterocyclic core, antimycobacterial activity of benzoxazole derivatives has been recently reported (Malapati et al. 2018; Lukowska-Chojnacka, Kowalkowska, and Napiorkowska 2018; Chacko et al. 2018).

The potent antimycobacterial *in vitro* activity and physicochemical space occupied by the benzoxazole-based oxime derivatives synthesized in our lab in contrast to FA derivatives suggested their potential utility as probes of cellular permeation to elucidate the parameters that might drive increased intracellular drug concentrations.

This chapter focuses on elucidating the physicochemical properties, cytotoxicities and *in vitro* activities of FA and its derivatives, and benzoxazole-based oxime derivatives selected to probe macrophage and *M. tuberculosis* permeation. Additionally, the interaction between selected compounds and *M. tuberculosis* in axenic culture was investigated to investigate *M. tuberculosis*-mediated drug metabolism.

2.3 Results

2.3.1 Physicochemical profiling of selected antimycobacterial agents

Compounds synthesized by members of our group (Chibale laboratory, Chemistry Department, University of Cape Town) which previously exhibited potent *in vitro* activity against *M. tuberculosis* H37Rv were selected from two drug classes: i) FA and derivatives (Figure 2.6) and ii) benzoxazole-based oxime derivatives (Figure 2.7).

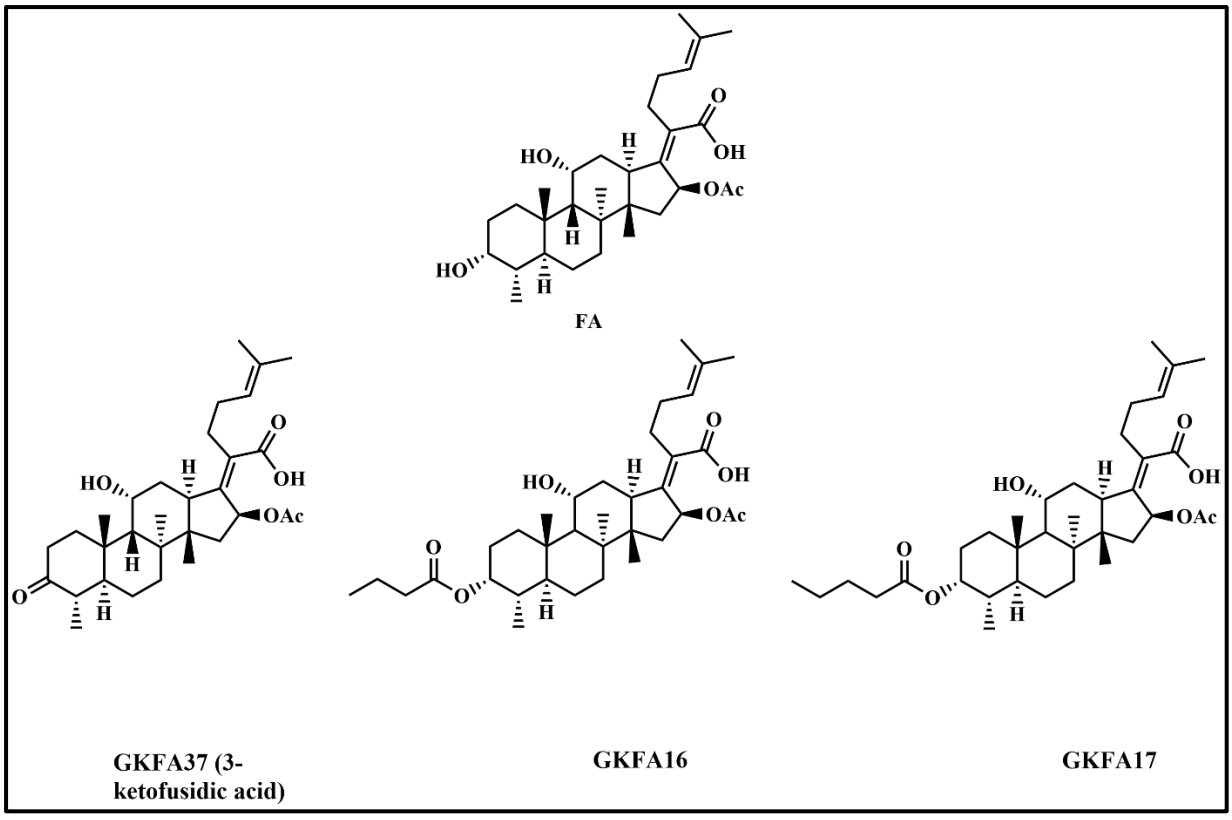

Figure 2.6. Fusidic acid and selected derivatives.

To profile the physicochemical parameters, the solubilities and permeabilities of all compounds selected for this study were first determined using standard *in vitro* assays described in detail

in chapter 6. Briefly, solubility under aqueous conditions was measured using either equilibrium or kinetic solubility methods. Using the equilibrium assay, test and control drug stocks were serially diluted in DMSO and phosphate buffer saline (PBS) over a concentration range, equilibrated and their absorbance read at 620nm. For kinetic solubility, also referred to as high-performance liquid chromatography (HPLC)-based method, drug stocks reconstituted in PBS were analyzed using HPLC-diode-array detector (DAD) with a calibration curve prepared in DMSO. Permeability was predicted using the parallel artificial membrane permeability assay (PAMPA) adapted from previously reported methods (Joshi et al. 2017). In addition, cLogP (calculated logP), and molecular weight values were calculated using ChemDraw Professional software (version 15.1). The cLogP value predicts the partitioning of a compound between water and *n*-octanol and is used as a measure of compound lipophilicity. The use of ChemDraw software as a tool to calculate logP was sufficient to rank compounds based on their lipophilicity. While I generated the kinetic solubility data, PAMPA and equilibrium solubility were done as part of routine assays in the Division of Clinical Pharmacology, Drug Discovery and Development Centre (H3D), University of Cape Town.

FA is a natural product with high lipophilicity properties; derivatization at the C-3 position through addition of alkyl-ester groups results in analogues with even higher clogP values (Table 2.3). While higher lipophilicity generally results in increased solubility liabilities, FA and the 3-ketoFA derivative (GKFA37) had good solubilities, both >200 µM. These two compounds are naturally occurring, with 3-ketoFA existing as the major human metabolite of FA both *in vitro* and *in vivo* (Turnidge 1999; Njoroge et al. 2019). This may explain their good solubility indices despite their high lipophilicities.

Replacing the C-3 OH group with alkyl ester groups significantly increased the lipophilicity by over 2 units, with clogP values of 9.29 and 9.82 observed for GKFA16 and GKFA17, respectively (Table 2.1). This expectedly led to a significant decrease in solubility, which

meant that permeability for these compounds could not be determined using PAMPA since the standard assay is performed at concentrations above their solubility limit. FA and GKFA37 were predicted to have higher PAMPA permeabilities (Table 2.1) than MXF (clogP -0.0824) **(**Table 2.2). MXF was selected on the basis of its preferential cellular lesion accumulation (Prideaux et al. 2015; Blanc et al. 2018), and a few other anti-TB drugs of varying lipophilic properties were included in the study (Table 2.2).

Table 2.1. Physicochemical parameters of selected FA analogues.

Compound code	**Structure**	**Molecular weight (g/mol)**	**cLogP**	**Aq. solubility[a] (pH 7.0, (µM))**	**PAMPA (Papp cm/s)**
FA	OH	516.7	7.28	>200	-4.90
GKFA37	O	514.7	6.88	>200	-3.93
GKFA16	$OCO(CH_2)_2CH_3$	586.8	9.29	25	ND
GKFA17	$OCO(CH_2)_3CH_3$	600.8	9.82	17	ND

-, not tested; ND: not determined or data not available due to analytical issues; *a:* solubility measured by a HPLC equilibrium method. PAMPA: low permeability, < -6.5cm/s; moderate permeability, -6.5 - -5.5cm/s; high permeability, > -5.5cm/s. clogP calculated using ChemDraw software (version 15.1).

Table 2.2. Physicochemical parameters of selected current TB drugs.

Compound code	Molecular weight (g/mol)	cLogP	Aq. solubility[a] (pH 7.0, (µM))	PAMPA (Papp cm/s)
MXF	401.4	-0.08	>200	-7.21
LVF	361.3	-0.51	>200	-
RIF	822.9	3.71	-	-
BDQ	555.5	7.25	-	-
CFZ	473.4	7.55	<5	-

-, not tested; ND: not determined or data not available due to analytical issues; *a:* solubility measured by kinetic methods. PAMPA: low permeability, < -6.5cm/s; moderate permeability, -6.5 - -5.5cm/s; high permeability, > -5.5cm/s. clogP calculated using ChemDraw software (version 15.1).

Benzoxazole-based oxime derivatives (Figure 2.7) were synthesized as part of SAR expansion of a hit compound from a NITD screening project (Figure 2.5). The NITD phenotypic HTS identified lead-like small polar molecules that occupy the conventional oral drug space (Kelly Chibale, personal communication).

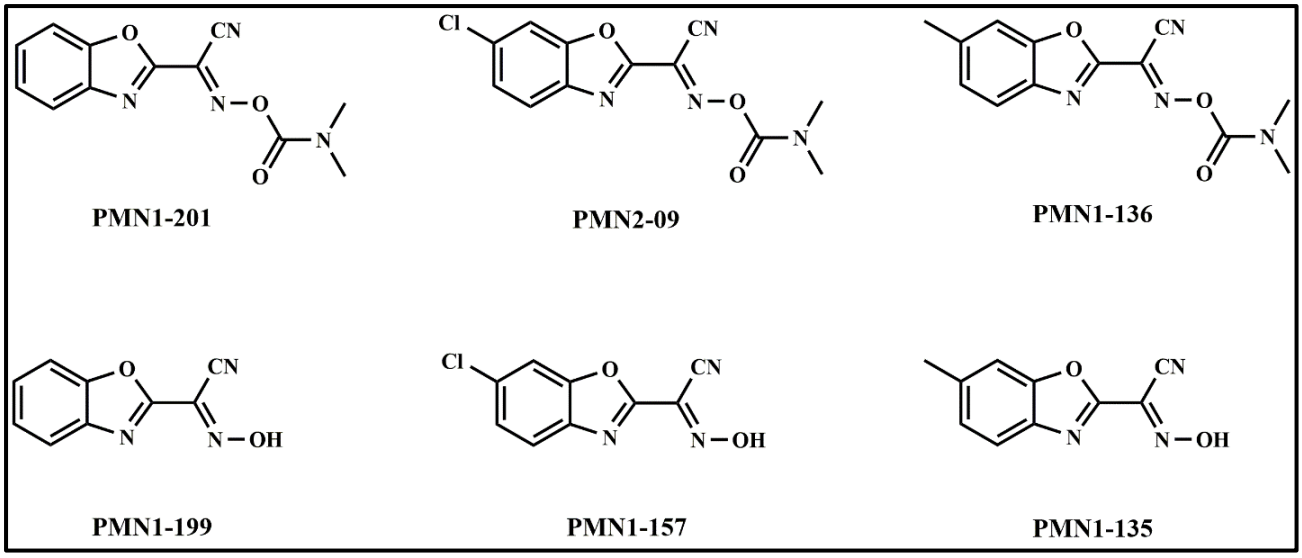

Figure 2.7. Selected benzoxazole-based oxime derivatives.

The benzoxazole-based oxime compounds all exhibited low clogP values <2, and MWs of <300 Da (Table 2.3). Due to the PAMPA and HPLC solubility testing not being an in-house assay, only a few representative compounds from this class were submitted to determine their solubility and predict permeability. In line with their lower lipophilic nature, both the free oxime and oxime carbamates tested, exhibited good solubility. The PAMPA results however, suggested that the tested compounds would have high permeability. While all the compounds are in the same range of MW, clogP and solubility, and likely to have similar permeability, testing the rest of the compounds would give more certainty to data interpretation.

Table 2.3. Physicochemical parameters of selected benzoxazole-based oxime analogues.

Compound code	**Structure**	**Molecular weight (g/mol)**	**cLogP**	**Aq. solubility[a] (pH 7.0, (µM))**	**PAMPA (Papp cm/s)**

	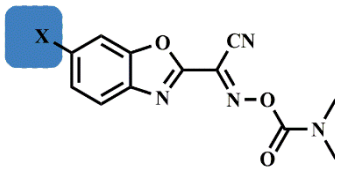				
PMN1-201	**H**	258.2	1.09	>200	-3.80
PMN1-136	**CH_3**	272.3	1.58	>200	-
PMN2-09	**Cl**	292.7	1.86	-	-
	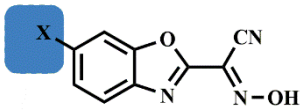				
PMN1-199	**H**	187.2	0.30	>200	-4.01
PMN1-135	**CH_3**	201.2	0.80	>200	-3.47
PMN1-157	**Cl**	221.6	1.07	-	-

-, not tested; *a:* solubility measured by kinetic methods. PAMPA: low permeability, < -6.5cm/s; moderate permeability, -6.5 - -5.5cm/s; high permeability, > -5.5cm/s. clogP calculated using ChemDraw software (version 15.1).

2.3.2 *In vitro* activity

FA derivatives were synthesized by members of the Chibale group as part of ongoing work aimed at the repositioning of FA for TB drug discovery. Previous structure-activity relationship (SAR) studies in our group resulted in FA derivatives of variable antimycobacterial activity (Njoroge et al. 2019; Dziwornu et al. 2019).

Briefly, *in vitro* screening of compounds against *M. tuberculosis* H37Rv was done by me or as part of routine testing in our laboratory to determine MIC values using a broth microdilution method, the Microplate Alamar Blue Assay (MABA). This method is routinely used as a high throughput means of determining growth and inhibition due to a specific compound or compounds in combination, however, one of its drawbacks is that it does not provide a measure of cidality. The cumbersome, colony forming unit (CFU) method remains the gold standard to measure cidality. The MABA assay determines the MIC of a compound over a concentration range created by serial dilution in a 96-well microplate. Following a period of incubation, typically 7days in the presence of the compound, the metabolic activity of the mycobacterial cells is measured by determining their ability to convert the resazurin dye (blue) to resorufin (pink). MIC values are then generated using either or both, visual detection and fluorescence-based quantification as viable and metabolically active cells convert the dye to resorufin, while non-viable cells remain blue.

The assay was set up under typically used culture media conditions (7H9 broth media enriched with albumin dextrose catalase (ADC), and a glucose or glycerol carbon source), and DMSO compound stocks were diluted by a two-fold serial dilution over a concentration range. Each compound was added in duplicate or triplicate, and the experiment repeated at least 3 times. Detailed experimental procedures are provided in Chapter 6. FA, GKFA37 (3-ketoFA) and the two C3 alkyl-ester derivatives, (GKFA16 and GKFA17), all showed good activity in both glucose and glycerol media (Table 2.5). Compounds GKFA16 and GKFA17 were less active in comparison to FA and GKFA37. Since the assay set up is based on two-fold serial dilutions, differences of this magnitude, were not regarded as significant. In addition, similar activities were observed in glycerol media, indicating that activity was not glycerol-dependent.

Furthermore, substitution of glucose or glycerol with cholesterol was investigated. *M. tuberculosis* has been reported to utilize host-derived lipids such as TAG, cholesterol and fatty

acids as carbon sources to ensure its survival (Daniel et al. 2011; Lee et al. 2013). *M. tuberculosis* is thought to drive dysregulation of host-lipid metabolism leading to formation of foamy macrophages, characterized by intra-cytosolic accumulation of neutral lipids in the form of lipid bodies (Peyron et al. 2008; Singh et al. 2012). Furthermore, the caseum is enriched with cholesterol and cholesterol ester amongst other lipid forms, thought to be from necrotic death of foamy cells (Kim et al. 2010). In cholesterol enriched media, all FA derivatives exhibited similar activities to the parental compound, FA. However, a slight loss in activity was observed compared to standard glycerol-based media (Table 2.5).

Table 2.4. *In vitro* activities of FA and derivatives against *M. tuberculosis* H37Rv in different media.

Compound		**MIC_{90} 7H9/GLU/ADC (µM)**	**MIC_{90} 7H9/GLY/ADC (µM)**	**MIC_{90} 7H9/cholesterol (µM)**
FA	OH	1.57(0.98-2.81)	1.28(0.98-4.45)	6.64
GKFA37	O	1.08(0.98-1.99)	0.91(0.49-0.98)	4.02
GKFA16	$OCO(CH_2)_2CH_3$	3.91(1.20-17.93)	3.91(0.78-8.24)	3.10
GKFA17	$OCO(CH_2)_3CH_3$	3.34(0.58-15.6)	2.26(0.49-15.6)	3.12
RIF		0.03(0.02-0.04)	0.03(0.02-0.04)	-

MIC values were determined as the lowest concentration of each drug(s) that prevented colour change of resazurin (blue) to resorufin (pink). MIC values are expressed as a median (range) value obtained from three biological replicates with at least 2 technical replicates each. MIC_{90}

7H9/cholesterol are expressed as mean value from a single experiment with 3 technical replicates. RIF was used as a positive control and not teste using cholesterol media.

FA activity against *S. aureus* is reportedly enhanced under acidic conditions (Lemaire et al. 2011). *M. tuberculosis* is thought to be exposed to an acidic intraphagosomal environment during macrophage infection, which may induce tolerance and drive intracellular survival (Levitte et al. 2016). For this reason, the effects of pH on activity of fusidic acid and derivatives was evaluated. Using base media supplemented with glycerol, the pH was adjusted to slightly acidic conditions with pH values of 5.83 and 4.96 in comparison to normal media conditions of pH 6.67, and MIC readings taken after a 14-day incubation. FA and the ketone, GKFA37, exhibited a 4-fold increase in activity at pH 5.83 against replicating *M. tuberculosis* H37Rv under normal aerobic conditions, while GKFA16 and GKFA17 MIC values remained unchanged (Figure 2.8). Delayed growth was observed at pH 5.83, while *M. tuberculosis* was unable to grow at pH 4.96 after 14 days of incubation.

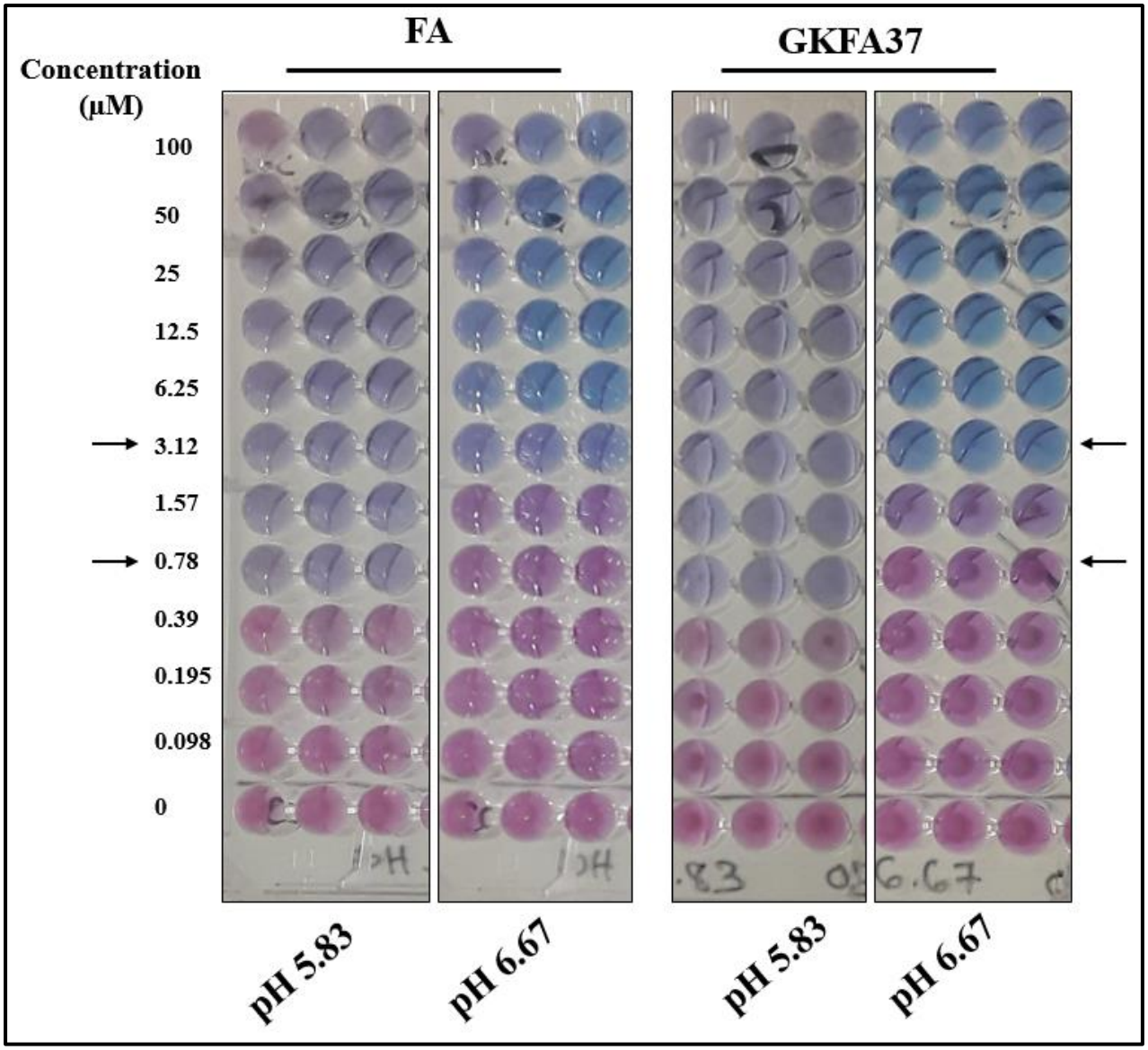

Figure 2.8. Activity of FA and 3-ketoFA (GKFA37) against replicating *M. tuberculosis* H37Rv under aerobic, acidic conditions.

Benzoxazole-based oxime carbamates (PMN1-201, PMN2-09 and PMN1-136) (synthesized by Paul Njaria, PhD - unpublished), were selected due to their potent *in vitro* antimycobacterial activity (Table 2.6). Their corresponding free oxime derivatives (PMN1-199, PMN1-157 and PMN1-135, respectively) were also synthesized, as it was hypothesized that the carbamates underwent hydrolysis to form the free oxime under the assay conditions. The carbamates

showed potent activity in both glucose and glycerol-supplemented media. The free oxime compounds however, generally exhibited loss of antimycobacterial activity compared to their parent compounds.

Table 2.5. *In vitro* activities of benzoxazole-based oxime derivatives against *M. tuberculosis* H37Rv.

Compound	**MIC_{90} 7H9/GLU/ADC (µM)**	**MIC_{90} 7H9/GLY/ADC (µM)**
PMN1-201	<0.244	<0.244
PMN1-199	>125	>125
PMN1-136	0.488	<0.122
PMN-135	>62.5	>62.5
PMN2-09	<0.122	<0.122
PMN1-157	>62.5	>62.5
RIF	0.03(0.02-0.04)	0.03(0.02-0.04)

MIC values were determined as the lowest concentration of each drug(s) that prevented colour change of resazurin (blue) to resorufin (pink). Most MIC values for the carbamates were below the lowest concentration tested or above the highest for the oxime compounds, MIC range could not be determined. Reported values are from a single experiment representative of at least two biological replicates and at least two technical replicates each. RIF was used as a positive control.

2.3.3 Evaluation of *in vitro* cytotoxicity

Optimization of drug leads during the drug discovery process requires that, in addition to determination of *in vitro* potency, compounds must be screened for potential safety liabilities, including cytotoxicity (Franzblau et al. 2012). *In vitro* cell-line assays provide a platform to evaluate human cytotoxicity rapidly at low cost. Prior to carrying out cellular drug uptake and determination of intracellular antimycobacterial efficacy, the monocyte-derived THP-1 cell-line was differentiated into macrophage-like cells, exposed to test compounds through a 2-fold serial dilution and incubated for 3 days at 37ºC under 5% CO_2. Table 2.4 shows the macrophage IC_{90} values of test compounds determined through a resazurin-based fluorescence assay. IC_{90} was defined as the lowest concentration that resulted in the loss of cell viability by 90%.

FA and its derivative GKFA37 generally exhibited good IC_{90} values and their selectivity indices (SIs) indicated a good safety margin. SI (defined as IC_{90}/ MIC_{90}) indicates the proportional difference in the concentration required to kill or inhibit bacterial growth and the concentration that is toxic to host cells. The benzoheterocyclic benzoxazole-based carbamates were well tolerated by THP-1 macrophages and had good SI values. PMN1-199, the corresponding free oxime of compound PMN1-201, was also less toxic to macrophages but displayed poor SI due to lack of antimycobacterial activity.

Table 2.6. Cytotoxicity measurements of test compounds on THP-1 cells.

Compound code	Structure	THP-1 IC_{90} (µM)	MIC_{90} 7H9/GLU/ADC (µM)	Selectivity index
	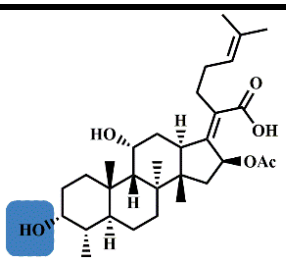			

FA	OH	>200	1.57	>100
GKFA37	O	>200	1.08	>100
GKFA16	$OCO(CH_2)_2CH_3$	52.1	3.91	13.3
GKFA17	$OCO(CH_2)_3CH_3$	104	3.34	31.2
	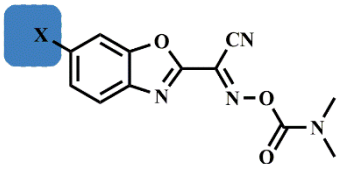			
PMN1-201	H	>80	<0.244	>100
PMN1-136	CH_3	>200	0.488	>100
PMN2-09	Cl	>100	<0.122	>100
	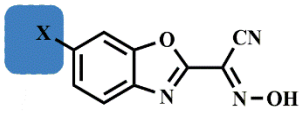			
PMN1-199	H	>200	>125	
PMN1-135	CH_3	ND	>62.5	
PMN1-157	Cl	ND	>62.5	

ND: not determined or data not available due to analytical issues

2.3.4 *In vitro* stability and *M. tuberculosis* mediated metabolism

3-ketoFA is a known human metabolite of FA while the two C-3 alkyl-esters derivatives (GKFA16 and GKFA17) were synthesized as prodrugs to improve the physicochemical and pharmacological parameters of FA. While, by definition, prodrugs are inactive derivatives of the parent drug, these FA analogues were found to be active against *M. tuberculosis*. Ongoing work in our research group towards repurposing of FA as an antimycobacterial agent has shown that FA lacks *in vivo* efficacy in a TB mouse model (Kelly Chibale – personal communication) which has been attributed to a species difference in metabolism between mice and humans *in*

vitro, utilizing rodent and human liver microsomes (Njoroge et al. 2019). Pharmacokinetic analysis further confirmed that FA was rapidly metabolized in mice to form 3-epiFA, therefore causing low FA exposure (Strydom et al. 2020). The authors also hypothesized that using C-3 alkyl ester prodrugs would improve the exposure of FA. C-3 alkyl esters improved absorption and tissue distribution, however the 3-epiFA metabolite was still predominantly formed in all organs, highlighting that FA *in vivo* optimization would require a non-rodent model such as marmoset or non-human primate (Strydom et al. 2020). In addition, it was shown that *M. tuberculosis* metabolized the C3-alkyl ester, GKFA17, when incubated over 48 hours to form FA (Njoroge et al. 2019).

The focus of this aspect of the thesis work was to further investigate the interaction of FA and derivatives with *M. tuberculosis* with a view to establishing which (if any) metabolic species were formed and were present during the time period in which the antimycobacterial activity (MIC) was determined, and would be present in infected macrophages (chapter 3 and 4).

FA and its derivative GKFA17 were incubated at sub-MIC concentrations (0.1 μM) with *M. tuberculosis* cells (live or heat-killed) or in cell-free media to determine general stability in aqueous growth media. In the presence of *M. tuberculosis*, GKFA17 was metabolized with complete loss of the compound observed after 4 days of incubation (Figure 2.9). Under the same conditions, compound exposed to heat-killed bacilli (and therefore presumed to be devoid of any enzymatic activity) remained stable, similar to incubation in growth media. Analysis of metabolites revealed an accumulation of FA in amounts equivalent to the hydrolyzed GKFA17, and very small amounts of the ketone, GKFA37. Further analysis of FA metabolism by *M. tuberculosis* showed that a small amount of the ketone accumulated in media. However, the amount of drug lost to metabolism did not correlate with the amount of metabolite formed, suggesting another unidentified metabolite might be formed (Figure 2.9). Figure 2.10 presents a suggested pathway of FA and C-3 alkyls esters metabolism by *M. tuberculosis*.

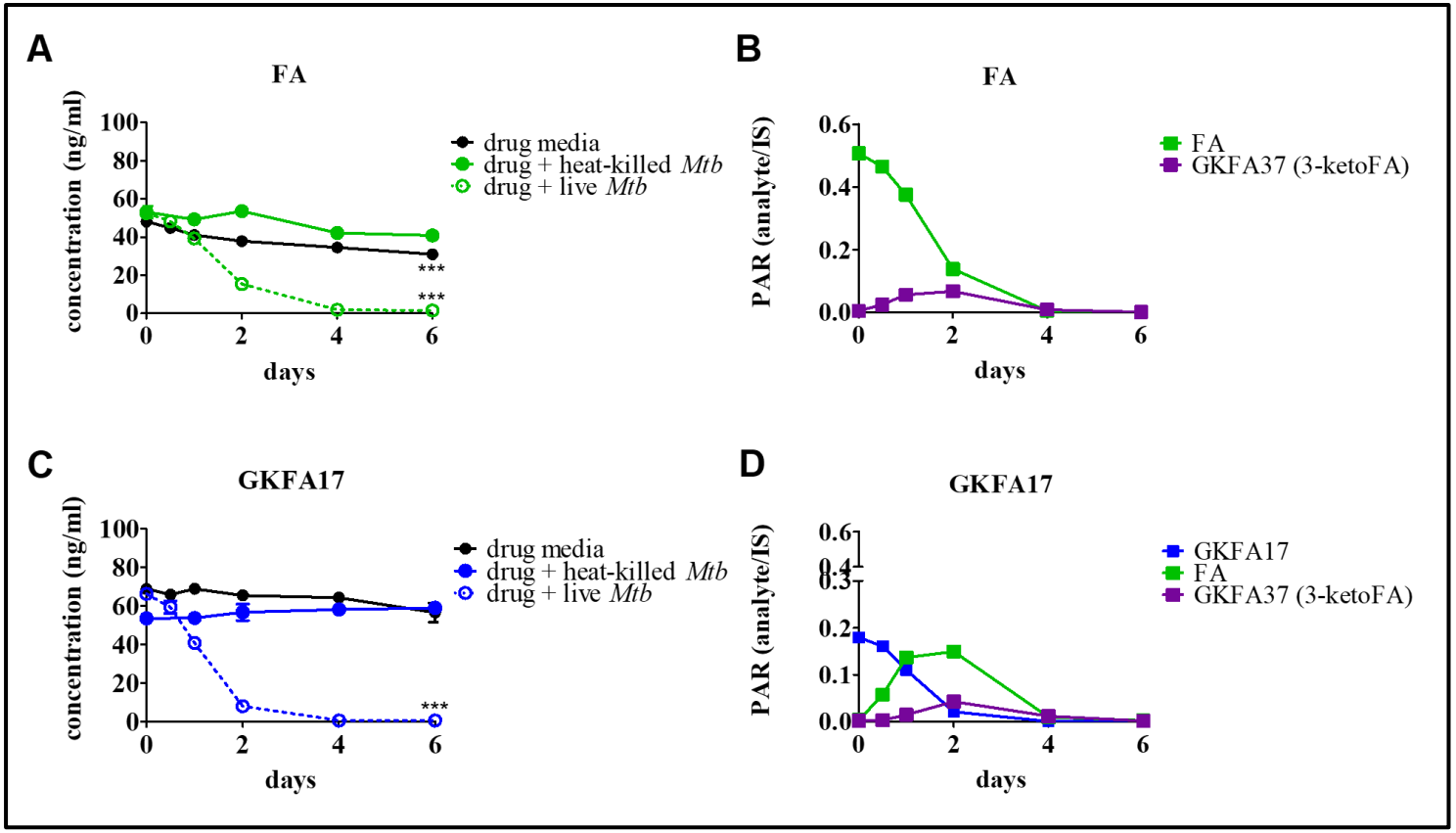

Figure 2.9. *M. tuberculosis* metabolism of FA and C-3 ester derivatives. A. FA metabolism by *M. tuberculosis* over 6 days at sub MIC concentrations, including heat-killed cells and media only control. B. formation of 3-ketoFA (GKFA37) from FA *M. tuberculosis* metabolism. C. Metabolism of C-3 alkyl-ester derivative, GKFA17 by *M. tuberculosis* and D. formation of FA and 3-ketoFA (GKFA37) from GKFA17 *M. tuberculosis* metabolism. *Mtb* - *M. tuberculosis*. Peak area ratio (PAR) = peak area of analyte/ peak area of internal standard (IS) Statistical significance at day 6 was assessed using 1-way ANOVA with Tukey's post hoc test, comparing against drug media. *P < 0.05; **P < 0.01, ***P < 0.001.

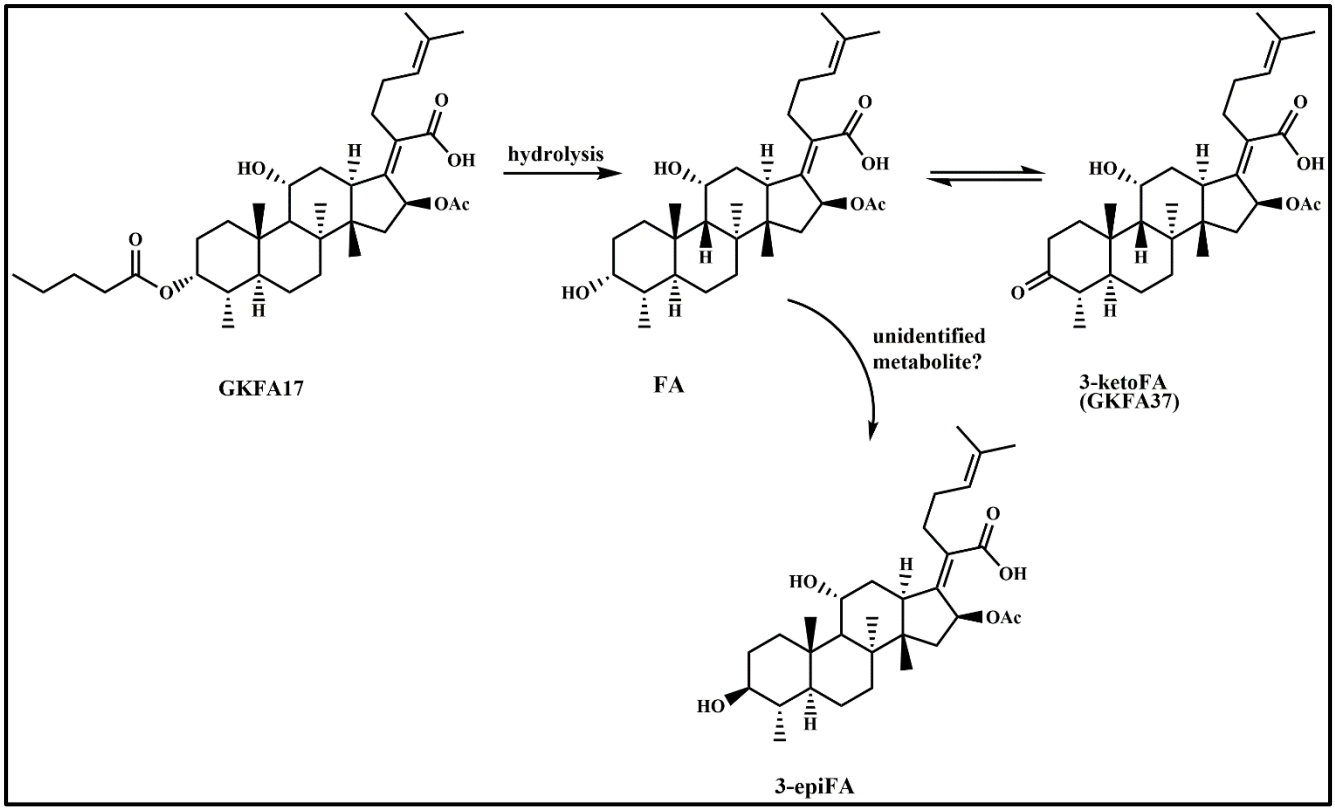

Figure 2.10. Proposed pathway for *M. tuberculosis* metabolism of FA and FA C3-alkyl esters.

Initial experiments to elucidate stability of the benzoxazole-based oxime compounds in media showed that the oxime carbamates - as indicated by the representative compound PMN2-09 - were susceptible to spontaneous degradation in both macrophage and *M. tuberculosis* culture media (Figure 2.11). The free oxime counterpart, PMN1-157, however, remained stable.

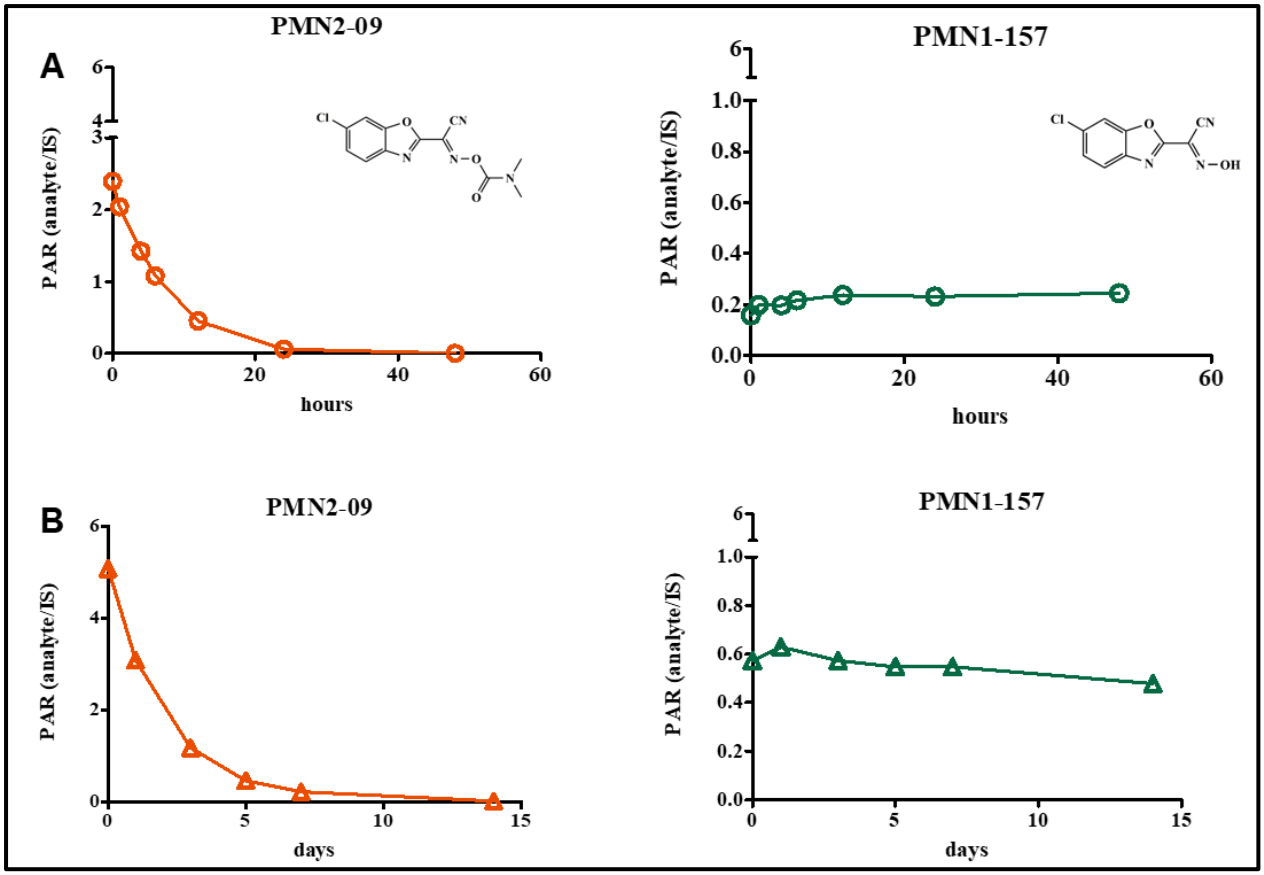

Figure 2.11. Benzoxazole-based carbamates and oximes stability in aqueous media conditions. Benzoxazole-based carbamate, PMN2-09 degraded while its corresponding free oxime, PMN1-157 remained stable in both RPMI-1640 (+10% fetal bovine serum) (Row A) and 7H9/OADC media (Row B).

The exposure of sub-MIC concentrations (0.1 µM) of the same compounds to *M. tuberculosis* suggested immediate breakdown of the oxime carbamate PMN2-09, with complete loss of the compound within 3 hours of incubation. Spontaneous degradation occurred in media, but at a slower rate. This loss of compound was accompanied by a correlated accumulation of the corresponding free oxime, suggesting that this was the only metabolite formed from the hydrolysis (Figure 2.12, A). The free oxime compound was stable to spontaneous degradation and *M. tuberculosis*-mediated metabolism (Figure 2.12, B). Figure 2.13 presents the proposed pathway for *M. tuberculosis*-mediated metabolism of the benzoxazole-based oxime carbamates.

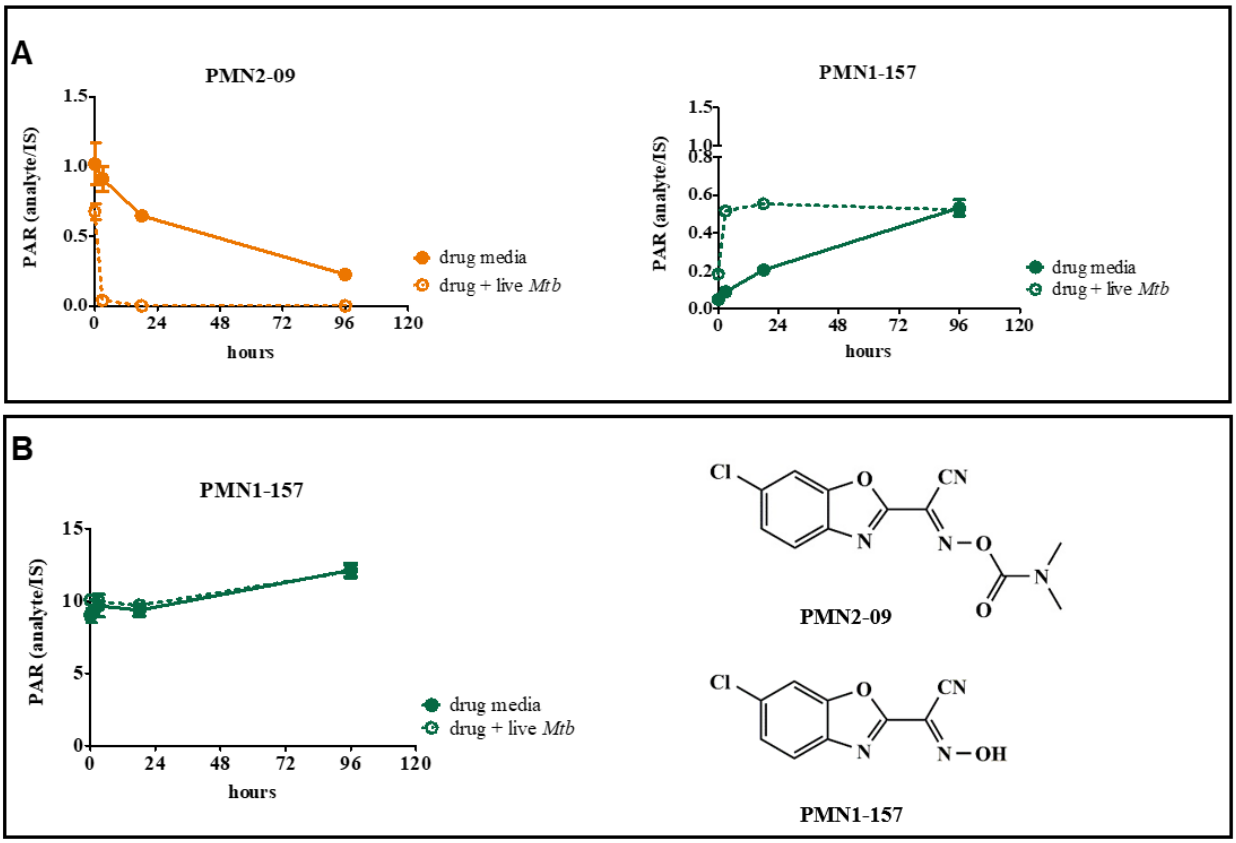

Figure 2.12. *M. tuberculosis* metabolism of benzoxazole-based oxime carbamates and their free oxime derivatives. A. (left); metabolism of oxime carbamate, compound PMN2-09, resulting accumulation of free oxime product (right). B. metabolism of the free oxime compound, PMN1-157. Compounds were incubated in 7H9/OADC growth medium (drug media) and added to log phase H37Rv WT culture (drug + live *Mtb*). *Mtb* - *M. tuberculosis*.

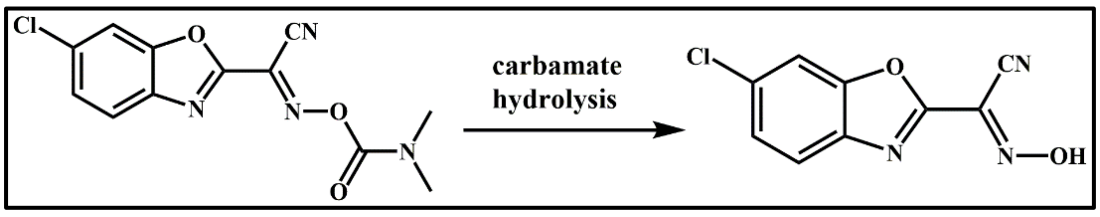

Figure 2.13. *M. tuberculosis* metabolism of benzoxazole-based oxime carbamates.

2.4 Discussion

The delivery of successful clinical drug candidates in the TB drug development pipeline depends to a large extent on comprehensive upstream optimization assays that will translate *in vitro* activity of antimycobacterial drug leads to *in vivo* efficacy in animal models (Franzblau et al. 2012; Dartois and Barry 2013). To probe *in vitro* drug permeation, active compounds with variable physicochemical properties were selected.

Repositioning efforts undertaken so far suggest that FA has a potential role as an antimycobacterial agent. The C3-ester derivatives GKFA16 and GKFA17 had similar activities, while the 3-ketoFA metabolite showed comparable activity to FA in both glucose and glycerol-based culture media, however, the differences amongst all compounds were not significant. Glycerol is often preferred for *in vitro* testing in axenic culture due to favorable *M. tuberculosis* growth, however, it may confound MIC measurements by increasing drug susceptibilities in compounds with glycerol-dependent activity (Franzblau et al. 2012). For example, glycerol-dependent *in vitro* activity was reported when pyrimidine imidazoles failed to show *in vivo* efficacy in an animal model and their potent *in vitro* activity was found to depend on the carbon source (Pethe et al. 2010). During host infection, some studies have reported that *M. tuberculosis* relies on glucose and fatty acid metabolism (Munoz-Elias and McKinney 2005; Marrero et al. 2013). Recent studies, however, have reported on a glycerol catabolism dependent ability of *M. tuberculosis* to develop drug tolerance, by inducing reversible mutations in the *glpK* gene encoding for glycerol-3-kinase (Safi et al. 2019; Bellerose et al. 2019). These findings directly implicate *M. tuberculosis* metabolism in drug efficacy therefore highlighting the importance of utilizing different carbon sources in *in vitro* assays.

M. tuberculosis activity in cholesterol-enriched media showed a 4-fold difference in FA and 3-ketoFA activity in comparison to glucose media, while no differences were observed for C3-

ester derivatives. The presence of a lipophilic alkyl side chain may be beneficial in a lipid-enriched environment where the interaction with cholesterol may increase the chance of reaching *M. tuberculosis*, while the less lipophilic FA and GKFA37 may suffer from drug binding and hence reduce the free fraction amount in media.

M. tuberculosis is exposed to acidic conditions in the phagolysosome, and it is these bacilli that may become non-replicating in response to the host acidic environment (Levitte et al. 2016). Finding drugs that have favorable cellular penetration properties and are potent at low pH, like PZA may be crucial in targeting these bacilli and prevent formation of non-replicating or slow growth bacteria in the macrophage cellular environment, would be particularly useful in cases of known PZA resistance. While there was an initial delayed growth in the slightly acidic pH conditions, *M. tuberculosis* was able to grow at pH 5.83 suggesting it becomes tolerant to acidic host conditions, in accordance with previous reports of mycobacterial acid tolerance (Vandal et al. 2008; Levitte et al. 2016). FA and its keto derivative were able to inhibit *M. tuberculosis* growth under acidic conditions by 4-fold in comparison to normal *in vitro* pH conditions, suggesting a potential for these compounds in intraphagosomal growth inhibition. Lemaire et al, (2011) reported that the lower MIC values of FA against *S. aureus*, observed in acidic conditions were associated with increased cellular uptake and drug accumulation; which was not observed for drugs such LZD whose MIC remained unaffected. They attributed this increase in part due to FA being a weak acid (pKa 4.7 to 5) whose lipophilicity increases when pH is reduced to 5. In addition, the ability of bacterial cells to maintain a pH gradient across their membranes through the proton motive respiratory chain system was though to facilitate FA permeation and FA intracellular trapping as the pH is likely more alkaline within the cells, therefore increasing the accessibility of FA molecules to its target (Lemaire et al. 2011). Future work could determine *M. tuberculosis* accumulation and metabolism of FA, and the C3-ester

derivatives under acidic conditions, to determine if M. tuberculosis-mediated metabolism could contribute to the improved *in vitro* activity.

The *in vitro* antimycobacterial data indicates that there is no glycerol-dependent activity for both the carbamates and their free oximes as compounds showed similar activity in both glucose and glycerol-supplemented media. The oximes, however, were inactive against *M. tuberculosis*. The findings that show hydrolysis of the carbamates even under culture conditions indicate that further studies should investigate substitution with a less labile group, while maintaining activity. From a drug development point of view, with these liabilities, the carbamates would likely suffer from limited bioavailability as potential breakdown in circulation would prevent the drug from reaching its site of action. For a disease such as TB, with complex pathology and a complicated drug route to reach the bacilli in their niche, poor stability would render these compounds ineffective.

Early *in vitro* optimization of physicochemical properties - solubility, lipophilicity (clogP or logD), permeability and stability - is essential in informing *in vitro* and *in vivo* PK/PD parameters (Sohlenius-Sternbeck et al. 2016; Dartois 2014). These parameters were profiled to tease out potential correlations between the physicochemical properties and *in vitro* cellular PK/PD. FA and derivatives are high molecular weight, high lipophilicity compounds (MW >500; clogP >5). Despite this violation of two of Lipinski's guidelines for oral drugs, these compounds are natural product derived, and therefore are highly likely to deviate from the 'normal' drug-likeness as is indeed the case for some clinically used TB drugs, which are not natural products. While a 'sweet spot' in lipophilicity is required for drug permeation through membranes, a limitation to increased lipophilicity is the drastic loss of solubility, which makes delivery of a drug difficult. PAMPA prediction showed high permeability for the lipophilic FA

and 3-ketoFA in comparison to the less lipophilic MXF. However, it is important to note that PAMPA predicts permeability based on passive diffusion using an artificial membrane, and such data should be extrapolated with caution. These compounds likely benefit from being semisynthetic derivatives of a natural product and permeation across the cell membrane could be possible through the highly diverse pool of active membrane transporters (International Transporter et al. 2010). While the clogP and MW properties fall outside the chemical space occupied by classical TB drugs, they do occupy a similar physicochemical space as BDQ, CFZ and DLM (Figure 2.1), all of which are currently recommended for DR-TB. This further emphasizes that anti-TB drugs do not have a defined physicochemical space.

GKFA16 and GKFA17 are prodrugs of FA through addition of alkyl ester groups at the C3 position. It was hypothesized that these FA derivatives would undergo cleavage by esterase enzyme activity intracellularly to release the potent FA. Although these compounds were found to be active against *M. tuberculosis*, data shows that they are hydrolyzed by *M. tuberculosis* to release FA and to a lesser extent, FA is further metabolized to form the active metabolite, 3-ketoFA. FA is likely metabolized to another unknown major metabolite by *M. tuberculosis*, and further studies to determine the nature of this metabolite is needed. Metabolism by liver enzymes of rodent species, identified epimerization of FA at C-3, or FA lactone formation at C-16 both of which could be potential *M. tuberculosis* metabolites (Njoroge et al. 2019). These data strongly imply *M. tuberculosis* esterase-mediated activity. Since C-3 esters, FA and 3-ketoFA are all active forms of FA, it is likely that *in vitro* activity is due to multiple species of the drug present in media. Furthermore, addition of an ester group at C-3 which has been shown to increase FA bioavailability and tissue distribution (Strydom et al. 2020), may be a good strategy to increase host intracellular FA exposure through slow release from the prodrug.

While the benzoxazole-based oxime carbamates showed potent *in vitro* activity, their main liability was the observed susceptibility to degradation in culture media (Fig 2.11). After administration, a drug should, with the right physiochemical properties, be able to traverse through biological membranes to reach the intracellular molecular target at sufficient concentrations required for activity (Dartois 2014). Some groups are more prone to spontaneous degradation or enzymatic cleavage (Awasthi and Freundlich 2017), which could affect the amount of drug available both in the bloodstream and the amount that reaches the drug target. This spontaneous degradation resulted in the more stable free oximes, which when tested for antimycobacterial activity were found to have some activity to complete loss of activity for others. It is hypothesized that the loss of activity seen with some of the free oxime is likely due to poor *M. tuberculosis* permeation. In addition, since the highly active carbamates underwent significant hydrolysis by *M. tuberculosis* enzymes within only 3 hours of incubation, it is further hypothesized that carbamates are likely responsible for *M. tuberculosis* permeation, and once within the bacilli, esterase activity releases the free oxime which is the drug species that reaches the molecular target and is responsible for activity. From a drug development perspective, developing carbamates with increased stability may not only facilitate uptake by *M. tuberculosis* cells, but with a slower rate of metabolism could potentially ensure increase cellular accumulation of the carbamate and subsequently more oxime drug molecules reaching the molecular target.

In vitro assessments of antimycobacterial activity ought to consider and simulate the host environments under which *M. tuberculosis* exists during infection. *M. tuberculosis* metabolic functions respond to human host mechanisms, and vice versa (Mashabela, de Wet, and Warner 2019); therefore, *in vitro* experimental assays are required (Franzblau et al. 2012) with conditions that recapitulate variations in pH, nutrient sources, oxygen and nitric oxide stress, to intramacrophage systems *in vitro* (Vandal et al. 2008; Vandal, Nathan, and Ehrt 2009; Rohde

et al. 2012; Singh et al. 2012; Russell et al. 2009), and *in vivo* animals and nonhuman primates (Martin et al. 2017; Lin et al. 2014). Investigation of drug activity under conditions which have been implicated in driving disease pathology may provide useful data to inform *in vivo* PK/PD analyses. For an intracellular pathogen, host cells may be exposed to higher intracellular drug accumulation which could affect host homeostatic functions. For this reason, safety indices must be evaluated to determine if effective drug concentrations risk cytotoxicity. The unique architecture of the *M. tuberculosis* bacilli plays a direct role on the permeability of drug molecules, and lesion microenvironments determine site specific drug exposure (Koul et al. 2011; Dartois 2014; Dartois and Barry 2013). Therefore, an emphasis ought to be placed on optimization of physicochemical properties of a drug. These optimizations should be in relation to uptake by the host cell containing *M. tuberculosis* bacilli, and caseum diffusion; and not just the ability to be absorbed in the gut.

Understanding drug-*M. tuberculosis* interactions in upstream analyses could aid the design of drugs that can possess both the right physicochemical properties to permeate the *M. tuberculosis* cell wall and circumvent any resistance mechanisms that may result from *M. tuberculosis*-mediated biotransformation. Given the diverse fates of a drug upon contact with the bacilli, which may also depend on the metabolic state of the bacilli, it is important to understand this early on during *in vitro* optimization. In addition, *M. tuberculosis*-drug interactions could facilitate the design of compounds with the right physicochemical properties to improve drug uptake but are less susceptible to mycobacterial efflux.

2.5 References

Adams, K. N., K. Takaki, L. E. Connolly, H. Wiedenhoft, K. Winglee, O. Humbert, P. H. Edelstein, C. L. Cosma, and L. Ramakrishnan. 2011. 'Drug tolerance in replicating mycobacteria mediated by a macrophage-induced efflux mechanism', *Cell*, 145: 39-53.

Awasthi, D., and J. S. Freundlich. 2017. 'Antimycobacterial Metabolism: Illuminating Mycobacterium tuberculosis Biology and Drug Discovery', *Trends in Microbiology*, 25: 756-67.

Bellerose, M. M., S. H. Baek, C. C. Huang, C. E. Moss, E. I. Koh, M. K. Proulx, C. M. Smith, R. E. Baker, J. S. Lee, S. Eum, S. J. Shin, S. N. Cho, M. Murray, and C. M. Sassetti. 2019. 'Common Variants in the Glycerol Kinase Gene Reduce Tuberculosis Drug Efficacy', *mBio*, 10.

Besier, S., A. Ludwig, V. Brade, and T. A. Wichelhaus. 2003. 'Molecular analysis of fusidic acid resistance in Staphylococcus aureus', *Molecular Microbiology*, 47: 463-9.

Blanc, L., I. B. Daudelin, B. K. Podell, P. Y. Chen, M. Zimmerman, A. J. Martinot, R. M. Savic, B. Prideaux, and V. Dartois. 2018. 'High-resolution mapping of fluoroquinolones in TB rabbit lesions reveals specific distribution in immune cell types', *Elife*, 7.

Byrd, C. M., D. W. Grosenbach, A. Berhanu, D. Dai, K. F. Jones, K. B. Cardwell, C. Schneider, G. Yang, S. Tyavanagimatt, C. Harver, K. A. Wineinger, J. Page, E. Stavale, M. A. Stone, K. P. Fuller, C. Lovejoy, J. M. Leeds, D. E. Hruby, and R. Jordan. 2013. 'Novel benzoxazole inhibitor of dengue virus replication that targets the NS3 helicase', *Antimicrobial Agents and Chemotherapy*, 57: 1902-12.

Chacko, S., H. I. M. Boshoff, V. Singh, D. M. Ferraris, D. R. Gollapalli, M. Zhang, A. P. Lawson, M. J. Pepi, A. Joachimiak, M. Rizzi, V. Mizrahi, G. D. Cuny, and L. Hedstrom. 2018. 'Expanding Benzoxazole-Based Inosine 5'-Monophosphate Dehydrogenase (IMPDH) Inhibitor Structure-Activity As Potential Antituberculosis Agents', *Journal of Medicinal Chemistry*, 61: 4739-56.

Cicek-Saydam, C., C. Cavusoglu, D. Burhanoglu, S. Hilmioglu, N. Ozkalay, and A. Bilgic. 2001. 'In vitro susceptibility of Mycobacterium tuberculosis to fusidic acid', *Clinical Microbiology and Infection*, 7: 700-2.

Collignon, P., and J. Turnidge. 1999. 'Fusidic acid in vitro activity', *International Journal of Antimicrobial Agents*, 12 Suppl 2: S45-58.

Daniel, J., H. Maamar, C. Deb, T. D. Sirakova, and P. E. Kolattukudy. 2011. 'Mycobacterium tuberculosis uses host triacylglycerol to accumulate lipid droplets and acquires a dormancy-like phenotype in lipid-loaded macrophages', *PLoS Pathogens*, 7: e1002093.

Dartois, V. 2014. 'The path of anti-tuberculosis drugs: from blood to lesions to mycobacterial cells', *Nature Reviews: Microbiology*, 12: 159-67.

Dartois, V., and C. E. Barry, 3rd. 2013. 'A medicinal chemists' guide to the unique difficulties of lead optimization for tuberculosis', *Bioorganic and Medicinal Chemistry Letters*, 23: 4741-50.

Duvold, T., M. D. Sorensen, F. Bjorkling, A. S. Henriksen, and N. Rastrup-Andersen. 2001. 'Synthesis and conformational analysis of fusidic acid side chain derivatives in relation to antibacterial activity', *Journal of Medicinal Chemistry*, 44: 3125-31.

Dziwornu, G. A., S. Kamunya, T. Ntsabo, and K. Chibale. 2019. 'Novel antimycobacterial C-21 amide derivatives of the antibiotic fusidic acid: synthesis, pharmacological evaluation and rationalization of media-dependent activity using molecular docking studies in the binding site of human serum albumin', *Medchemcomm*, 10: 961-69.

Franzblau, S. G., M. A. DeGroote, S. H. Cho, K. Andries, E. Nuermberger, I. M. Orme, K. Mdluli, I. Angulo-Barturen, T. Dick, V. Dartois, and A. J. Lenaerts. 2012. 'Comprehensive analysis of methods used for the evaluation of compounds against Mycobacterium tuberculosis', *Tuberculosis (Edinb)*, 92: 453-88.

Fuursted, K., D. Askgaard, and V. Faber. 1992. 'Susceptibility of strains of the Mycobacterium tuberculosis complex to fusidic acid', *APMIS*, 100: 663-7.

Godtfredsen, W. O., W. Von Daehne, L. Tybring, and S. Vangedal. 1966. 'Fusidic acid derivatives. I. Relationship between structure and antibacterial activity', *Journal of Medicinal Chemistry*, 9: 15-22.

International Transporter, Consortium, K. M. Giacomini, S. M. Huang, D. J. Tweedie, L. Z. Benet, K. L. Brouwer, X. Chu, A. Dahlin, R. Evers, V. Fischer, K. M. Hillgren, K. A. Hoffmaster, T. Ishikawa, D. Keppler, R. B. Kim, C. A. Lee, M. Niemi, J. W. Polli, Y. Sugiyama, P. W. Swaan, J. A. Ware, S. H. Wright, S. W. Yee, M. J. Zamek-Gliszczynski, and L. Zhang. 2010. 'Membrane transporters in drug development', *Nat Rev Drug Discov*, 9: 215-36.

Joshi, M. C., J. Okombo, S. Nsumiwa, J. Ndove, D. Taylor, L. Wiesner, R. Hunter, K. Chibale, and T. J. Egan. 2017. '4-Aminoquinoline Antimalarials Containing a Benzylmethylpyridylmethylamine Group Are Active against Drug Resistant Plasmodium falciparum and Exhibit Oral Activity in Mice', *Journal of Medicinal Chemistry*, 60: 10245-56.

Kim, M. J., H. C. Wainwright, M. Locketz, L. G. Bekker, G. B. Walther, C. Dittrich, A. Visser, W. Wang, F. F. Hsu, U. Wiehart, L. Tsenova, G. Kaplan, and D. G. Russell. 2010. 'Caseation of human tuberculosis granulomas correlates with elevated host lipid metabolism', *EMBO Molecular Medicine*, 2: 258-74.

Koul, A., E. Arnoult, N. Lounis, J. Guillemont, and K. Andries. 2011. 'The challenge of new drug discovery for tuberculosis', *Nature*, 469: 483-90.

Lakshminarayana, S. B., T. B. Huat, P. C. Ho, U. H. Manjunatha, V. Dartois, T. Dick, and S. P. Rao. 2015. 'Comprehensive physicochemical, pharmacokinetic and activity profiling of anti-TB agents', *Journal of Antimicrobial Chemotherapy*, 70: 857-67.

Laurberg, M., O. Kristensen, K. Martemyanov, A. T. Gudkov, I. Nagaev, D. Hughes, and A. Liljas. 2000. 'Structure of a mutant EF-G reveals domain III and possibly the fusidic acid binding site', *Journal of Molecular Biology*, 303: 593-603.

Lee, W., B. C. VanderVen, R. J. Fahey, and D. G. Russell. 2013. 'Intracellular Mycobacterium tuberculosis exploits host-derived fatty acids to limit metabolic stress', *Journal of Biological Chemistry*, 288: 6788-800.

Lemaire, S., F. Van Bambeke, D. Pierard, P. C. Appelbaum, and P. M. Tulkens. 2011. 'Activity of fusidic acid against extracellular and intracellular Staphylococcus aureus: influence of pH and comparison with linezolid and clindamycin', *Clinical Infectious Diseases*, 52 Suppl 7: S493-503.

Levitte, S., K. N. Adams, R. D. Berg, C. L. Cosma, K. B. Urdahl, and L. Ramakrishnan. 2016. 'Mycobacterial Acid Tolerance Enables Phagolysosomal Survival and Establishment of Tuberculous Infection In Vivo', *Cell Host Microbe*, 20: 250-8.

Lin, P. L., C. B. Ford, M. T. Coleman, A. J. Myers, R. Gawande, T. Ioerger, J. Sacchettini, S. M. Fortune, and J. L. Flynn. 2014. 'Sterilization of granulomas is common in active and latent tuberculosis despite within-host variability in bacterial killing', *Nature Medicine*, 20: 75-9.

Lipinski, C. A., F. Lombardo, B. W. Dominy, and P. J. Feeney. 2001. 'Experimental and computational approaches to estimate solubility and permeability in drug discovery and development settings', *Adv Drug Deliv Rev*, 46: 3-26.

Lukowska-Chojnacka, E., A. Kowalkowska, and A. Napiorkowska. 2018. 'Lipase-catalyzed kinetic resolution of novel antitubercular benzoxazole derivatives', *Chirality*, 30: 457-68.

Malapati, P., V. S. Krishna, R. Nallangi, R. R. Srilakshmi, and D. Sriram. 2018. 'Identification and development of benzoxazole derivatives as novel bacterial glutamate racemase inhibitors', *European Journal of Medicinal Chemistry*, 145: 23-34.

Marakalala, M. J., R. M. Raju, K. Sharma, Y. J. Zhang, E. A. Eugenin, B. Prideaux, I. B. Daudelin, P. Y. Chen, M. G. Booty, J. H. Kim, S. Y. Eum, L. E. Via, S. M. Behar, C.

E. Barry, 3rd, M. Mann, V. Dartois, and E. J. Rubin. 2016. 'Inflammatory signaling in human tuberculosis granulomas is spatially organized', *Nature Medicine*, 22: 531-8.

Marrero, J., C. Trujillo, K. Y. Rhee, and S. Ehrt. 2013. 'Glucose phosphorylation is required for Mycobacterium tuberculosis persistence in mice', *PLoS Pathogens*, 9: e1003116.

Martin, C. J., A. M. Cadena, V. W. Leung, P. L. Lin, P. Maiello, N. Hicks, M. R. Chase, J. L. Flynn, and S. M. Fortune. 2017. 'Digitally Barcoding Mycobacterium tuberculosis Reveals In Vivo Infection Dynamics in the Macaque Model of Tuberculosis', *mBio*, 8.

Mashabela, G. T., T. J. de Wet, and D. F. Warner. 2019. 'Mycobacterium tuberculosis Metabolism', *Microbiol Spectr*, 7.

Munoz-Elias, E. J., and J. D. McKinney. 2005. 'Mycobacterium tuberculosis isocitrate lyases 1 and 2 are jointly required for in vivo growth and virulence', *Nature Medicine*, 11: 638-44.

Njoroge, M., G. Kaur, M. Espinoza-Moraga, A. Wasuna, G. A. Dziwornu, R. Seldon, D. Taylor, J. Okombo, D. F. Warner, and K. Chibale. 2019. 'Semisynthetic Antimycobacterial C-3 Silicate and C-3/C-21 Ester Derivatives of Fusidic Acid: Pharmacological Evaluation and Stability Studies in Liver Microsomes, Rat Plasma, and Mycobacterium tuberculosis culture', *ACS Infect Dis*, 5: 1634-44.

O'Shea, R., and H. E. Moser. 2008. 'Physicochemical properties of antibacterial compounds: implications for drug discovery', *Journal of Medicinal Chemistry*, 51: 2871-8.

Omollo, C., V. Singh, E. Kigondu, A. Wasuna, P. Agarwal, A. Moosa, T.R. Ioerger, V. Mizrahi, K. Chibale, and D. F. Warner. 2019. 'Developing synergistic drug combinations to restore antibiotic sensitivity in drug-resistant Mycobacterium tuberculosis', *bioRxiv*.

Pethe, K., P. C. Sequeira, S. Agarwalla, K. Rhee, K. Kuhen, W. Y. Phong, V. Patel, D. Beer, J. R. Walker, J. Duraiswamy, J. Jiricek, T. H. Keller, A. Chatterjee, M. P. Tan, M. Ujjini, S. P. Rao, L. Camacho, P. Bifani, P. A. Mak, I. Ma, S. W. Barnes, Z. Chen, D. Plouffe, P. Thayalan, S. H. Ng, M. Au, B. H. Lee, B. H. Tan, S. Ravindran, M. Nanjundappa, X. Lin, A. Goh, S. B. Lakshminarayana, C. Shoen, M. Cynamon, B. Kreiswirth, V. Dartois, E. C. Peters, R. Glynne, S. Brenner, and T. Dick. 2010. 'A chemical genetic screen in Mycobacterium tuberculosis identifies carbon-source-dependent growth inhibitors devoid of in vivo efficacy', *Nat Commun*, 1: 57.

Peyron, P., J. Vaubourgeix, Y. Poquet, F. Levillain, C. Botanch, F. Bardou, M. Daffe, J. F. Emile, B. Marchou, P. J. Cardona, C. de Chastellier, and F. Altare. 2008. 'Foamy

macrophages from tuberculous patients' granulomas constitute a nutrient-rich reservoir for M. tuberculosis persistence', *PLoS Pathogens*, 4: e1000204.

Prideaux, B., L. E. Via, M. D. Zimmerman, S. Eum, J. Sarathy, P. O'Brien, C. Chen, F. Kaya, D. M. Weiner, P. Y. Chen, T. Song, M. Lee, T. S. Shim, J. S. Cho, W. Kim, S. N. Cho, K. N. Olivier, C. E. Barry, 3rd, and V. Dartois. 2015. 'The association between sterilizing activity and drug distribution into tuberculosis lesions', *Nature Medicine*, 21: 1223-7.

Pu, Y., Z. Zhao, Y. Li, J. Zou, Q. Ma, Y. Zhao, Y. Ke, Y. Zhu, H. Chen, M. A. B. Baker, H. Ge, Y. Sun, X. S. Xie, and F. Bai. 2016. 'Enhanced Efflux Activity Facilitates Drug Tolerance in Dormant Bacterial Cells', *Molecular Cell*, 62: 284-94.

Rida, S. M., F. A. Ashour, S. A. El-Hawash, M. M. ElSemary, M. H. Badr, and M. A. Shalaby. 2005. 'Synthesis of some novel benzoxazole derivatives as anticancer, anti-HIV-1 and antimicrobial agents', *European Journal of Medicinal Chemistry*, 40: 949-59.

Rohde, K. H., D. F. Veiga, S. Caldwell, G. Balazsi, and D. G. Russell. 2012. 'Linking the transcriptional profiles and the physiological states of Mycobacterium tuberculosis during an extended intracellular infection', *PLoS Pathogens*, 8: e1002769.

Russell, D. G., P. J. Cardona, M. J. Kim, S. Allain, and F. Altare. 2009. 'Foamy macrophages and the progression of the human tuberculosis granuloma', *Nature Immunology*, 10: 943-8.

Safi, H., P. Gopal, S. Lingaraju, S. Ma, C. Levine, V. Dartois, M. Yee, L. Li, L. Blanc, H. P. Ho Liang, S. Husain, M. Hoque, P. Soteropoulos, T. Rustad, D. R. Sherman, T. Dick, and D. Alland. 2019. 'Phase variation in Mycobacterium tuberculosis glpK produces transiently heritable drug tolerance', *Proceedings of the National Academy of Sciences of the United States of America*, 116: 19665-74.

Sarathy, J., V. Dartois, T. Dick, and M. Gengenbacher. 2013. 'Reduced drug uptake in phenotypically resistant nutrient-starved nonreplicating Mycobacterium tuberculosis', *Antimicrobial Agents and Chemotherapy*, 57: 1648-53.

Sarathy, J. P., F. Zuccotto, H. Hsinpin, L. Sandberg, L. E. Via, G. A. Marriner, T. Masquelin, P. Wyatt, P. Ray, and V. Dartois. 2016. 'Prediction of Drug Penetration in Tuberculosis Lesions', *ACS Infect Dis*, 2: 552-63.

Shanson, D. C. 1990. 'Clinical relevance of resistance to fusidic acid in Staphylococcus aureus', *Journal of Antimicrobial Chemotherapy*, 25 Suppl B: 15-21.

Singh, V., S. Jamwal, R. Jain, P. Verma, R. Gokhale, and K. V. Rao. 2012. 'Mycobacterium tuberculosis-driven targeted recalibration of macrophage lipid homeostasis promotes the foamy phenotype', *Cell Host Microbe*, 12: 669-81.

Sohlenius-Sternbeck, A. K., J. Janson, J. Bylund, P. Baranczewski, A. Breitholtz-Emanuelsson, Y. Hu, C. Tsoi, A. Lindgren, O. Gissberg, T. Bueters, S. Briem, S. Juric, J. Johansson, M. Bergh, and J. Hoogstraate. 2016. 'Optimizing DMPK Properties: Experiences from a Big Pharma DMPK Department', *Curr Drug Metab*, 17: 253-70.

Strydom, N., G. Kaur, G. A. Dziwornu, J. Okombo, L. Wiesner, and K. Chibale. 2020. 'Pharmacokinetics and Organ Distribution of C-3 Alkyl Esters as Potential Antimycobacterial Prodrugs of Fusidic Acid', *ACS Infect Dis*, 6: 459-66.

Te Brake, L. H. M., G. J. de Knegt, J. E. de Steenwinkel, T. J. P. van Dam, D. M. Burger, F. G. M. Russel, R. van Crevel, J. B. Koenderink, and R. E. Aarnoutse. 2018. 'The Role of Efflux Pumps in Tuberculosis Treatment and Their Promise as a Target in Drug Development: Unraveling the Black Box', *Annual Review of Pharmacology and Toxicology*, 58: 271-91.

Turnidge, J. 1999. 'Fusidic acid pharmacology, pharmacokinetics and pharmacodynamics', *International Journal of Antimicrobial Agents*, 12 Suppl 2: S23-34.

Turnidge, J., and P. Collignon. 1999. 'Resistance to fusidic acid', *International Journal of Antimicrobial Agents*, 12 Suppl 2: S35-44.

Van Caekenberghe, D. 1990. 'Comparative in-vitro activities of ten fluoroquinolones and fusidic acid against Mycobacterium spp', *Journal of Antimicrobial Chemotherapy*, 26: 381-6.

van der Westhuyzen, R., S. Winks, C. R. Wilson, G. A. Boyle, R. K. Gessner, C. Soares de Melo, D. Taylor, C. de Kock, M. Njoroge, C. Brunschwig, N. Lawrence, S. P. Rao, F. Sirgel, P. van Helden, R. Seldon, A. Moosa, D. F. Warner, L. Arista, U. H. Manjunatha, P. W. Smith, L. J. Street, and K. Chibale. 2015. 'Pyrrolo[3,4-c]pyridine-1,3(2H)-diones: A Novel Antimycobacterial Class Targeting Mycobacterial Respiration', *Journal of Medicinal Chemistry*, 58: 9371-81.

Vandal, O. H., C. F. Nathan, and S. Ehrt. 2009. 'Acid resistance in Mycobacterium tuberculosis', *Journal of Bacteriology*, 191: 4714-21.

Vandal, O. H., L. M. Pierini, D. Schnappinger, C. F. Nathan, and S. Ehrt. 2008. 'A membrane protein preserves intrabacterial pH in intraphagosomal Mycobacterium tuberculosis', *Nature Medicine*, 14: 849-54.

Zhang, H. Z., Z. L. Zhao, and C. H. Zhou. 2018. 'Recent advance in oxazole-based medicinal chemistry', *European Journal of Medicinal Chemistry*, 144: 444-92.

CHAPTER 3

EVALUATING PERMEATION AND INTRACELLULAR EFFICACIES OF ANTIMYCOBACTERIAL AGENTS IN *M. TUBERCULOSIS*-INFECTED MACROPHAGES

3.1 Introduction

The *M. tuberculosis*-infected macrophage represents a crucial feature in TB disease pathogenesis. The adaptation of *M. tuberculosis* to life as an intracellular pathogen has already been discussed in Chapter 1. *M. tuberculosis* survives the intraphagosomal environment, characterized by acidic pH and reactive oxygen and nitrogen intermediates (ROI and RNI, respectively), through adaptation mechanisms that allow for its continued replication or shift to a non-replicating state in the intracellular niche (Rohde et al. 2007). The different metabolic states adopted by bacilli in macrophages are critical from a therapeutic viewpoint as sufficient intracellular drug concentrations are required to target not only the replicating, but non-replicating, tolerant bacilli. *In vitro* transcriptional analyses indicate genetic variations in response to host macrophage-derived stresses. Differential expression of genes associated with β-oxidation of fatty acids, nitrosative and oxidative stress, iron metabolism, cell envelope modifications and induction of DosR dormancy regulon, were reported in *in vitro* macrophage infection experiments simulating early *in vivo* infection events (Schnappinger et al. 2003; Rohde et al. 2012). Rohde et al., (2012) reported that *M. tuberculosis* transcriptional signatures alter dramatically following the initial phagosomal encounter. However, some genes return to normal transcriptional levels as *M. tuberculosis* adapts to life in the macrophage phagosome. Significant evidence exists to support our understanding of how intracellular *M. tuberculosis*, in response to macrophage antimicrobial mechanisms, undergoes metabolic and physiological

changes or induces changes in host metabolism to ensure its survival (Ehrt, Schnappinger, and Rhee 2018; Mashabela, de Wet, and Warner 2019; Gleeson et al. 2016; Shi et al. 2015) The upregulation of dormancy genes suggests that at least a subpopulation of intracellular *M. tuberculosis* bacilli are non-replicating or slow-growing, and the associated metabolic shift may allow its survival in the phagosome in a state of clinical latency. Intracellular macrophage residence necessitates efficient delivery of drugs to inhibit bacterial growth and achieve sterilization. Therefore, understanding cellular PK/PD is crucial to optimize drugs that possess favorable characteristics for intracellular permeation (Dartois 2014; Dartois and Barry 2013; Tanner et al. 2018).

In recent years, more studies have focused on investigating the differential abilities of anti-TB drugs to penetrate and accumulate in macrophages *in vitro*. Utilizing host cell infection models in early investigations could elucidate the relationship between cellular drug penetration, physicochemical properties of drugs and their ability to kill intracellular bacillary subpopulations. These data could be used to inform drug penetration into alveolar macrophages and other infected host cells *in vivo*. For example, differential accumulation of fluoroquinolones in *in vitro* cell cultures has been reported and suggests a potential for different treatment outcomes against intracellular bacteria for this class of anti-TB drugs. Michot et al., showed that MXF had superior intracellular accumulation compared to other fluoroquinolones (LVF, ciprofloxacin (CPX), and garenoxacin) and was less susceptible to the efflux transporter responsible for CPX efflux (Michot et al. 2005; Michot et al. 2004). Reduced accumulation of CPX in J774 macrophages was associated with efflux by a multidrug resistance-associated protein (MRP), a member of the ATP-binding cassette transporter superfamily (Michot et al. 2004; Marquez et al. 2009). MRP efflux activity was dependent on pH, as acidic pH increased intracellular concentrations owing to reduced efflux (Michot et al. 2004). These findings

suggest that intracellular concentrations are a function of drug influx and efflux; and that their differences are likely influenced by differences in physicochemical properties of drugs. While in bacteria efflux is mostly a mechanism of drug tolerance (Adams et al. 2011), efflux in eukaryotic cells is an important factor for determining drug cellular PK and overall tissue accumulation.

Drug ion imaging data showed favorable cellular distribution of MXF in comparison to caseum, while *in vitro* macrophage data showed that the MXF intracellular/extracellular (I/E) ratio was superior to other anti-TB drugs, second only to CFZ (Prideaux et al. 2015). These data, showing poor caseum penetration of MXF, provided insight into the failure of MXF-containing regimens in sterilizing persisters and shortening TB treatment (Gillespie et al. 2014; Warner and Mizrahi 2014). They also highlighted the importance of utilizing animal models which recapitulate key pathologic features of TB disease in humans. Increasing drug accumulation was associated with increasing lipophilicity of the drugs, with CFZ being the most lipophilic (clogP 7.26) (Prideaux et al. 2015). Substantial accumulation of CFZ in macrophages has been reported, with formation of crystal-like structures *in vitro* and *in vivo*. This is likely due to the low solubility of CFZ which causes it to precipitates out of an aqueous environment (Harbeck et al. 1999; Baik et al. 2013; Baik and Rosania 2012). With a very high tissue distribution and a longer half-life, physicochemical properties drive macrophage accumulation of CFZ leading to increased cellular lesion exposure. For this reason, CFZ still retains its use as an anti-TB drug in MDR-TB therapies.

The pioneering work of Dartois and colleagues envisions the path of a drug from administration to target site, and calls for interrogation and optimization steps to be taken to influence the amount of drug reaching the molecular target (Dartois 2014). In this chapter, the focus is on

how the physicochemical properties of a drug influence macrophage penetration, and on how the differences in intracellular accumulation affect inhibition of bacterial growth. In addition, the influence of macrophage bacterial burden on the amount of drug accumulated in infected host cells was investigated. Furthermore, the previous chapter reported *M. tuberculosis*-mediated metabolism of FA and its prodrugs in axenic culture; here, *M. tuberculosis*-mediated drug metabolism in the host intracellular environment is also investigated. The selected compounds, FA and benzoxazole-based oxime derivatives have varying lipophilicities which enable an investigation of the effect of this physicochemical property on drug accumulation and efficacy.

3.2 Results

3.2.1 Accumulation of FA and derivatives in resting macrophages

Drug cellular uptake was investigated by exposing a monolayer of PMA-differentiated THP-1 cells to a single concentration (10µM) of the selected compounds over time. After washing off extracellular compound, liquid chromatography tandem mass spectrometry (LC-MS/MS) methods were used to quantify intracellular drug concentrations. As expected, after 48 hours of incubation, the more lipophilic FA ester derivatives, GKFA16 and GKFA17, were found to be highly accumulated intracellularly, by approximately 7- and 10-fold, respectively, in comparison to the parent compound (Figure 3.1 and 3.2). The RPMI drug medium was changed every second day and, while THP-1 macrophages maintained increasing levels of GKFA16 and GKFA17 over time, the intracellular concentrations of FA and GKFA37 peaked at about 24 hours and thereafter slowly decreased. MXF, with a lower clogP value of -0.082, accumulated at levels comparable to the least lipophilic of the FA compounds, GKFA37, despite their large differences in clogP. MXF showed a steady-state accumulation over the incubation period.

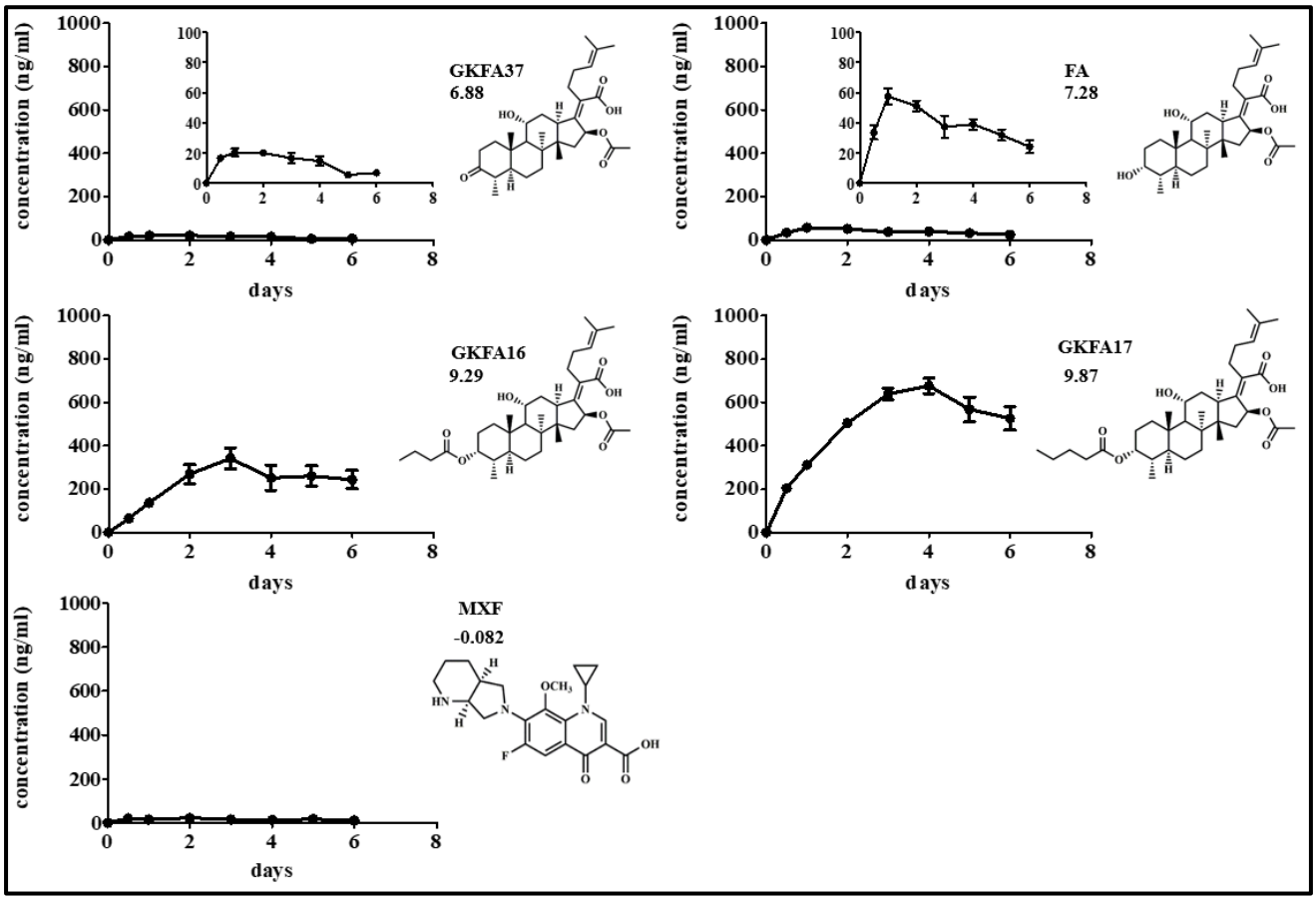

Figure 3.1. Concentrations of FA and derivatives accumulated in resting macrophages over a 6-day incubation period. Data represent mean ± SEM of 3 independent experiments for GKFA16 and GKFA17, and 2 independent experiments for FA, GKFA37 and MXF, performed in triplicate.

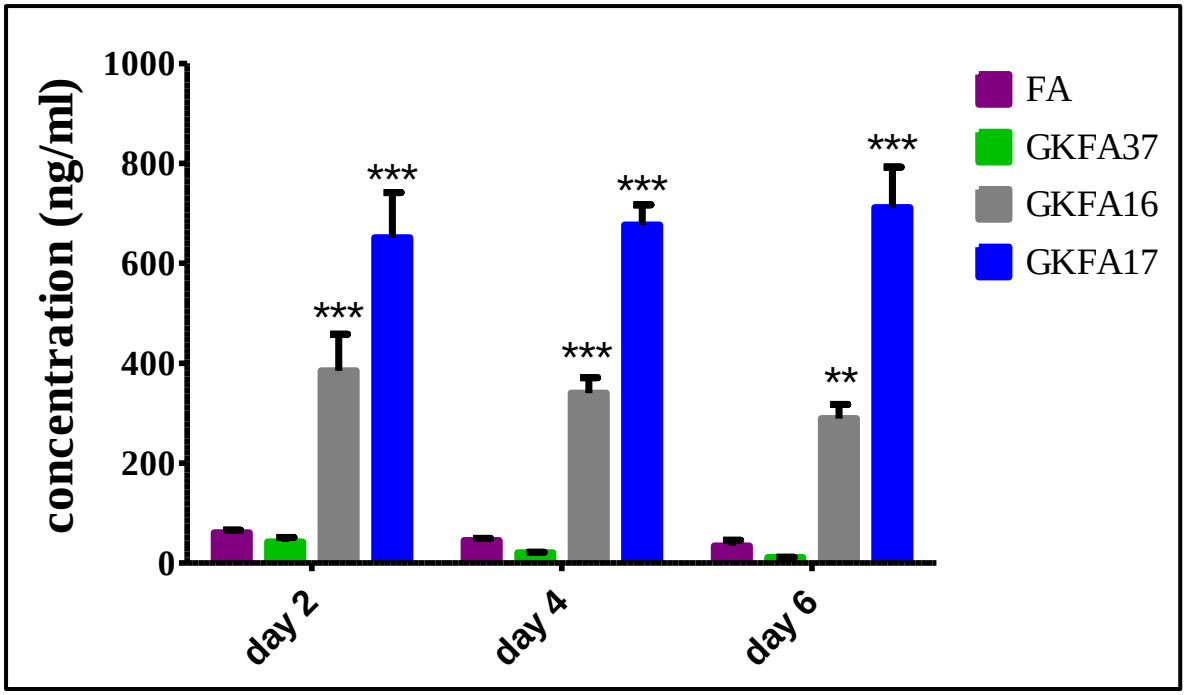

Figure 3.2. Comparison of intracellular drug concentrations after 2, 4 and 6 days of incubation with resting macrophages. Data represent mean ± SEM of at least 2 independent experiments performed in triplicate. Statistical significance was assessed using 1-way ANOVA with Tukey's post hoc test, comparing against FA at each time-point. *P < 0.05; **P < 0.01, ***P < 0.001.

LC-MS/MS methods can be used to quantify drug concentrations in tissue samples with accuracy and specificity. However, unlike MALDI-MSI imaging (Prideaux et al. 2015) or the correlated light, electron and ion microscopy (Greenwood et al. 2019) techniques which can determine specific drug spatial distribution in lung tissue and host cells, respectively, determination of drug protein or membrane binding utilizing LC-MS/MS would require prior fractionation of the sample. The concentrations reported in Figure 3.2 were quantities associated with the total cell lysate. However, given that cellular membranes are lipophilic structures with macromolecules spanning the surface, it is likely that a portion of the total drug measured was membrane bound. To determine how much of the measured drug amount represented free drug available intracellularly, and how much was associated with (non-specific) membrane-binding, macrophages were exposed to compounds for 48 hours. Following treatment, cells were lysed with deionized water, centrifuged and rinsed with

deionized water once more and both supernatant portions were collected to determine intracellular drug concentrations. The cell debris (containing membrane-bound drug) was resuspended in an equal volume of water and all portions were analyzed using LC-MS/MS.

The total amount measured from both pellets and supernatant combined was similar to the 2-day time-point (Figure 3.2), as expected. Only about 3.2% of the total FA measured was associated with the cell membrane, and the alkyl-esters (GKFA16 and GKFA17) had 6.6% and 19.1% of the compound bound to the cell membrane, respectively (Table 3.1). Taking this into account, the portion of the total drug fraction available intracellularly was still significantly higher than FA, approximately 7- and 10-fold for GKFA16 and GKFA17, respectively.

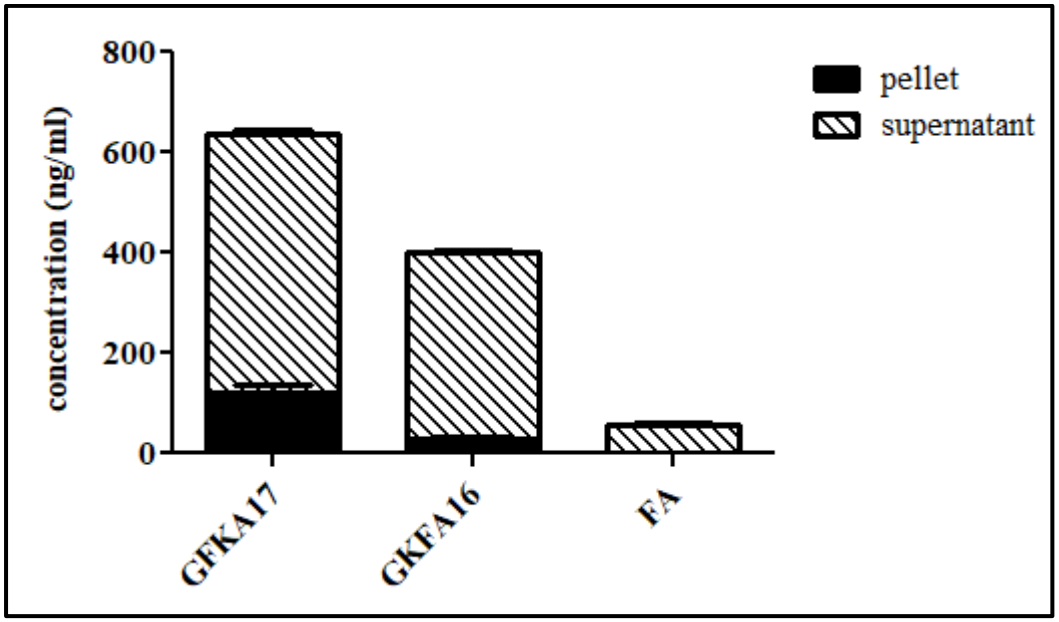

Figure 3.3. Cell membrane binding after 48 hours of incubation with resting macrophages.

Table 3.1. Fraction of membrane-bound drug.

Compound	Average % membrane bound
FA	3.2
GKFA16	6.6
GKFA17	19.1

3.2.2. Drug uptake during infection

M. tuberculosis infection of macrophages induces various changes within both the host cell and bacillus. In this thesis work, it was hypothesized that infection likely alters the ability of macrophages to accumulate drugs, which may be due to upregulation of mechanisms such as efflux transporters induced by *M. tuberculosis* resulting in decreased drug accumulation; or upregulation in protein or lipid phagocytosis resulting in increased uptake of lipid or protein-bound drug. Macrophage-induced drug tolerance of mycobacteria through upregulation of efflux transporters has been reported, and is reversible when treated with verapamil, (Adams et al. 2011; Adams, Szumowski, and Ramakrishnan 2014). However, it remains unclear whether *M. tuberculosis* induces macrophage drug transporters leading to alterations in intracellular concentrations and therefore affecting response to treatment. The effect of macrophage bacterial burden on drug accumulation was therefore investigated.

THP-1 macrophages were infected with a fluorescent reporter mutant, *M. tuberculosis* H37Rv MA :: (*smyc*'::mCherry (=pCherry3)) (Carroll et al. 2010) for 4 hours at multiplicities of infection (MOI) of 1, 2 and 5. The percentage of infected cells was determined by flow cytometry. In addition, infected cells were treated with GKFA17, the FA derivative that accumulated at the highest concentration, to enable the determination of whether infection had any effect on drug accumulation. Increasing bacterial exposure increased the number of host cells infected (Figure 3.4). However, no significant differences in drug accumulation were observed between infected and uninfected cells at all MOIs (Figure 3.5). For further infection experiments, macrophages were infected at MOI =1, which was determined to result in approximately 50% of cells infected (Figure 3. 4).

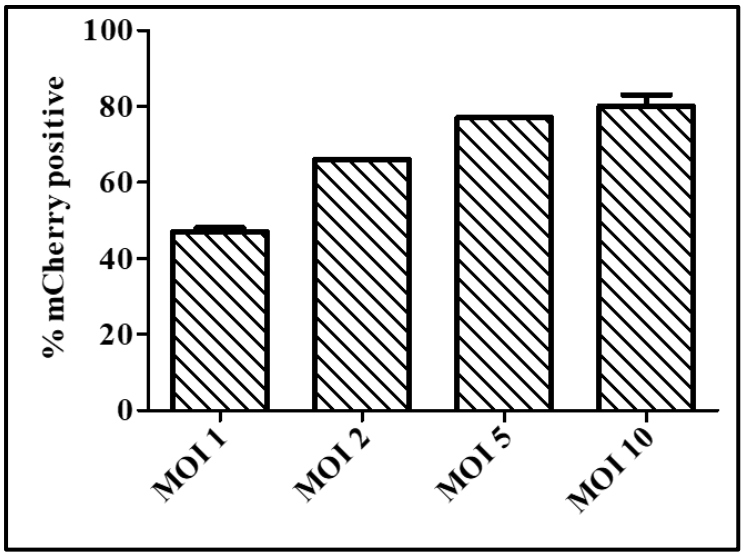

Figure 3.4. Percentage cells infected with a fluorescent reporter mutant, *M. tuberculosis* H37Rv MA:: (*smyc*'::mCherry (=pCherry3)) after 4 hours of incubation.

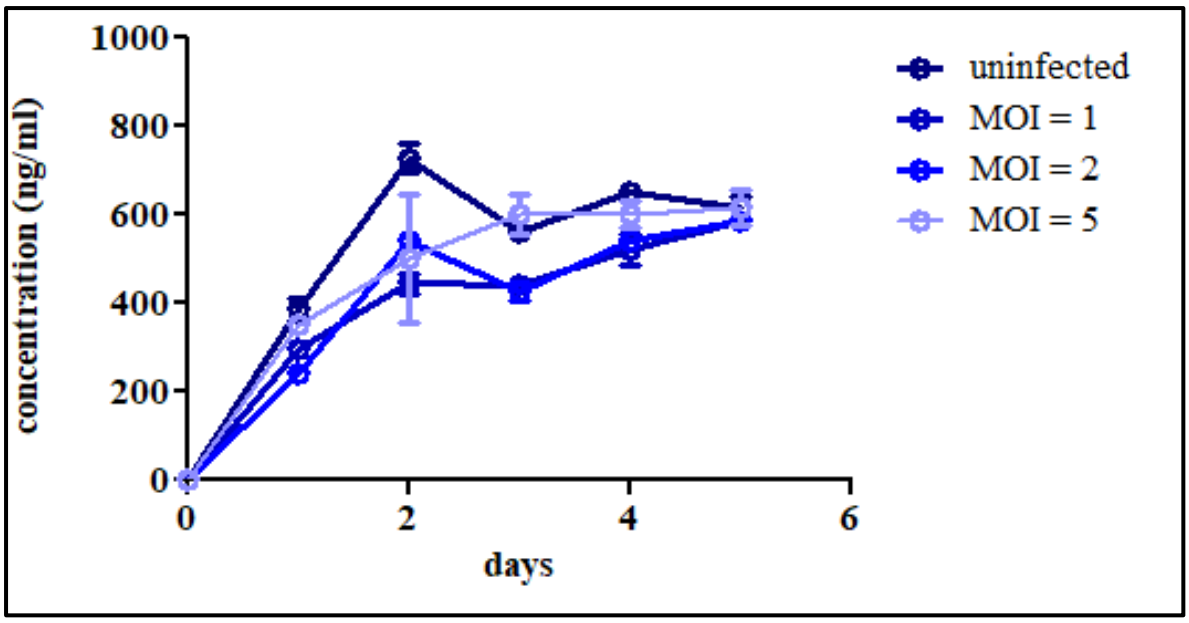

Figure 3.5. Macrophage drug accumulation as a function of host cell bacterial burden. Infected cells were treated with GKFA17 at a single concentration, 10 µM. Data are from a single experiment performed in triplicate sample. Error bars indicate standard deviations, calculated from the mean.

3.2.3 Efficacies of FA and derivatives in infected macrophages

Applying the same concentration used to treat resting macrophages (10 µM; Figure 3.1), macrophages were infected at MOI = 1 for 4 hours and treated. At each time point, cells were washed to remove extracellular drug, lysed, and lysate plated for CFU enumeration to determine intramacrophage antimycobacterial activity. While the more lipophilic compounds, GKFA16 and GKFA17, accumulated at levels 7 and 10-fold greater than that of FA and GKFA37, the efficacies against intracellular *M. tuberculosis* were similar, with approximately 1-1.5 log reduction in CFU.

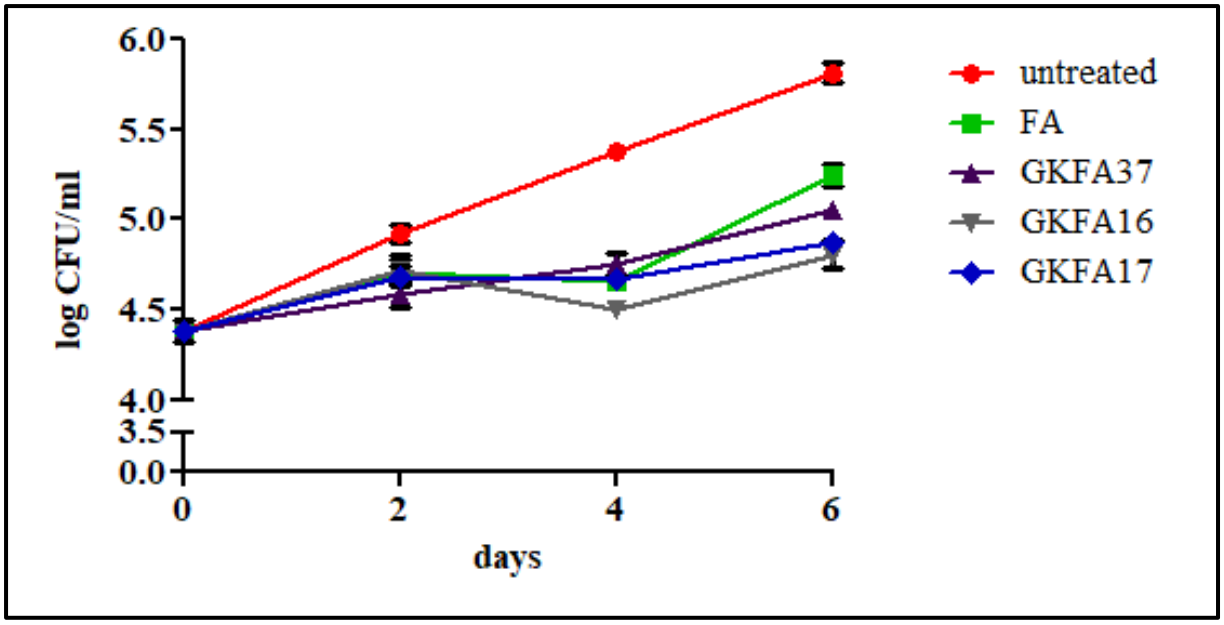

Figure 3.6. Bacterial survival in macrophages treated with FA and derivatives at a single concentration, 10 µM. Data are representative of two biological replicates with three technical replicates. Error bars indicate standard deviations, calculated from the mean of triplicate samples.

FA and its derivatives exhibited similar MIC values of approximately 1 µM (Chapter 2) against *M. tuberculosis in vitro*. At 10X MIC treatment, which equates to similar concentrations, FA, GKFA37 and GKFA16, all had a similar effect on intracellular bacterial growth despite GKFA16 accumulating at significantly higher concentrations than the other two compounds (Figure 3.1), consistent with the results presented in Figure 3.6. GKFA17, the most lipophilic (clogP 9.87) of the compounds, was highly concentrated within host macrophages and at 10X MIC treatment showed a slight advantage over the other two with respect to reduction of intracellular bacterial growth with approximately a 2-log difference relative to the untreated control. At 10X MIC (~1.5µM), MXF showed superior intramacrophage efficacy, with greater than 4-fold reduction in CFU. A further increase in concentration to 50X MIC achieved a complete sterilization of intracellular bacterial growth.

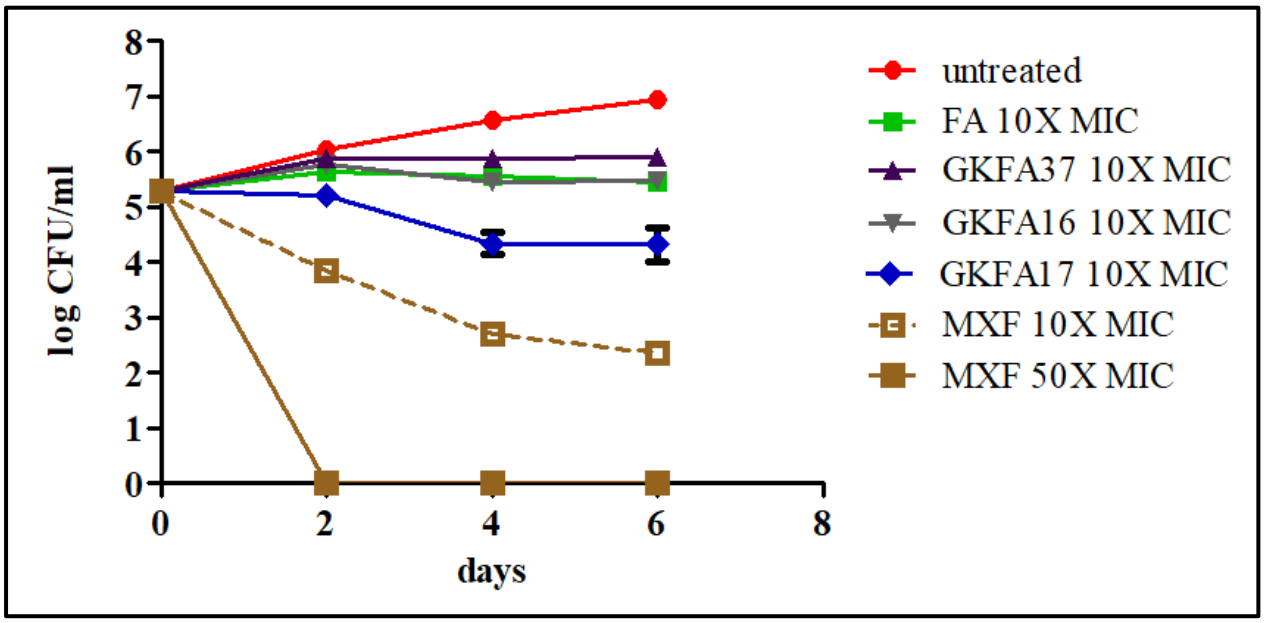

Figure 3.7. Intramacrophage efficacy as a function of MIC. Data are from a representative experiment of two replicate experiments each comprising three technical replicates. Error bars indicate standard deviations, calculated from the mean of triplicate samples.

3.2.4 Intra-macrophage drug metabolism

In Chapter 2, it was shown that the alkyl ester prodrugs GKFA16 and GKFA17 underwent *M.tuberculosis*-mediated metabolism to form FA, which further underwent metabolism to form 3-keto FA (GKFA37). It is also known that humans metabolize FA to form the ketone (Turnidge 1999; Njoroge et al. 2019). In the analysis of samples incubated in 24-well plates for drug accumulation studies, these metabolites could not be detected in either infected or uninfected host cells. It was hypothesized that host cells are likely to possess esterases capable of hydrolysing the alkyl esters and the inability to detect FA or GKFA37 was due to low cell numbers resulting in small undetectable amounts of the metabolites in the samples. In addition, in the case of infected cells, the number of bacilli per macrophage was significantly less than

the biomass present during *in vitro* culture for *M. tuberculosis* metabolism experiments. Therefore, macrophages were infected in culture flasks instead of plates, at MOI = 4 and both infected and uninfected cells were treated at a single concentration. Large sample volumes were collected and extracted according to the standard protocol, but adjusting for volumes. The samples were concentrated under inert N_2 gas, reconstituted in mobile phase buffer and analyzed.

After 2 and 4 days of treatment with GKFA17, uninfected macrophages had significantly higher relative levels of the compound in comparison to infected cells (Figure 3.8). In addition, on day 6, both infected and uninfected cells had significantly decreased relative levels of GKFA17 in comparison to day 2. In the same samples, FA metabolite accumulated at similar relative levels on days 2, 4 and 6, albeit, the amounts of FA had significantly reduced on day 6.

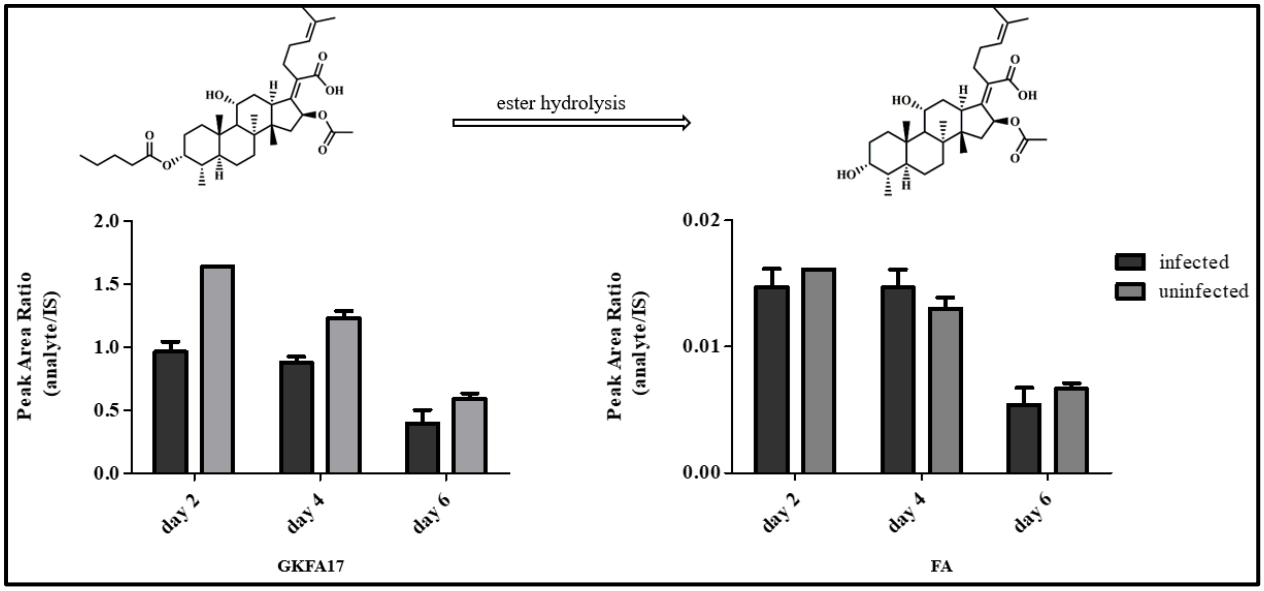

Figure 3.8. Metabolism of GKFA17 in both *M. tuberculosis*-infected and uninfected macrophages. Data are from a single experiment. Error bars indicate standard deviations, calculated from the mean of triplicate samples.

These results suggest that host cells are able to metabolize the prodrugs to release FA intracellularly. Furthermore, intracellular *M. tuberculosis* drives further hydrolysis as suggested, by further reduction in the levels of GKFA17 levels in infected cells. The corresponding increase in FA levels, however, was similar under both conditions, suggesting that *M. tuberculosis* may drive further biotransformation of FA to form other metabolites at a faster rate than that of the host intracellular enzymes. The decreasing levels of FA on day 6 could be attributed to the metabolism of FA to another unidentified metabolite; which is presumed to be either 3-ketoFA or the C-3 epimer epiFA. Alternatively, the loss of FA could be attributed to efflux mechanisms as seen in Figure 3.1.

3.2.5 Accumulation and intracellular *M. tuberculosis* activity of benzoxazole-based oxime derivatives

As demonstrated in Chapter 2, the selected benzoxazole-based oxime carbamates were unstable and underwent hydrolysis in the RPMI medium used to culture THP-1 macrophages. Although their corresponding free oximes were stable under media conditions, they were less active against *M. tuberculosis*. To determine intracellular drug accumulation of these compounds, THP-1 macrophages were treated with the compounds at 10 µM for 3 hours. Samples were collected and analyzed using LC-MS/MS as described in the methods detailed in Chapter 6. PMN2-09 and PMN1-157 had retention times at 3.34 and 3.18, respectively, when compounds were spiked in the mobile phase and injected into the LC-MS/MS (Figure 3.9A). On analysis of macrophage samples (Figure 3.9B), there was no detectable levels of either compound after 3 hours of incubation as all peaks were at baseline level. This was also observed for compounds PMN1-201, PMN1-199, PMN1-136 and PMN1-135 (data not shown).

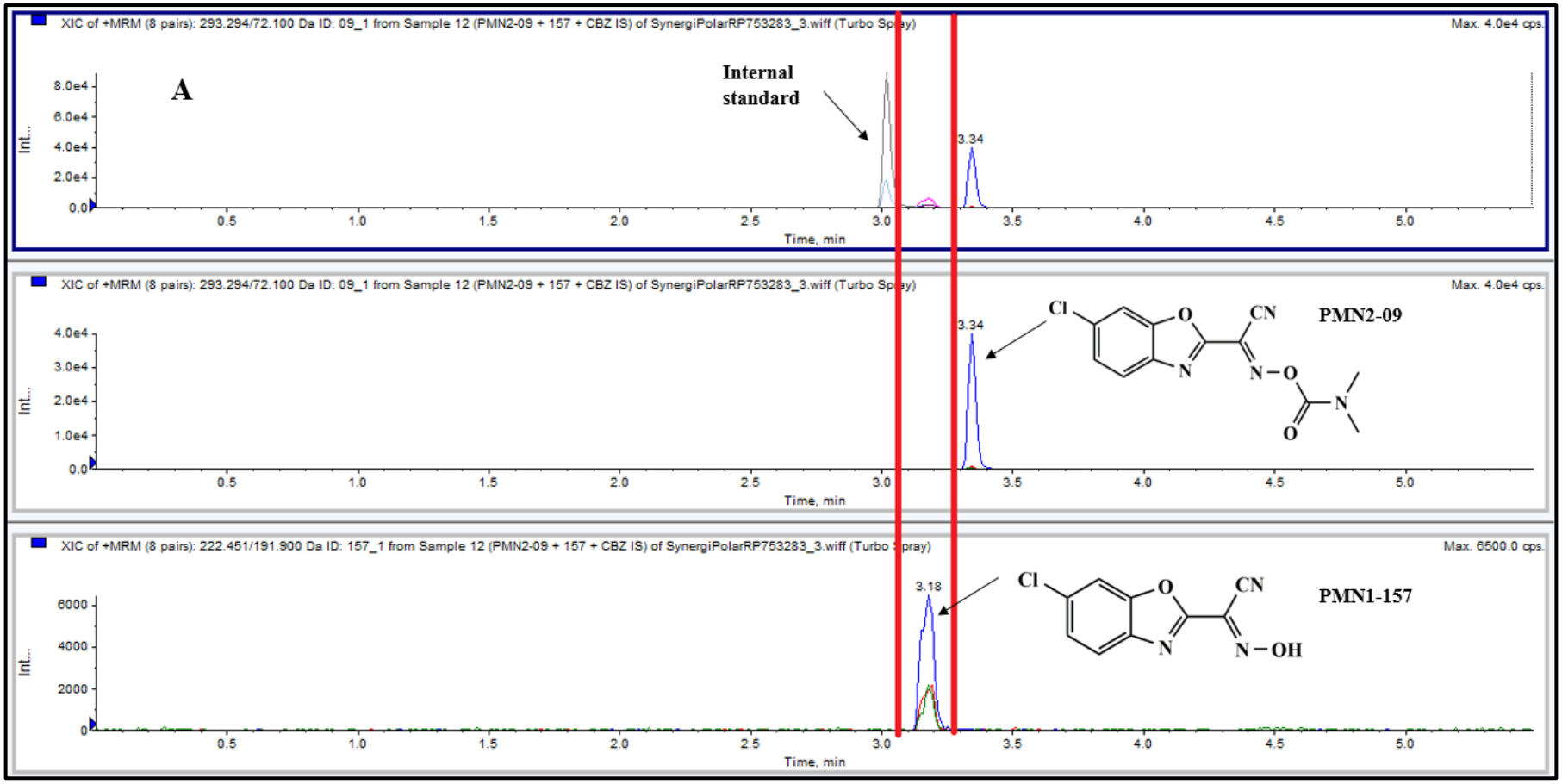
XIC of +MRM (8 pairs): 293.294/72.100 Da ID: 09_1 from Sample 12 (PMN2-09 + 157 + CBZ IS) of SynergiPolarRP753283_3.wiff (Turbo Spray)
Max. 4.0e4 cps.
A
Internal standard
3.34
Int...
Time, min
XIC of +MRM (8 pairs): 293.294/72.100 Da ID: 09_1 from Sample 12 (PMN2-09 + 157 + CBZ IS) of SynergiPolarRP753283_3.wiff (Turbo Spray)
Max. 4.0e4 cps.
3.34
PMN2-09
XIC of +MRM (8 pairs): 222.451/191.900 Da ID: 157_1 from Sample 12 (PMN2-09 + 157 + CBZ IS) of SynergiPolarRP753283_3.wiff (Turbo Spray)
Max. 6500.0 cps.
3.18
PMN1-157

Figure 3.9. Representative chromatograms of compounds PMN2-09 and PMN1-157. A) Compounds were spiked in acetonitrile: water mobile phase buffer to determine their retention times. B) Representative chromatograms of macrophage samples incubated with both compounds at 10 µM.

In Chapter 2, results demonstrated that the carbamates had good antimycobacterial activities *against M. tuberculosis in vitro*. To further analyze the effect of these compounds, infected macrophages were treated with both the carbamates and free oximes. The drug media was replenished every 24 hours to counter any compound spontaneous media degradation. However, despite the potent *in vitro* activities of benzoxazole-based oxime carbamates against *M. tuberculosis*, these compounds lacked activity against intracellular bacilli (Figure 3.10).

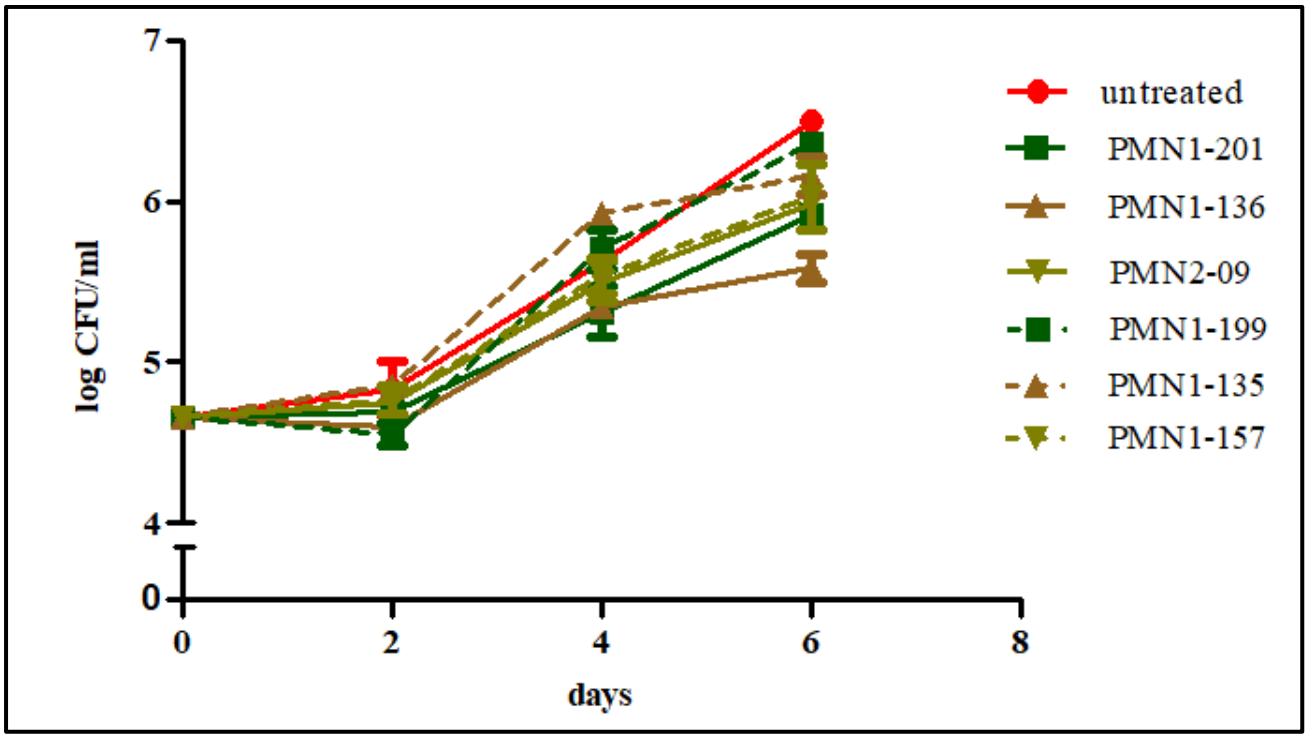

Figure 3.10. Bacterial survival in infected macrophages treated with oxime carbamates, PMN1-201, PMN1-136 and PMN2-09 and their corresponding free oximes, PMN1-199, PMN1-135 and PMN1-157 at 10µM. Data are representative of two independent experiments performed in triplicate. Error bars indicate standard deviations, calculated from the mean of triplicate samples.

3.3 Discussion

The highly lipophilic FA derivatives accumulated at significantly higher concentrations than the parent compound, FA, suggesting lipophilicity was the main driver of intracellular drug accumulation. This was expected as more lipophilic compounds are likely to permeate the cell membrane phospholipid bilayer. While these compounds (GKFA16 and GKFA17) maintained higher levels of intracellular drug, the levels of FA and GKFA37 decreased over time despite replenishment of drug media every 48 hours. Intracellular concentrations are the net result of drug influx and efflux rates and, in some cases, intracellular metabolism (Te Brake et al. 2018; Awasthi and Freundlich 2017). For FA and GKFA37, the rate of efflux appears to exceed that of macrophage uptake. In contrast, the accumulation of GFKA16 and GKFA17 suggests that either the efflux rate was slower than the rate of uptake. It is possible, too, that these compounds engage a different membrane efflux transporter. The latter is in part supported by the findings of Michot et al (2005) who showed that the structurally related drugs MXF and CPX were not effluxed by the same mechanism, with MXF exhibiting superior macrophage accumulation. It was shown in this thesis work that MXF reached a steady-state accumulation in THP-1 macrophages, suggesting that drug uptake and efflux likely occur at the same rate.

Macrophage efflux transporters are an important determinant of host cell drug accumulation, and macrophage residency has implications on mycobacterial efflux, with consequences on drug susceptibility (Adams et al. 2011). Although verapamil acts as a protonophore against *M. tuberculosis* (Chen et al. 2018), it is known to have calcium channel blocking capabilities, and restored drug susceptibility of intra-macrophage *M .tuberculosis* (Adams, Szumowski, and Ramakrishnan 2014). The role of macrophage efflux has also been reported, for example, CPX in J774 macrophages was susceptible to efflux by the MRP transporter, *MRP4*, while the efflux of RIF and EMB in THP-1 was linked to another member of the ABC super family of

transporters, P-glycoprotein (P-gp) (Marquez et al. 2009; Hartkoorn et al. 2007). Gemfibrozil, an unspecific MRP inhibitor inhibited CPX efflux in CPX-resistant macrophages with increased efflux rates (Marquez et al. 2009). Intracellular activity of RIF and EMB was reported to significantly increase in the presence of a P-gp inhibitor, tariquidar (Hartkoorn et al. 2007). This suggests potential for macrophage efflux inhibitors as a strategy to increase host cell drug accumulation. Another possibility for the sustained accumulation of the more lipophilic FA alkyl esters may be intracellular macromolecular binding causing less free drug fraction being available to be effluxed out of the cell.

While increasing lipophilicity increases the amount of intracellular drug accumulated in host cells, more lipophilic compounds are more susceptible to plasma protein binding. FA has been shown to bind to albumin with up to 95-97% (Turnidge 1999; Guttler, Tybring, and Engberg-Pedersen 1971), Recent investigations informed by molecular docking studies to rationalize media-dependent activity of FA derivatives, driven by binding to albumin, provides a basis for the rational design of compounds with reduced albumin binding and increased plasma bioavailability (Dziwornu et al. 2019). In addition, although the more lipophilic derivatives accumulate at significantly higher levels, they suffer increased non-specific cell membrane binding (Figure, 3.3), which affects the amount of drug reaching the bacilli in the intracellular environment. Furthermore, highly lipophilic drugs are predicted to distribute poorly into the caseum environment due to poor diffusion and increased macromolecular binding (Sarathy et al. 2016). Therefore, it is likely that FA and its derivatives will poorly distribute into the caseum. For example CFZ was shown to exhibit poor caseum penetration while strongly accumulating in cellular lesions (Prideaux et al. 2015). This perhaps explains CFZ efficacy in BALB/c mice which develop cellular lesions but poor efficacy in C3HeB/FeJ mice whose lesions have a necrotic core (Irwin et al. 2014; Irwin et al. 2015). From the perspective of combination therapy, the ability of more lipophilic FA derivatives to concentrate in

macrophages implies that they will target intracellular bacilli effectively rather than that found in the caseum, suggesting they should be combined with drugs of known caseum penetration. Further repurposing efforts of FA as an anti-TB drug should consider plasma binding, non-specific cell membrane-binding and caseum macromolecular binding as determinants of the amount of drug that eventually reaches bacilli in the lesion microenvironments.

In addition to lipophilicity driving drug accumulation, a drug's intrinsic activity against *M. tuberculosis* is important; that is, whether the drug is bacteriostatic or bactericidal. For example, it was shown in this thesis work that despite the over 7- and 10-fold difference in accumulation of GKFA16 and GKFA17 (Figure 3.2), these compounds exhibit comparable activity against intracellular bacilli (Figure 3.6). This effect may be due to the ester prodrugs undergoing hydrolysis followed by oxidation to form FA and the ketone as a metabolite. It has previously been shown by work from our laboratories, also confirmed in Chapter 2 of this thesis, that the alkyl esters undergo *M. tuberculosis*-mediated metabolism *in vitro* (Njoroge et al. 2019), and in the host cell environment during infection (Figure 3.8), to form FA. This suggests that the intracellular activity of GKFA16 and GKF17 may be due to both the prodrug and the resulting parent compound FA, which is known to be bacteriostatic. While FA only accumulates at lower levels, the use of C-3 ester prodrugs which are susceptible to enzymatic cleavage in the intracellular environment may prove to be a promising strategy to increase the accumulation of FA within the host cells and in turn increase its intracellular exposure over time.

FA and derivatives exhibited a bacteriostatic effect against intracellular *M. tuberculosis* at a single concentration (10μM), despite the increased intracellular concentration of GKFA16 and GKFA17. This is likely due to the bacteriostatic activity of these compounds, which masks the effect different intracellular concentrations. While the data on GKFA17 at 10X MIC (Figure 3.7) seems to suggest that increasing the applied concentrations may result in further reduction

of intracellular *M. tuberculosis* growth; it is likely an effect of the compound precipitating out of solution due to its low solubility causing host cell cytotoxicity at the concentrations used. GKFA17 was shown to be metabolized by both the host cell and *M. tuberculosis* to form intracellular FA, therefore it is unlikely that this effect is due to GKFA17 targeting a different protein. MXF accumulates in macrophages better than other fluoroquinolones and shows favorable *in vivo* distribution into cellular lesions (Prideaux et al. 2015; Michot et al. 2005; Blanc et al. 2018). MXF, however, is predicted to accumulate at lower levels than FA using PAMPA (chapter 2). At the same concentration, it shows lower cellular uptake relative to FA and the alkyl ester derivatives GKFA16 and GKFA17, but comparable to the 3-ketoFA metabolite, GKFA37 (Figure 3.1). Furthermore, MXF is known to be highly bactericidal against *M. tuberculosis* both *in vitro* and *in vivo* (Nuermberger et al. 2004; Miyazaki et al. 1999; Ji et al. 1998).

The approach of using more lipophilic prodrugs to increase the concentration of the active parent compound within host cell may even be more effective for compounds such as MXF with cidal antimycobacterial activity. MXF, as expected due to its lower clogP, only achieved lower intracellular concentrations than FA and its derivatives. However, due to its superior MIC, MXF was able to significantly reduce *M. tuberculosi*s growth. It is therefore hypothesized that structural analogues of MXF with cleavable side groups that will increase its lipophilicity to moderate levels similar to RIF which gradually accumulates in the caseum (Prideaux et al. 2015), could potentially increase not only the intracellular accumulation but improve distribution into the caseum where the cidal activity would be crucial to sterilize persister bacilli. In addition, while lipophilicity can predict drug accumulation in the cellular lesion compartment, the superior intracellular efficacy of MXF suggests that it is not only intracellular concentrations that predicts efficacy, but MIC indices. Cellular PK/PD indices such as cellular AUC/MIC or C_{max}/MIC ratios could determine host cell drug efficacies. For

example, a hollow fiber model of disseminated *M. avium* infection showed that killing of intracellular bacteria by azithromycin (AZT) and efflux-induced emergence of resistance were closely associated with intra-macrophage AUC/MIC ratio (Schmalstieg et al. 2012).

As already discussed, in addition to a drug's intrinsic physicochemical properties, we note that human macrophage efflux transporters may play an important role in host cell drug accumulation (Te Brake et al. 2018). As bacilli continue to replicate in infected host macrophages, it is known that *M. tuberculosis* upregulates certain functions including efflux pumps to adapt to intracellular host stress (Schnappinger et al. 2003; Rohde et al. 2012). However, it is likely that as *M. tuberculosis* proliferates, driving host cells towards necrotic death at the cellular-caseum interface, the bacilli induce host cell efflux mechanisms in macrophages laden with high bacillary loads therefore reducing drug accumulation in those cells. This would consequently allow *M. tuberculosis* to thrive under suboptimal intracellular conditions causing drug tolerance in bacilli that eventually end up in the caseum after host cell necrotic death, partly explaining why caseum bacilli exhibit increased drug tolerance (Sarathy et al. 2018; Adams et al. 2011). From a therapeutic point of view, drug distribution into these cells is therefore critical. It was observed, however, that resting macrophages infected with high bacterial numbers did not significantly reduce the amount of drug (GKFA17) accumulated in the host cells.

Benzoxazole-based oxime compounds failed to achieve any intra-macrophage accumulation likely due to poor penetration properties, this despite the high permeability predicted using the PAMPA assay. While compound stability may have been the main liability, early compound macrophage incubation time points taken over 3 hours (prior to complete degradation of compound in media) showed a lack of analyte signal in the cell samples. In addition, presuming that the oxime carbamate hydrolyzed resulting in accumulation of the free oxime in extracellular drug media (as shown in chapter 2), this analyte was also not observed in these

samples. The free oxime itself was not observed in host cells when directly incubated with the media. The free oximes were not susceptible to spontaneous degradation, therefore any amount of compound accumulated would have been detected via LC-MS/MS analysis.

It was initially hypothesized that the poor activity shown by the free oximes was due to poor *M. tuberculosis* cellular uptake, and that the potent oxime carbamates penetrated the bacilli. Furthermore, since it was shown that *M. tuberculosis* completely hydrolyses the oxime carbamates within only a few hours of drug exposure, it was also hypothesized that the free oxime released upon *M. tuberculosis*-mediated metabolism was responsible for the observed activity within the bacilli. However, the macrophage incubation data suggests that the failure of both the free oximes and the parent carbamates to permeate into the host cells, limits the potential of these compounds for further development as drug leads unless further SAR optimization is undertaken to address stability and permeability issues. The inability of these compounds to accumulate in host cells was evident in their failure to control host cell bacterial growth at high concentrations (Figure 3.10).

3.4 References

Adams, K. N., J. D. Szumowski, and L. Ramakrishnan. 2014. 'Verapamil, and its metabolite norverapamil, inhibit macrophage-induced, bacterial efflux pump-mediated tolerance to multiple anti-tubercular drugs', *Journal of Infectious Diseases*, 210: 456-66.

Adams, K. N., K. Takaki, L. E. Connolly, H. Wiedenhoft, K. Winglee, O. Humbert, P. H. Edelstein, C. L. Cosma, and L. Ramakrishnan. 2011. 'Drug tolerance in replicating mycobacteria mediated by a macrophage-induced efflux mechanism', *Cell*, 145: 39-53.

Awasthi, D., and J. S. Freundlich. 2017. 'Antimycobacterial Metabolism: Illuminating Mycobacterium tuberculosis Biology and Drug Discovery', *Trends in Microbiology*, 25: 756-67.

Baik, J., and G. R. Rosania. 2012. 'Macrophages sequester clofazimine in an intracellular liquid crystal-like supramolecular organization', *PloS One*, 7: e47494.

Baik, J., K. A. Stringer, G. Mane, and G. R. Rosania. 2013. 'Multiscale distribution and bioaccumulation analysis of clofazimine reveals a massive immune system-mediated xenobiotic sequestration response', *Antimicrobial Agents and Chemotherapy*, 57: 1218-30.

Blanc, L., I. B. Daudelin, B. K. Podell, P. Y. Chen, M. Zimmerman, A. J. Martinot, R. M. Savic, B. Prideaux, and V. Dartois. 2018. 'High-resolution mapping of fluoroquinolones in TB rabbit lesions reveals specific distribution in immune cell types', *Elife*, 7.

Carroll, P., L. J. Schreuder, J. Muwanguzi-Karugaba, S. Wiles, B. D. Robertson, J. Ripoll, T. H. Ward, G. J. Bancroft, U. E. Schaible, and T. Parish. 2010. 'Sensitive detection of gene expression in mycobacteria under replicating and non-replicating conditions using optimized far-red reporters', *PloS One*, 5: e9823.

Chen, C., S. Gardete, R. S. Jansen, A. Shetty, T. Dick, K. Y. Rhee, and V. Dartois. 2018. 'Verapamil Targets Membrane Energetics in Mycobacterium tuberculosis', *Antimicrobial Agents and Chemotherapy*, 62.

Dartois, V. 2014. 'The path of anti-tuberculosis drugs: from blood to lesions to mycobacterial cells', *Nature Reviews: Microbiology*, 12: 159-67.

Dartois, V., and C. E. Barry, 3rd. 2013. 'A medicinal chemists' guide to the unique difficulties of lead optimization for tuberculosis', *Bioorganic and Medicinal Chemistry Letters*, 23: 4741-50.

Dziwornu, G. A., S. Kamunya, T. Ntsabo, and K. Chibale. 2019. 'Novel antimycobacterial C-21 amide derivatives of the antibiotic fusidic acid: synthesis, pharmacological evaluation and rationalization of media-dependent activity using molecular docking studies in the binding site of human serum albumin', *Medchemcomm*, 10: 961-69.

Ehrt, S., D. Schnappinger, and K. Y. Rhee. 2018. 'Metabolic principles of persistence and pathogenicity in Mycobacterium tuberculosis', *Nature Reviews: Microbiology*, 16: 496-507.

Gillespie, S. H., A. M. Crook, T. D. McHugh, C. M. Mendel, S. K. Meredith, S. R. Murray, F. Pappas, P. P. Phillips, A. J. Nunn, and R. EMoxTB Consortium. 2014. 'Four-month moxifloxacin-based regimens for drug-sensitive tuberculosis', *New England Journal of Medicine*, 371: 1577-87.

Gleeson, L. E., F. J. Sheedy, E. M. Palsson-McDermott, D. Triglia, S. M. O'Leary, M. P. O'Sullivan, L. A. O'Neill, and J. Keane. 2016. 'Cutting Edge: Mycobacterium tuberculosis Induces Aerobic Glycolysis in Human Alveolar Macrophages That Is

Required for Control of Intracellular Bacillary Replication', *Journal of Immunology*, 196: 2444-9.

Greenwood, D. J., M. S. Dos Santos, S. Huang, M. R. G. Russell, L. M. Collinson, J. I. MacRae, A. West, H. Jiang, and M. G. Gutierrez. 2019. 'Subcellular antibiotic visualization reveals a dynamic drug reservoir in infected macrophages', *Science*, 364: 1279-82.

Guttler, F., L. Tybring, and H. Engberg-Pedersen. 1971. 'Interaction of albumin and fusidic acid', *British Journal of Pharmacology*, 43: 151-60.

Harbeck, R. J., G. S. Worthen, T. D. Lebo, and C. A. Peloquin. 1999. 'Clofazimine crystals in the cytoplasm of pulmonary macrophages', *Annals of Pharmacotherapy*, 33: 250.

Hartkoorn, R. C., B. Chandler, A. Owen, S. A. Ward, S. Bertel Squire, D. J. Back, and S. H. Khoo. 2007. 'Differential drug susceptibility of intracellular and extracellular tuberculosis, and the impact of P-glycoprotein', *Tuberculosis (Edinb)*, 87: 248-55.

Irwin, S. M., E. Driver, E. Lyon, C. Schrupp, G. Ryan, M. Gonzalez-Juarrero, R. J. Basaraba, E. L. Nuermberger, and A. J. Lenaerts. 2015. 'Presence of multiple lesion types with vastly different microenvironments in C3HeB/FeJ mice following aerosol infection with Mycobacterium tuberculosis', *Disease Models & Mechanisms*, 8: 591-602.

Irwin, S. M., V. Gruppo, E. Brooks, J. Gilliland, M. Scherman, M. J. Reichlen, R. Leistikow, I. Kramnik, E. L. Nuermberger, M. I. Voskuil, and A. J. Lenaerts. 2014. 'Limited activity of clofazimine as a single drug in a mouse model of tuberculosis exhibiting caseous necrotic granulomas', *Antimicrobial Agents and Chemotherapy*, 58: 4026-34.

Ji, B., N. Lounis, C. Maslo, C. Truffot-Pernot, P. Bonnafous, and J. Grosset. 1998. 'In vitro and in vivo activities of moxifloxacin and clinafloxacin against Mycobacterium tuberculosis', *Antimicrobial Agents and Chemotherapy*, 42: 2066-9.

Marquez, B., N. E. Caceres, M. P. Mingeot-Leclercq, P. M. Tulkens, and F. Van Bambeke. 2009. 'Identification of the efflux transporter of the fluoroquinolone antibiotic ciprofloxacin in murine macrophages: studies with ciprofloxacin-resistant cells', *Antimicrobial Agents and Chemotherapy*, 53: 2410-6.

Mashabela, G. T., T. J. de Wet, and D. F. Warner. 2019. 'Mycobacterium tuberculosis Metabolism', *Microbiol Spectr*, 7.

Michot, J. M., C. Seral, F. Van Bambeke, M. P. Mingeot-Leclercq, and P. M. Tulkens. 2005. 'Influence of efflux transporters on the accumulation and efflux of four quinolones (ciprofloxacin, levofloxacin, garenoxacin, and moxifloxacin) in J774 macrophages', *Antimicrobial Agents and Chemotherapy*, 49: 2429-37.

Michot, J. M., F. Van Bambeke, M. P. Mingeot-Leclercq, and P. M. Tulkens. 2004. 'Active efflux of ciprofloxacin from J774 macrophages through an MRP-like transporter', *Antimicrobial Agents and Chemotherapy*, 48: 2673-82.

Miyazaki, E., M. Miyazaki, J. M. Chen, R. E. Chaisson, and W. R. Bishai. 1999. 'Moxifloxacin (BAY12-8039), a new 8-methoxyquinolone, is active in a mouse model of tuberculosis', *Antimicrobial Agents and Chemotherapy*, 43: 85-9.

Njoroge, M., G. Kaur, M. Espinoza-Moraga, A. Wasuna, G. A. Dziwornu, R. Seldon, D. Taylor, J. Okombo, D. F. Warner, and K. Chibale. 2019. 'Semisynthetic Antimycobacterial C-3 Silicate and C-3/C-21 Ester Derivatives of Fusidic Acid: Pharmacological Evaluation and Stability Studies in Liver Microsomes, Rat Plasma, and Mycobacterium tuberculosis culture', *ACS Infect Dis*, 5: 1634-44.

Nuermberger, E. L., T. Yoshimatsu, S. Tyagi, R. J. O'Brien, A. N. Vernon, R. E. Chaisson, W. R. Bishai, and J. H. Grosset. 2004. 'Moxifloxacin-containing regimen greatly reduces time to culture conversion in murine tuberculosis', *American Journal of Respiratory and Critical Care Medicine*, 169: 421-6.

Prideaux, B., L. E. Via, M. D. Zimmerman, S. Eum, J. Sarathy, P. O'Brien, C. Chen, F. Kaya, D. M. Weiner, P. Y. Chen, T. Song, M. Lee, T. S. Shim, J. S. Cho, W. Kim, S. N. Cho, K. N. Olivier, C. E. Barry, 3rd, and V. Dartois. 2015. 'The association between sterilizing activity and drug distribution into tuberculosis lesions', *Nature Medicine*, 21: 1223-7.

Rohde, K. H., D. F. Veiga, S. Caldwell, G. Balazsi, and D. G. Russell. 2012. 'Linking the transcriptional profiles and the physiological states of Mycobacterium tuberculosis during an extended intracellular infection', *PLoS Pathogens*, 8: e1002769.

Rohde, K., R. M. Yates, G. E. Purdy, and D. G. Russell. 2007. 'Mycobacterium tuberculosis and the environment within the phagosome', *Immunological Reviews*, 219: 37-54.

Sarathy, J. P., L. E. Via, D. Weiner, L. Blanc, H. Boshoff, E. A. Eugenin, C. E. Barry, 3rd, and V. A. Dartois. 2018. 'Extreme Drug Tolerance of Mycobacterium tuberculosis in Caseum', *Antimicrobial Agents and Chemotherapy*, 62.

Sarathy, J. P., F. Zuccotto, H. Hsinpin, L. Sandberg, L. E. Via, G. A. Marriner, T. Masquelin, P. Wyatt, P. Ray, and V. Dartois. 2016. 'Prediction of Drug Penetration in Tuberculosis Lesions', *ACS Infect Dis*, 2: 552-63.

Schmalstieg, A. M., S. Srivastava, S. Belkaya, D. Deshpande, C. Meek, R. Leff, N. S. van Oers, and T. Gumbo. 2012. 'The antibiotic resistance arrow of time: efflux pump induction is

a general first step in the evolution of mycobacterial drug resistance', *Antimicrobial Agents and Chemotherapy*, 56: 4806-15.

Schnappinger, D., S. Ehrt, M. I. Voskuil, Y. Liu, J. A. Mangan, I. M. Monahan, G. Dolganov, B. Efron, P. D. Butcher, C. Nathan, and G. K. Schoolnik. 2003. 'Transcriptional Adaptation of Mycobacterium tuberculosis within Macrophages: Insights into the Phagosomal Environment', *Journal of Experimental Medicine*, 198: 693-704.

Shi, L., H. Salamon, E. A. Eugenin, R. Pine, A. Cooper, and M. L. Gennaro. 2015. 'Infection with Mycobacterium tuberculosis induces the Warburg effect in mouse lungs', *Scientific Reports*, 5: 18176.

Tanner, L., P. Denti, L. Wiesner, and D. F. Warner. 2018. 'Drug permeation and metabolism in Mycobacterium tuberculosis: Prioritising local exposure as essential criterion in new TB drug development', *IUBMB Life*, 70: 926-37.

Te Brake, L. H. M., G. J. de Knegt, J. E. de Steenwinkel, T. J. P. van Dam, D. M. Burger, F. G. M. Russel, R. van Crevel, J. B. Koenderink, and R. E. Aarnoutse. 2018. 'The Role of Efflux Pumps in Tuberculosis Treatment and Their Promise as a Target in Drug Development: Unraveling the Black Box', *Annual Review of Pharmacology and Toxicology*, 58: 271-91.

Turnidge, J. 1999. 'Fusidic acid pharmacology, pharmacokinetics and pharmacodynamics', *International Journal of Antimicrobial Agents*, 12 Suppl 2: S23-34.

Warner, D. F., and V. Mizrahi. 2014. 'Shortening treatment for tuberculosis--to basics', *New England Journal of Medicine*, 371: 1642-3.

CHAPTER 4

EFFECTS OF HOST-PATHOGEN INTERACTIONS ON MACROPHAGE DRUG ACCUMULATION AND *IN VITRO* EFFICACY AGAINST *M. TUBERCULOSIS*

4.1 Introduction

During infection, *M. tuberculosis* must adapt its metabolic pathways in response to the host cell, whose own metabolic status may be influenced by both the bacillus and host immune processes (Mashabela, de Wet, and Warner 2019). The interplay between immunometabolism (O'Neill, Kishton, and Rathmell 2016; Russell, Huang, and VanderVen 2019) and pathometabolism (Eisenreich et al. 2015) is critical to infection outcomes. From a therapeutic viewpoint, the immune status of a host cell may impact on drug efficacy in distinct ways: i) host cell status may cause upregulation of intrinsic *M. tuberculosis* resistance mechanisms, such increased activity of mycobacterial efflux pumps to limit the amount of drug reaching the molecular target; ii) host cell status may affect mycobacterial metabolism, making an essential target conditionally "non-essential" ; iii) host cell killing mechanisms may synergize with the antimycobacterial drug and; iv) changes in the host cell processes to limit the amount of drug available intracellularly, such as upregulation of host cell efflux, decreased permeation, or non-specific binding to host organelles and intracellular bodies. The latter was investigated in this chapter.

At bacillary level, the induction of bacterial efflux pumps upon macrophage infection increasing drug tolerance, likely due to insufficient drug levels reaching the molecular target, is an example of how the host cell environment influences changes in the bacilli (Adams et al. 2011). Furthermore, tolerant bacteria were only observed in a subset of infected macrophages likely indicating heterogeneity of macrophage phenotypes *in vivo* (Adams et al. 2011). The

indication of differential induction of bacterial efflux pumps, and thus tolerance, will impact on drug efficacy in cellular lesion microenvironments.

From a metabolic perspective, changes in local host metabolism may directly impact a drug target in an essential *M. tuberculosis* metabolic pathway (Mashabela, de Wet, and Warner 2019). For example, the *guaB2*-encoded mycobacterial inosine monophosphate dehydrogenase (IMPDH), which is essential in *de novo* purine biosynthesis *in vitro*, was considered not vulnerable *in vivo* owing to the presence in TB lesions of guanine concentrations sufficient for *M. tuberculosis* to scavenge (Singh et al. 2017; Park et al. 2017).

Host metabolic processes may cause inadequate intracellular drug concentrations in different ways. TB drugs may be differentially susceptible to macrophages membranes influx and efflux transporters such as the organic anion transporting polypeptide transporter, P-glycoprotein, multidrug resistance proteins (MRP) etc., therefore drug penetration and accumulation into the intracellular host environment (Te Brake et al. 2018; Moreau et al. 2011). In addition, host immune responses may play a role in modulating their function. MRP1 efflux protein which has been implicated in ciprofloxacin efflux was reportedly upregulated in response to cytotoxic levels of NO (Marquez et al. 2009; Lok et al. 2016), suggesting that accumulation of MRP1 efflux susceptible drugs would be impacted. The most considerable metabolic shift in the infected macrophage during host infection is perhaps lipid metabolism. The resulting foamy macrophage phenotype, described in Chapter 1, filled with intracellular LBs, is closely linked with mycobacterial persistence and disease progression (Russell et al. 2009; Peyron et al. 2008). The implications on drug efficacy are two-fold: tolerant bacterial phenotype are associated with foamy macrophage, suggesting higher concentrations would be required to achieve efficacy; and secondly, the LBs are highly lipophilic cellular structures with the ability of antimycobacterial drugs to reach their molecular target owing to lipid binding particularly for highly lipophilic drugs (Sarathy et al. 2016). While studies prioritizing the role of foamy

macrophage drug accumulation and its impact on efficacy are limited, a recent study showed that the highly lipophilic BDQ accumulated primarily in LBs within foamy macrophages (Greenwood et al. 2019). However, the authors argued that this association was favorable as the lipid bound drug constituted a reservoir of easily transferable drug to enhance intracellular efficacy (Greenwood et al. 2019). Non-replicating bacteria reportedly induced in foamy macrophages may be tolerant to antimycobacterial agents further diminishing intracellular drug efficacy. Non-replicating bacilli induced *in vitro* through the nutrient-starvation model have been reported to be phenotypically resistant to existing drugs, and reduce drug uptake (Sarathy et al. 2013; Betts et al. 2002). Although the non-replicating state induced *in vitro* under starvation conditions may differ from that induced in foamy macrophages, both tolerance mechanisms are associated with a metabolic shift and upregulation of dormancy genes (Peyron et al. 2008; Daniel et al. 2011; Betts et al. 2002).

Several *in vitro* assays have been described for studying the effect of foamy macrophages *in vitro*. Some studies have utilized lipid rich macrophages isolated *in vivo* from animal models while others reported that macrophages grown under hypoxic conditions induced formation of lipid bodies (Santucci et al. 2016; Daniel et al. 2011; Bostrom et al. 2006). Infection of macrophages with *M. tuberculosis* H37Rv, but not the avirulent H37Ra, induced lipid body formation, and upregulated TAG levels (Singh et al. 2012). Exposure to extracellular lipids to induce macrophages to differentiate into a foamy phenotype has been widely reported (Sarathy et al. 2016; Podinovskaia et al. 2013; den Hartigh et al. 2010; Agarwal et al. 2020). While all these models induce host cell LBs, interpretation of data and the potential implications for *in vivo* granuloma macrophages vary from one model to another.

In this chapter, the hypothesis tested was that macrophage activation could potentially affect the ability of host cells to accumulate drug, with impact on intra-macrophage drug efficacy. It was hypothesized that the intrinsic physicochemical properties of antibiotic compounds determine their intracellular accumulation and distribution in the presence of LBs. For *M. tuberculosis*-macrophage interactions, the possibility that differential distributions between foamy and non-foamy macrophages would impact drug efficacy was particularly compelling.

4.2 Results

4.2.1 Effect of macrophage activation on intracellular drug accumulation and *M. tuberculosis* survival

Macrophages were exposed to interferon (IFN)-γ and LPS for activation using previously reported methods (Liu et al. 2016). Briefly, macrophage-like THP-1 cells were differentiated using PMA for 24 hours, after which the media was replaced with activation media containing both (IFN)-γ and LPS at previously reported concentrations (Liu et al. 2016). To assess the effect of activation on intracellular drug accumulation, activated and resting macrophages were exposed to the most accumulated derivative of FA, GKFA17 (10 µM), and samples analyzed as described earlier. Activated macrophages exhibited a significant reduction in the concentration of drug accumulated over time, with approximately half the concentration accumulated *versus* that determined for resting macrophages (Figure 4.1). This effect was also observed in infected activated and resting macrophages (Figure 4.1).

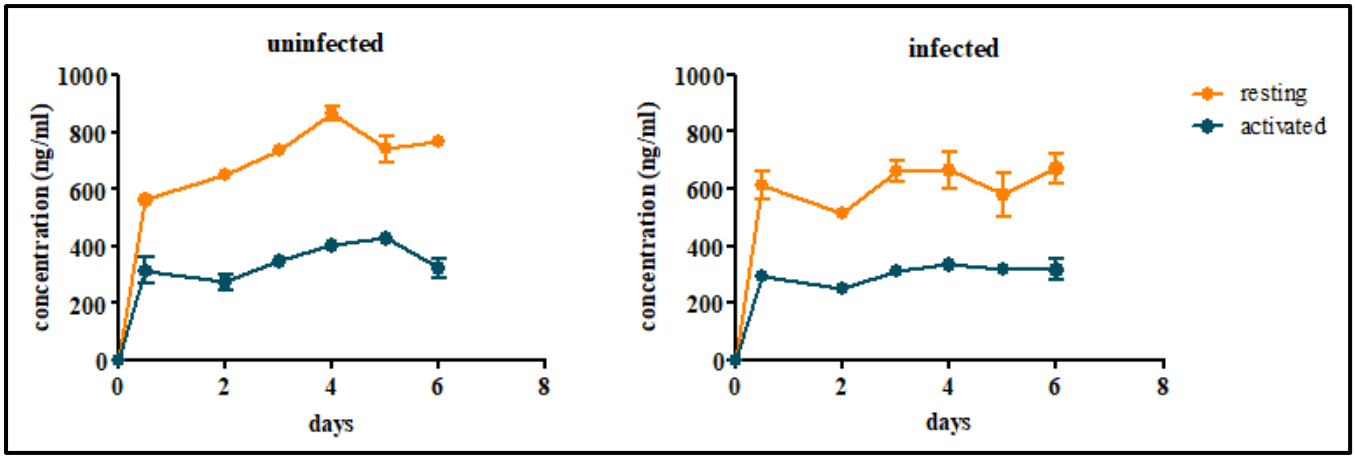

Figure 4.1. Effect of host cell activation on accumulation FA derivative, GKFA17. Data represent a single experiment performed in triplicate. Error bars represent standard error of the mean.

Previous studies have reported the induction of proinflammatory responses, and implicated cytotoxic effects of LPS against human cells (Vogel, Marshall, and Rosenstreich 1979; Xaus et al. 2000; Li et al. 2016). Even though concentrations that have been reported in literature were used, most of the studies investigated immunological effects, with no consideration of the potential effects on cellular membrane integrity. Drug accumulation depends on cellular uptake and intact cellular membranes to retain the drug within the intracellular environment. To eliminate the possibility of membrane damage as the reason for reduced drug accumulated in activated cells, cells were detached with 5 mM EDTA solution and stained with propidium iodide (PI). PI is excluded by intact plasma membranes, and only stains cells with compromised membrane integrity. Cells were analyzed via flow cytometry acquisition with PI on the x-axis of the gating windows.

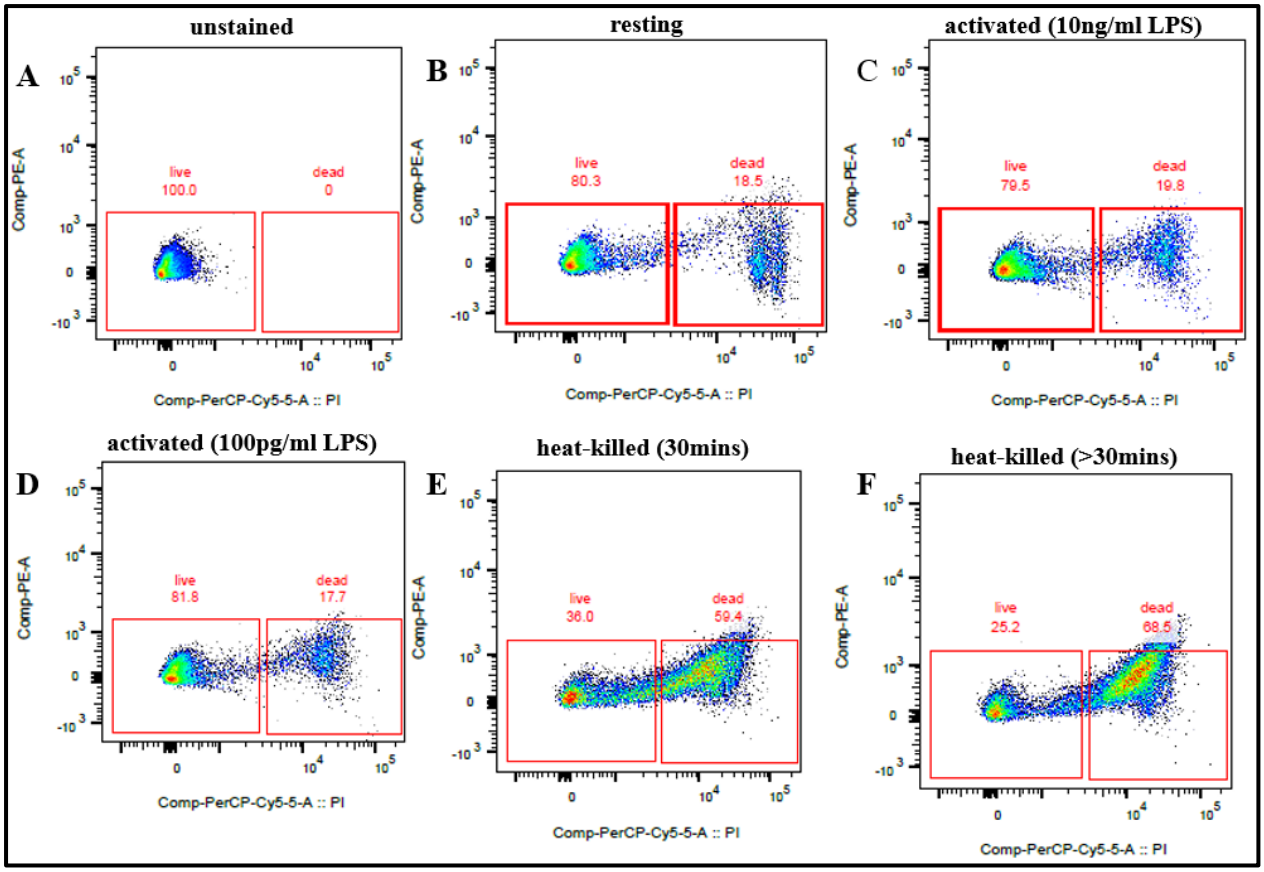

Figure 4.2. Flow cytometry analysis of propidium iodide (x-axis) cellular uptake to determine host cell membrane damage. Cell acquisition was conducted using BD FACSCalibur, FACSDiva version 6.1.3 software. Data were analyzed using FlowJo V10.

The unstained control was used to set the negative and positive gates (Figure 4.2). Approximately 20% of the cell population of both non-activated (resting) and activated cells (10 ng/ml concentration used for cell activation in all experiments) stained positive for PI. At the lower LPS concentration, no differences were observed. A positive control of resting macrophages exposed to heat in a water bath for 30 minutes to ensure membrane damage confirmed an increased percentage (~60%) PI positive cells, with a further increase detected when cells were incubated for longer. These results suggested that LPS activation did not impact membrane integrity, thus eliminating this as a potential confounder.

CFU plating to enumerate intracellular bacterial survival revealed that despite the significantly reduced drug accumulated in activated samples, these cells were better able to control bacterial

growth: an increased CFU reduction was observed relative to resting macrophages. These observations suggested the importance of immune response mechanisms in controlling *M. tuberculosis* growth (Figure 4.3).

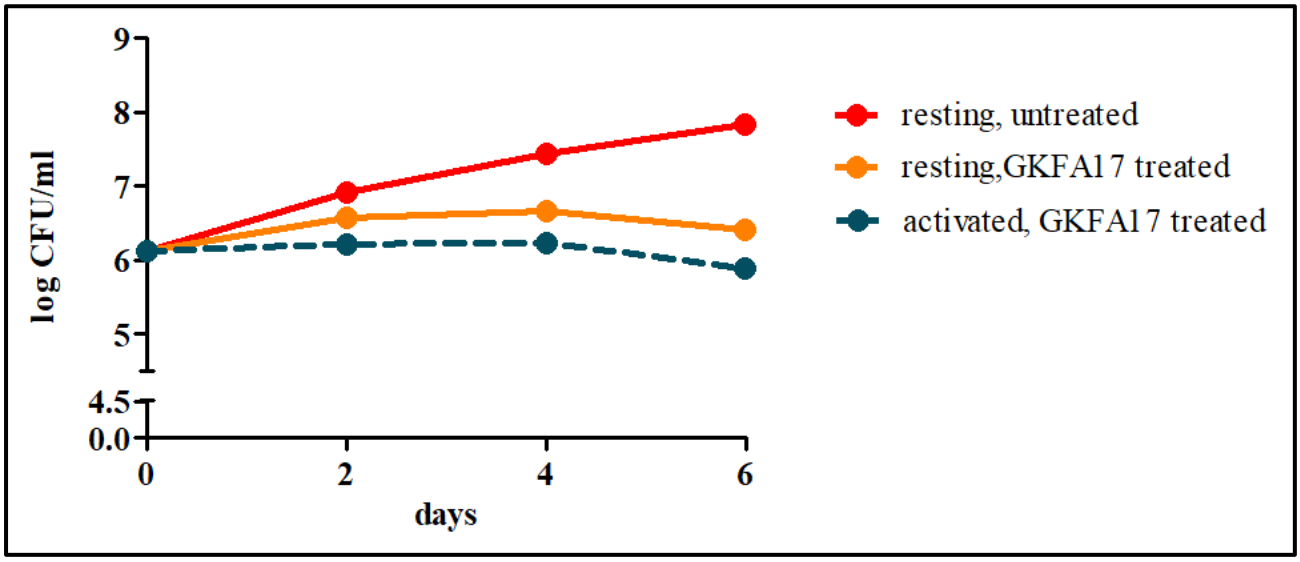

Figure 4.3. Intracellular bacterial survival in resting and activated macrophages treated with FA derivative, GKFA17.

It was hypothesized that the reduced drug accumulation observed in activated macrophages could be drug class-specific since different drug classes may be subject to influx and efflux by different membrane transporter systems. Liu et al., reported that J774- macrophages exhibited comparable accumulation of the first line anti-TB drugs (RIF, INH, PZA and EMB) to those determined in resting macrophages (Liu et al. 2016). Treatment with RIF and BDQ suggested comparable relative concentrations accumulated in both activated and resting THP-1 macrophages (Figure 4.4). BDQ showed an increasing accumulation over time, whereas RIF levels initially increased before decreasing after 24 hours, implying RIF could be susceptible to macrophage efflux transporters.

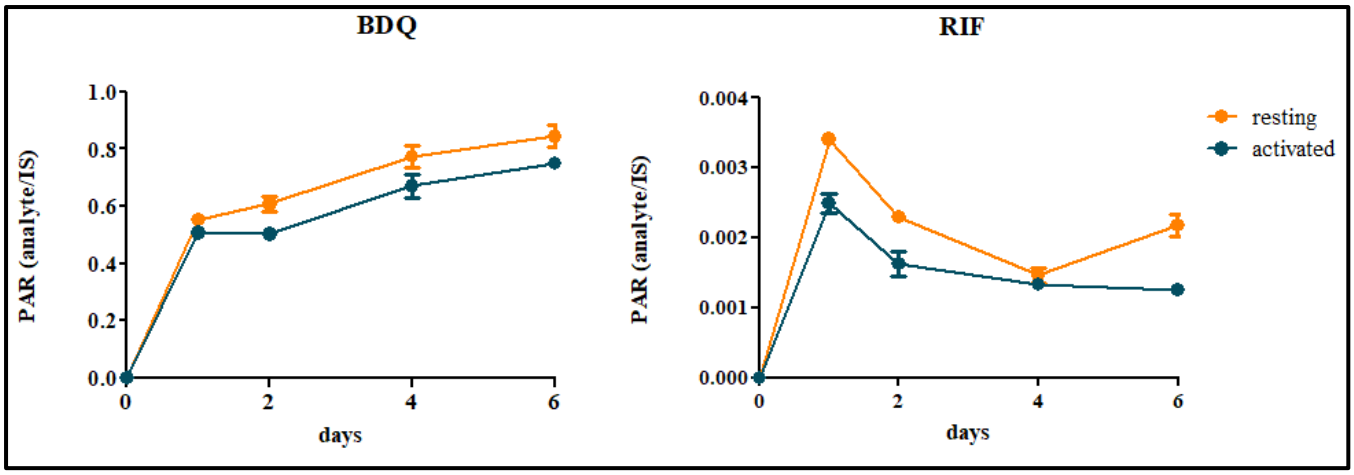

Figure 4.4. Effect of host cell activation on drug accumulation of BDQ and RIF (5 and 10 µM treatment respectively; selected based on solubility). Data represent a single experiment performed in triplicate. Error bars represent standard error of the mean.

4.2.2 Accumulation of FA and derivatives in foamy macrophages

THP-1 macrophages were differentiated and foamy macrophages induced with exposure to oleic acid enriched medium using a published protocol (Agarwal et al. 2020), adopted from a previously described method by Sarathy et al., (2016). Formation of LBs within macrophages was visualized via fluorescence microscopy using a green fluorescent LipidTox stain, which binds neutral lipids; confocal imaging confirmed the presence of LBs which were significantly more abundant in oleic acid-treated cells compared to the untreated control (Figure 4.5).

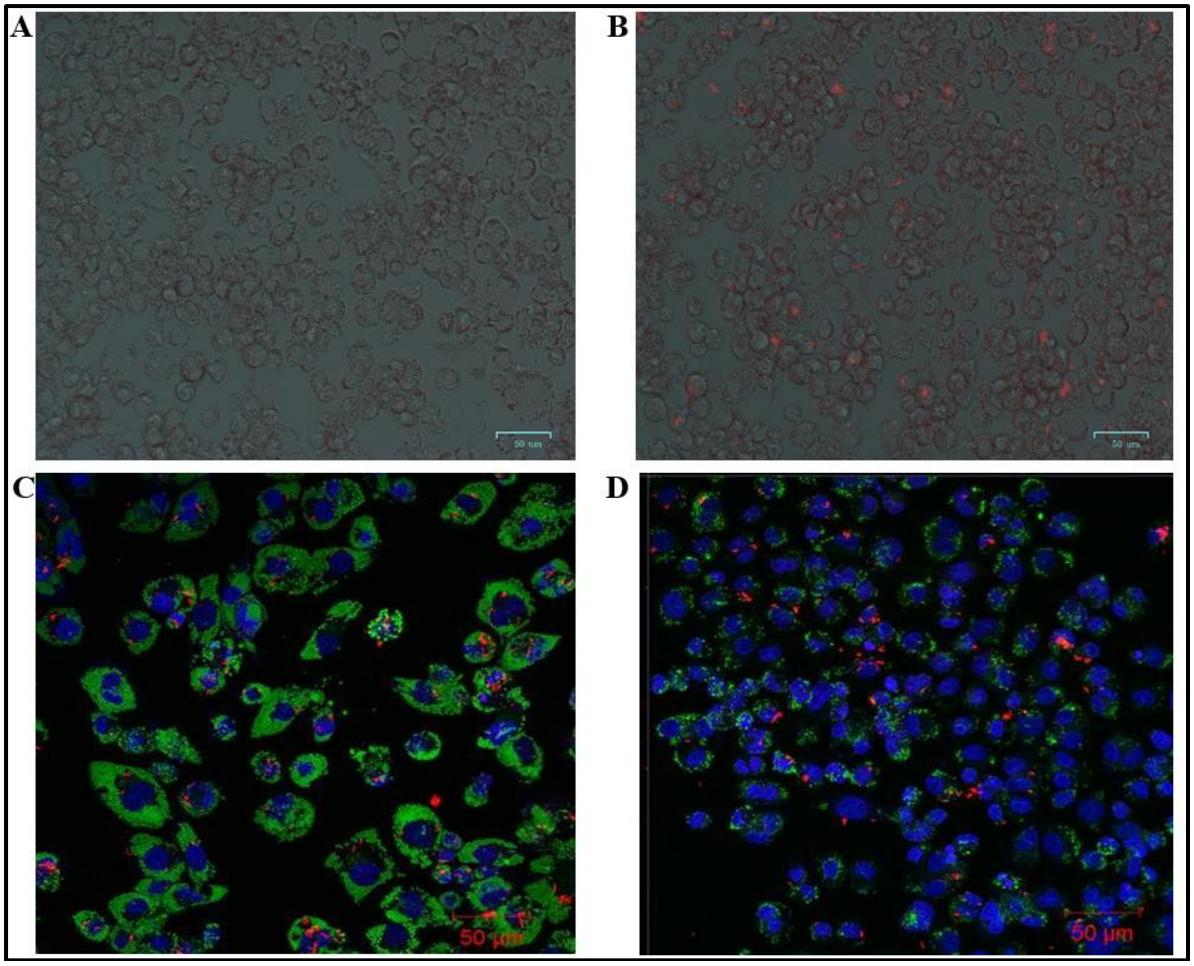

Figure 4.5. Comparison of LB content in oleic acid differentiated THP-1 foamy macrophages *in vitro*. A) THP-1 macrophages treated with 400 µM oleic acid, and B) infected with *M. tuberculosis* H37Rv MA :: (smyc'::mCherry (=pCherry3)) (red). C) LBs were stained with LipidTox (green) and cell nuclei with DAPI (blue) in *M. tuberculosis* infected foamy macrophages *versus* D) non-foamy macrophages. (A, B) images were generated using a BioRad ZOE microscope, (C,D) images were generated using a Zeiss LSM 880 with Fast Airyscan module confocal microscope (Carl Zeiss, Jena, Germany). LipidTOX (green) =Argon 488nm laser, mCherry (red) = 561nm laser and DAPI (blue) = 405nm laser using a Plan Apochromat 63X/1.4 NA Oil DIC objective. Images were analysed using ZEN software.

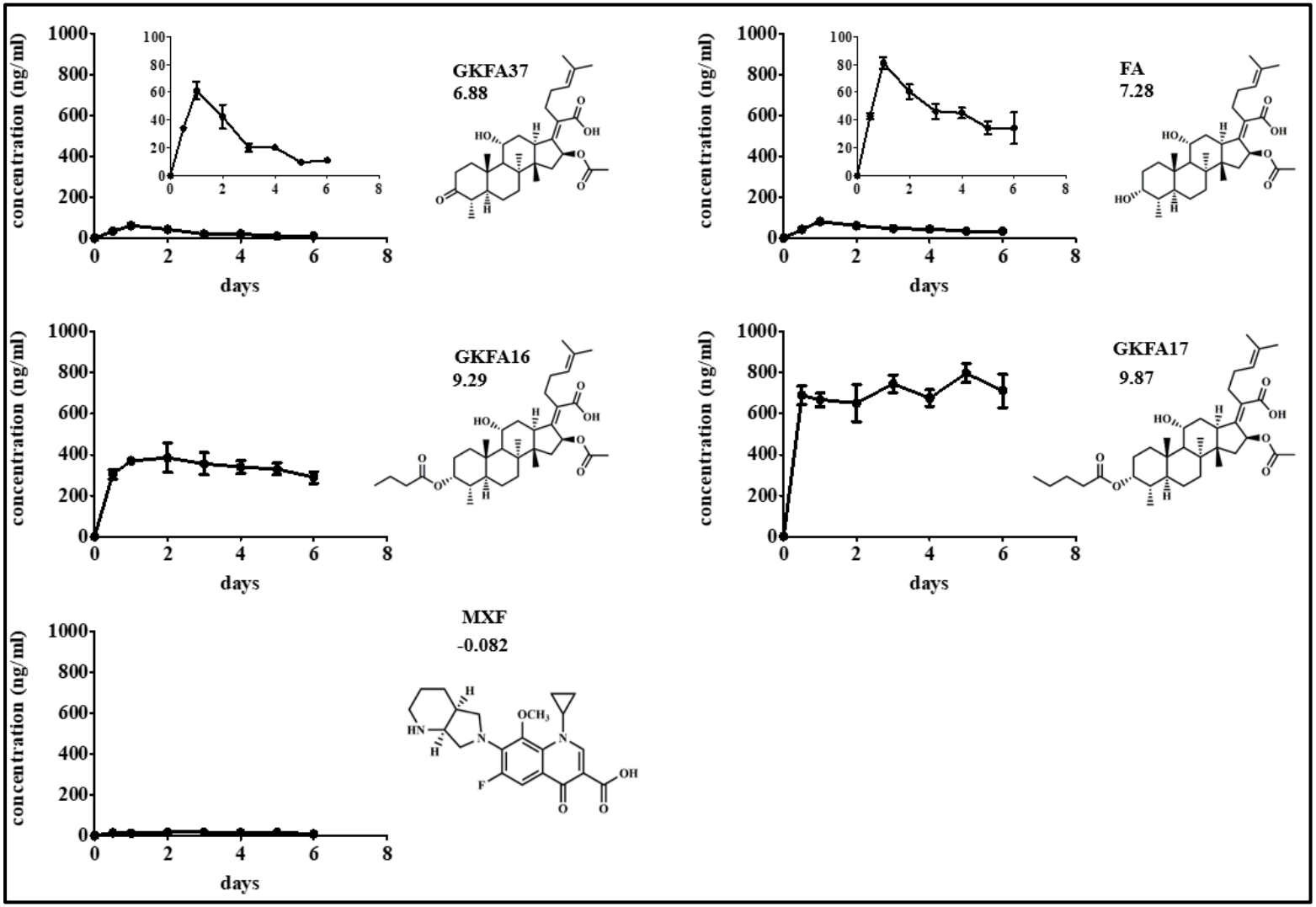
concentration (ng/ml)
days
GKFA37
6.88
FA
7.28
GKFA16
9.29
GKFA17
9.87
MXF
-0.082

Figure 4.6. Concentrations of FA and derivatives accumulated in foamy macrophages over a 6-day incubation period. Data are from representative experiments performed in at least two biological replicates with three technical replicates each. Error bars represent standard error of the mean.

THP-1-derived foamy macrophages where then exposed to FA and derivatives to determine intracellular accumulation. GKFA16 and GKFA17 accumulated in significantly higher amounts than both FA and GKFA37 (Figure 4.6). In the lipid-rich foamy macrophages, slightly higher intracellular accumulation was also observed for each compound in comparison to resting non-foamy cells, particularly in the first 48 hours following drug exposure (Figure 4.7).

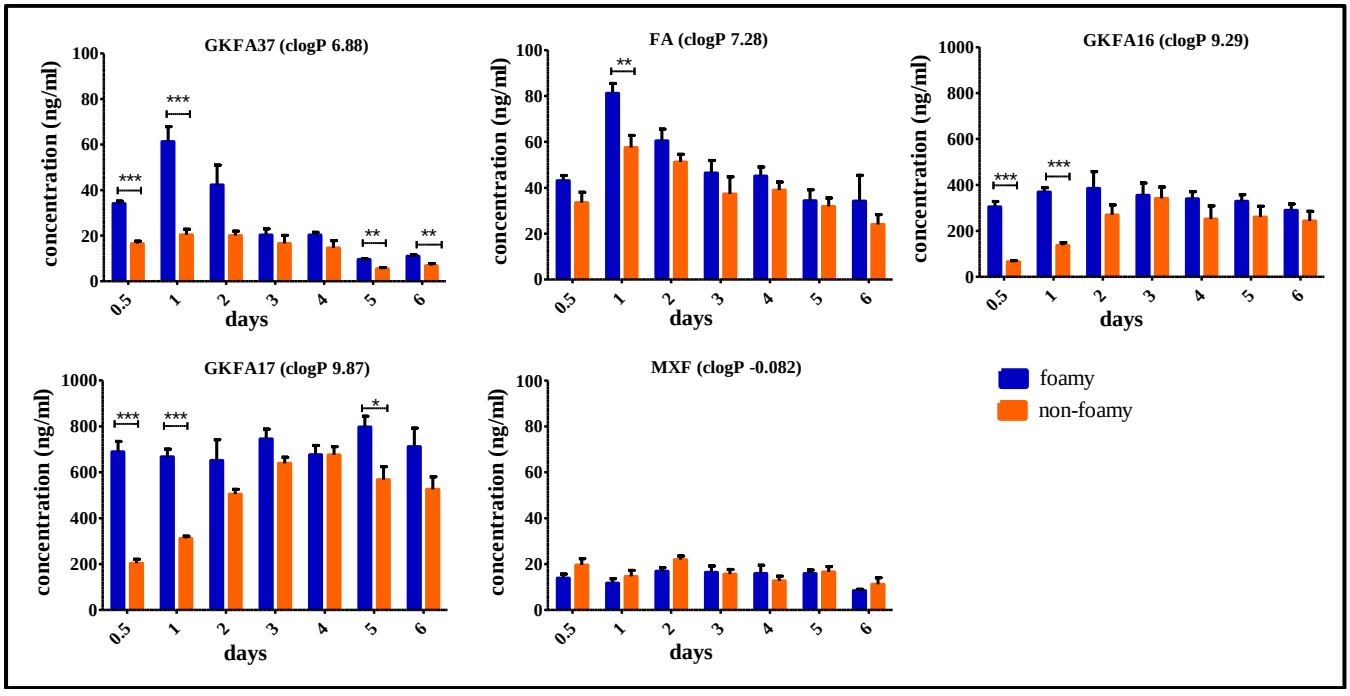

Figure 4.7. Differences in drug accumulation in foamy compared to resting, non-foamy macrophages. Data represent mean ± SEM of 3 independent experiments for GKFA16 and GKFA17, and 2 independent experiments for FA, GKFA37 and MXF, performed in triplicate. The significance between foamy and non-foamy cells at each time point was evaluated using Mann-Whitney tests. *P* values of <0.05 were considered significant. *P < 0.05; **P < 0.01, ***P < 0.001.

Measurements of intracellular uptake in comparison to extracellular drug concentration indicated that all FA compounds were able to concentrate within the cell to achieve significantly higher intracellular concentrations (Figure 4.8). The intracellular to extracellular (I/E) concentration ratios were also significantly greater *versus* resting non-foamy cells. Notably, MXF concentrated within macrophages with a I/E concentration ratio of approximately according to 7, and no differences were observed between foamy and non-foamy cells.

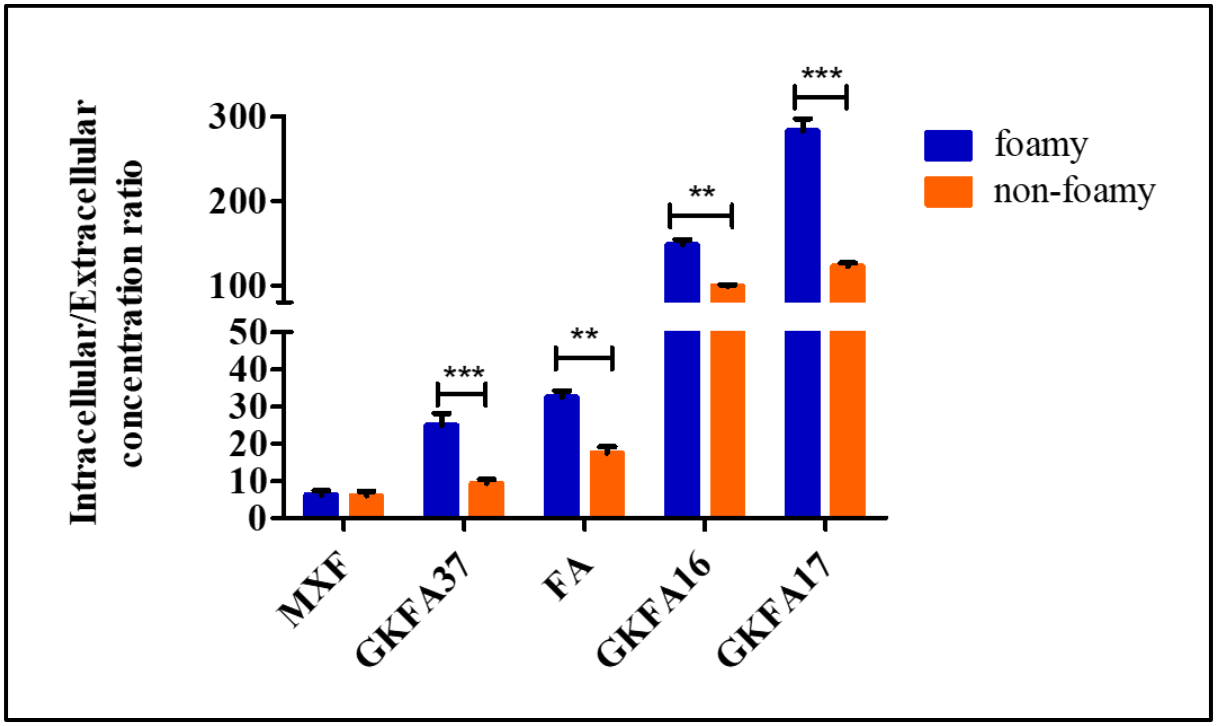

Figure 4.8. Intracellular: extracellular (I/E) concentration ratios of foamy and non-foamy macrophages after 24 hours of drug exposure. Intracellular: extracellular (I/E) concentration ratios of foamy and non-foamy macrophages after 24 hours of drug exposure. Data represent mean ± SEM and are representative of 3 independent experiments for GKFA16 and GKFA17, and 2 independent experiments for FA, GKFA37 and MXF, performed in triplicate. The significance between foamy and non-foamy cells for each compound was evaluated using Mann-Whitney tests. *P* values of <0.05 were considered significant. *P < 0.05; **P < 0.01, ***P < 0.001.

Macrophage differentiation into foamy cells by uptake of external lipids likely occurs via endocytosis and may increase the presence of lipids on the cell membrane surface and

subsequently affect membrane binding of an applied drug. To investigate whether the apparent increase in drug uptake by foamy cells instead reflected extracellular drug lipid binding, we determined how much of the drug was freely available intracellularly and how much was associated with membrane binding in comparison to non-foamy cells following a 48 hour exposure. Samples were prepared as described in chapter 3, and drug associated with cell debris (pellet) and supernatant was measured for FA, GKFA16 and GKFA17. While the amount of drug bound to the cell pellet slightly increased foamy macrophages, the amount of total drug measured significantly increased, suggesting an increase in the intracellular drug (Figure 4.9). However, these data did not provide any information of intracellular drug distribution. Treatment with CFZ, a naturally fluorescent anti-TB drug with high lipophilicity, indicated co-localization of the drug with LBs in foamy macrophages in comparison to non-foamy cells (Figure 4.10).

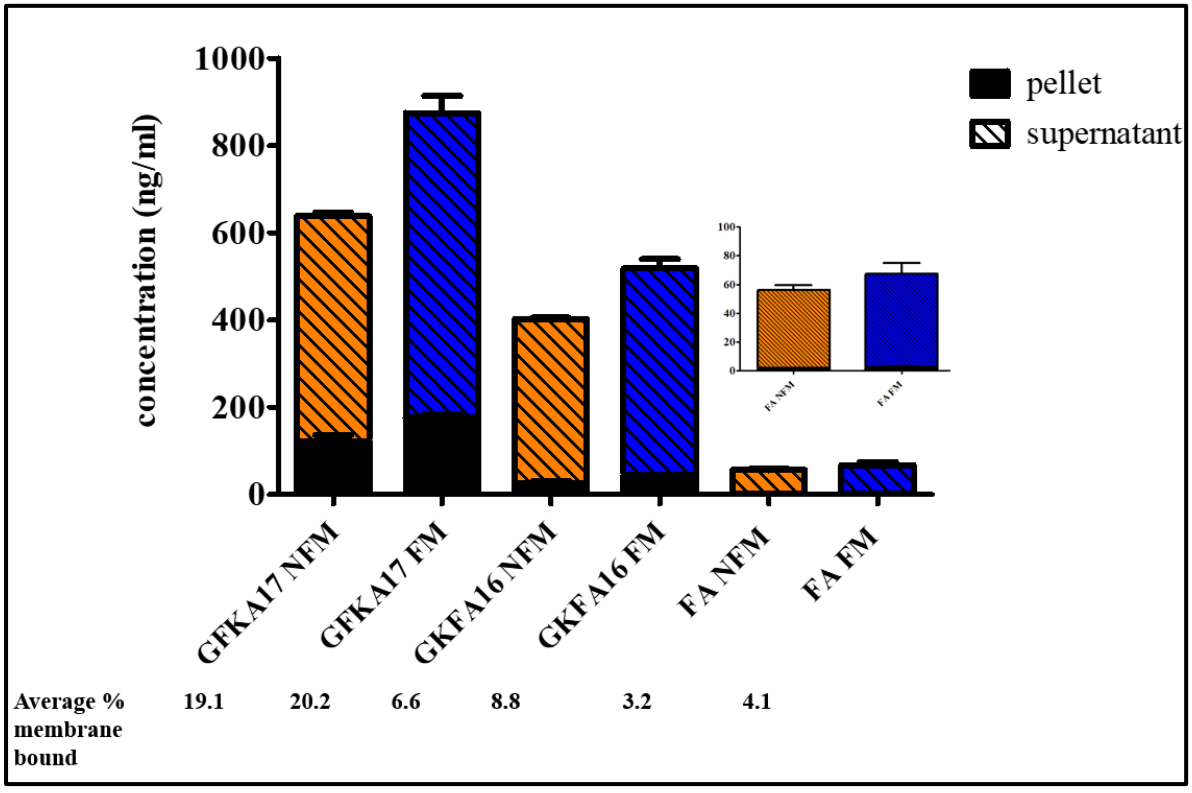

Figure 4.9. Comparison of cell membrane drug binding between foamy and non-foamy macrophages. NFM – non-foamy macrophages, FM – foamy macrophages.

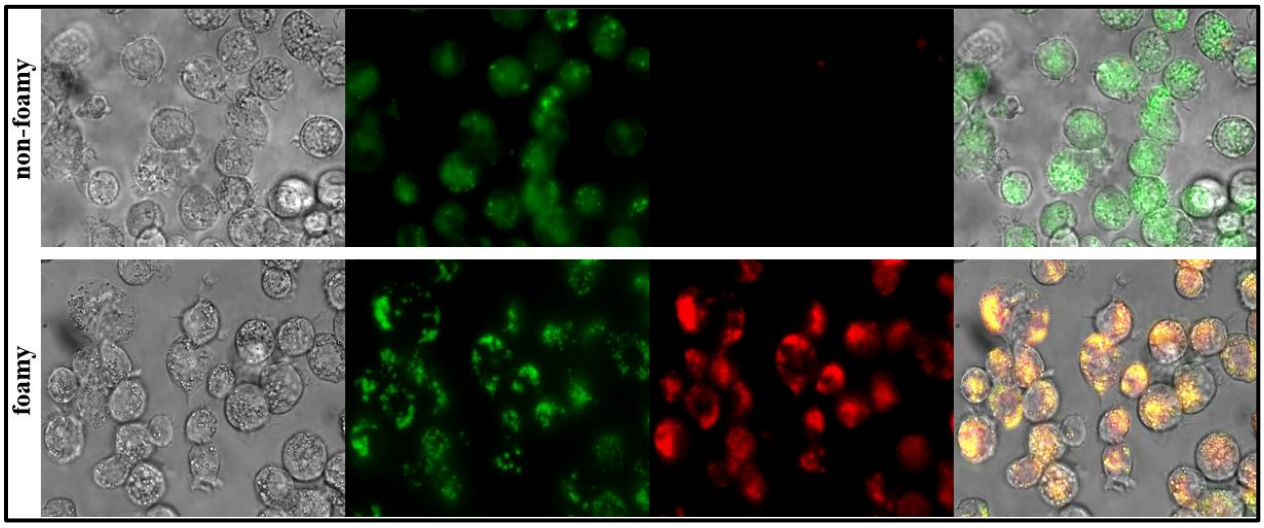

Figure 4.10. Foamy and non-foamy macrophages were treated with CFZ for 30 minutes, stained with LipidTox green. Imaging was done using the Axio Observer 7 equipped with a 100x plan-apochromatic phase 3 oil immersion objective with numerical aperture of 1.4. Zeiss ZEN software was used for imaging and images processed with ImageJ.

M. tuberculosis in foamy macrophages has been reported to alter host cell homeostatic functions, and drive mechanisms for progressing host cell death (Caceres et al. 2009). Foamy macrophages were infected with *M. tuberculosis* H37Rv at MOIs of 1, 2 and 5 to determine whether the presence of intracellular bacilli affects drug uptake by macrophages. Infected macrophages were exposed to compound GKFA17 at 10 µM. Increasing macrophage bacterial burden had no impact on the amount of drug accumulated. However, at MOI = 5, host cell death was observed in foamy macrophages with loss of surface adherence after 2 days of infection (Figure 4.11). This effect was only observed in the case of foamy macrophages, and not in infected non foamy cells (chapter 3), despite exposure to the same bacterial counts and similar percentage of cells infected at MOI = 5 (Figure 4.12).

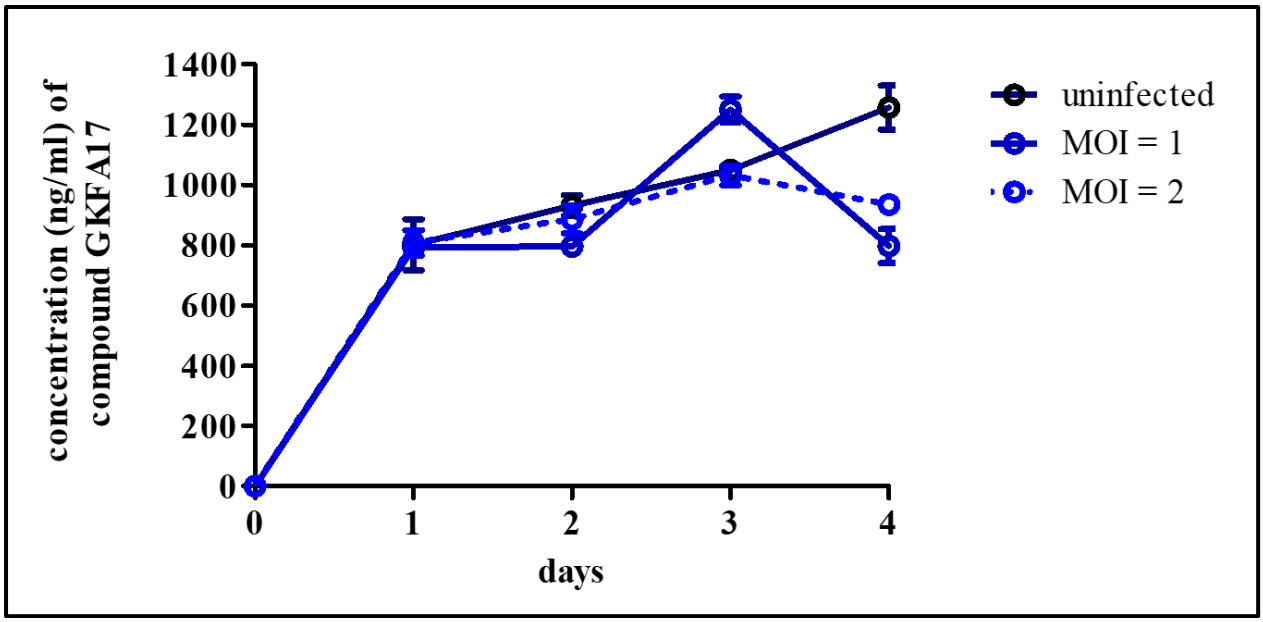

Figure 4.11. Intracellular accumulation of compound GKFA17, as a function of foamy macrophage bacterial burden. Data are from an experiment performed in technical triplicate.

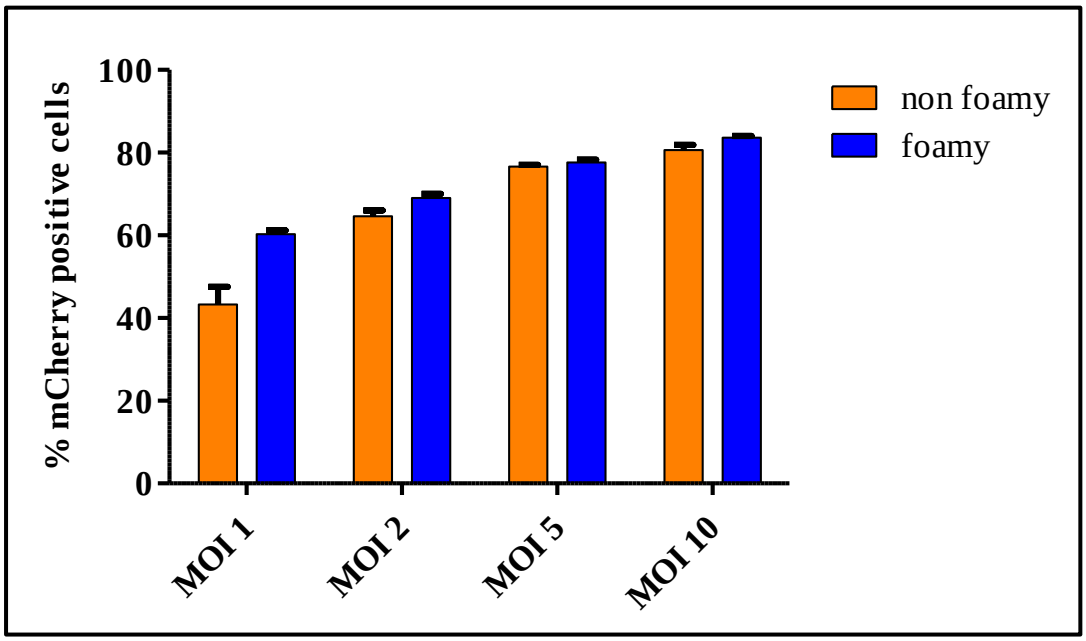

Figure 4.12. Percentage of cells infected after 4 hours of bacterial exposure at MOI =1, 2, 5,or 10.

4.2.3 Efficacy of antimycobacterial agents in foamy macrophages

The results so far indicated that foamy macrophages accumulated higher levels of FA and derivatives and that GKFA16 and GKFA17 accumulated more than FA and GKFA37. An investigation was then carried out to determine if this translated into more rapid reduction in intracellular bacterial numbers. At the same drug concentration (10 µM), infected foamy macrophages (MOI = 1) were treated and, at specific time points, cells were lysed and plated for CFU enumeration. Despite the significant differences in uptake of GKFA16 and GKFA17 in comparison to FA and GKFA37, the same effect was observed as in non-foamy cells: for all drugs, intracellular bacillary numbers were reduced to a similar extent (approximately one log-fold) relative to the untreated control (Figure 4.13). This was supported by the mean fluorescence intensity of the *M. tuberculosis* H37Rv MA :: (smyc'::mCherry (=pCherry3)) intracellular signal which remained constant while the untreated control increased, indicating a bacteriostatic intracellular effect of FA and derivatives, and continued *M. tuberculosis* growth in the untreated control (Figure 4.14).

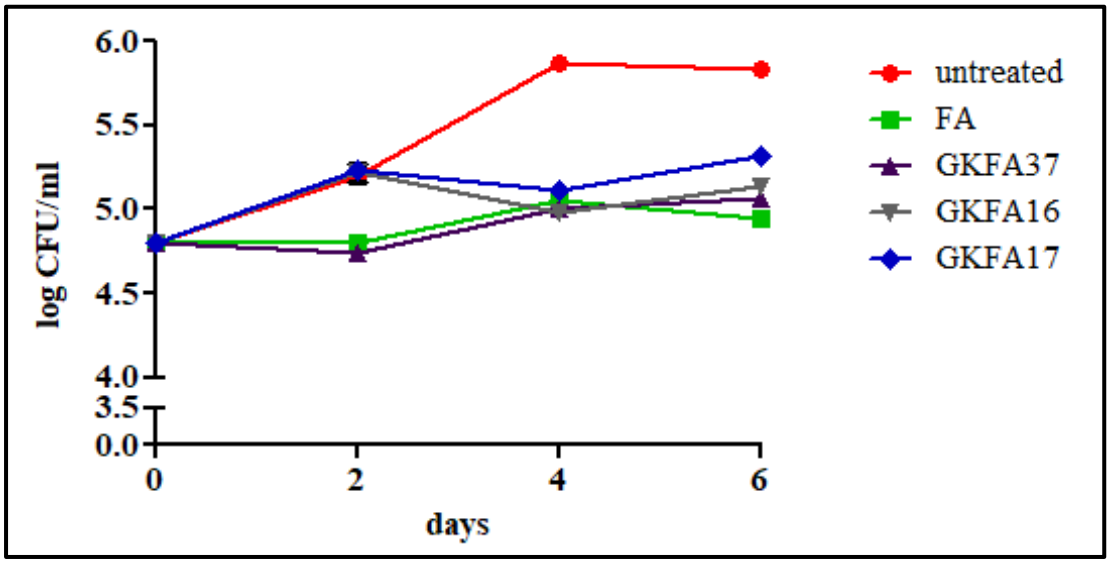

Figure 4.13. Intracellular bacterial survival in foamy macrophages treated with FA and derivatives at 10 µM concentration.

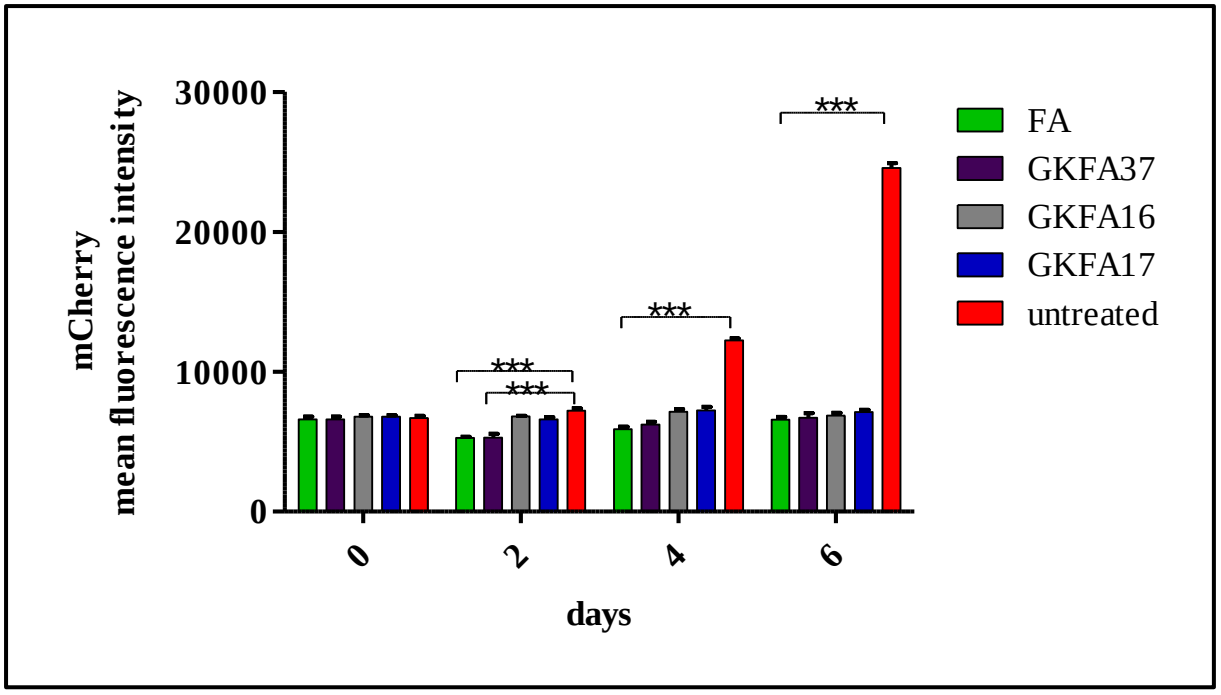

Figure 4.14. Mean fluorescence intensities of intracellular *M. tuberculosis* H37Rv MA :: (smyc'::mCherry (=pCherry3)) during treatment (10 μM for all compounds) of foamy macrophages Error bars represent standard error of the mean. Multiple comparisons with the control untreated group were analyzed using a 1-way ANOVA with Dunnett's post analysis. *P* values of <0.05 were considered significant. *P < 0.05; **P < 0.01, ***P < 0.001.

The bacteriostatic effect of FA and derivatives in the foamy macrophage phenotype (Figures 4.13 and 4.14) and in resting macrophages (Chapter 3) suggested that differential intracellular drug concentrations did not drive cellular efficacy for these compounds. Further analysis was therefore done to discern the effects of host cell immune status and changes in host cell LBs. Earlier results indicated that GKFA17-treated activated macrophages significantly reduced drug accumulation relative to resting cells, while foamy cells showed an even improved intracellular accumulation relative to resting cells. Foamy and activated macrophages were generated as described earlier and treated with 10X MICs of FA and derivatives with bacteria enumerated by CFU counts. This analysis suggested that activated macrophages drive intracellular bacterial killing, indicated by the greater than 2-fold reduction in bacterial numbers relative to the unactivated control (Figure 4.15). The distinction between activated untreated and treated macrophages indicate that host cell activation potentiates further

intracellular activity of these compounds. It further confirmed that the effect of differential drug concentrations cannot be discerned using bacteriostatic compounds, indicated by the clustering of all compounds in the resting and foamy group, distinct from the activated group.

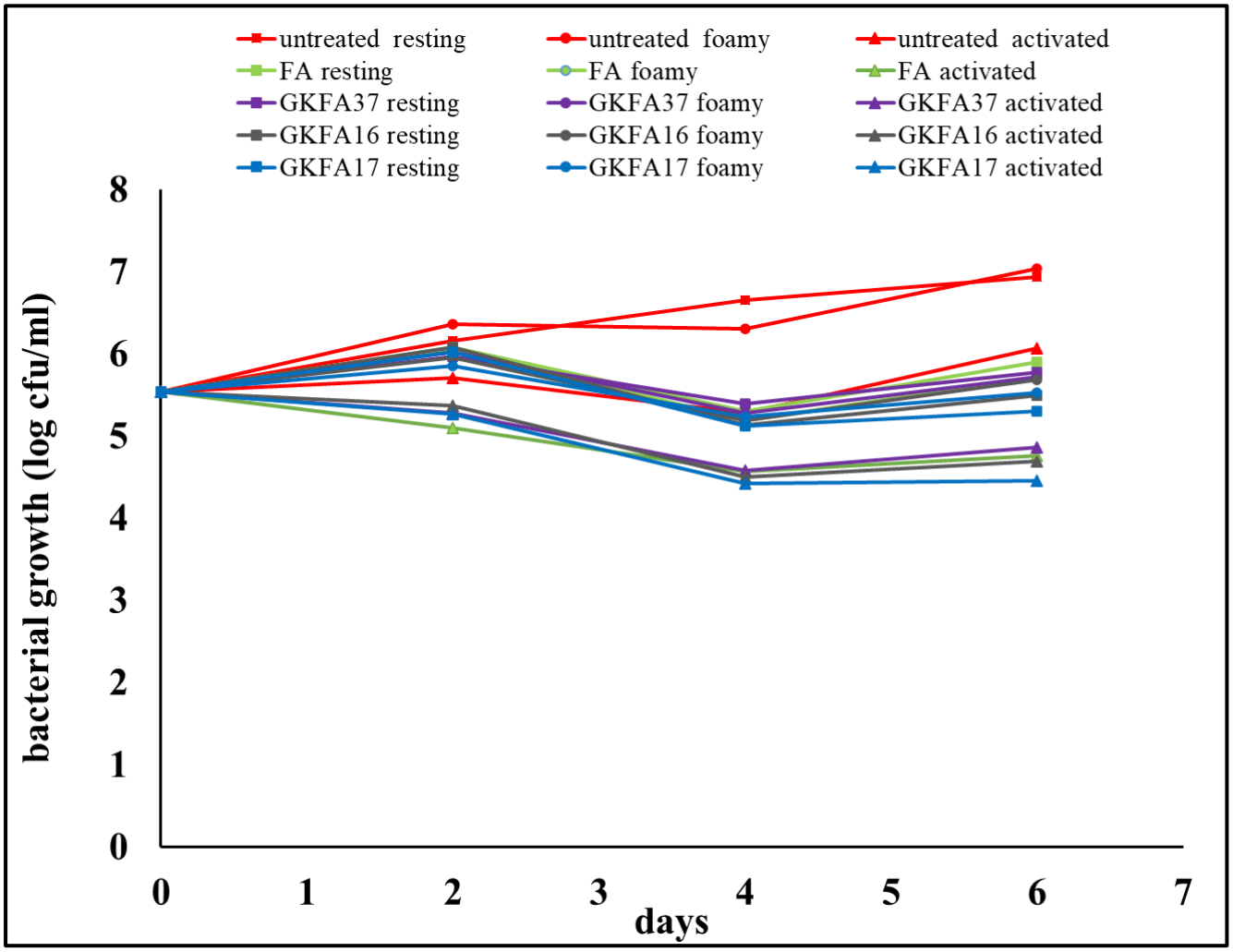

Figure 4.15. A comparison of bacterial survival in resting, foamy and activated macrophages at 10x MIC of the indicated compounds.

FA and derivatives were bacteriostatic at the tested concentrations, and further increasing concentrations would impact solubility and potentially cause host cell cytotoxicity. The effect

of a lipid-rich environment on the intracellular activity of clinically used anti-TB drugs, RIF, BDQ, MXF and LVF was next investigated. These drugs are known to effect cidal activity against replicating *M. tuberculosis in vitro* and *in vivo* (Lakshminarayana et al. 2015; Johnson et al. 2006). MXF has been reported to have superior antimycobacterial activity and to achieve higher intracellular concentrations and cellular lesion distribution than other fluoroquinolones including LVF (Sarathy et al. 2019; Michot et al. 2005; Lakshminarayana et al. 2015). However, given the differences in lipophilicity of these two compounds, it was of interest to determine the effect of host LBs on intracellular drug distribution and ability to reach *M. tuberculosis* bacilli in their niche.

BDQ is the most lipophilic, and was shown to accumulate more in the cellular lesion, with poor caseum diffusion (Irwin et al. 2016; Sarathy et al. 2016). RIF is a key sterilizing drug and has been shown to distribute into both caseum and cellular lesion compartments (Prideaux et al. 2015). Since BDQ and RIF are more lipophilic than both MXF and LVF, an investigation into the impact of the presence of lipid bodies in foamy macrophages on intracellular activity of these drugs was carried out. Both macrophage phenotypes were treated with 10 µM of each drug and media were replenished every second day. The efficacy of RIF on intracellular bacilli as determined by CFU enumeration was the same for both foamy and non-foamy cells, with a 3-log reduction in bacillary counts observed relative to the untreated control (Figure 4.16). MXF and LVF are both bactericidal against intracellular bacilli and, in non-foamy cells both drugs eliminated all intracellular bacteria (day 6), with MXF showing an early cidal effect within 48 hours of treatment. In foamy macrophages, however, MXF exhibited a delayed effect with near complete sterilization of intracellular bacteria only at day 6, whereas LVF failed to eliminate all intracellular bacilli by day 6. BDQ reduced bacillary counts by ~2-fold and 3-fold

in foamy and non-foamy in comparison to the untreated control at day 4, respectively. These results suggested an impact of host LBs on cellular drug efficacy.

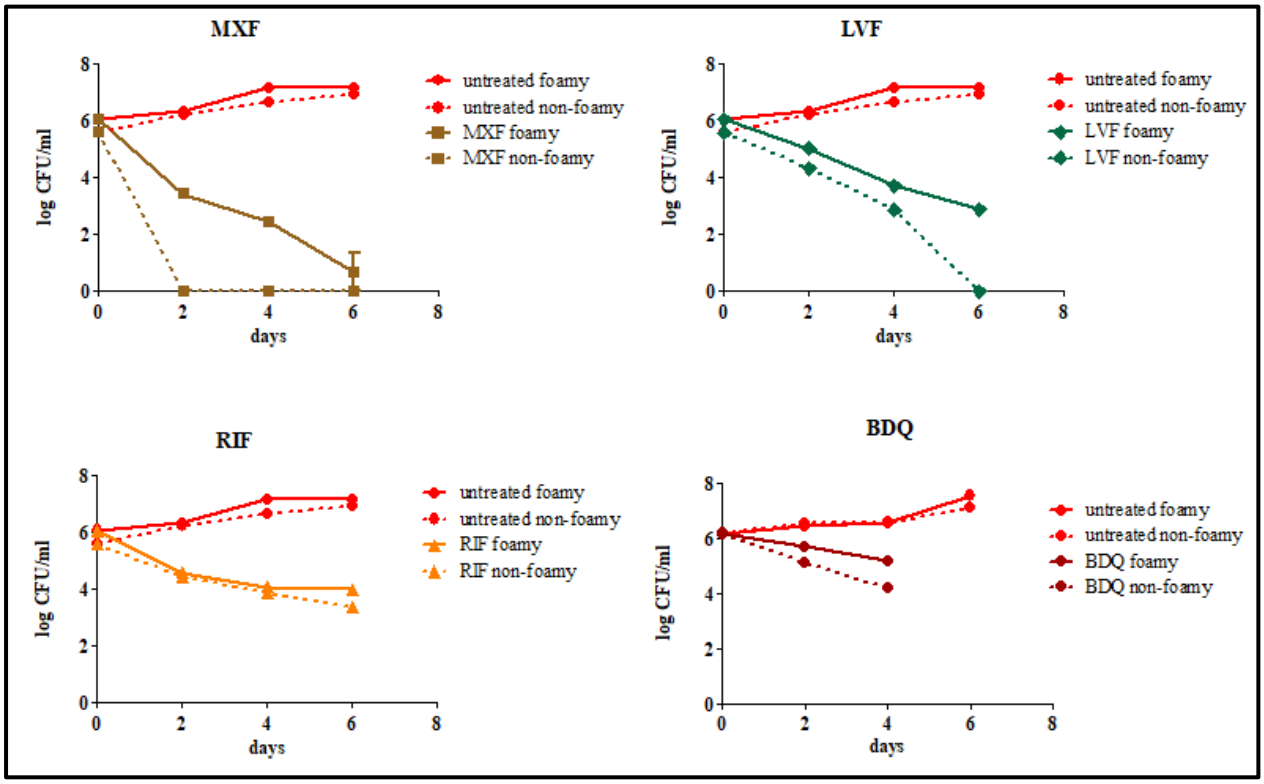

Figure 4.16. A comparison of intracellular bacillary survival in foamy and non-foamy macrophages treated with anti-TB drugs (10 µM for MXF, LVF, and RIF; 5 µM for BDQ). BDQ data was collected over a 4-day period due to limited compound availability for repeat experiment. Data are representative of two biological replicates for RIF (single experiment for MXF, LVF and BDQ, discussed later in the chapter) with three technical replicates each. Error bars represent standard error of the mean.

4.3 Discussion

To test the effect of host immune response on cellular drug accumulation, activated macrophages were induced by stimulation of THP-1-derived macrophages towards a classical pro-inflammatory M1 phenotype using IFN-γ and LPS. Following drug treatment, both

infected and uninfected activated macrophages significantly reduced the amount of GKFA17 (Figure 4.1) in comparison to resting cells. This drug loss from activated macrophages was not due to host cell membrane damage as both resting and activated cells stained similarly with PI, a dye that penetrates cells with compromised membrane integrity. It is hypothesized that macrophage activation induces host cell efflux pumps that actively reduce the amount of drug accumulated or prevent cellular uptake. Plating samples for CFU enumeration from the infected activated cells showed that despite reduced drug levels, activated macrophages further reduced intracellular bacterial counts after 6 days of incubation in comparison to resting cells with higher drug levels. This suggests that, for these compounds, host killing mechanisms potentiate the intracellular antimycobacterial activity of the compound. However, the extent of contribution of the compound at this concentration or the activation status of the cell will require that untreated activated cells be added as a control in future experiments. At 10X MIC, activated treated macrophages were even more effective than foamy macrophages, which accumulated higher compound levels than resting (non-foamy) cells, suggesting that the activation status of the cell was the major driver of the decrease in bacterial burden (Figure 4.15).

The phagosomal pH of activated macrophages is more acidic than that of resting macrophages. In this thesis work, it has been shown that FA and GKFA37 are more active in slightly acidic conditions *in vitro* (Chapter 1). The C-3 alkyl esters GKFA16 and GKFA17 undergo hydrolysis to FA, which can in turn be metabolized to 3-ketoFA (GKFA37). Untreated activated macrophages reduced CFU by a similar magnitude to treated resting or foamy cells (Figure 4.14). Treatment of activated cells seemed to further reduce CFU growth despite lower drug levels suggesting FA compounds may be more effective against bacteria in a low pH intraphagosomal environment. The resting untreated control increased bacterial growth as expected, indicating active host cell *M. tuberculosis* replication. FA is a translation inhibitor

that is active against replicating *M. tuberculosis*. Therefore, FA compounds could be effective against replicating phagosomal *M. tuberculosis* in activated host cells.

The accumulation of RIF and BDQ in activated macrophages was not affected by the activation status of the host cells, suggesting that these two drugs were not susceptible to efflux in activated cells. These data agree with the observation by Liu et al., (2016) who showed that RIF and the other first line drugs accumulated to similar levels in resting and activated J774 macrophages. These data highlight that host immune response directly impact accumulation of some drugs, probably by upregulation of macrophage efflux transporters. Inclusion of activated macrophage assays to predict intracellular exposure will be crucial to support cellular lesion penetration data.

The role of foamy macrophages in the efficacy of antimycobacterial agents against intracellular *M. tuberculosis* was explored by adopting a previously described method of oleic acid to induce foamy macrophage differentiation (Sarathy et al. 2016). The differences in LB accumulation in foamy cells were confirmed by visualization of the green fluorescent LipidTox stain. Drug exposure of foamy cells revealed similar uptake patterns to those observed for non-foamy cells, with GKFA16 and GKFA17 accumulating in significantly higher concentrations than either FA or GKFA37. Furthermore, foamy macrophages showed significantly higher early drug accumulation than non-foamy cells (Figure 4.7), suggesting an increased early drug uptake and that the presence of LB within the host cell environment helps sequester the lipophilic compounds intracellularly. Greenwood et al, reported that LBs did not help sequester the highly lipophilic BDQ, but rather that lipid bound drug constituted a reservoir that could be transferred into the bacilli as they take up lipids and therefore improve intracellular drug efficacy (Greenwood et al. 2019). Given the same range in lipophilicity of BDQ and the test compounds

in this thesis work, it was hypothesized that FA and its derivatives accumulate in LB in foamy cells. Due to high lipophilicity of FA compounds, LBs may facilitate initial drug binding translating to increased concentrations in earlier time-points. However, once saturation is reached, it is likely that metabolism and efflux contribute to reduce intracellular concentrations and this effect is more pronounced in the less lipophilic FA and GKFA37 as they are the least accumulated, and are likely to bind to LBs with less affinity in comparison to the alkyl esters. CFZ is another lipophilic TB drug with comparable clogP to the test compounds used in this thesis work. Taking advantage of its natural red color and fluorescence which allowed for visualization using microscopy, it was shown that CFZ concentrates in LBs within foamy cells (Figure 4.10). In addition, the increase in accumulation of FA compounds in foamy macrophages was not associated with increased non-specific membrane binding as both macrophage phenotypes had comparable percentage of mean membrane bound drug. The observed effect was solely due to the presence of intracellular LBs.

Untreated non-foamy and foamy macrophages permitted bacterial growth at a similar rate up to 6 days (Figure 4.15) despite non-foamy cells having been implicated in induction of a non-replicating state. These observations are in line with results reported by Peyron et al, who showed that a non-replicating state was only induced after 6 days of infection, while resting cells permitted continued exponential growth (Peyron et al. 2008). In addition, using a similarly induced foamy phenotype, Agarwal et al., (2020) reported that *M. tuberculosis* replicates within both foamy and non-foamy cells, although foamy cells seemed to effect a slight control in bacillary growth. These differences to data reported here may be due to the inoculum used, at higher MOI foamy cells may be induced to activate immune mechanisms to control bacterial growth (Agarwal et al., 2020). Alternatively, the interaction of *M. tuberculosis* with LBs due to increased proximity at a higher MOI, may have an effect on its growth. The similar control of bacterial growth at constant CFU, effected by FA compounds in both foamy and non-foamy

cells seemed to suggest that the LBs had no effect on intracellular bacterial survival. This contradicted the theory of LB-mediated transfer of drug into *M. tuberculosis*. In addition, as observed in non-foamy macrophages, the alkyl esters GKFA16 and GKFA17, with significantly higher macrophage concentrations also showed comparable intracellular efficacy to FA and GKFA37 as scored by both CFU and mCherry mean fluorescence intensity. The bacteriostatic effect of FA compounds against intracellular bacilli at tested concentrations could be masking the effect of drug lipid binding on intracellular efficacy.

RIF (clogP value of 3.71), BDQ (7.25), MXF (-0.0824) and LVF (-0.508) showed variable intra-macrophage efficacy in foamy and non-foamy cells. The effect of RIF, with moderate lipophilicity, appeared not to be impacted by the presence of LBs as the drug reduced CFU by a comparable ~3-fold log difference relative to the untreated control. MXF and LVF exhibited a delayed bactericidal effect in foamy macrophage bacilli, which suggested that LBs play a role in their intracellular distribution. BDQ, the most lipophilic of the four drugs, exhibited a more bactericidal effect in non-foamy compared to foamy cells, a similar trend with the fluoroquinolones, despite differences in lipophilicities These results contrast the model proposed by Greenwood et al (2019), which suggested that foamy cells improve efficacy by concentrating the drug in LBs, allowing transfer to the bacilli. MXF has a lower clogP than BDQ, which might result in different LB binding capacity. MXF accumulated less than the lipophilic FA compounds (same lipophilic range as BDQ), albeit it showed similar intracellular concentrations in both foamy and non-foamy cells, which were not affected by infection. BDQ relative concentrations (data not shown), were similar for both foamy and non-foamy cells. MXF reached higher intracellular than extracellular concentrations with a I/E ratio of ~7, which is comparable to that previously reported in bone marrow derived non-foamy macrophages (Blanc et al. 2018).

Despite the favorable drug uptake characteristics of MXF, the macrophage efficacy results suggest a lipophilicity-driven outcome of drug distribution and hence the observed activity in the lipid rich foamy cells. It can be hypothesized that LBs bind intracellular drug and may increase drug accumulation in foamy cells, as the intracellular concentration of FA compounds, and CFZ co-localization data reported in this thesis work and BDQ co-localization reported previously (Greenwood et al. 2019), seem to suggest. However, the amount of unbound drug fraction may not be affected in a similar manner for the more lipophilic compounds, as it is for less lipophilic compounds. The outcome of efficacy likely depends on the inherent activity of the drug (cidal or static), whether the drug achieves intracellular concentrations far above those required for activity and the extent of lipid binding. The less lipophilic MXF and LVF, even in the absence of LBs, accumulate to adequate concentrations to impart the observed effective bacterial killing. However, the binding of LB in foamy macrophages significantly affects the amount of free drug available intracellularly, even though a lower percentage of both MXF and LVF may be lipid bound compared to RIF, BDQ and the other more lipophilic drugs. For BDQ, with less sterilizing activity than the fluoroquinolones, it likely achieves sufficient intracellular concentration, however due to very high lipophilicity, the extent of binding significantly affects the levels of remaining unbound drug. RIF, with moderate lipophilicity, seems to achieve a balance between these factors, hence there was no LB-mediated reduced efficacy.

To support this hypothesis, an experiment was designed and conducted to determine the extent of LB binding, intracellular drug distribution and the effects on cellular efficacy. Briefly, foamy and non-foamy macrophages were treated with MXF, LVF, BDQ, CFZ, RIF and the highly lipophilic, bacteriostatic test compounds, FA and GKFA17. Following drug exposure over 48 hours, which our previous results suggest peak intracellular concentrations, drug media was removed and replaced with fresh media in a subset of both foamy and non-foamy macrophage samples (subset 1). In the remaining samples, drug media was replenished every 48 hours

(subset 2) and both samples were incubated for another 4-day period. At days 0, 2, 4 and 6, macrophages were lysed and plated for CFU enumeration. Unfortunately, the intervention of the COVID-19 pandemic – with enforced, ongoing shutdown of our research laboratory – has meant that the data cannot be collected. The predicted outcomes, in accordance to the theory proposed by Greenwood et al., (2019), would be that the foamy macrophages in subset 1 should exhibit superior control of intracellular bacillary growth in comparison to non-foamy cells, supporting a role for LBs as a reservoir for intracellular drug and therefore a sustained transfer of drug into *M. tuberculosis*. The second expected outcome supporting our hypothesis would be more complex as not only the extent of lipophilicity-driven drug penetration and drug-lipid binding influencing the unbound drug fraction is important but also the inherent activity (cidal or static) of the compound would determine efficacy against *M. tuberculosis*. The data generated so far highlight the utility of this *in vitro* macrophage infection and drug penetration assay in discerning the effect of intracellular drug accumulation and distribution on efficacy for cidal drugs. However, for static antimycobacterial agents, the data may be more difficult to interpret as the static effect masks the effect of differential intracellular drug concentrations.

4.4 References

Adams, K. N., K. Takaki, L. E. Connolly, H. Wiedenhoft, K. Winglee, O. Humbert, P. H. Edelstein, C. L. Cosma, and L. Ramakrishnan. 2011. 'Drug tolerance in replicating mycobacteria mediated by a macrophage-induced efflux mechanism', *Cell*, 145: 39-53.

Agarwal, P., T.W. Combes, F. Shojaee-Moradi, B.A. Fielding, S.N. Gordon, V. Mizrahi, and F.O. Martinez. 2020. 'Foam Cells Control Mycobacterium tuberculosis Infection', *Frontiers in Microbiology*.

Betts, J. C., P. T. Lukey, L. C. Robb, R. A. McAdam, and K. Duncan. 2002. 'Evaluation of a nutrient starvation model of Mycobacterium tuberculosis persistence by gene and protein expression profiling', *Molecular Microbiology*, 43: 717-31.

Blanc, L., I. B. Daudelin, B. K. Podell, P. Y. Chen, M. Zimmerman, A. J. Martinot, R. M. Savic, B. Prideaux, and V. Dartois. 2018. 'High-resolution mapping of fluoroquinolones in TB rabbit lesions reveals specific distribution in immune cell types', *Elife*, 7.

Bostrom, P., B. Magnusson, P. A. Svensson, O. Wiklund, J. Boren, L. M. Carlsson, M. Stahlman, S. O. Olofsson, and L. M. Hulten. 2006. 'Hypoxia converts human macrophages into triglyceride-loaded foam cells', *Arteriosclerosis, Thrombosis, and Vascular Biology*, 26: 1871-6.

Caceres, N., G. Tapia, I. Ojanguren, F. Altare, O. Gil, S. Pinto, C. Vilaplana, and P. J. Cardona. 2009. 'Evolution of foamy macrophages in the pulmonary granulomas of experimental tuberculosis models', *Tuberculosis (Edinb)*, 89: 175-82.

Daniel, J., H. Maamar, C. Deb, T. D. Sirakova, and P. E. Kolattukudy. 2011. 'Mycobacterium tuberculosis uses host triacylglycerol to accumulate lipid droplets and acquires a dormancy-like phenotype in lipid-loaded macrophages', *PLoS Pathogens*, 7: e1002093.

den Hartigh, L. J., J. E. Connolly-Rohrbach, S. Fore, T. R. Huser, and J. C. Rutledge. 2010. 'Fatty acids from very low-density lipoprotein lipolysis products induce lipid droplet accumulation in human monocytes', *Journal of Immunology*, 184: 3927-36.

Eisenreich, W., J. Heesemann, T. Rudel, and W. Goebel. 2015. 'Metabolic Adaptations of Intracellullar Bacterial Pathogens and their Mammalian Host Cells during Infection ("Pathometabolism")', *Microbiol Spectr*, 3.

Greenwood, D. J., M. S. Dos Santos, S. Huang, M. R. G. Russell, L. M. Collinson, J. I. MacRae, A. West, H. Jiang, and M. G. Gutierrez. 2019. 'Subcellular antibiotic visualization reveals a dynamic drug reservoir in infected macrophages', *Science*, 364: 1279-82.

Irwin, S. M., B. Prideaux, E. R. Lyon, M. D. Zimmerman, E. J. Brooks, C. A. Schrupp, C. Chen, M. J. Reichlen, B. C. Asay, M. I. Voskuil, E. L. Nuermberger, K. Andries, M. A. Lyons, V. Dartois, and A. J. Lenaerts. 2016. 'Bedaquiline and Pyrazinamide Treatment Responses Are Affected by Pulmonary Lesion Heterogeneity in Mycobacterium tuberculosis Infected C3HeB/FeJ Mice', *ACS Infect Dis*, 2: 251-67.

Johnson, J. L., D. J. Hadad, W. H. Boom, C. L. Daley, C. A. Peloquin, K. D. Eisenach, D. D. Jankus, S. M. Debanne, E. D. Charlebois, E. Maciel, M. Palaci, and R. Dietze. 2006. 'Early and extended early bactericidal activity of levofloxacin, gatifloxacin and moxifloxacin in pulmonary tuberculosis', *International Journal of Tuberculosis and Lung Disease*, 10: 605-12.

Lakshminarayana, S. B., T. B. Huat, P. C. Ho, U. H. Manjunatha, V. Dartois, T. Dick, and S. P. Rao. 2015. 'Comprehensive physicochemical, pharmacokinetic and activity profiling of anti-TB agents', *Journal of Antimicrobial Chemotherapy*, 70: 857-67.

Li, Z., M. J. Scott, E. K. Fan, Y. Li, J. Liu, G. Xiao, S. Li, T. R. Billiar, M. A. Wilson, Y. Jiang, and J. Fan. 2016. 'Tissue damage negatively regulates LPS-induced macrophage necroptosis', *Cell Death and Differentiation*, 23: 1428-47.

Liu, Y., S. Tan, L. Huang, R. B. Abramovitch, K. H. Rohde, M. D. Zimmerman, C. Chen, V. Dartois, B. C. VanderVen, and D. G. Russell. 2016. 'Immune activation of the host cell induces drug tolerance in Mycobacterium tuberculosis both in vitro and in vivo', *Journal of Experimental Medicine*, 213: 809-25.

Lok, H. C., S. Sahni, P. J. Jansson, Z. Kovacevic, C. L. Hawkins, and D. R. Richardson. 2016. 'A Nitric Oxide Storage and Transport System That Protects Activated Macrophages from Endogenous Nitric Oxide Cytotoxicity', *Journal of Biological Chemistry*, 291: 27042-61.

Marquez, B., N. E. Caceres, M. P. Mingeot-Leclercq, P. M. Tulkens, and F. Van Bambeke. 2009. 'Identification of the efflux transporter of the fluoroquinolone antibiotic ciprofloxacin in murine macrophages: studies with ciprofloxacin-resistant cells', *Antimicrobial Agents and Chemotherapy*, 53: 2410-6.

Mashabela, G. T., T. J. de Wet, and D. F. Warner. 2019. 'Mycobacterium tuberculosis Metabolism', *Microbiol Spectr*, 7.

Michot, J. M., C. Seral, F. Van Bambeke, M. P. Mingeot-Leclercq, and P. M. Tulkens. 2005. 'Influence of efflux transporters on the accumulation and efflux of four quinolones (ciprofloxacin, levofloxacin, garenoxacin, and moxifloxacin) in J774 macrophages', *Antimicrobial Agents and Chemotherapy*, 49: 2429-37.

Moreau, A., M. Le Vee, E. Jouan, Y. Parmentier, and O. Fardel. 2011. 'Drug transporter expression in human macrophages', *Fundamental and Clinical Pharmacology*, 25: 743-52.

O'Neill, L. A., R. J. Kishton, and J. Rathmell. 2016. 'A guide to immunometabolism for immunologists', *Nature Reviews: Immunology*, 16: 553-65.

Park, Y., A. Pacitto, T. Bayliss, L. A. Cleghorn, Z. Wang, T. Hartman, K. Arora, T. R. Ioerger, J. Sacchettini, M. Rizzi, S. Donini, T. L. Blundell, D. B. Ascher, K. Rhee, A. Breda, N. Zhou, V. Dartois, S. R. Jonnala, L. E. Via, V. Mizrahi, O. Epemolu, L. Stojanovski, F. Simeons, M. Osuna-Cabello, L. Ellis, C. J. MacKenzie, A. R. Smith, S. H. Davis, D. Murugesan, K. I. Buchanan, P. A. Turner, M. Huggett, F. Zuccotto, M. J. Rebollo-Lopez, M. J. Lafuente-Monasterio, O. Sanz, G. S. Diaz, J. Lelievre, L. Ballell, C. Selenski, M. Axtman, S. Ghidelli-Disse, H. Pflaumer, M. Bosche, G. Drewes, G. M. Freiberg, M. D. Kurnick, M. Srikumaran, D. J. Kempf, S. R. Green, P. C. Ray, K. Read, P. Wyatt, C. E. Barry, 3rd, and H. I. Boshoff. 2017. 'Essential but Not Vulnerable: Indazole Sulfonamides Targeting Inosine Monophosphate Dehydrogenase as Potential Leads against Mycobacterium tuberculosis', *ACS Infect Dis*, 3: 18-33.

Peyron, P., J. Vaubourgeix, Y. Poquet, F. Levillain, C. Botanch, F. Bardou, M. Daffe, J. F. Emile, B. Marchou, P. J. Cardona, C. de Chastellier, and F. Altare. 2008. 'Foamy macrophages from tuberculous patients' granulomas constitute a nutrient-rich reservoir for M. tuberculosis persistence', *PLoS Pathogens*, 4: e1000204.

Podinovskaia, M., W. Lee, S. Caldwell, and D. G. Russell. 2013. 'Infection of macrophages with Mycobacterium tuberculosis induces global modifications to phagosomal function', *Cellular Microbiology*, 15: 843-59.

Prideaux, B., L. E. Via, M. D. Zimmerman, S. Eum, J. Sarathy, P. O'Brien, C. Chen, F. Kaya, D. M. Weiner, P. Y. Chen, T. Song, M. Lee, T. S. Shim, J. S. Cho, W. Kim, S. N. Cho, K. N. Olivier, C. E. Barry, 3rd, and V. Dartois. 2015. 'The association between sterilizing activity and drug distribution into tuberculosis lesions', *Nature Medicine*, 21: 1223-7.

Russell, D. G., P. J. Cardona, M. J. Kim, S. Allain, and F. Altare. 2009. 'Foamy macrophages and the progression of the human tuberculosis granuloma', *Nature Immunology*, 10: 943-8.

Russell, D. G., L. Huang, and B. C. VanderVen. 2019. 'Immunometabolism at the interface between macrophages and pathogens', *Nature Reviews: Immunology*, 19: 291-304.

Santucci, P., F. Bouzid, N. Smichi, I. Poncin, L. Kremer, C. De Chastellier, M. Drancourt, and S. Canaan. 2016. 'Experimental Models of Foamy Macrophages and Approaches for Dissecting the Mechanisms of Lipid Accumulation and Consumption during Dormancy and Reactivation of Tuberculosis', *Front Cell Infect Microbiol*, 6: 122.

Sarathy, J., L. Blanc, N. Alvarez-Cabrera, P. O'Brien, I. Dias-Freedman, M. Mina, M. Zimmerman, F. Kaya, H. P. Ho Liang, B. Prideaux, J. Dietzold, P. Salgame, R. M. Savic, J. Linderman, D. Kirschner, E. Pienaar, and V. Dartois. 2019. 'Fluoroquinolone Efficacy against Tuberculosis Is Driven by Penetration into Lesions and Activity against Resident Bacterial Populations', *Antimicrobial Agents and Chemotherapy*, 63.

Sarathy, J., V. Dartois, T. Dick, and M. Gengenbacher. 2013. 'Reduced drug uptake in phenotypically resistant nutrient-starved nonreplicating Mycobacterium tuberculosis', *Antimicrobial Agents and Chemotherapy*, 57: 1648-53.

Sarathy, J. P., F. Zuccotto, H. Hsinpin, L. Sandberg, L. E. Via, G. A. Marriner, T. Masquelin, P. Wyatt, P. Ray, and V. Dartois. 2016. 'Prediction of Drug Penetration in Tuberculosis Lesions', *ACS Infect Dis*, 2: 552-63.

Singh, V., S. Donini, A. Pacitto, C. Sala, R. C. Hartkoorn, N. Dhar, G. Keri, D. B. Ascher, G. Mondesert, A. Vocat, A. Lupien, R. Sommer, H. Vermet, S. Lagrange, J. Buechler, D. F. Warner, J. D. McKinney, J. Pato, S. T. Cole, T. L. Blundell, M. Rizzi, and V. Mizrahi. 2017. 'The Inosine Monophosphate Dehydrogenase, GuaB2, Is a Vulnerable New Bactericidal Drug Target for Tuberculosis', *ACS Infect Dis*, 3: 5-17.

Singh, V., S. Jamwal, R. Jain, P. Verma, R. Gokhale, and K. V. Rao. 2012. 'Mycobacterium tuberculosis-driven targeted recalibration of macrophage lipid homeostasis promotes the foamy phenotype', *Cell Host Microbe*, 12: 669-81.

Te Brake, L. H. M., G. J. de Knegt, J. E. de Steenwinkel, T. J. P. van Dam, D. M. Burger, F. G. M. Russel, R. van Crevel, J. B. Koenderink, and R. E. Aarnoutse. 2018. 'The Role of Efflux Pumps in Tuberculosis Treatment and Their Promise as a Target in Drug Development: Unraveling the Black Box', *Annual Review of Pharmacology and Toxicology*, 58: 271-91.

Vogel, S. N., S. T. Marshall, and D. L. Rosenstreich. 1979. 'Analysis of the effects of lipopolysaccharide on macrophages: differential phagocytic responses of C3H/HeN and C3H/HeJ macrophages in vitro', *Infection and Immunity*, 25: 328-36.

Xaus, J., M. Comalada, A. F. Valledor, J. Lloberas, F. Lopez-Soriano, J. M. Argiles, C. Bogdan, and A. Celada. 2000. 'LPS induces apoptosis in macrophages mostly through the autocrine production of TNF-alpha', *Blood*, 95: 3823-31.

CHAPTER 5

CONCLUSIONS AND FUTURE RECOMMENDATIONS

5.1 Conclusions

There is an urgent need to sustain the TB drug pipeline by preloading the preclinical phase of drug development. Developing effective new clinical candidates and optimizing current TB drugs to ensure that they are effective against *M. tuberculosis* subpopulations that exist in lung lesions are high priorities. The aim of this thesis was to utilize an *in vitro* macrophage infection model to study the relationship between physicochemical properties of novel antimycobacterial agents and some current TB drugs, and their cellular permeation, distribution and efficacy in *M. tuberculosis* infected macrophages. These efforts were aimed at informing a rational design of anti-TB drug leads with favorable physicochemical properties that drive drug cellular accumulation to deliver effective concentrations that can be translated to *in vivo* efficacy.

Chapter 2 focused on profiling the physicochemical properties, activities and *in vitro* interaction of compounds with *M. tuberculosis*. Two classes of experimental compounds synthesized in the Chibale laboratories were selected: high MW, high lipophilicity FA and analogues; and the small, polar benzoxazole-based oxime carbamates and free oxime derivatives. In addition, a few selected currently used TB drugs with varying lipophilic properties were used as reference compounds. TB disease primarily affects the lung, and it has been established that its pathology presents as highly heterogeneous lung lesions (Dartois and Barry 2013; Lenaerts, Barry, and Dartois 2015). The target profile for a TB drug therefore requires that it possesses properties that will enable the drug to reach the target organ and distribute into the various lesion compartments at effective concentrations. This necessitates

the inclusion of disease-relevant *in vitro* assays that can be used for profiling of experimental compounds in early investigations, with the intent to select for those compounds whose physicochemical properties drive drug cellular uptake and favorable caseum distribution. For example, it was shown in this thesis that despite their promising potent *in vitro* activity, the benzoxazole-based carbamates showed poor stability and permeation into macrophages which resulted in poor control of intramacrophage bacillary growth, and hence limited further investigations.

Furthermore, *in vitro M. tuberculosis* metabolism studies can provide important information on whether *M. tuberculosis*-mediated biotransformation likely activates or inactivates experimental compounds. Prodrugs in drug discovery are defined as inactive drug molecules that become activated, usually by an enzymatic process *in vivo* to release the active drug moiety. A significant number of currently used TB drugs follow this approach. An example is INH, which is activated by *M. tuberculosis* KatG, a catalase peroxidase enzyme that converts it to INH-NAD adducts which then inhibit another key enzyme involved in mycolic biosynthesis, InhA (Vilcheze and Jacobs 2007). The use of C3-alkyl FA prodrugs is a favorable approach that can be used to release and accumulate FA in the lung tissue *in vivo* (Strydom et al. 2020), and specifically in the macrophage host cell as shown in this thesis. *M. tuberculosis* and host cell-mediated hydrolysis of C3-alkyl esters (GKFA16 and GKFA17) could therefore be used to increase the exposure of FA within the intracellular environment. On the other hand, the presence of easily cleavable groups may not be favorable for certain chemical scaffolds as demonstrated by the benzoxazole carbamates which were drastically hydrolyzed by *M. tuberculosis* to their poorly active free oxime counterparts. Further studies should therefore focus on optimization of the highly active oxime carbamates through suitable replacements that

will result in improved stability and permeability while retaining activity against *M. tuberculosis*.

Chapters 3 and 4 focused on establishing the ability of compounds to permeate and accumulate in the *M. tuberculosis*-infected macrophage – the 'minimal unit of infection' (VanderVen et al. 2016) – and whether this depended on their lipophilicity. Furthermore, it was investigated whether the amount of drug accumulated translated into effective killing of intracellular *M. tuberculosis* in macrophage phenotypes that may be present within the human host during disease. While lipophilicity is a key driver of drug cellular permeation, a combination of the amount of drug accumulated within macrophages and the intrinsic activity of a compound against *M. tuberculosis* drives the outcome of infection. This was shown with the highly cidal MXF which only demonstrated moderate cellular accumulation but with sterilizing effects against intracellular *M. tuberculosis*. For bacteriostatic drugs like FA and its derivatives, increasing lipophilicity and therefore drug accumulation, had little to no effect on infected macrophage treatment outcome. This highlighted that the impact of differential drug permeation and accumulation on intracellular efficacy of bacteriostatic drugs cannot be discerned with this assay. However, its strength in highlighting the continued increase in FA prodrug accumulation, further affirms that the prodrug strategy could be effective to increase intracellular drug concentrations therefore maintaining prolonged high FA levels within the host cell.

The induction of foamy macrophages through oleic acid exposure showed the formation of lipid bodies within the macrophages which allowed investigating the effect of the presence of LBs on drug uptake and infection outcome in comparison to the non-foamy, resting cells. For the bacteriostatic FA compounds, the inability to distinguish the effect of drugs in foamy macrophages further validated that this assay cannot be used to provide resolution on the

impact of penetration, accumulation and intracellular distribution of bacteriostatic drugs. In contrast, for cidal drugs, LBs in foamy cells seem to impact the ability of MXF, LVF and BDQ to reach and kill intracellular bacilli, while RIF was not affected. This suggests that the extent of drug lipid binding may influence the fate of foamy macrophages at the cellular/necrotic interface during treatment. For drugs that fail to achieve target unbound free fraction, there will likely be reduced efficacy against intracellular bacilli. The implications may be the development of phenotypic drug tolerance.

The results may vary based on the method used to induce the foamy state, the number of LBs accumulated by the host cell and the bacilli inoculum used, which may all inform the level of interaction or proximity between the bacilli and LBs inside the cell. While for some drugs the diffusion into lipid bodies can serve as a reservoir to facilitate the continuous accumulation of the drug inside cells, for some compounds this lipid binding may be unfavorable. Limitations of *in vitro* macrophage assays using the THP-1 cell line with a limited lifespan include the inability to characterize long-term effects of intracellular drug accumulation and distribution as well as activity against *M. tuberculosis* in both foamy and non-foamy cells.

5.2 Future Recommendations

The results in this thesis demonstrate the potential of utilizing *in vitro* macrophage infection assays to predict which antimycobacterial agents will accumulate in the cellular lesions and if this accumulation will translate into bacterial killing or inhibition of growth. Further work could look into evaluating drug combinations to explore within-macrophage synergistic interactions. This would particularly be beneficial for those drugs that are less efficacious in foamy macrophages likely due to their increased lipid binding, to be used in combination with compounds that demonstrate less lipid interactions. In addition, for drugs that show lower

macrophage uptake, synergistic interactions in combinations with other drugs could translate the low intracellular concentrations into efficient killing of the *M. tuberculosis.*

Secondly, the predictive model for macrophage accumulation could potentially identify drugs that are susceptible to efflux and therefore lower their intracellular concentrations over time. The implication of macrophage efflux is reduced drug efficacy due to sub-therapeutic intracellular exposure. For example, it was shown in this work that the accumulation of RIF, FA and GKFA37 was reduced over time. Although investigation of efflux mechanisms was beyond the scope of this project, future work could explore whether this reduced accumulation was due to drug efflux. Consequently, it would be worth investigating the potential of efflux inhibitors to improve the exposure of drugs in macrophages and determine whether this translates into improved macrophage efficacy.

Thirdly, the lipophilicity driven drug cellular accumulation observed in chapters 3 and 4 suggests that there is potential for this physiochemical property to be exploited to design drugs or prodrugs that will improve cellular lesion accumulation. In addition, when used in conjunction with the *in vitro* caseum binding assays developed by Dartois and colleagues, this predictive model has the potential for designing of new drug combinations that are not only effective against *M. tuberculosis*, but are complimentary in their ability to reach both the cellular and caseum bacilli populations in the granuloma.

Finally, the overall aim of this thesis was to contribute to strategies for optimization of current TB drugs and new antimycobacterial agents to enable the rational design of drug leads in early preclinical stages to progress them faster through the drug discovery cascade. Through the development of *in vitro* models that can predict drug lesion distribution, compounds with preferential accumulation and macrophage efficacy could translate to in *vivo* efficacy. These

strategies could contribute to the final goal of treatment shortening therapy currently required for TB disease (Connolly, Edelstein, and Ramakrishnan 2007).

5.3 References

Connolly, L. E., P. H. Edelstein, and L. Ramakrishnan. 2007. 'Why is long-term therapy required to cure tuberculosis?', *PLoS Medicine*, 4: e120.

Dartois, V., and C. E. Barry, 3rd. 2013. 'A medicinal chemists' guide to the unique difficulties of lead optimization for tuberculosis', *Bioorganic and Medicinal Chemistry Letters*, 23: 4741-50.

Lenaerts, A., C. E. Barry, 3rd, and V. Dartois. 2015. 'Heterogeneity in tuberculosis pathology, microenvironments and therapeutic responses', *Immunological Reviews*, 264: 288-307.

Strydom, N., G. Kaur, G. A. Dziwornu, J. Okombo, L. Wiesner, and K. Chibale. 2020. 'Pharmacokinetics and Organ Distribution of C-3 Alkyl Esters as Potential Antimycobacterial Prodrugs of Fusidic Acid', *ACS Infect Dis*, 6: 459-66.

VanderVen, B. C., L. Huang, K. H. Rohde, and D. G. Russell. 2016. 'The Minimal Unit of Infection: Mycobacterium tuberculosis in the Macrophage', *Microbiol Spectr*, 4.

Vilcheze, C., and W. R. Jacobs, Jr. 2007. 'The mechanism of isoniazid killing: clarity through the scope of genetics', *Annual Review of Microbiology*, 61: 35-50.

CHAPTER 6

EXPERIMENTAL

6.1 Reagents and solvents

FA was purchased from Avachem Scientific (Texas, USA). All FA (Singh et al. 2020) and benzoxazole-based oxime derivatives (unpublished) were synthesized in Kelly Chibale laboratories in the Chemistry department (University of Cape Town, South Africa). MXF, LVF, RIF and CFZ were purchased from Sigma-Aldrich (South Africa). BDQ was a donation from the Division of Clinical Pharmacology (University of Cape Town, South Africa), originally purchased from Toronto Research Chemicals (Canada). All solvents, additives for chromatography work (at least HPLC grade), laboratory reagents and other consumables for cell culture were purchased from Sigma-Aldrich or Merck (South Africa). Deionized water for buffer preparation and HPLC mobile phases was from a Millipore water purification system (Merck, South Africa). THP-1 cell line were in-house laboratory liquid nitrogen stocks, originally purchased from ATCC. *M. tuberculosis* H37Rv MA (wild-type, WT) and *M. tuberculosis* H37Rv MA :: (*smyc*'::mCherry (=pCherry3))fluorescent reporter strains were from freezer stocks maintained by the Molecular Mycobacteriology Research Unit (University of Cape Town, South Africa) at -80 ^{o}C. Prof. David Russell (Cornell University, USA) kindly donated the plasmid and Dr. Vinayak Singh prepared the *M. tuberculosis* H37Rv MA :: (*smyc*'::mCherry (=pCherry3)) strain.

6.2 *In vitro* screening

6.2.1 *M. tuberculosis* growth and MIC determination using the Microplate Alamar Blue Assay (MABA)

All *M. tuberculosis* experiments were performed in a Biosafety Level 3 laboratory. Freezer stocks stored at -80 °C were thawed at room temperature and inoculated in Middlebrook 7H9 medium supplemented with 10% oleic acid-albumin-dextrose-catalase (7H9/OADC) (Difco™) at 37 °C for approximately 3 days, sub-cultured and grown further to attain log phase, OD_{600} ~0.5-0.8. For the fluorescent *M. tuberculosis* H37Rv MA :: (*smyc*'::mCherry (=pCherry3)) strain, 50 µg/ml final concentration of hygromycin was added each time a culture was started or sub-cultured.

MICs for the selected anti-TB drugs and test compounds were determined by broth microdilution Microplate Alamar Blue Assay (MABA). 10mM drug stocks were prepared in DMSO and stored at -20 ºC. In 96-well, U-bottom microplates, 50 µl of 7H9/OADC was added to all wells from Rows 2-12. In row 1, 100 µl 7H9 media containing test drugs at desired starting concentration were added, and two-fold serial dilutions performed by removing 50 µl volume from row 1 to row 2 well and mixing by pipette. Another 50 µl was removed from row 2 to row 3 and this was repeated until row 11, with the last 50µl volume discarded. Row 12 was used as a no drug control, and a single column was used as maximal growth inhibition control by adding 1 mg/ml RIF. Log phase *M. tuberculosis* H37Rv WT cultures grown in 7H9 media were diluted a 200-fold and 50 µl inoculum added to each drug and control wells (final volume of 100 µl per well). For testing in acidic media, pH was adjusted by adding HCl or NaOH (1N) to culture media.

The plates were incubated for 7 or14 days at 37 ºC, 5% CO_2, after which alamar blue was added and plates further incubated. The following day, a change from blue to pink indicated growth of bacteria. Alamar blue (resazurin) is a blue, non-fluorescent oxidation-reduction indicator used in cell viability assays which is reduced to a highly fluorescent resorufin (pink) by live cells. MIC_{90} was defined as the lowest concentration

of the drug where there was no visual color change; or the concentration that inhibited more than 90% of the bacterial population by fluorescence readouts measured with a SpectraMax i3 microplate reader (Separations) using excitation and emission wavelengths of 485 and 508 nm, respectively.

6.2.2 THP-1 cell culture and assessment of viability

All macrophage drug uptake and infection experiments were performed using a THP-1 macrophage-like cell line. Briefly, THP-1 cells were grown in RPMI 1640 medium supplemented with 10% fetal bovine serum (FBS) in filtered cap culture flasks at 37 ºC, 5% CO_2 to reach ~$8x10^5$ -$1x10^6$ cells/ml, sub-culturing every second day. Cell viability was assessed using the trypan blue dye exclusion protocol and cells were counted using a TC20 cell counter (BioRad). Cells were then differentiated into a monolayer of macrophages either in flasks, 24 well or 96-well flat-bottom microplates, depending on the experimental setup.

6.2.3 THP-1 cytotoxicity

THP-1 monocytes were differentiated into macrophage-like phenotype by adding phorbol 12-myristate 13-acetate (PMA) at a final concentration of 200 nM. 100 µl of cells in RPMI media containing 10% FBS at a concentration of $1x10^6$ cells/ml were transferred into each well in a 96-well flat bottom plate, and adhered onto the plate surface overnight.

PMA-containing media was replenished with 100 µl fresh media in each well. Drug solutions were added to the cells by serial dilution, ensuring a final DMSO concentration of <1% in each well. In the first wells, drugs were added at 2 times the desired concentration (100 µl volume) and serially diluted until the last 100 µl was

discarded. Each plate was incubated at 37 ^{o}C, 5% CO_2 for two days, after which the resazurin solution was added to each well and incubated overnight. Plates were read on a BMG fluorescence plate reader (excitation at 485 nm and emission at 520 nm).

The wells with cells and media only were used for background subtraction for experimental wells. To calculate the effect of drug on cells, percentage cell survival was defined as 1-(test well fluorescence units/mean fluorescence units of max. cell death wells) x 100. The lowest drug concentration effecting 90% cell viability was considered the IC_{90}.

Selectivity index (SI) of drug = IC_{90}/ MIC_{90}

6.3 Solubility

i) Turbidimetric method

A turbidimetric method adapted from Bevan and Lloyd was used to estimate aqueous solubility at pH 7.4 (Bevan and Lloyd 2000). 10 mM stock solutions of test and control compounds were prepared in DMSO, and 50 µl volume was placed in triplicate in row H of a 96-well microplate. 8 mM (100 µl) compound solutions in DMSO were prepared in row G and serially diluted by transferring 50 µl to the wells above (row F up to B, containing 50 µl DMSO). This generated pre-dilution solutions with concentration range from 0.00 in row A to 10.00 mM in row H (Figure 6.1).

In a secondary 96-well microplate, dilutions were prepared from the pre-dilution plate in DMSO (wells in columns 1–6) and 0.01 M pH 7.4 phosphate buffered saline (PBS) (wells in columns 7–12) in triplicate, such that only two test compounds could be accommodated per plate (Figure 6.2). 4 µl of each pre-dilution solution was added to the corresponding well of the second plate containing 196 µl of the appropriate diluent (DMSO or PBS). The final concentration of DMSO in the PBS wells was 2% v/v. The total volume per well was 200 µl

and the assay solutions had concentrations of 0.0, 5.0, 10.0, 20.0, 40.0, 80.0, 160.0, and 200.0 μM from A down to H.

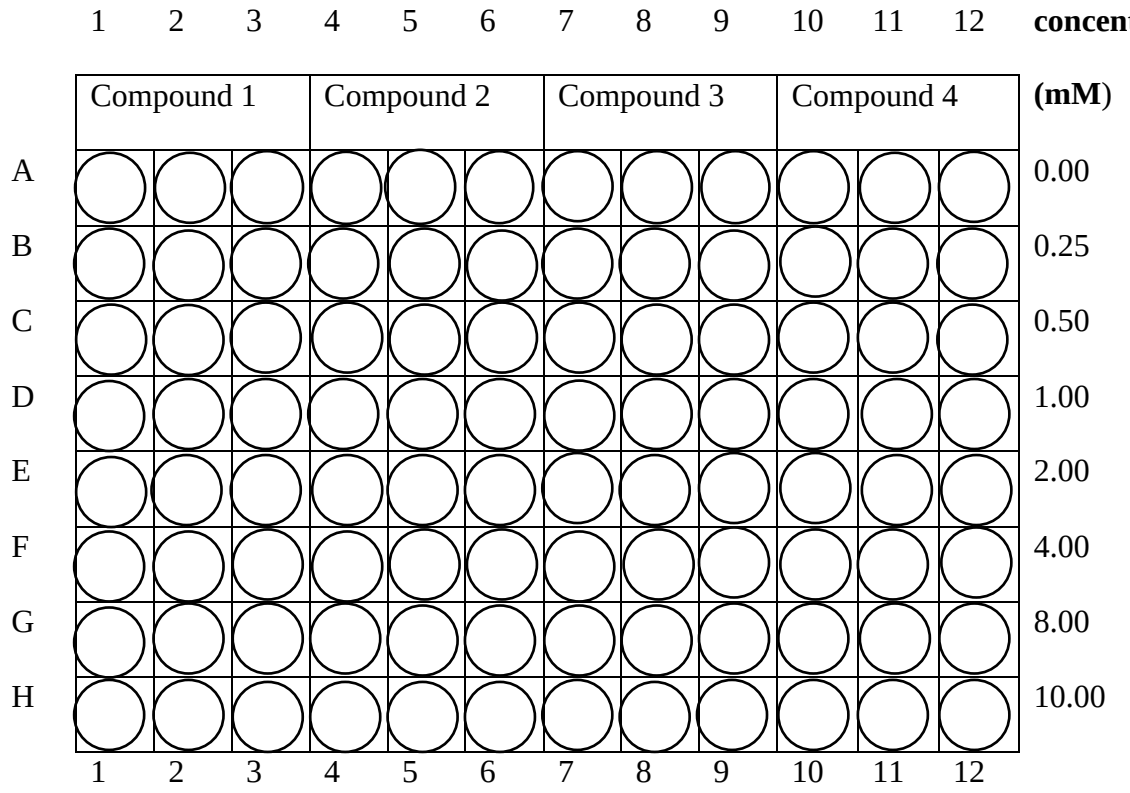

Figure 6.1. A pre-dilution plate set-up for turbidimetric solubility.

The covered plates were equilibrated at room temperature for 2 hours, and UV-VIS absorbances read at 620 nm using a SpectraMax 340PC384 microplate reader (Molecular Devices, CA). DMSO (column 1-6), and 0 μM (row A) wells served as control and blank respectively. For each compound, a line graph of corrected absorbance (that is; absorbance of PBS solution minus the absorbance of the corresponding DMSO solution) against concentration was plotted. At concentrations above the limit of solubility, undissolved particles precipitated out of solution, resulting in increased apparent absorbance. Therefore, the concentration at which increased absorbance was noted was deemed the approximate solubility of the compounds, this corresponded with a shift in absorbance from the zero (DMSO) line.

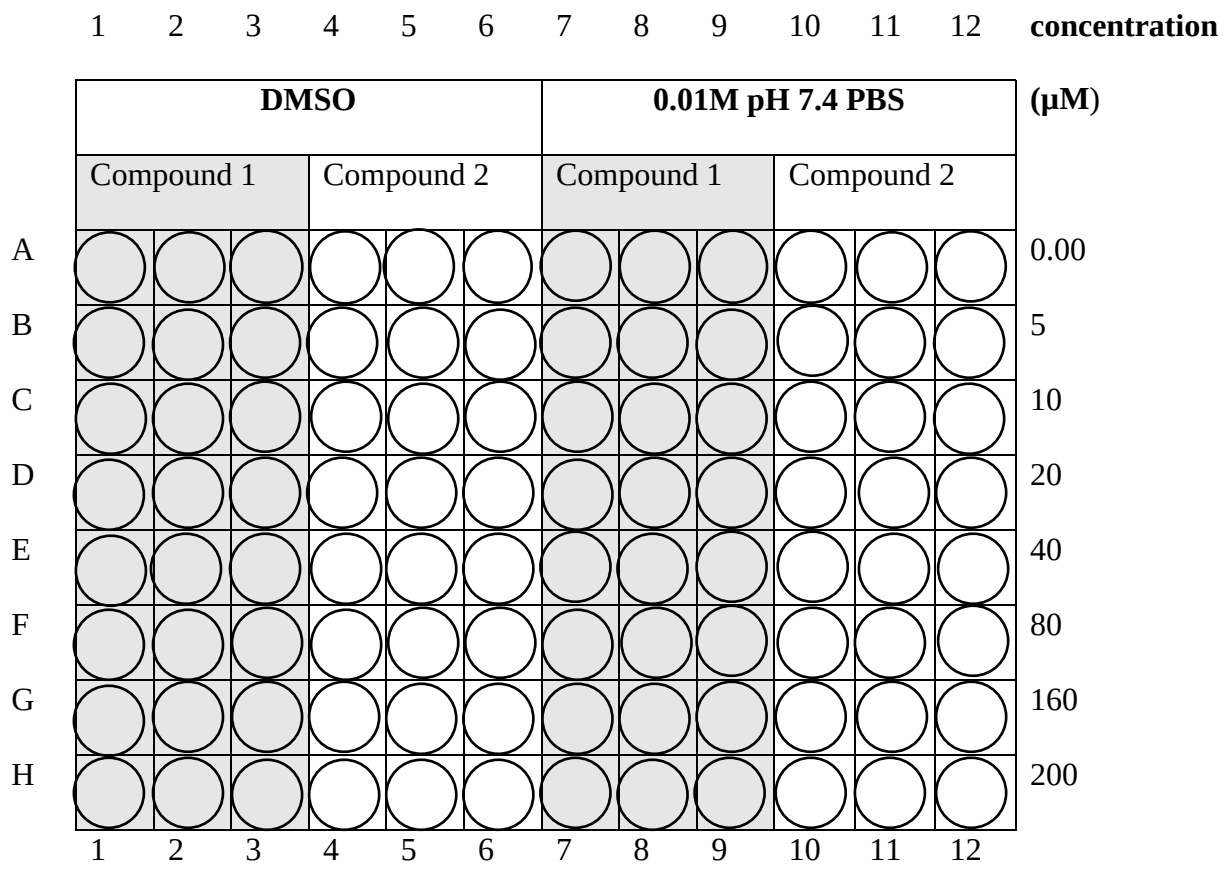

Figure 6.2. Test plate set-up for turbidimetric solubility.

ii) HPLC-based method

Solubility was measured using a miniaturized shake-flask method adapted to a 96-well microplate. (Zhou et al. 2007; Alelyunas et al. 2009). Briefly, 4 µl of a 10mM drug stock in DMSO was added to a 96-well microplate and evaporated using a GeneVac system. Phosphate buffer (pH 7.4) was then added to each well and the plate was incubated at 25 °C for 24 h with shaking. The samples were then centrifuged at 3500 g for 15 min and transferred to an analysis plate. A calibration curve in DMSO was prepared for each sample with concentrations between 10 – 220 µM and included in the analysis plate. Analysis was performed by HPLC-DAD

(Agilent 1200 Rapid Resolution HPLC with a diode array detector) and solubility of each sample determined from the corresponding calibration curve.

6.4 Parallel artificial membrane permeability assay (PAMPA)

PAMPA was performed using a previously described method (Joshi et al. 2017). Briefly, 96-well MultiScreen Filter plates (Millipore, 0.4 µM PCTE Membrane) were used to perform the assay in triplicate. Prior to the assay, membrane filters were pre-coated with 5% hexadecane in hexane and allowed to dry. Lucifer yellow, a membrane integrity marker was then added to the apical wells of the pre-coated MultiScreen plate donor/drug solutions containing test compound. Phosphate buffer (pH7.4) was added to the acceptor plate. 10 mM test compound was used to spike (1 µM) the donor buffer at pH 7.4, and the donor plate slotted into the acceptor plate. The plates were then incubated with gentle shaking at 40-50 rpm for 4 hours at room temperature. Following the incubation, sample from the acceptor wells and theoretical equilibrium wells were transferred to the analysis plate and matrix matched with blank donor buffer. The internal standard, carbamazepine (0.0236 µg/mL) in acetonitrile was added to all samples and analysed by LC-MS/MS (Agilent Rapid Resolution HPLC, AB SCIEX 4500 MS). The normalised (analyte/internal) peak areas were used to calculate the apparent permeability (Papp). Membrane integrity was assessed by calculating the Papp of Lucifer Yellow (acceptable values <50 nm/s) using a Modulus microplate reader (Excitation 490nm, Emission 510 – 570 nm) (Wohnsland and Faller 2001).

6.5 *M. tuberculosis* drug metabolism and aqueous stability

i) *M. tuberculosis* drug metabolism

M. tuberculosis H37Rv MA was grown to an $O.D_{600}$ of 0.5 in six flasks each containing 50 ml of 7H9/OADC. Cultures were centrifuged at 4000 rpm for 10 minutes at room temperature. The supernatant was discarded and pellets re-suspended in an equal volume

of PBS (0.05% Tween80) pH 7.4. A second cycle of centrifugation was performed and supernatant discarded. The pellets were re-suspended in 15 ml volume of the PBS media containing Tween80. This culture was split into 5 ml aliquots in tubes to ensure triplicate samples for each compound to be tested. For the heat-killed cultures, the washing procedure above was preceded by heating the cultures in a water bath at 80^{o}C for 1 hour. Each compound was added to achieve a concentration of 0.1 µM and DMSO ≤ 1% in the final PBS cultures. After each compound was added in triplicate, samples were incubated in a 37 ^{o}C incubator. At pre-defined time-points, 200 µl from each sample was transferred into microtubes. Samples were extracted with 400 µl 3:1 (v/v) chloroform/methanol containing internal standard, for sterilization, and centrifuged at 10000rpm for 10 minutes. The organic layer was transferred to a new plate, evaporated and prepared for LC-MS/MS analysis as described in detail below.

ii) Compound media stability

Triplicate samples were prepared by adding compounds into warm RPMI media containing 10% fetal bovine serum at a concentration of 2 µM for all benzoxazole-based oxime derivatives, and 1 µM for FA and its derivatives GKFA37, GKFA16 and GKFA17. Drug solutions were vortexed and incubated at 37 ^{o}C, 5% CO_2. 100 µl aliquots were sampled at pre-defined time intervals and stored at -20 ^{o}C. For LC-MS/MS analysis, samples were thawed on ice. Extraction was done by liquid-liquid extraction using 200 µl acetonitrile containing internal standard. GKFA122 was used as internal standard for FA compounds series, whereas carbamazepine (CBZ) was used for the benzoxazole-based oxime compounds. Samples were vortexed for 2 minutes and centrifuged at 10200rpm for 5 minutes. 200 ul of supernatant was transferred onto a 96-well deep plate for analysis.

6.6 Macrophage drug uptake assay

Drug uptake into THP-1 macrophages was performed using methods adapted from Prideaux et al, (2015). THP-1 cells were propagated to >90% viability at $8x10^5$-$1.0x10^6$cells/ml. The assay was conducted in a 24-well plate format with $5x10^5$ cells per well, differentiated with 200 nM PMA. Drugs were added at a final concentration of 10 µM or desired concentration as specified; and drug media changed every second day. At pre-determined time points, macrophages were then washed 4 times to remove traces of extracellular drug and detached with 50 µM EDTA solution by gently pipetting after 5 min incubation. 10 µl sample was used to quantify the number of cells/well using the trypan blue method. Further incubation in the dilute EDTA solution allowed for cell lysis, and 200 µl lysate was transferred to microtubes and stored at -20 ºC for quantitation by LC-MS/MS.

For activated macrophages, after differentiation of $5x10^5$ cells per well in a 24 well plate, cells were rinsed once and treated with media containing LPS (10ng/ml) and IFN-γ (10ng/ml) overnight before drug treatment. For foamy macrophages, after differentiation of $5x10^5$ cells per well in a 24 well plate, cells were rinsed once and treated with media containing 1 mL, 400 µM oleic acid for 24 hours before drug treatment (Agarwal et al. 2020).

Calculation of intracellular to extracellular concentration (I/E) ratio

Expression of drug accumulation as a ratio of intracellular to extracellular drug concentration (I/E) was calculated as follows:

$$I/E = \text{intracellular concentration} / \text{extracellular concentration},$$

where extracellular concentration is the concentration of drug added to the macrophages. Intracellular drug concentration was calculated using the drug concentration of the cell lysate determined by LC-MS/MS analysis as described above and adjusting for the number of cells and cell volume. Chen et al, (2018) determined using confocal microscopy that the average THP-1 cell diameter was 11.3 µM, therefore calculated the average cell volume to be 755.5 μm^3 per cell (Chen et al. 2018).

Intracellular concentration = (lysate concentration x lysate volume) / (cell number x cell volume)

6.7 Determination of percentage non-specific drug membrane binding

Cells were prepared as described in the protocol for drug uptake assay. After washing to remove traces of extracellular drug, 200 µl deionized water was added to lyse the cells. The lysates were transferred to microtubes and centrifuged at 10000 rpm for 2 minutes. 200 µl supernatant was collected in tubes and stored for analysis. An additional 200 µl deionized water was added to the pellet in each tube, vortexed and centrifuged again. The second supernatant was collected in different tubes and the pellet resuspended in an equal volume of water. The three samples were stored at -20 ^{o}C and analyzed by LC-MS/MS. The amount of drug associated with the pellet was determined, as a percentage of total drug amount.

6.8 Macrophage infection efficacy

THP-1 cells were propagated and seeded on 24-well plates as described in the macrophage drug uptake assay or at approximately $5x10^4$ cells/well in a 96-well flat bottom plate *M. tuberculosis* H37Rv MA :: (*smyc*'::mCherry (=pCherry3)) strain was cultured to log phase growth (OD_{600} 0.6) in hygromycin-containing 7H9/OADC media. The bacterial culture was centrifuged at 10000 rpm for 10 minutes and washed twice with PBS. The pellet was resuspended in RPMI media containing 10% FBS and filtered with a 5 µm filter to remove bacterial clumps. Bacterial cell density was adjusted to achieve the cell concentration required for MOI = 1. THP-1 cells were washed once with warm incomplete media and infected with *M. tuberculosis* for 4 hours, after which extracellular bacteria was washed off with pre-warmed media and uptake of bacteria by macrophages visualized using microscopy. Drug-containing media was added at the desired concentration and was replenished every 48 hours. At predetermined time points, 210 µl 50 µM EDTA solution was added to each well to detach cells from plate surface.

For CFU determination, a 100 µl portion of the infected macrophage cell lysate was added to 900 µl dH_2O. 10-fold dilutions of the lysate were performed using PBS and plated on solid hygromycin-7H10/OADC media plates. The plates were sealed, incubated at 37 ^oC and CFU counts were taken after ~28 days. Infected (untreated) controls were included. To determine intracellular concentration, the remaining 100 µl infected macrophage cell suspension portion was extracted by adding 200 µl chloroform/methanol containing 100 nM internal standard to sterilize the samples and prepared as described for LC-MS/MS sample preparation.

6.9 Flow cytometry

To determine macrophage percentage infection, cells were infected as described above with multiplicities of infection of 1, 2, 5 and 10. Cells were detached with EDTA as described above and immediately transferred into tubes containing PBS for flow cytometry acquisition. 7-AAD

(7-amino-actinomycin D) was used for live/dead staining (1:1000 v/v). Cell acquisition was performed on a BD FACSAria Fusion and data analyzed using FlowJo software (V10).

To determine the effect of macrophage activation on cell membrane integrity, PMA-differentiated macrophages were rinsed and activation media added containing either 10ng/ml 100pg/ml final concentration of LPS. Cells were incubated overnight followed by a single rinse, detached with 5mM EDTA and stained with propidium iodide (PI) (1:1000 v/v). Control wells were incubated with 'normal' media, and stained as above. Heated control cells were prepared by incubation in a water bath at 60^{o}C for 30 minutes or more, prior to staining with PI. Cell acquisition and analysis was performed as described above.

6.10 Microscopy

Foamy cells were washed with PBS and stained with green LipidTOX (Invitrogen) and DAPI (Sigma) as per manufacturer's instruction and processed for confocal microscopy in a Zeiss LSM 880 with Fast Airyscan module confocal microscope (Carl Zeiss, Jena, Germany). The LipidTOX (green) was detected with the Argon 488 nm laser, mCherry (red) with the 561 nm laser and DAPI, a nuclear stain (blue) with the 405 nm laser using a Plan Apochromat 63X/1.4 NA Oil DIC objective. Images were analysed using ZEN software.

For imaging CFZ uptake in foamy macrophages, cells were differentiated onto microscopy slides placed within the 24-well culture plates. After 24 h incubation, culture media was rinsed off with PBS and drug media added for 30 minutes. A second wash was done and cells stained with LipidTOX green. Imaging was done using the Axio Observer 7 equipped with a 100x plan-apochromatic phase 3 oil immersion objective with numerical aperture of 1.4. Zeiss ZEN software was used for imaging and images processed with ImageJ.

6.11 LC/MS/MS methods

6.11.1 Sample preparation

Briefly, 200 µl cell lysate samples from each well were extracted by liquid-liquid extraction using 400µl methanol: chloroform (1:3) containing a structurally similar internal standard (100 nM GKFA122) for FA derivatives or 125nM carbamazepine (CBZ) for all other compounds. Each sample was vortexed for 2 minutes, centrifuged for 10 minutes at 10,000 rpm, and 200 µl organic layer was transferred to a deep 96-well plate, solvent evaporated under inert N_2 gas and reconstituted in 200 µl mobile phase buffer for LC/MS-MS analysis. Standards (STD) and quality control (QC) samples were prepared by spiking known concentrations of each drug into a macrophage lysate matrix prepared from THP-1 cells. For foamy macrophages samples, the lysate matrix was prepared using oleic induced foamy macrophages accordingly.

6.11.2 Instrumentation

Analysis was performed with a Agilent 1200 Rapid Resolution (600 bar) HPLC system consisting of a binary pump, degasser, autosampler, and temperature-controlled column compartment coupled to an AB Sciex 4000 QTRAP mass spectrometer with an electrospray ion (ESI) source in positive and multiple reaction-monitoring mode. The following general mass spectrometer settings were used: curtain gas (psi) = 40, ion spray voltage (V) = 5000, source temperature = 500, gas 1 (psi) = 50 and gas 2 (psi) = 60. The resulting ammonium adducts for FA derivatives and M+1 (*m/z*) ions for the remaining analytes are listed in Table 6.1.

Table 6.1. LC/MS/MS transitions.

Analyte	**Q1 (Da)**	**Q3 (Da)**
FA	534.421	457.400
GKFA37 (3-ketoFA)	532.390	455.300
GKFA16	604.380	527.400
GKFA17	618.364	541.400
PMN1-201	259.299	72.000
PMN1-199	188.319	157.900
PMN1-136	274.640	88.000
PMN1-135	202.506	172.000
PMN2-09	293.294	72.000
PMN1-157	222.451	191.900
MXF	402.191	384.100
BDQ	555.210	57.000
RIF	823.918	791.200

6.11.3 HPLC conditions

Gradient chromatography was performed on a Phenomenex® Gemini C18 (2.0 x 50 mm, 5 μm) reversed phase column for FA derivatives, MXF, RIF and BDQ; and Phenomenex® Synergi 2.5μm Polar-RP 100Å (2mm x 50mm) column for benzoxazole-based oximes derivatives. Analytes were eluted at a flow rate of 600 μl/min with mobile phases: A. 5% ammonium acetate, 5% (v/v) acetonitrile in water, and B. 5% (v/v) ammonium acetate in

acetonitrile for FA derivatives; and 500 µl/min with 0.1% (v/v) formic acid in water (A) and acetonitrile (B) for MXF, BDQ, RIF, and benzoxazole-based oxime derivatives.

Table 6.2. Gradient chromatography steps for FA compounds.

Time (min)	**Flow rate (µl)**	**Mobile phase A (%)**	**Mobile phase B (%)**
0.00	600	90	10
0.50	600	90	10
4.00	600	5	95
5.00	600	5	95
5.10	600	90	10
8.00	600	90	10

The gradient steps used mobile phases A. 5% ammonium acetate, 5% acetonitrile (v/v) in water, and B. 5% ammonium acetate (v/v) in acetonitrile on a Phenomenex® Gemini C18 (2.0 x 50 mm, 5 µm) reverse phase column.

Table 6.3. Gradient chromatography steps for MXF.

Time (min)	**Flow rate (µl)**	**Mobile phase A (%)**	**Mobile phase B (%)**
0.00	500	95	5
0.50	500	95	5
2.00	500	5	95
3.00	500	5	95
3.60	500	95	5
6.00	500	95	5

The gradient steps used mobile phases A; 0.1% formic acid:water (v/v) and B; 0.1% formic acid :acetonitrile (v/v) on a Phenomenex® Gemini C18 (2.0 x 50 mm, 5 µm) reverse phase column.

6.11.4 Quantification

STD and QC samples were extracted and analyzed in parallel with each batch of samples. Analytes were quantified over a range of 5-200 ng/ml (FA, GKFA37), 5-2000 ng/ml (GKFA16, GKFA17) and 5-1000 ng/ml (MXF). For BDQ, RIF and benzoxazole-based oxime derivatives, relative quantities were measured by determining the ratio of analyte peak area to internal standard peak area. Representative calibration curves of analysed batches for the FA compounds and MXF with their respective regression values are shown below (Figure 6.3-6.7). Quantification used quadratic regression of the analyte area/internal standard area vs concentration with specified weighting. All calibration curves showed regression above 0.99.

Quantification accuracy and precision were measured for high, medium and low QCs for all analytes (Tables 6.4-6.8). Analyst v1.6, ABSciex (Johannesburg, South Africa) was used for instrumentation control and data acquisition.

Table 6.4. Quantification statistics of FA calibration curve.

Expected Concentration	Sample Name	Number Of Values Used	Mean	Standard Deviation	Precision (%CV)	Accuracy (%Norm)
5	S7	2 of 2	5.71	0.62	10.9	114
7.5	S6	2 of 2	7.57	0.19	2.46	101
10	S5	2 of 2	9.46	0.63	6.68	95
25	S4	2 of 2	23.0	1.98	8.59	92
50	S3	2 of 2	43.8	1.70	3.89	88
100	S2	2 of 2	114	12.8	11.3	114
200	S1	2 of 2	195	14.7	7.54	97
15	QC3 (low)	2 of 2	14.1	0.88	6.27	94
60	QC2	2 of 2	52.7	1.16	2.20	88
120	QC1 (high)	2 of 2	112	12.4	11.1	93

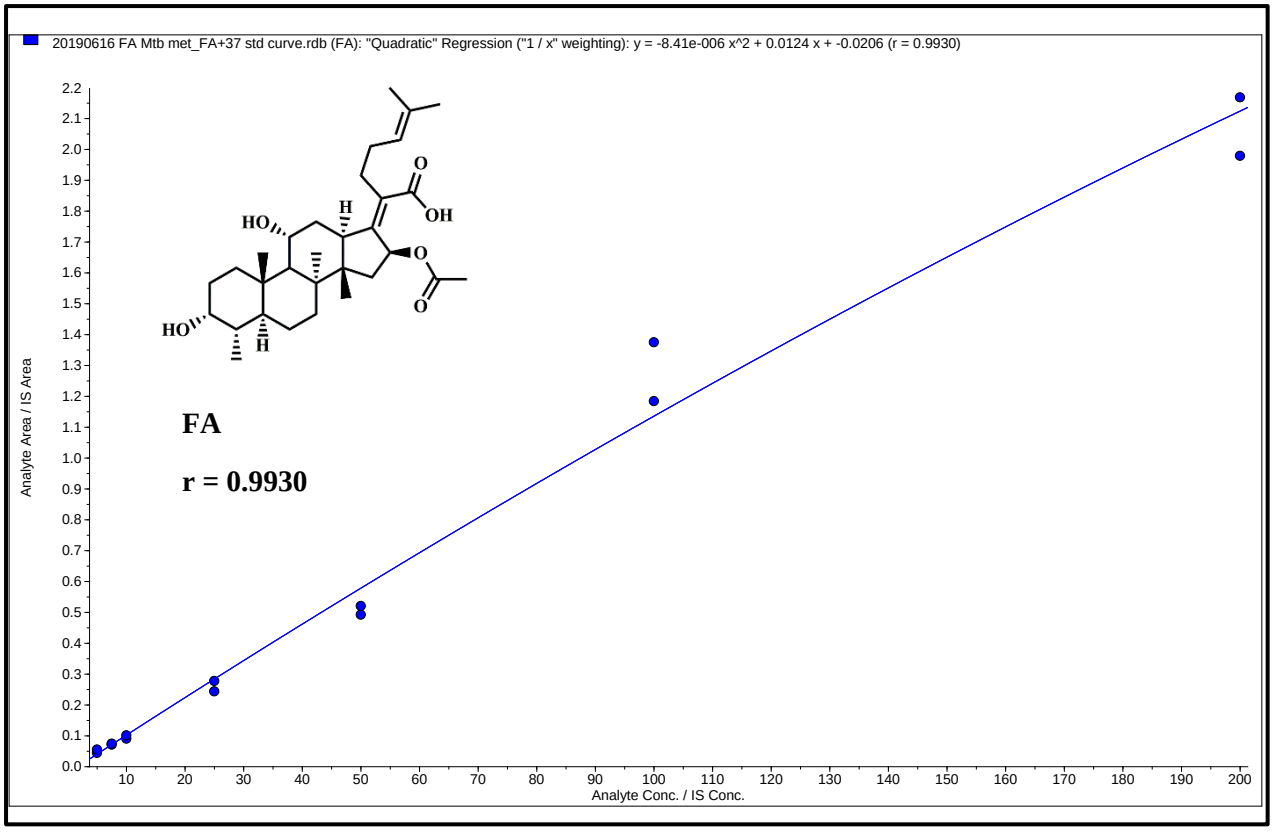

Figure 6.3. Representative calibration curve of FA.

Table 6.5. Quantification statistics of GKFA37 (3-ketoFA) calibration curve.

Expected Concentration	Sample Name	Number Of Values Used	Mean	Standard Deviation	Precision (%CV)	Accuracy (%Norm)
5	S7	2 of 2	5.62	0.14	2.56	112
7.5	S6	2 of 2	7.60	0.04	0.54	101
10	S5	2 of 2	9.85	0.45	4.60	99
25	S4	2 of 2	22.1	1.66	7.51	88
50	S3	2 of 2	44.3	0.91	2.06	89
100	S2	2 of 2	115	4.11	3.59	115
200	S1	2 of 2	193	6.04	3.12	97
15	QC3 (low)	2 of 2	14.10	0.75	5.29	94
60	QC2	2 of 2	53.46	0.27	0.50	89
120	QC1 (high)	2 of 2	107.0	6.76	6.32	89

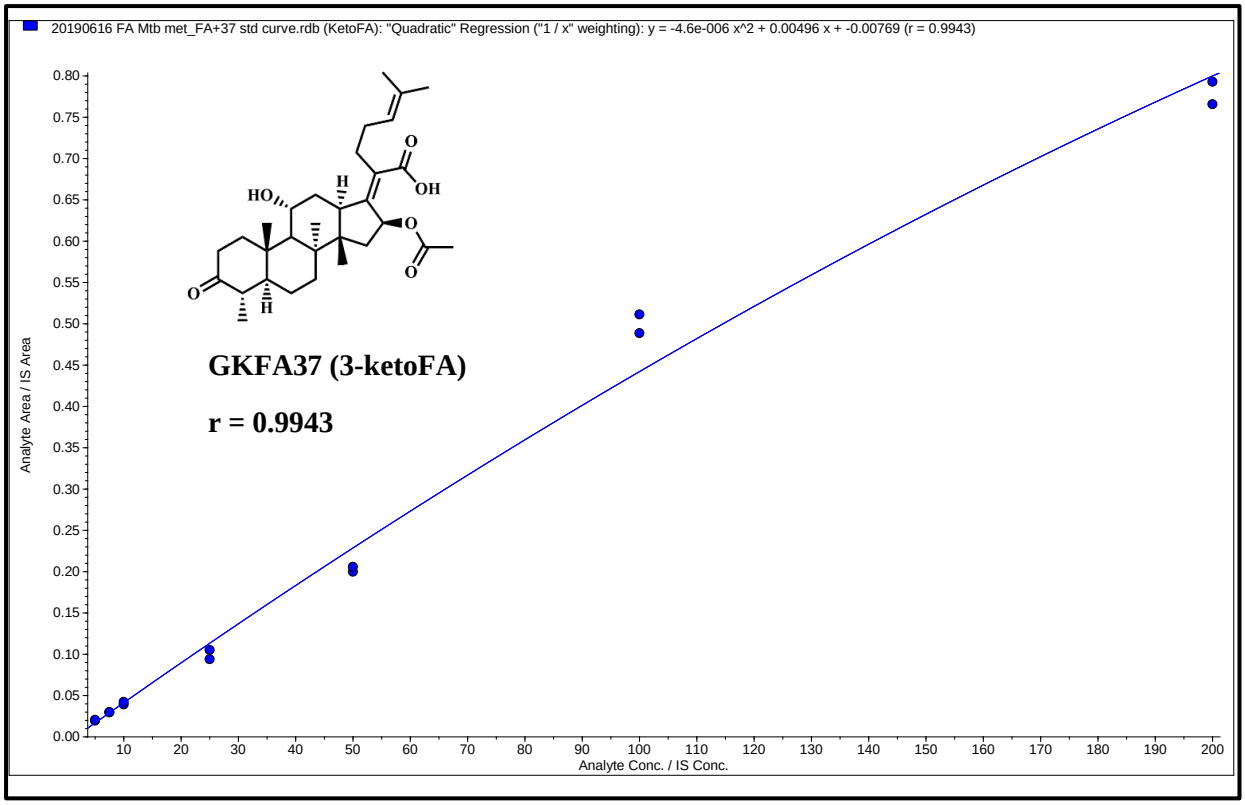

Figure 6.4. Representative calibration curve of GKFA37 (3-ketoFA).

Table 6.6. Quantification statistics of GKFA17 calibration curve.

Expected Concentration	Sample Name	Number Of Values Used	Mean	Standard Deviation	Precision (%CV)	Accuracy (%Norm)
5	S8	2 of 2	4.2	0.8	18.9	84
10	S7	2 of 2	10.7	1.7	15.7	107
50	S6	2 of 2	51.7	5.9	11.5	103
100	S5	2 of 2	107	2.5	2.3	107
250	S4	2 of 2	256	6.2	2.4	103
500	S3	2 of 2	489	31.4	6.4	98
1000	S2	2 of 2	986	32.6	3.3	99
2000	S1	2 of 2	2011	0.14	0.007	101
15	QC4 (low)	2 of 2	14.6	0.3	2.2	98
300	QC3	2 of 2	298	14.0	4.7	99
600	QC2	2 of 2	651	7.3	1.1	109
1200	QC1 (high)	2 of 2	1259	59	4.7	105

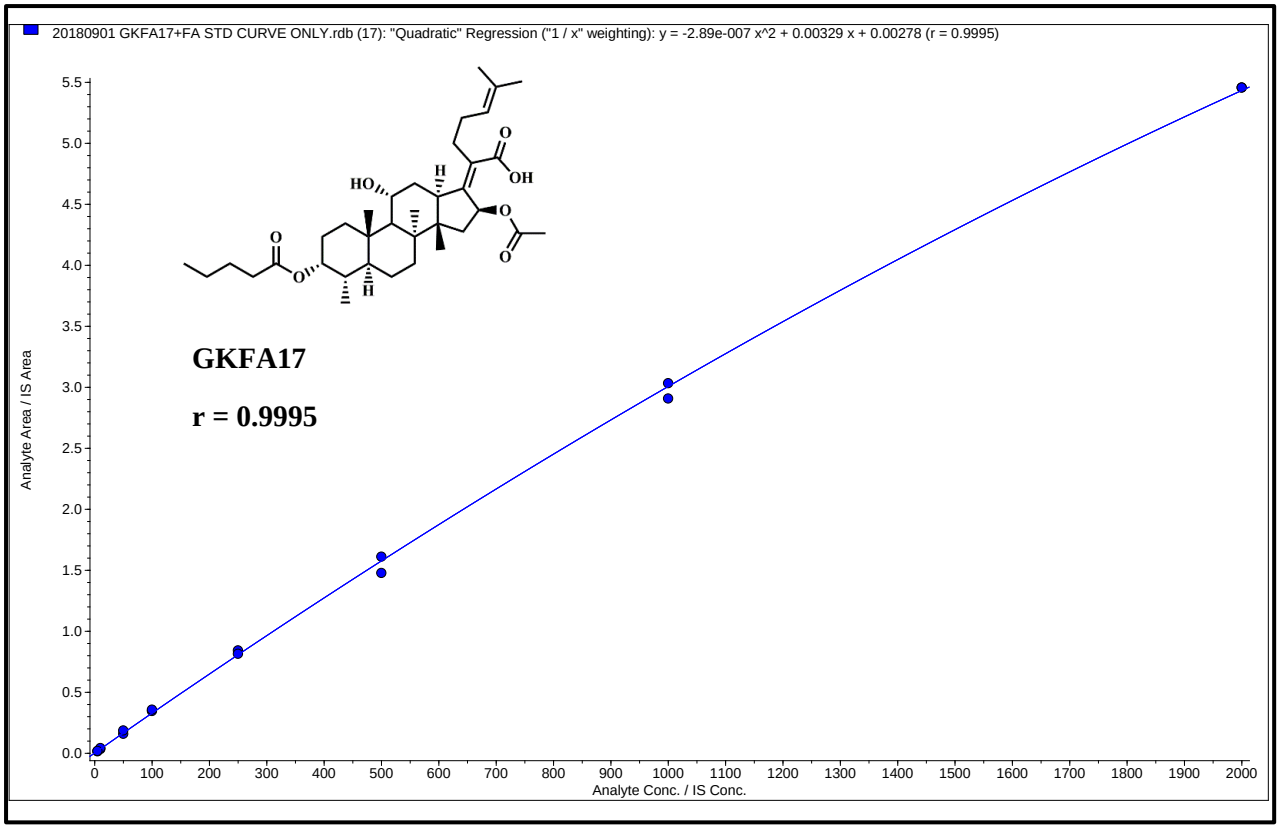

Figure 6.5. Representative calibration curve of GKFA17.

Table 6.7. Quantification statistics of GKFA16 calibration curve.

Expected Concentration	Sample Name	Number Of Values Used	Mean	Standard Deviation	Precision (%CV)	Accuracy (%Norm)
5	S8	2 of 2	5.28	0.64	12.0	106
10	S7	2 of 2	9.67	1.41	14.6	97
50	S6	2 of 2	50.6	2.85	5.63	101
100	S5	2 of 2	96.8	0.50	0.52	97
250	S4	2 of 2	248	3.82	1.54	99
500	S3	2 of 2	496	2.61	0.53	99
1000	S2	2 of 2	1016	6.36	0.63	102
2000	S1	2 of 2	1992	53.5	2.69	100
15	QC4 (low)	2 of 2	14.6	0.32	2.2	98
300	QC3	2 of 2	298	14.0	4.7	99
600	QC2	2 of 2	651	7.3	1.1	109
1200	QC1 (high)	2 of 2	1259	59	4.7	105

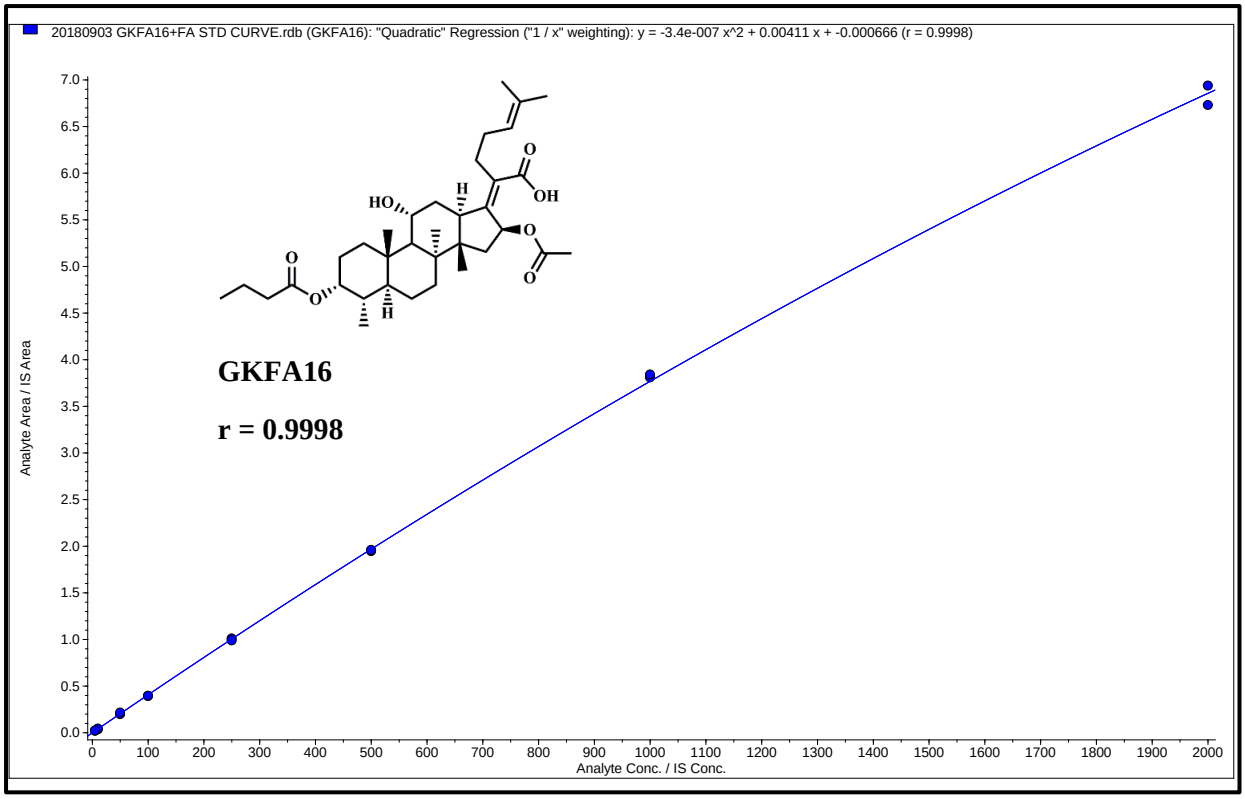

Figure 6.6. Representative calibration curve of GKFA16.

Table 6.8. Quantification statistics of MXF calibration curve.

Expected Concentration	Sample Name	Number Of Values Used	Mean	Standard Deviation	Precision (%CV)	Accuracy (%Norm)
5	S8	2 of 2	6.01	0.08	1.27	120
10	S7	2 of 2	9.58	0.59	6.17	96
25	S6	2 of 2	23.2	0.32	1.39	93
50	S5	2 of 2	46.0	0.24	0.53	92
100	S4	2 of 2	96.3	1.30	1.35	96
250	S3	2 of 2	251	11.1	4.40	100
500	S2	2 of 2	517	36.2	7.01	103
1000	S1	2 of 2	991	138.9	14.01	99
7.5	QC5 (low)	2 of 2	7.14	0.35	4.96	95
15	QC4	2 of 2	12.19	1.32	10.8	81
30	QC3	2 of 2	25.51	3.31	13.0	85
300	QC2	2 of 2	296	47.66	16.1	99
600	QC1 (high)	2 of 2	602	47.35	7.87	100

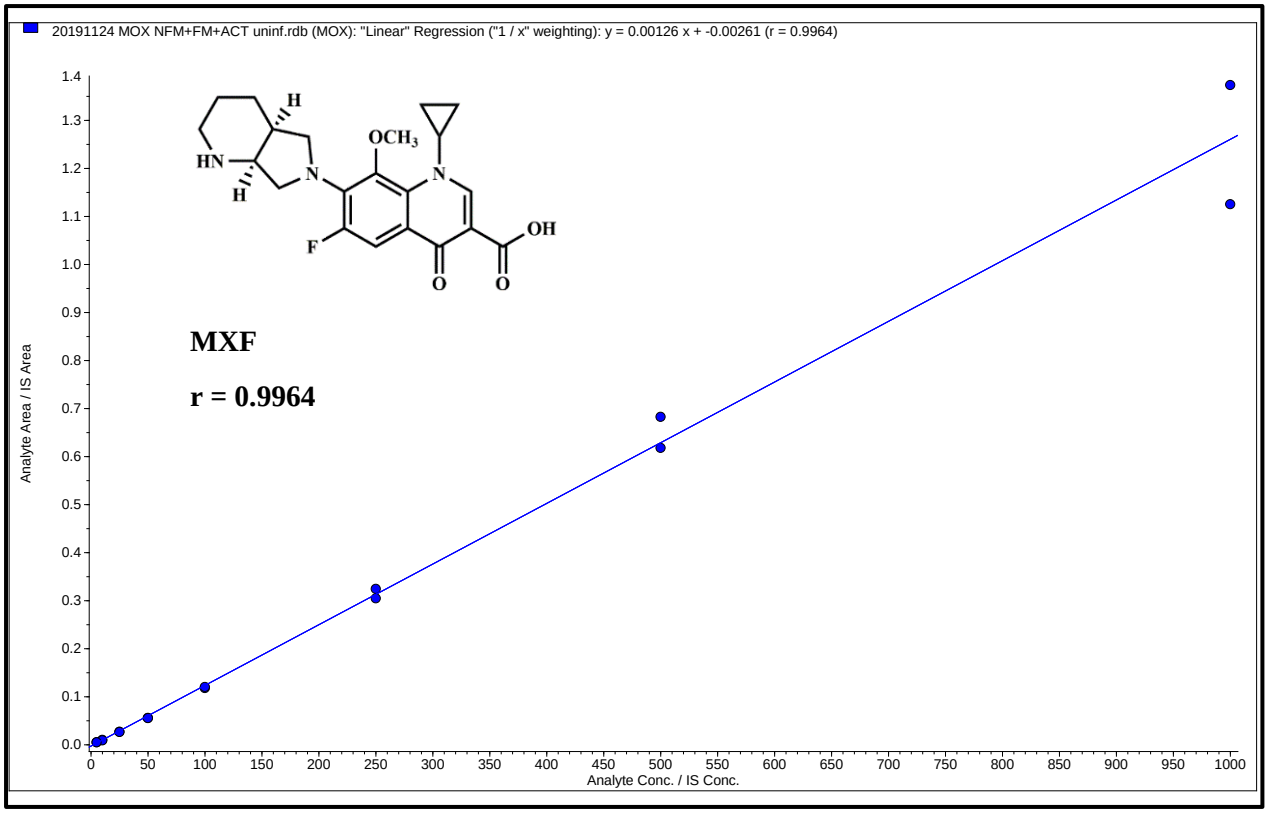

Figure 6.7. Representative calibration curve of MXF.

6.12 References

Alelyunas, Y. W., R. Liu, L. Pelosi-Kilby, and C. Shen. 2009. 'Application of a Dried-DMSO rapid throughput 24-h equilibrium solubility in advancing discovery candidates', *European Journal of Pharmaceutical Sciences*, 37: 172-82.

Bevan, C. D., and R. S. Lloyd. 2000. 'A high-throughput screening method for the determination of aqueous drug solubility using laser nephelometry in microtiter plates', *Analytical Chemistry*, 72: 1781-7.

Chen, C., S. Gardete, R. S. Jansen, A. Shetty, T. Dick, K. Y. Rhee, and V. Dartois. 2018. 'Verapamil Targets Membrane Energetics in Mycobacterium tuberculosis', *Antimicrobial Agents and Chemotherapy*, 62.

Joshi, M. C., J. Okombo, S. Nsumiwa, J. Ndove, D. Taylor, L. Wiesner, R. Hunter, K. Chibale, and T. J. Egan. 2017. '4-Aminoquinoline Antimalarials Containing a

Benzylmethylpyridylmethylamine Group Are Active against Drug Resistant Plasmodium falciparum and Exhibit Oral Activity in Mice', *Journal of Medicinal Chemistry*, 60: 10245-56.

Singh, K., G. Kaur, P. S. Shanika, G. A. Dziwornu, J. Okombo, and K. Chibale. 2020. 'Structure-activity relationship analyses of fusidic acid derivatives highlight crucial role of the C-21 carboxylic acid moiety to its anti-mycobacterial activity', *Bioorganic and Medicinal Chemistry*: 115530.

Wohnsland, F., and B. Faller. 2001. 'High-throughput permeability pH profile and high-throughput alkane/water log P with artificial membranes', *Journal of Medicinal Chemistry*, 44: 923-30.

Zhou, L., L. Yang, S. Tilton, and J. Wang. 2007. 'Development of a high throughput equilibrium solubility assay using miniaturized shake-flask method in early drug discovery', *Journal of Pharmaceutical Sciences*, 96: 3052-71.